JPL Publication 90-27

Proceedings of the Fourteenth NASA Propagation Experimenters Meeting (NAPEX XIV) and the Advanced Communications Technology Satellite (ACTS) Propagation Studies Miniworkshop

Held in Austin, Texas, May 11–12, 1990

Faramaz Davarian
Editor

July 1, 1990

National Aeronautics and Space Administration

Jet Propulsion Laboratory
California Institute of Technology
Pasadena, California

JPL Publication 90-27

Proceedings of the Fourteenth NASA Propagation Experimenters Meeting (NAPEX XIV) and the Advanced Communications Technology Satellite (ACTS) Propagation Studies Miniworkshop

Held in Austin, Texas, May 11–12, 1990

Faramaz Davarian
Editor

July 1, 1990

NASA
National Aeronautics and
Space Administration

Jet Propulsion Laboratory
California Institute of Technology
Pasadena, California

This publication was prepared by the Jet Propulsion Laboratory, California Institute of Technology, under a contract with the National Aeronautics and Space Administration.

PREFACE

The NASA Propagation Experimenters Meeting (NAPEX) is a forum convened to discuss the studies supported by the NASA Propagation Program. The reports delivered at this meeting by the management and the investigators of the program summarize the recent activities as well as plans for the future. Representatives from domestic and international organizations who conduct radio wave propagation studies are invited to NAPEX for discussions and exchange of information. This proceedings records the content of NAPEX XIV and the ACTS miniworkshop that followed it.

NAPEX XIV, which took place on May 11, 1990 at Austin, Texas, was organized into two sessions. The morning session, chaired by Mr. Dean Olmstead of NASA, was devoted to K-band studies for the Advanced Communications Technology Satellite (ACTS) and the Olympus spacecraft. A total of seven papers were presented at this session. The afternoon session entitled "Fixed and Mobile Satellite Propagation Studies and Experiments," was jointly chaired by Dr. Faramaz Davarian of JPL and Mr. John Kiebler of NASA. The number of papers delivered at this session was eight.

The three-member review panel was represented by Professor Gert Brussaard of Eindhoven University of Technology. The other two panel members, Drs. David Rogers and Stewart McCormick, were unable to attend. Professor Brussaard elaborated on the material presented in the meeting in the form of remarks made at the conclusion of the conference. Professor Brussaard's remarks are provided in this proceedings.

NAPEX XIV was hosted by the University of Texas. I must commend Dr. Wolfhard Vogel and his colleagues, Mr. Jeoffrey Torrence and Wanda Turner, for superbly arranging the local logistics. Thanks to their efforts, the one-and-a-half day activity was quite orderly, and it was very pleasant for the attendees.

I would like to express my appreciation to all participants of NAPEX XIV. I would also like to thank Dr. Ernest Smith and his colleagues, Dr. Warren Flock and Ms. Lisa Leonard, for their outstanding contributions in organizing this NAPEX meeting. Furthermore, I wish to extend my gratitude to Harold Yamamoto of JPL for his assistance in compiling and preparing the proceedings for publication.

NAPEX XV is planned for June 28, 1991. Although the meeting site has not been selected yet, southern Ontario will be a likely candidate because the U.S. URSI will be meeting in London, Ontario, during June 24-27, 1991.

Faramaz Davarian

ABSTRACT

The NASA Propagation Experimenters Meeting (NAPEX), supported by the NASA Propagation Program, is convened annually to discuss studies made on radio wave propagation by investigators from domestic and international organizations. NAPEX XIV was held on May 11, 1990, at the Balcones Research Center, University of Texas, Austin, Texas. Participants included representatives from Canada, Italy, Japan, The Netherlands, United Kingdom, and the United States. The meeting was organized into two technical sessions: The first was devoted to propagation studies for the Advanced Communications Technology Satellite (ACTS) and the Olympus Spacecraft, while the second focused on the fixed and mobile satellite propagation studies and experiments.

Following NAPEX XIV, the ACTS Miniworkshop was held at the Hotel Driskill, Austin, Texas, on May 12, 1990, to review ACTS propagation activities since the First ACTS Propagation Studies Workshop was held in Santa Monica, California, on November 28 and 29, 1989. Five papers were presented by contributors from government agencies, private industries, and research institutions.

CONTENTS

NAPEX XIV MEETING

ACTS PROPAGATION STUDIES MINIWORKSHOP

NAPEX XIV ATTENDEES

Mr. Kenneth C. Allen
ITS/NTIA, Radio Bldg.
325 Broadway
Boulder, CO 80303
Phone: 303 497 3412
FAX: 303 497 5993

Mr. Bertram Arbesser-Rastburg
ESA-ESTEC, Mailcode: XEP
P.O. Box 299
NL-2200 AG Noordwick
The Netherlands
Phone: +31-1719-84541
FAX: +31-1719-84547

Mr. Robert Bauer
NASA Lewis Research Center
21000 Brookpark Road
Cleveland, OH 44135
Phone: 216-433-4313
FAX: 216-433-6371

Dr. Charles W. Bostian
Virginia Tech
Dept. of Electrical Engineering
Blacksburg, VA 24061
Phone: 703-231-8400
FAX: 703-231-3355

Dr. Gert Brussaard
Faculty of Electical Engineering
Eindhoven University of Technology
HH 12.33
5600 MB Eindhoven #513
The Netherlands
Phone: +31 40 473890
FAX: +31 40 448375

Dr. Stanley Butman
Jet Propulsion Lab.
4800 Oak Grove Drive
Pasadena, CA 91109
Phone: 818 354 7948
FAX: 818 393 4643

Dr. Dayamoy Chakraborty
Jet Propulsion Lab, MS 161-228
4800 Oak Grove Drive
Pasadena, CA 91109
Phone: 818-354-1877
FAX: 818-393-4643

Mr. Robert Chang
Stanford Telecommunications
1761 Business Center
Reston, VA 22090
Phone: 703-438-8020
FAX: 703-438-8112

Dr. Michael D. Cousins
SRI International, G-102
33 Ravenswood Ave.
Menlo Park, CA 94025
Phone: 415-859-3341
FAX: 415-322-2318

Dr. Faramaz Davarian
Jet Propulsion Lab., 161-228
4800 Oak Grove Drive
Pasadena, CA 91109
Phone: 818-354-4820
FAX: 818-393-4643

Dr. Khaled Dessouky
Jet Propulsiona Lab., 161-228
4800 Oak Grove Drive
Pasadena, CA 91109
Phone: 818-354-0412
FAX: 818-393-4643

Dr. Warren L. Flock
University of Colorado
Campus Box 425
Boulder, CO 80309
Phone: 303-492-7012
FAX: 303-492-2758

Dr. Yoji Furuhama
ATR Optical and Radio
Communications Research Labs.
Seika-cho Soraka-gun Kyoto 619-02 JAPAN
Phone: +81-7749-5-1511
FAX: +81-7749-5-1508

Mr. Frank Gargione
GE Astrospace
P.O. Box 800
Princeton, NJ 0853-0800
Phone: 609-490-2337
FAX: 609-490-2444

Mr. Richard Gibbon
Mitre Corporation
600 Maryland SW, Ste 200A
Washington, DC 20034
Phone: 202-453-9223
FAX: 202-755-0659

Dr. Julius Goldhirsh
Applied Physics Lab.
Johns Hopkins Road
Laurel, MD 20723-6099
Phone: 301-953-5042
FAX: 301-953-1093

Dr. Nasser Golshan
Jet Propulsion Lab., 161-228
4800 Oak Grove Drive
Pasadena , CA 91109
Phone: 818-354-0459
FAX: 818-393-4643

Ms. Loretta Ho
Jet Propulsion Lab
4800 Oak Grove Drive
Pasadena, CA 91109
Phone: 818-354-1724
FAX: 818-393-4643

Mr. Robert Hughes
4800 Oak Grove Drive
Pasadena, CA 91109
Phone: 818-354-2438
FAX: 818-354-2825

Mr. John Kiebler
14520 Dowling Drive
Burtonsville, MO 20866
Phone: 301-384-9614

Mr. Peter MacDoran
University of Colorado
Campus Box 431
Boulder, CO 80309
Phone: 303-492-4426
FAX: 303-492-2825

Antonio Martellucci
Fondazione Ugo Bordoni
Via B. Castiglione 59
00142 Roma ITALY

Dr. T. Menabe
ATR Optical and Radio
Communications Research Labs.
Seik-cho Soraka-gun Kyoto 619-02 JAPAN
Phone: +81-7749-5-1511
FAX: +81-7749-5-1508

Dr. John McKeeman
SATCOM Group, Dept. of EE
Virginia Tech
Blacksburg, VA 24061
Phone: 703-231-6834
FAX: 703-231-6390

Dr. Donald H. Messer
330 Independence Ave.
SW Room 4512
Washington, DC 20547
Phone: 202-485-3212
FAX: 202-485-1781

Mr. Masoud Motamedi
Jet Propulsion Lab., 161-228
4800 Oak Grove Drive
Pasadena, CA 91109
Phone: 818-354-8514
FAX: 818-393-4643

Mr. Dean Olmstead
NASA Headquarters, Code EC
600 Independence Ave.
Washington, DC 20456
Phone: 202-453-1506
FAX: 202-755-9234

Dr. Roderic L. Olsen
Communications Research Center
P.O. Box 11490 Station H
Ottawa CANADA K2H 8S2
Phone: 613-998-2564
FAX: 613-990-7787

Mr. Edward Schwartz
Harris Corp. Building #1-5361
Melbourne, Fl 32902
Phone: 407-729-2421
FAX: 407-727-4663

Dr. Harry Smith
School of Info.
Systems Engineering
University of Bradford
Bradford, ENGLAND
Phone: 274-733466 X6199
FAX: 274-305340

Dr. Ernest K. Smith
University of Colorado
Campus Box 425
Boulder, CO 80309
Phone: 303-492-7123
FAX: 303-492-2758

Dr. Jack B. Snider
NOAA/ERL/WPL, R/E/WPS
325 Broadway
Boulder , CO 80303
Phone: 303-497-6735
FAX: 303-497-6978

Dr. W.L. Stutzman
Virginia Tech
EE Department
Blacksburg, VA 24061-0111
Phone: 703-231-6834 or 8401
FAX: 703-231-6390

Mr. Kenji Tanaka
CRL
Kashima Space Research Center
Communications Research Laboratory, MPT
Kashima, Ibaraki 314 Japan
Phone: +81 229 82 1211
FAX: +81 299 83 5728

Mr. Geoffrey Torrence
Univ. of Texas, EE Research Lab.
10100 Burnett Road
Austin, Texas 78758
Phone: 512 -471-8608
FAX: 512-471-8609

Dr. Wolfhard J. Vogel
University of Texas, EE Research Lab.
10100 Burnett Road
Austin, Texas 78758
Phone: 512 -471-8608
FAX: 512-471-8609

Dr. Edgeworth R. Westwater
NOAA/ERL/WPL, R/E/WPS
325 Broadway
Boulder, CO 80303
Phone: 303-497-6527
FAX: 303-497-6978

NAPEX XIV SUMMARY

F. Davarian
Jet Propulsion Laboratory
California Institute of Technology
Pasadena, CA 91109

Ernest K. Smith
NASA Propagation Information Center
University of Colorado
Boulder, CO 80309-0425

The fourteenth of the current (1980s) series of NASA Propagation Experimenters Meetings (NAPEX XIV) was held on Friday, May 11, 1990, at the Balcones Research Centre of the University of Texas at the invitation of Dr. Wolfhard (Wolf) J. Vogel. The facilities, as can be seen in the photograph, were ideal, and the hospitality afforded by Wolf Vogel, assisted by Geoffrey Torrence and Wanda Turner, was much appreciated. Wolf had chosen the Driskill Hotel, an old traditional emporium, in downtown Austin next to the 6th Street entertainment district for the conference site. This proved to be a very popular choice. The banquet was held Friday evening at the Driskill and featured the Lounge Lizards, in lieu of the traditional after-dinner speaker. The Lounge Lizards turned out to be a local folk/bluegrass group featuring Hank Card, lead and rhythm guitar. (Card is a lawyer and administrative judge during the daytime.) This may well mark the demise of after-dinner speakers at our banquets.

The attendance for NAPEX XIII in San Jose was the highest to that time but it was exceeded by NAPEX XIV. There were 42 registered for NAPEX XIV, 38 at the reception and banquet and 32 at the ACTS Propagation Mini-Workshop Saturday morning at the Driskill. Wolf escorted 6 participants on a tour of the University of Texas campus in Austin Saturday afternoon.

The final agenda for the activities of the May 11/12 period is included in this summary as Tables 1 - 3 taken from the registration materials. Registration fees were $30 for the NAPEX meeting, the reception and banquet was $35, and the Mini-Workshop came to $15.

Two new features of NAPEX XIV were the mini-workshop on ACTS Propagation aspects - a follow-on to the First ACTS Propagation Studies Workshop held in Santa Monica Nov. 28-29, 1989, and the placement of the banquet after rather than before the NAPEX technical meeting. There were two reasons for the latter decision. The first was the lengthy travel time between the Dallas AP-S/URSI meeting, and the second was that by putting the banquet on Friday night it would bridge the NAPEX meeting and the ACTS Workshop, thus serving both meetings.

As can be seen in Table 2, Dr. David Rogers could not attend the meeting but did provide a text. It was made public at the meeting that he was joining Dr. Rod Olsen's group at the Communications Research Centre in Ottawa effective June 1. His new address is:

Dr. David V. Rogers
Microwave Propagation Group
Communications Research Centre
P.O. Box 11490, Station H
Ottawa, Canada K2H 8S2
Phone (c/o R. Olsen) 613-998-2564
Fax 613-990-4077

We wish him well in his new position. Dr. Rogers was a member of the Booker Science Review Panel in 1986 along with Drs. Gert Brussaard and K.S. (Stu) McCormick, and with the latter two is now a member of the Review Committee for the NASA Propagation Program. The Committee attends formally every two years at odd numbered NAPEX meetings, but we were privileged to have Dr. Brussaard with us at NAPEX XIV.

Faramaz Davarian announced that the next NAPEX meeting will be in Canada on June 28, 1991 with possible locations of London, Ontario or Ottawa. In 1991 US-URSI and Canadian URSI join forces and meet June 24-27, 1991, at the University of Western Ontario, London, Ontario. NAPEX is normally held in geographical and temporal proximity to the Spring/Summer URSI meeting.

TABLE 1

General Schedules of Activities
NAPEX XIV and ACTS Miniworkshop
Austin, Texas May 10-12, 1990
Chairman, Local Arrangements: Dr. Wolfhard Vogel
Balcones Research Center, University of Texas at Austin

Thursday, May 10

Check into the Driskill Hotel anytime after 3 PM.
(No activities have been planned for Thursday.)

Friday, May 11

8:00 AM	The NAPEX bus will leave the Driskill Hotel.
8:30-8:50	Registration at the University of Texas Balcones Research Center for NAPEX XIV, the banquet, and the ACTS Propagation Miniworkshop.
8:50-9:00	Welcoming remarks.
9:00-11:45	NAPEX Session #1 Propagation Studies for the Advanced Communications Technology Satellite (ACTS) and Olympus Spacecraft.
1:45-1:15	Lunch
1:15-5:00	NAPEX Session #2 Fixed and Mobile Propagation Studies and Experiments.
5:10 PM	Bus leaves Balcones Research Center for the Driskill Hotel.
7:00 PM	Reception at the Driskill
8:00-11:00	Dinner at the Driskill followed by musical entertainment by the Lounge Lizzards

Saturday, May 12

8:00 AM	(Checkout at the Driskill is 12 noon.)
8:20-8:30	Registration at the Driskill
8:30-11:30	ACTS Propagation Miniworkshop at the Driskill.
Note:	For those staying over, there will be a tour of the university campus Saturday afternoon which will include the Gutenberg Bible and Magna Carta.

TABLE 2

May 11, 1990

AGENDA NAPEX XIV

SESSION 1. Propagation Studies for the Advanced Communications Technology Satellite (ACTS) and the Olympus Spacecraft.

Chairman: D. Olmstead, ACTS Program Mgr., NASA Headquarters

9:00 1) A Summary of the First ACTS Propagation Workshop
D.V. Rogers, Comsat Labs (presented by E.K. Smith)

9:20 2) ACTS Propagation Program
F. Davarian, JPL

9:40 3) OPEX Propagation Measurements and Studies
B. Arbesser-Rastburg, ESA-ESTEC

10:00 COFFEE BREAK

4) Olympus Propagation Studies in the U.S.

10:20 I. Propagation Terminal Hardware and Experiments
W.L. Stutzman, Virginia Tech

10:50 II. Receiver Development and the Data Acquisition System
J.C. McKeeman, Virginia Tech

11:05 III. Olympus Receiver Evaluation and Phase Noise Measurements
R.L. Campbell, Michigan Tech

11:15 5) Communication and Propagation Experiments for Ka Band Mobile Applications
K. Dessouky, JPL

11:35 LUNCH BREAK

SESSION 2. Fixed and Mobile Satellite Propagation Studies and Experiments

Chairman: F. Davarian, JPL, Part A
J. Kiebler, NASA/PSSC, Part B

PART A

1:30 1) Deep Space Propagation Experiments at Ka-Band
S. Butman, JPL

1:45 2) Attenuation Statistics Derived from Emission Measurements by a Network of Ground-Based Microwave Radiometers.
E.R. Westwater, J.B. Snider, WPL, NOAA

2:05 3) Satellite Sound Broadcast Propagation Studies and Measurements
W.J. Vogel, Univ. of Texas

2:30 4) Satellite Sound Broadcast Work at CRL
K. Tanaka, CRL, Tokyo

2:50 COFFEE BREAK

PART B

3:15 5) A Description of Results from the "Handbook on Signal Fade Degradation for the Land Mobile Satellite Service"
J. Goldhirsh, Johns Hopkins/APL

3:35 6) Codeless GPS Applications to Multi-Path: CGAMP
P.F. MacDoran, Colorado
J. Lemmon, ITS/NTIA

4:00 7) Mobile Field Experiments in Australia
L. Ho, K. Dessouky, JPL

4:20 8) NASA Propagation Information Center
W.L. Flock, E.K. smith, Univ. Of Colorado

4:30 DISCUSSION AND CLOSING REMARKS

a) Representatives of the Advisory Committee
b) J. Kiebler, PSSC/NASA
c) F. Davarian, JPL

5:00 ADJOURN

TABLE 3

May 12, 1990

AGENDA
ADVANCED COMMUNICATIONS TECHNOLOGY SATELLITE PROPAGATION STUDIES MINIWORKSHOP

Chairmen: D. (Jack) Chakraborty and F. Davarian

8:30 AM	A Status Report on the ACTS Propagation Experiments Program J. Kiebler, PSSC; D. Olmstead, NASA
8:55	ACTS Propagation Terminal Prototype Planning and Design D. Chakraborty, JPL
9:15	ACTS Update F. Gargione, GE
9:30	LBR Terminal Update E.A. Schwartz, Harris Corp.
9:45	A Review of Fade Detection Techniques F. Pergal, JPL
10:05	Discussion
11:30	Meeting Adjourns

OPENING REMARKS

F. Davarian
Jet Propulsion Laboratory
California Institute of Technology
Pasadena, CA 91109

It is customary in the NAPEX meetings to devote a whole session to a topic with the most activity in the program. Therefore, in this meeting, a whole session is devoted to K-band measurements using ACTS and Olympus. This indicates the degree of our involvement in the ACTS and Olympus campaigns. Our interest in these spacecraft is not coincidence. The Propagation Program has always looked for satellites of opportunity to conduct propagation experiments. We can recall the last satellite experiment using ETS-V and MARECS-B2 satellites for L-band mobile satellite studies in Australia in 1988. The launch of Olympus by ESA less than a year ago has provided us with a unique opportunity that we are determined to take advantage of. Likewise, NASA's ACTS will provide us with another excellent opportunity in about two years. Therefore, K-band propagation studies will be a focal point for us in the next few years.

Until a year ago, MSAT constituted the area of most concentrated effort. Since a year ago, we have reduced our efforts in this area to evaluate our products and provide a new direction to the campaign. Our current activity in this regime includes the writing of a handbook on propagation effects for land mobile satellite systems. Although our efforts in this area have been reduced and have a new scope, continued support of MSAT is foreseen for some time.

The NAPEX XIV agenda includes a presentation entitled "Deep Space Propagation Experiments at Ka-Band." I would like to see some interaction between the Propagation Program and the Deep Space Network (DSN). I hope this will be the beginning of a fruitful cooperation between the two groups.

Our ground-based radiometric measurements for studying the effects of the atmosphere on 20, 30, and 90 GHz signal transmission and noise have been well received. We will continue this effort in the coming year with emphasis given to the Olympus/ACTS studies. We are planning to move NOAA's 3-channel radiometer to Blacksburg, Virginia, so that measurements can be made in conjunction with our Olympus experiments this fall.

Satellite sound broadcast is a new domain for the Propagation Program. The University of Texas is leading this effort. We hope our findings will become available in time to influence WARC 1992.

You may recall that in the past we had tried to perform a delay spread measurement using signals transmitted by GPS satellites. Admittedly, we had not been very successful in doing so. Recently, ESA has joined forces with us, and now we are jointly supporting an effort at the University of Colorado to develop a codeless GPS receiver for delay spread measurements. It is hoped that field measurements will begin in late 1990 or early 1991.

Our information center at the University of Colorado will continue its support of the Propagation Program. This center has been publishing quarterly newsletters that help to publicize our work.

NAPEX XIV

Session 1

PROPAGATION STUDIES FOR THE ADVANCED COMMUNICATIONS TECHNOLOGY SATELLITE (ACTS) AND THE OLYMPUS SPACECRAFT

Chairman:

Dean Olmstead
NASA Headquarters

ADVANCED COMMUNICATIONS TECHNOLOGY SATELLITE (ACTS) PROGRAM

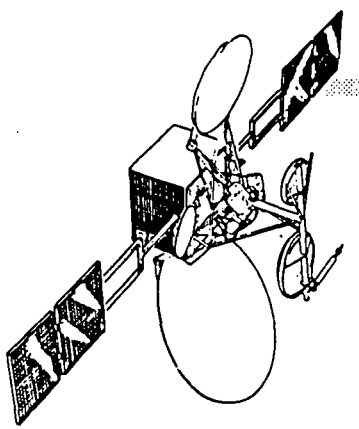

Presentation to
NAPEX WORKSHOP

DEAN A. OLMSTEAD
May 11, 1990

ACTS

NASA

ACTS PROGRAM
KEY EVENTS

EVENT	DATE
• ACTS Experiments Briefing to Adm. Truly	February, 1990 (C)
• ACTS University NRA Release	March, 1990 (C)
• AIAA International Communications Satellite Conference, Los Angeles, CA	March 11-15, 1990 (C)
• ACTS Experimenters Workhop Phoenix, AZ	March 28, 1990 (C)
• Pacific Telecom Meeting with Dr. Fisk	April 5, 1990 (C)
• ACTS Gigabit Users Workshop, Boulder, CO	April 10 - 11, 1990 (C)
• ACTS Terminal Investment CBD Announcement	April 20, 1990 (C)
• ACTS Regional Meeting, Princeton, NJ	May 9, 1990 (C)

KEY EVENTS (con't)

EVENT	DATE
• ACTS Propagation Workshop, Austin, TX	May 11-12, 1990
• ACTS Cost/Schedule Review, LeRC	May 16-17, 1990
• Int'l Mobile Satellite Conference, (with WARC'92 Planning) Ottawa, Canada	June 17 - 20, 1990
• ACTS Experiments Workshop, Seattle, WA	July, 1990
• ACTS Experiments Workshop, Boulder, CO	Aug./Sept., 1990
• ACTS Conference '90 (in Conjunction with SCUC) Las Vegas, Nevada	October 17 - 18, 1990

ACTS BASELINE SCHEDULE
(MAY 1992 LAUNCH)

PLAN DATE : 1/30/89

PREPARED BY : DJF

PAGE : 1

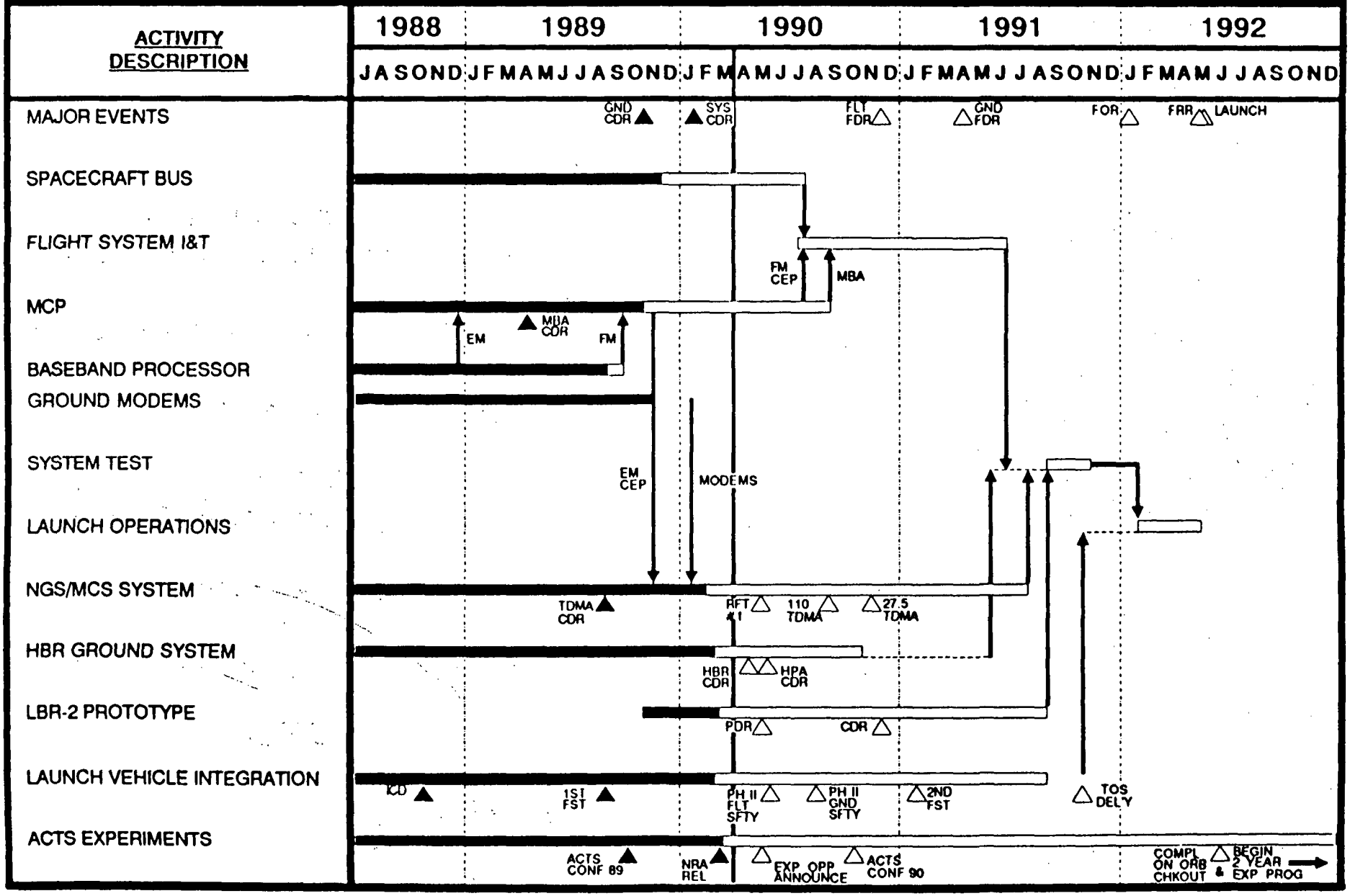

4/03/90

PROGRAM 89% FUNDED

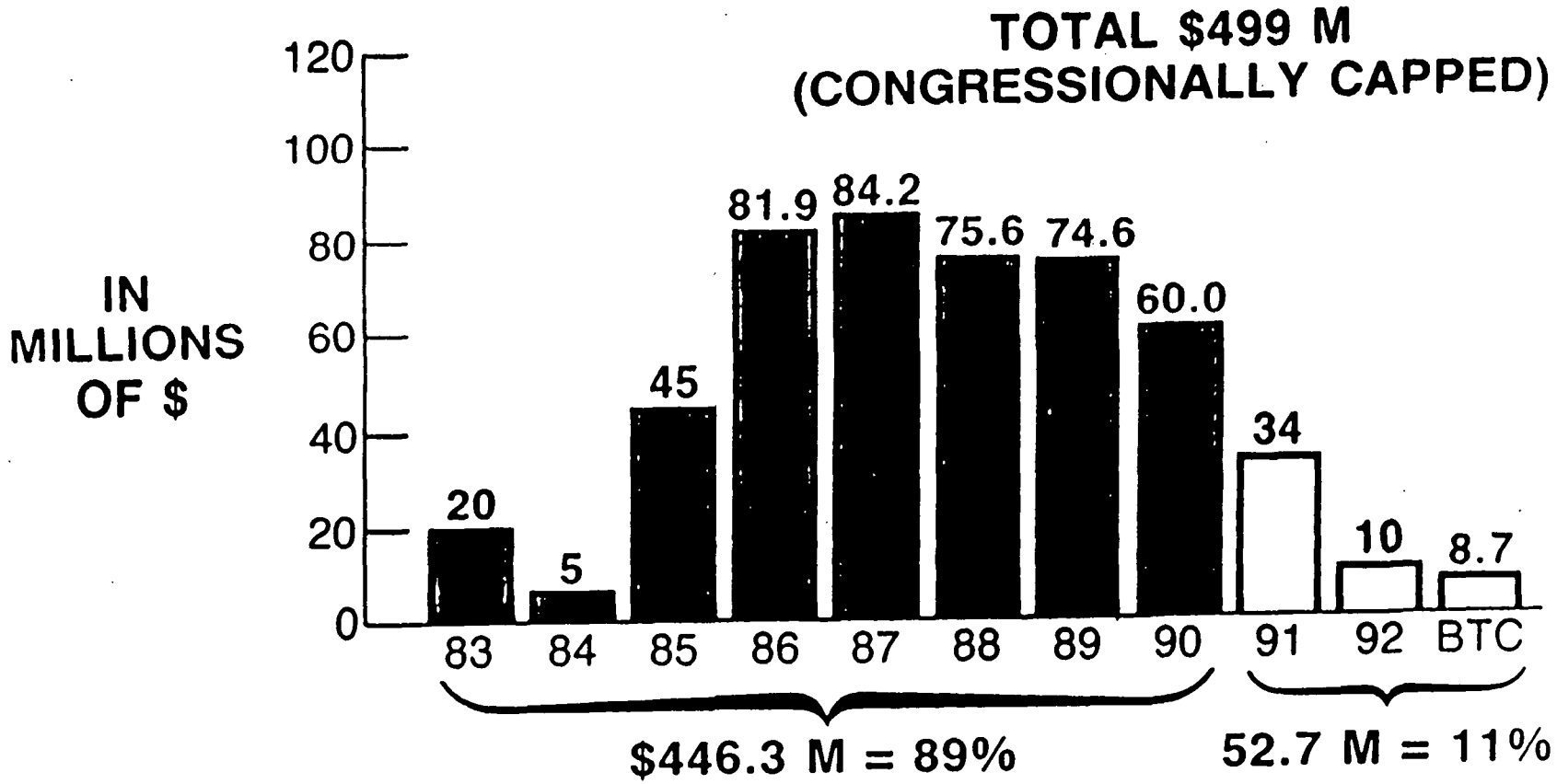

ACTS

CD-46656

NASA

ACTS EXPERIMENTS PROGRAM
Experimenter Terminal Categories

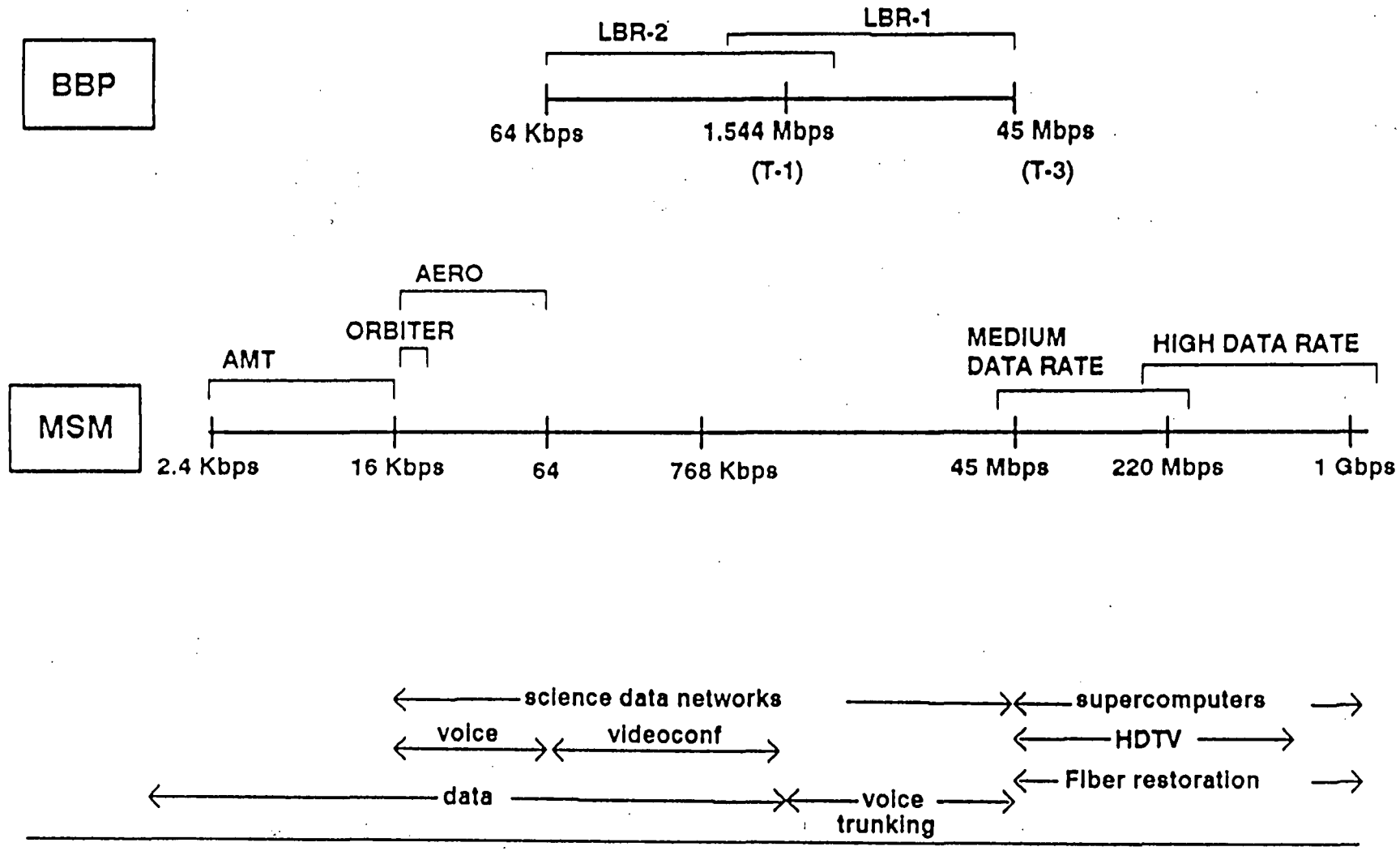

SUMMARY OF THE FIRST ACTS PROPAGATION WORKSHOP

David V. Rogers
COMSAT Laboratories
Clarksburg, MD 20871-9475

1. BACKGROUND

The first ACTS Propagation Studies Workshop (APSW I), organized by NASA/JPL to plan propagation experiments and studies with NASA's Advanced Communications Technology Satellite (ACTS), convened in Santa Monica, California, during November 28-29, 1989. The objectives of APSW I were to identify general and ACTS-related propagation needs, and to prepare recommendations for a study plan incorporating scientific and systems requirements related to deployment of 8-10 propagation terminals in the USA in support of ACTS experimental activities.

2. WORKSHOP ACTIVITIES

Two sessions were held on the first day. R. Bauer of NASA Lewis Research Center chaired Session I, "A Review of ACTS Propagation Features," a synopsis of parameters for both the space and ground segments of the ACTS system with emphasis on elements related to propagation concerns. Topics included: an ACTS System Overview; Spacecraft Beacon Characteristics; the NASA Ground Station (NGS) Beacon Measurement Subsystem; the NGS Fade Detection Algorithm; and the Harris "Mean Squared Over Variance" fade-sensing technique proposed for NASA's Low-Burst-Rate (LBR) communication terminals. F. Davarian of JPL chaired Session II, "NASA Propagation Experiments Plan," including The View From NASA Headquarters; VPI&SU Olympus Propagation Experiments; and A Look at the ACTS Opportunity.

The second day was devoted to parallel discussions within Working Group (WG) 1 - Scientific Studies, and WG 2 - Systems Applications & Receiver Architecture. F. Davarian set the agenda with an introductory presentation. Special presentations were made by R.K. Crane (20/30 GHz Propagation Effects Study), W.J. Vogel (ACTS to Antarctica); J. Goldhirsh (ACTS - Mobile Experiment); R.M. Manning (Markov Random Process Models for Adaptive Fade Algorithms); and K.C. Allen (Pattern Recognition Techniques Applied to Adaptive Compensation). Both WGs prepared reports on their work, results of which are reproduced below.

Complete proceedings of APSW I are available in Publication JPL D-6918, edited by F. Davarian, dated December 15, 1989. The following discussion, based on elements extracted from the proceedings, emphasizes ACTS requirements and corresponding plans.

3. PLANNING GUIDELINES

Planning for ACTS propagation experiments and studies should accommodate the ACTS spacecraft specifications (e.g., beacon characteristics); goals of the ACTS program (demonstration of advanced technology such as dynamic fade compensation); trends in satellite communications (small-margin terminals, etc.), and the need to remedy deficiencies in available propagation information (such as the lack of data for some climates). Activities on the first day of APSW I were organized to provide the participants with such information.

Session I focused on ACTS spacecraft features, and Session II on propagation-related goals. General propagation needs and specific ACTS needs enumerated by F. Davarian included:

- Propagation data for VSATs with small power margins
- Propagation data on short-term fades and fade slope
- Fade countermeasures
- Nationwide joint impairment statistics
- Fade prediction and countermeasure techniques, rain attenuation models, etc.
- Unified effort to respond to ACTS propagation needs
- Provide advice and assistance to ACTS communication experimenters.

4. RESULTS OF WORKSHOP DELIBERATIONS

The two APSW I working groups deliberated on the second day, and prepared detailed reports, available in the proceedings. Those reports are summarized below.

4.1 WG 1 - Scientific Studies

WG 1, Chaired by Robert K. Crane, Dartmouth College, considered propagation experiments that could be conducted with ACTS, and recommended experiments to:

- complete models for the prediction of attenuation statistics in climate regions of the USA that have not been studied
- obtain a statistical description of attenuation for annual time percentages of 1% to 10% needed for the design of low-margin communication systems
- provide a statistical description of the physical processes that give rise to attenuation in the next higher frequency window (~ 90 GHz) needed for the design of higher frequency communication systems
- obtain information needed for the evaluation of the schemes for attenuation compensation employed in the ACTS program and to provide additional data for the design of new mitigation techniques
- explore the use of the 20/30 GHz band for the development of new services, and
- obtain information on the vertical structure of the atmosphere for use in refining attenuation prediction models and in developing inversion algorithms for remote sensing systems.

WG 1 gave consideration to available propagation data for North America, summarized in Fig. 1, noting that most of the rain climate zones have not been well sampled. At least three years of observations were recommended for five of the seven climate regions within the USA for at least 7 new locations, as follows:

Climate Zone	Institution	Location
B2	NOAA/WPL	Colorado
C	?	W. Washington
D1	Michigan Tech	Michigan
D1	Dartmouth College	New Hampshire
D3	?	Tenn., N. Carolina
E	?	Florida
F	Jet Propulsion Lab	California

Three additional climate regions were identified as critical for construction of valid rain attenuation models on a global basis: the Arctic (zone A) and the tropics (zones G and H). The steerable ACTS antenna could be used in conjunction with radiometer measurements for observations in these regions. To extend existing data to time percentages above 1%, measurements were also recommended for zones B1 and D2, in the latter at locations already represented in the data base (Austin, TX; Blacksburg, VA; and Washington, D.C. area).

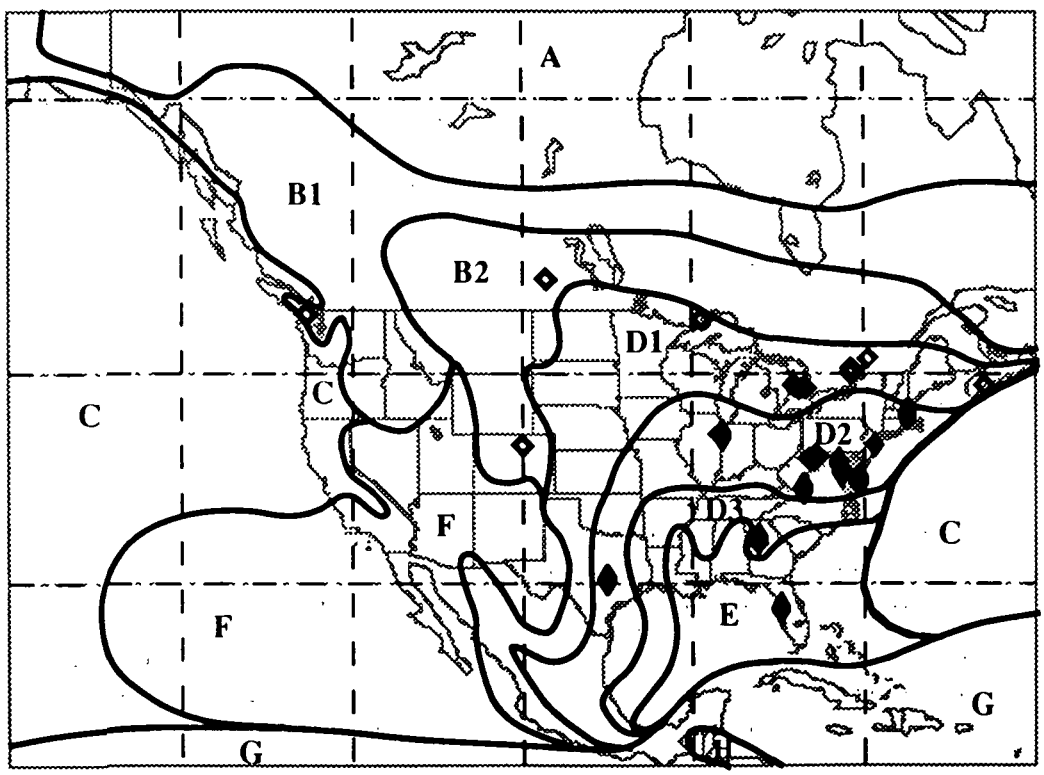

Figure 1. North American Slant Path Observations

For several applications, the complementary capabilities of beacon and radiometer measurements were noted. WG 1 recommended radiometer measurements in support of beacon measurements to obtain data for annual time percentages of 1% to 10%; for identification of the physical processes that cause propagation impairments; and to investigate the vertical structure of the atmosphere. For the compilation of attenuation data for time percentages of 1% to 10%, WG 1 recommended the use of radiometers to establish accurate clear-sky baseline levels and extend the dynamic range of the beacon measurements down to 0.2 dB, while complementary beacon measurements are required to extend the dynamic range of the radiometer terminals. This combination is necessary to provide the required dynamic range of 0.2 dB to 15 dB with an accuracy of better than 15% for the attenuation measurements. WG 1 identified the requirement for a beacon dynamic range of 26 dB (6 dB above the nominal received level to 20 dB below) for this application.

For development of impairment mitigation techniques, WG 1 recommended recording fading signals at a sampling rate of 1 Hz for the compilation of statistics of fade duration, interfade intervals, and fading rates, and to provide time series data needed to test the behavior of fade detection and forecast schemes. Measurements of signal level statistics for propagation through trees and roadside obstructions were recommended to support a move to higher frequencies by the land mobile-satellite services. In particular, measurements in Maryland were recommended to augment the existing UHF and L-band data base.

WG 1 made several general recommendations to ensure data quality and uniformity of data processing. These included: deployment of an optical rain gauge at each site, and use of a Wang device that can identify the precipitation phase (rain, snow, ice) at locations that experience significant occurrences of mixed precipitation; measurement of surface weather conditions at each site; use of a single data format and set of data processing algorithms by all experimenters; establishment of uniform instrument-calibration procedures before the experiment begins; uniform documentation and data preparation/reporting procedures should be used; and a uniform procedure for handling equipment downtime should be established prior to the measurements.

4.2 WG 2 - Systems Applications & Receiver Architecture

Working Group 2, Chaired by David V. Rogers, COMSAT Labs, considered a variety of communication system needs (not necessarily completely consistent with scientific requirements identified by Working Group 1). A variety of propagation requirements for future systems, with particular emphasis on ACTS needs and applications, were identified:

- dynamic allocation of communication resources, with related need for details of individual propagation events (fading rates, fade durations and interfade intervals at specified thresholds, etc.), and associated control algorithms;
- small-margin systems (VSATs) and similar requirements for adaptive decision-making at low fade levels where gaseous absorption, cloud losses, and tropospheric scintillation components should be separately identified;
- mobile systems, which have a secondary frequency allocation in the Ka-bands, and the related problems of multipath and shadowing/blockage;
- dual-polarization system studies (e.g., effects of power control on crosspolar interference, joint coding for fading and depolarization), possibly requiring propagation study;

- the JPL Personal Access Satellite Service (PASS) terminals, which will be small and transportable; and
- site diversity with small terminals at small separations.

Most of the aforementioned needs can be adequately addressed by monitoring the ACTS beacons, although supplementary radiometric (skynoise) data were also recommended.

WG 2 considered the desirability of recording various propagation parameters and the associated sampling bandwidth, dynamic range, and resolution for measurements conducted with the ACTS beacons, and recommended that the terminal be configured to record the following propagation and meteorological parameters:

- 20- and 30-GHz GHz beacon receive signal levels;
- 20- and 30-GHz GHz radiometric skynoise (brightness) temperatures;
- point rain rate near the terminal;
- atmospheric temperature and humidity at the earth's surface; and
- ambient temperature of sensitive components affecting the measurement of beacon receive signal level and radiometric skynoise temperature.

WG 2 recommended that: the terminal be designed to sample the beacon receive signal level at rates up to 100 Hz (though data may be recorded at lower rates during normal operation); that detection bandwidth of the beacon receivers vary with sampling rate in accordance with the Nyquist criterion; that radiometer data be sampled at the same rate as the beacon data for ease of handling; and that the recorded data include the periodic calibration levels. Humidity and temperature can be sampled as slowly as once every 10 minutes to conserve data storage space. Time stamps stored with the data should be in terms of universal time, and accurate within ± 2 seconds.

Effective mitigation of Ka-band path attenuation requires properly-designed algorithms to identify and respond to fading in real time. Five major areas were identified and recommended for investigation and development: fade detection; propagation effect identification; baseline determination and extraction; adaptive fade response and compensation; and frequency scaling. Appropriate propagation parameters should be measured and recorded with regard to the requirements of these five areas.

WG 2 considered a variety of questions regarding the terminals required for the JPL ACTS propagation measurements, noting that substantial development in these areas is ongoing under the NASA Propagation Program, and that the results will strongly affect any final design. The main recommendations included:

- for the beacon measurements: 0.1 dB resolution; accuracy of 0.5 dB rms believed achievable; 10-15 dB dynamic range needed to give reliable data in the 0-5 dB range (of particular interest for VSATs and adaptive algorithms);
- it is preferable to continuously monitor an injected signal from a stable source for calibration but this approach is expensive (easier to implement with digital receiver);
- a rain gauge is essential, and temperature and humidity data are desirable;
- a reliable Uninterruptible Power Supply (UPS) is essential;

- a self-test feature is highly desirable (could be remote);
- data collection with a 12-bit A/D was a popular choice; storage should be binary with a time stamp; real time displays with variable time histories (e.g., 8 min, 2 hr, 1 day, 2 days);
- a modem interface to a phone line is necessary for remote monitoring and checking;
- all terminals should be of standard design and produce standardized data.

Propagation experiments that make use of the communications channel capabilities of the ACTS (both Low Burst Rate and High Burst Rate modes) were considered, although beyond the capabilities of envisaged ACTS beacon-monitoring terminals. The HBR mode provides over 800 MHz of bandwidth, with an EIRP of nearly 60 dBW, in a nonregenerative hard-limited "bent-pipe" mode. Experiments were considered that would make use of a channel-characterization signal transmitted on the uplink from a single reference station in a broadcast mode to any of 3 selected antenna systems on the downlink. These experiments provide unique and novel capabilities that cannot be obtained with the ACTS beacons, and could increase the scope and value of ACTS in providing Ka-band propagation results for system applications. These experiments may be classed into the following categories:

- channel probe experiments to measure the impulse-response function of the radio transmission channel in conjunction with performance assessment (e.g., BER);
- Ka-band aeronautical mobile experiments in the HBR mode to measure and evaluate transmission characteristics of Ka-band aeronautical mobile links, including signal fading, elevation-angle dependence, E_b/N_0 as a function of aircraft antenna gain, and effects of aircraft surface multipath on system performance;
- Land mobile-satellite experiments to establish the feasibility of and requirements for mobile satellite systems at 20 and 30 GHz; acquire a data base of fading caused by trees and terrain at these frequencies; and evaluate the advantage of spread spectrum techniques to overcome terrain multipath.
- Outer/inner coding techniques based on concatenated coding with combined (e.g., Reed-Solomon and convolutional) codes for adaptive power control, where the two coding schemes are invoked separately to provide graduated levels of coding gain.

N91-11956

ACTS PROPAGATION PROGRAM

F. Davarian
Jet Propulsion Laboratory
California Institute of Technology
Pasadena, CA 91109

Introduction

The Advanced Communications Technology Satellite (ACTS) Propagation Program is organized to fulfill certain needs and requirements of the ACTS community. It is hoped that issues related to propagation effects in the context of ACTS experiments can be addressed and resolved by this program.

The objectives of the ACTS Propagation Program are included in but not limited to the following:

- Plan for propagation measurements and studies using ACTS.
- Organize propagation experimenters who want to use ACTS into one group.
- Develop observation stations for ACTS propagation measurements.
- Supervise data collection, analysis, and ensure uniformity of data recording among various experimenters.
- Assist the ACTS Program Office to carry out its objectives.

This program is organized and managed by the NASA Propagation Program at JPL. Financial support for this program is provided by NASA.

Planning

Planning for the ACTS Propagation Program is done cooperatively by many contributors including:

- NASA Propagation Program
- NASA ACTS Program
- Propagation Community
- ACTS Experimenters

The main vehicle for planning is the ACTS propagation studies workshops. Planning for the ACTS propagation terminal was addressed in the First ACTS Propagation Studies Workshop, November 28-29, 1989. The workshop was convened to develop a plan for the ACTS Propagation Program. At the end of two days, the participants delivered a set of recommendations regarding propagation studies and experiments using ACTS. These recommendations covered a range of topics including the configuration and the number of propagation terminals.

Thirty-seven people attended the workshop. Table 1 shows the organizational distribution of the attendees. The workshop presentations were compiled in a document. Three hundred copies of this document have been distributed since.

The workshop participants provided guidelines regarding the ACTS propagation stations. Furthermore, due to the approaching spacecraft launch date and the satellite's short life span, it was strongly suggested that the work on the development of the terminals start without delay. The workshop participants agreed that it would be best to collect propagation data for a minimum of three years, an objective that can be achieved only if the terminal development effort starts immediately.

A preliminary set of observation locations was proposed during the workshop. Table 2 shows these locations with candidate hosts for these stations at some of the locations.

In response to the workshop recommendations, a plan was put forth for developing nine observation stations. This plan consists of two developmental parts: terminal prototype and experimental terminals. With the May 1992 launch date for ACTS, the experimental terminals must be ready for shipping by July 1990. Therefore a terminal development schedule with a July 1992 delivery date was produced which is shown in Figure 1. This schedule is a preliminary one and its final form will be presented in the next ACTS Propagation Studies Workshop in November 1990. Table 3 shows a preliminary cost estimate for the observation stations.

Observation Station

Each observation station will be capable of making 20/30 GHz beacon and radiometric measurements. Furthermore meteorological data, such as point rain rate, ambient temperature and humidity, will be recorded. Each station will be equipped with a data acquisition system with capability to process and display data.

Data Collection and Analysis

The observation stations will be loaned to volunteer organizations for data collection. The collected data will be put in a depository for centralized processing and analysis. A small amount of funding will be available to support host organizations for maintaining the observation stations and for data collection. A reasonable supply of spare parts will be kept at JPL for maintenance and repair of the observation stations.

Summary

The ACTS Propagation Program is an umbrella organization responding to the needs and requirements of the ACTS propagation community. This program is organized by the NASA Propagation Program at JPL and is funded by NASA. Planning for ACTS experiments is the prime objective of this program. About nine observation stations will be developed under this program, which will be loaned to experimenters for propagation measurements. This program will supervise data collection and analysis. The findings of the ACTS propagation campaign will be documented in a report and distributed to the propagation community.

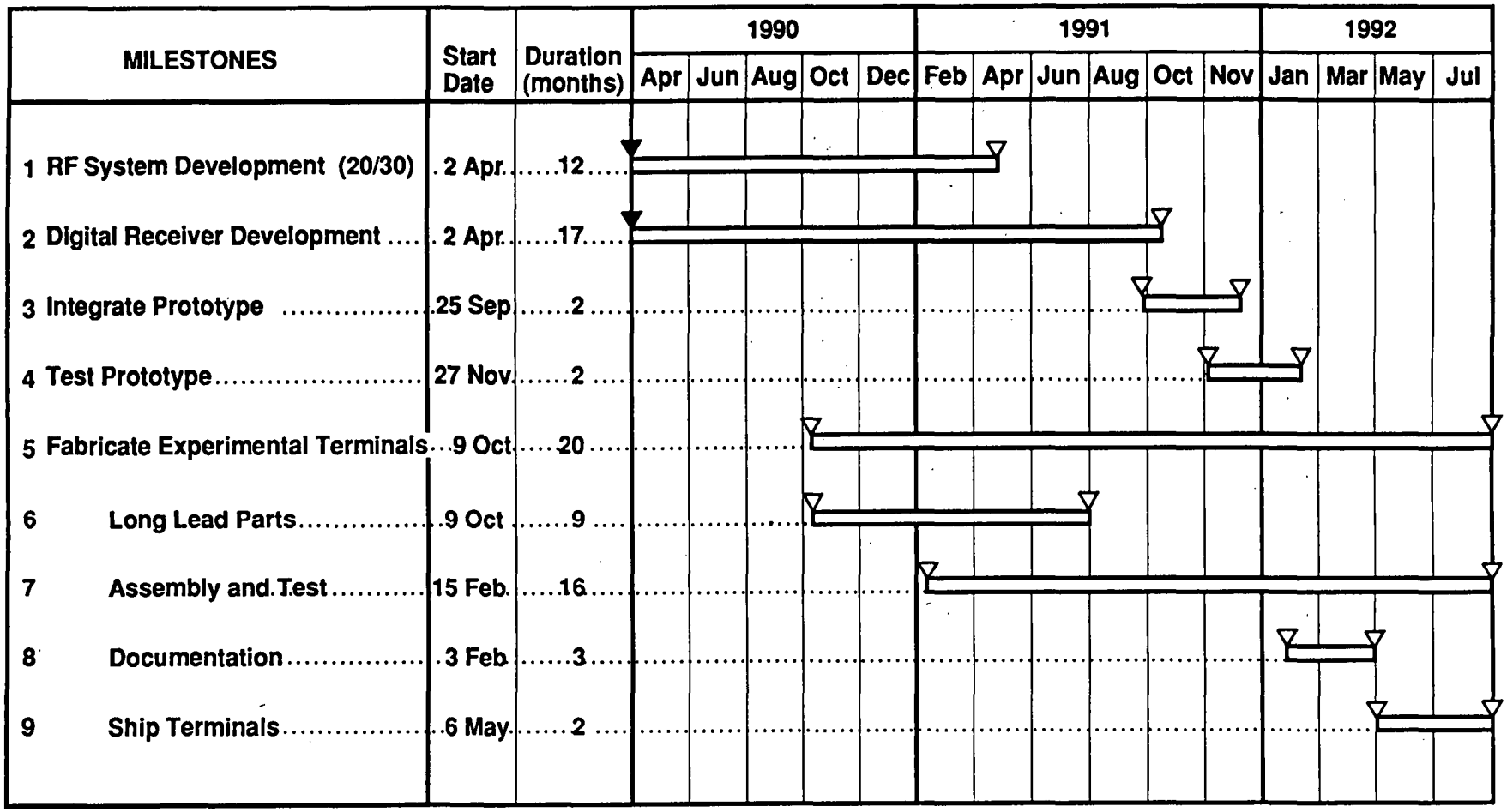

Figure 1. ACTS Experimenter's Terminal Development Schedule

Table 1. Organizational Distribution of Workshop Attendees

Organization	Attendees
NASA	6
JPL	6
University	12
Government	3
Others	10

Table 2. Preliminary Observation Locations with Candidate Hosts

Climate Zone	Institution	Location
B2	NOAA/WPL	Colorado
C	?	Western Washington
D1	Michigan Tech	Michigan
D1	Dartmouth College	New Hampshire
D3	?	Tennessee/North Carolina
E	?	Florida
F	JPL	California

Table 3. Preliminary Cost Estimates per Terminal

Parts & Materials	
Meteorological Equipment	10,000.00
Antennal Subsystem (Prodelin)	8,500.00
RF Subsystem	24,000.00
IF Subsystem	6,000.00
Base Band Subsystem	12,000.00
Computer/DAS/UPS	5,000.00
Total Parts & Materials	65,500.00
Shrinkage:	X 1.05
	68,800.00
JPL Procurement:	X 1.15
	79,100.00
Labor:	25,000.00
Total Mfg. Cost:	104,100.00
Spare Assemblies:	X 1.20
	124,900.00
Cost Uncertainty	X 1.20
Total Cost per Terminal (9 ea.)	$149,900.00

Notes: •Cost does not include site preparation or shelters
•Price is FOB Pasadena

OPEX PROPAGATION MEASUREMENTS AND STUDIES

Bertram Arbesser-Rastburg

ESA - European Space Research and Technology Centre
Noordwijk, The Netherlands

Abstract -- With the launch of the OLYMPUS satellite a new area began for the OPEX group. The years of preparations are now paying off- the experiments are underway and the co-operative effort is now turning its attention to the processing and analysis of data and to the interpretation of results. The aim of this paper is to give a short review of the accomplishments made since NAPEX 13 and the work planned for the future.

1. Introduction

When ESA's telecommunications satellite OLYMPUS was launched in summer of 1989 it carried a payload producing three unmodulated beacons at 12.5, 19.8 and 29.7 GHz. The main purpose of these beacons is to enable scientists to carry out long term slant path propagation experiments at these frequencies. The Olympus Propagation Experimenters group, OPEX, which was set up under ESA auspices in 1980, had been preparing for this event very carefully. The specifications for the equipment to be used and the elaboration of standard procedures for data processing and analysis have been worked out jointly. Today the OPEX community includes approximately 30 groups of experimenters.

2. In-Orbit Performance of the Propagation Payload

Immediately after achieving platform stability at the orbital location at 341 degrees east, ESA performed the In-Orbit Tests. Most measurements were carried out at the IOT station of Redu in Belgium using terminals specially developed for this purpose. Table 1 gives a summary of the test results.

It shall be noted that the EIRP variations quoted in Table 1 are including propagation variations. The real variations occurring on the satellite are much smaller. The redundancy for B1 was lost because of a failure between multiplier and tube and the redundant B2 tube displayed a fault immediately after the first in-orbit switch-on.

For the B1/B2 signals further tests are planned with the new TMS-7 test station. After the measurements are completed in Europe, it is planned to ship the TMS-7 station to Ottawa, Canada and to Blacksburg (VA), USA, for measurements of co-and crosspolar signal power.

3. Geographical Distribution of Experiments

In virtually all member-countries of ESA and in a couple of other countries OLYMPUS propagation experiments are being planned. In 12 sites the experiments have already started. At the majority of sites more than one beacon is received and radiometers are co-located to facilitate bias removal at clear sky conditions.

Table 2 gives an overview of the locations of these experiments. In addition to the experiments listed in table 2, there are measurements planned in Raleigh, NC (USA), Madrid (Spain), about 20 more sites in Italy, in two sites in Yugoslavia, in Spitzbergen (Norway) and a number of other places. In a special effort supported by the Italian government plans are made for experiments in tropical regions of Africa ("TROPEX").

In most places the experimenters are carrying out the bulk of the data analysis in house; in England a group of Universities have agreed to jointly analyze the data coming from the Rutherford-Appleton Laboratory in Chilton.

4. Working Groups

For some time a small group of experimenters have been supporting the Agency in the definition of preprocessing and analysis routines, data formats and the like. This support also included participation in the progress meetings with the software house writing the code. A high level of both expertise and motivation have provided the basis for the success of this group. At the last OPEX meeting (OPEX XIII, held in Noordwijk in March 1990) the formation of new working groups has been proposed and accepted. The work of these groups will be focused on data analysis but also special measurement questions will be addressed.

The following groups have been established:

- Data Processing Software ("Dapper") Evaluation
  This is an extension of the activities of the "Small User Group" which will give advice on questions of software revision and maintenance.

- Radiometry
  The proper processing of data from single- and multi-frequency radiometers to provide bias removal for the beacon data and questions of set-up, calibration and operation of the radiometers are being treated.

- Attenuation
  All aspects of the analysis of attenuation data such as annual and worst month cumulative statistics, diurnal distribution, fade duration, fade slope, scintillations, site diversity, frequency scaling are being investigated. An area of special interest for 20/30 GHz systems is the cloud attenuation.

- XPD
  Rain- and ice-induced crosspolarization effects are analyzed as functions of attenuation and rainrate. Also the dynamic behaviour of the XPD is of interest.

- Polarimetric 20 GHz measurements
  A special feature of the Olympus 19.8 GHz beacon is the continuous switching of the polarization plane. This allows to make co-and crosspolar measurements in two orthogonal planes to investigate the anisotropy of the propagation medium. The working group will focus on the analysis of these data.

- Radar measurements
  Some Experimenters have access to specialized meteorological radars in the vicinity of the Olympus receiver station. In particular, radars with dual polarization which are capable of scanning the beacon receiver's antenna beam can provide special insights into the fine scale characteristics of precipitation. Rain can be clearly distinguished from ice and the drop size distribution can be established. The Radar-Opex ("ROPEX") working group will co-ordinate the observation and analysis procedures.

In addition to the above mentioned working groups a steering group has been set up which will deal with the overall co-ordination, with the organization of meetings and with the setting up of agreements for use of software and exchange of data.

5. Software

The standardized data-preprocessing software has been completed in its pre-release version for 80386 machines. Distribution to a limited number of experimenters who have volunteered to beta-test the package will follow. The analysis part of the software is also coming along well. The development fell behind schedule when the XENIX development system did not appear on the market and a decision had to be made to switch to UNIX instead. As a result of this the minimum requirements for the computer hardware have increased. A hard-disk of 150 Mbyte capacity and 8 Mbyte of RAM are now required.

The single parameter standard analysis results are listed in Table 3 and the Joint statistics are listed in Table 4. User defined channels can also be analyzed and class sizes can be altered for special purposes.

6. Plans for the coming year

When the 80386-users will have received the software, the porting to other target machines will start. On 15 October 90 the next OPEX meeting will be held which will present the first outputs from the new working groups. For April 1991 a workshop is scheduled at ESTEC to compare the results from the first year's data.

PARAMETER \ Beacon:	**B0**	**B1**	**B2**
Frequency [GHz]	12.501866	19.770393	29.655589
Frequency offset [kHz] over 24 hours	-1.77	-2.80	-4.20
Freq. variation [kHz] over 24 hours	0.31	0.49	0.74
EIRP [dBW]	13.1	31.7	27.7
EIRP Variations [dB] peak-to-peak over 24 h	0.25	0.4	0.86
XPI [dB]	35	>43	-
Polarisation (X or Y)	Y	X/Y	Y
Pol. sw. frequency [Hz]	-	933.000525	-
Redundancy	Full	No	No

Table 1: Results of OLYMPUS propagation package in-orbit test.

LOCATION		LAT	LON	ALT	EL
City	Country	[deg] N	[deg] E	[m]	[deg]
Blacksburg, VA	USA	37.220	-80.450	300	13.4
Ottawa	CAN	45.000	-76.000	50	13.5
Coventry	UK	52.417	-1.517	100	27.8
Chilton	UK	51.567	-1.283	100	28.6
Martlesham	UK	52.060	1.286	25	27.5
Gometz La Ville	F	48.671	2.121	168	30.3
La Folie Bessin	F	48.653	2.196	160	30.3
Delft	NL	52.000	4.372	60	26.6
Leidschendam	NL	52.092	4.389	8	26.6
Louvain	B	50.667	4.617	160	27.6
Lessive	B	50.130	5.150	162	27.9
Eindhoven	NL	51.448	5.487	30	26.8
Torino	I	45.067	7.667	238	32.0
Darmstadt	D	49.869	8.625	180	26.9
Milano	I	45.413	9.495	84	30.4
Kjeller	N	59.983	11.033	20	17.4
Oberpfaffenhofen	D	48.050	11.160	580	26.9
Munich	D	48.189	11.629	514	26.6
Albertslund	DK	55.680	12.360	30	20.6
Rome	I	41.830	12.470	50	32.0
Graz	A	47.068	15.495	489	25.7
Metsahovi	SF	60.218	24.394	300	12.3

Table 2: List of OPEX Propagation experiments reported active or near completion in March 1990. Listing sorted by longitude.

Parameter	Class size
Co-polar Att 12 GHz (CPA)	0.2 dB
Copolar Att.20 and 30 GHz (CPA)	0.5 dB
Ratio CPA 30/12 GHz (RCPA)	.2
Ratio CPA 30/20 GHz and 20v/12 GHz	.1
Radiometer Att. 12 GHz (CPARM)	0.2 dB
Radiometer Att. 20 and 30 GHz	0.3 dB
CPA hor-vert 20 GHz	0.1 dB
XPD 12, 20v, 20h, 30 GHz	1 dB
Fade Duration 12, 20 & 30 GHz (τ)	1 or $32*2^n$s
CPA-Rate of Change (S), 12,20&30 GHz	0.05 dB/s
Std Dev of log Ampl.scint. (σx)	0.1 dB
Real & Imag Part of anisotropy	3 deg
Canting angle	1 deg
Circ Pol copol unbalance	0.1 dB
Copolar phase (CPH) at 12,20 &30 GHz	1 deg
Crosspolar phase (XPH) 12,20 &30 GHz	1 deg
Std Dev cop. phase (σph) 12,20&30GHz	1 deg
Rain rate (R)	2 mm/h
Water vapour density (ρ_w)	0.58g/m^3
Ground temperature (Tgnd)	1 K
Pressure (P)	1 mBar
Wind Velocity (Vw)	0.5 m/s
Transversal Wind speed (Vwt)	0.5 m/s
Wind direction (Dw)	1 deg
Cloud-cover (CC)	octals
Radar Reflectivity (Z)	1 dB
Diff Reflectivity (ZDR)	0.1 dBz
Bit error rate (BER)	

Table 3: Cumulative distributions produced by DAPPER.

Parameter Y / Parameter X	Class sizes
CPA vs CPA (30/12,30/20,20/12 GHz)	0.2 /0.2 dB
RCPA (20/12) / CPA(12)	0.2 /0.5 dB
RCPA(30/20)/CPA20;RCPA(20,12)/CPA12	0.1 /0.5 dB
CPA / CPARM at 12,20 & 30 GHz	0.5 /0.5 dB
CPA / Z	1.0 /1.0 dB
CPA / τ at 12, 20 & 30 GHz	0.5 dB/1s
CPA / S at 12, 20 & 30 GHz	.5dB/.05dB/s
CPA / XPD at 12, 20 & 30 GHz	0.5 /1.0 dB
XPD / XPH at 12, 20 & 30 GHz *	2 dB/ 3 deg
CPAh-CPAv/CPHv-CPHh (20 GHz) *	.1dB/ 3 deg
XPD / CPAh-CPAv (20 GHz)	3 dB /.1 dB
XPH / CPAh-CPAv (20 GHz)	3 dB /.1 dB
XPD / XPD (30/20,30/12,20/12 GHz) *	2.0/ 2.0 dB
σ_x^2 / ρ_w	.01dB^2/.5g/m^3
σ_x^2 / Tgnd	.01dB^2 / 1K
CPHv-CPHh / XPH (20 GHz) *	3.0/3.0 deg
Z / ZDR	1 dB/.2 dBz
BER / CPA	
BER / XPD	
BER / σ_x^2	

Table 4: Joint Statistics provided for by the DAPPER software. For the entries marked with "*" multiple curves are being produced with CPA as parameter in 2 dB steps.

OLYMPUS PROPAGATION STUDIES IN THE U.S. - Propagation Terminal Hardware and Experiments

Warren L. Stutzman
for the
Satellite Communications Group
Bradley Department of Electrical Engineering
Virginia Tech
Blacksburg, VA 24061-0111

Abstract - Virginia Tech is performing a comprehensive set of propagation measurements using the OLYMPUS satellite beacons at 12.5, 20, and 30 GHz. These data will be used to characterize propagation conditions on VSAT - type networks for next generation small aperture Ka-band systems.

1. Introduction

The European Space Agency (ESA) satellite OLYMPUS was launched July 12, 1989. The spacecraft contains a sophisticated package of propagation beacons operating at 12.5, 19.77, and 29.66 GHz (referred to as 12.5, 20, and 30 beacons). These beacons cover the east coast of the United States with sufficient power for attenuation measurements. The Virginia Satellite Communications Group is completing the hardware construction phase and will begin formal data collection in June.

As satellite communication systems move toward the 20/30 GHz frequency range for wider bandwidth and reduced interference, the role of small earth terminals (VSATs) becomes increasingly important. Previous satellite communications systems used large earth terminals with wide fade margins to achieve high reliability. Past propagation experiments were aimed at accumulating data for these wide margin systems. VSATs, however, with their modest propagation reliability requirements coupled with fade compensation techniques and low margins have now become practical. Propagation research must now shift to the measurement and modelling of low margin systems. This requires accurate measurement of fade statistics and fade dynamics for low to moderate fading, 3 to 5 dB. Fade dynamics are also important to the design of compensation schemes. The objective of our experiment is to investigate propagation effects on future Ku- and Ka-band communications systems. The Advanced Communications Technology Satellite (ACTS), scheduled for launch in 1992, will provide another opportunity for Ka-band propagation studies throughout North America.

The experiment program at Virginia Tech offers some unique opportunities. The collection of simultaneous data at three frequencies spanning the 12 to 30 GHz region is extremely useful in frequency scaling studies. This is possible because all links have the same path (14° elevation, 108° azimuth). The 14° elevation angle is relatively low and data in this region is also very useful in its own right because this is at the lower limit for CONUS coverage with domestic satellites. Our experiment was designed to record low-fade events accurately. This is valuable in amassing a data base for low margin operational satellite links such as VSAT systems. Another feature of our OLYMPUS program is that it provides a test bed for ACTS due to the similarity of frequencies (ACTS beacons are at 20.2 and 27.5 GHz). In particular, we have designed and built a beacon receiver for OLYMPUS which can be used for ACTS.

2. The Measurement System

The propagation experiment system at Virginia Tech will continuously measure the 12.5, 20, and 30 GHz OLYMPUS beacons for one year. The east coast of the United States is far off boresight of the OLYMPUS 20 and 30 GHz antennas; however, there is sufficient EIRP from the beacons in our direction for good propagation measurements using moderate sized antennas. Cross-polarization measurements are not possible as the satellite antennas have low XPD well away from boresight.

Four separate receiving systems are used; one each for 12.5, 20, and 30 GHz, as well as a 20 GHz diversity terminal. The receiving antennas are 12, 5, and 4 feet in diameter at 12.5, 20 and 30 GHz, respectively. Thus, the 20/30 GHz portions of the experiment employ VSAT class terminals. The second 20 GHz terminal will be used to determine the advantages of small scale site diversity reception using VSAT terminals.

A unique feature of the OLYMPUS beacon package is that the three spacecraft beacons are coherent since they are derived from a common oscillator. The Virginia Tech OLYMPUS receivers take advantage of their coherence by deriving frequency locking information from the 12.5 receiver. This information is used to maintain lock for all four receivers. In effect, this widens the dynamic range of the 20 and 30 GHz receivers, which experience more fading during a rain event than does the 12.5 GHz receiver.

The receivers at all three frequencies are very similar. Each receiver has a low noise amplifier followed by a mixer-preamp whose output IF frequency is 1120 MHz. A motorized attenuator is included in the RF section to aid in system calibration. The 1120 MHz IF is subsequently mixed down to produce lower IF frequencies of 70 MHz and 10 kHz. The 10 kHz signal is then used in detection and tracking.

A hybrid analog/digital receiver is used in our detection scheme for the 12.5 GHz system. The analog portion of the receiver tracks the carrier frequency and maintains the signal within a 3 Hz window. Simultaneously, the 10 kHz carrier is sampled at a 40 kHz rate by a 12 bit A/D converter. Each sample is then filtered by a digital FIR filter and the resulting 16 bit I and Q values are recorded by the data acquisition system.

Clouds and scintillation can produce up to 3 dB of attenuation at 30 GHz on a 14° elevation-angle path and may be present for a large percentage of the time. Therefore, it is important in a slant-path propagation experiment to be able to set the clear air reference level accurately. Radiometers operate at each beacon frequency in our receiving system to aid in setting this clear air reference level. The radiometers are of the total power design; the RF and IF sections are housed in a temperature controlled environment to keep gain constant. The radiometer design is unique in that it uses the same RF chain as the beacon receiver.

The output of the receivers and radiometers are continuously monitored by the data acquisition system (DAS), which is discussed in a companion paper.

3. The Experiment Program

The objectives of the experiment are summarized in Table 2. Attenuation data will be collected from the 12.5, 20 and 30 GHz OLYMPUS beacons for a one year period. Radiometric data will be collected to assist in setting reference levels to improve low level attenuation measurement accuracies. However, such data may be useful in its own right.

To examine small-scale diversity, we will operate a second 20 GHz receiver which will be located near the main 20 GHz terminal. Although widely spaced diversity terminals have been studied for deep fades, short baseline diversity for low/moderate fading has not. Attenuation data at the diversity station will be compared to that of the main terminal during the same sub-year time interval. Diversity gain will be examined for each station as a function of baseline distance.

For the fade slope portion of the experiment, statistics on the rate at which individual fades begin and end (in dB per second) will be accumulated and correlated with the physics of propagation. Fade slope data are useful in studies of various modulation schemes for Ka-band VSAT systems.

Attenuation data at 30 GHz will be used to test various algorithms to predict how fading can be relieved using uplink power control.

4. Receiver Development

The 12.5 GHz signal suffers much less fading than the 30 GHz signal. Attenuation in rain increases approximately as the square of the frequency, so a 10 dB fade at 12.5 GHz is accompanied by a 57 dB fade at 30 GHz and a 25 dB fade at 20 GHz. Locking the receiver to the 12.5 GHz signal means that it will stay in lock when the higher frequencies are below the minimum measurement level of the receiver, and there will be no hysteresis effect when the fade ends and the signal levels rise to the point where measurements can continue. The dynamic range of our 12.5 GHz receiver is 30 dB. We might expect to experience one event a year in which attenuation exceeds 30 dB at 12.5 GHz on our 14° slant path from OLYMPUS. A fade of this severity will cause loss of lock in the receiver, but we expect the outage to be very brief.

The heart of our receiver is a frequency lock loop (FLL) operating at a 10 kHz IF frequency with a bandwidth of less than 20 Hz. We are using a FLL in preference to a phase lock loop (PLL) for two reasons. We can achieve a narrower locking bandwidth with the FLL, and hysteresis effects when the FLL loses lock and must reacquire on a weak signal are less severe than with the PLL. Our FLL locks the three beacon signals into a 3 Hz bandwidth, providing a dynamic measurement range in excess of 40 dB in the 20 and 30 GHz receiver channels. The 12.5 GHz receiver has been bench tested giving over 30 dB dynamic range. It also has been tested with the spacecraft beacon for several weeks demonstrating excellent performance in clear air and in fading.

5. Initial Results

An intense rain cell moved across the Virginia Tech Tracking Station on April 21. At the time we were monitoring the 12.5 GHz beacon signal for stability by strip chart recording. The results of the beacon fade are shown in Fig. 1. A large fade of over 20 dB occurred first, followed by a second fade of a few dB; the system was not calibrated for use with a strip chart recorder. During the second fade 12.5 GHz radiometer data were recorded by hand and later plotted as shown in Fig. 2. The agreement to the beacon signal is very good, indicating the value of the radiometer for low fades.

Table 1

Characteristics of OLYMPUS Receivers at Virginia Tech

Terminal	12	20 & 20D	30
Frequency (GHz)	12.5	19.77	29.65
Polarization	V	Switched V,H	V
Switching loss (dB)	-	4	-
EIRP toward Blacksburg (dBW)	9.1	19.7	19.7
Antenna Size (m)	4.0	1.5	1.2
Power available from antenna (dBW)	-147.0	-145.0	-146.8
C/N in 3 Hz BW (dB)	49.9	48.5	45.3

Table 2

Objectives of the Virginia Tech OLYMPUS Experiment

Attenuation Measurements:

- Fade statistics
- Frequency scaling of attenuation
- Fade duration
- Fade interval
- Fade slope

Radiometric Measurements

Small Scale Diversity

Uplink Power Control

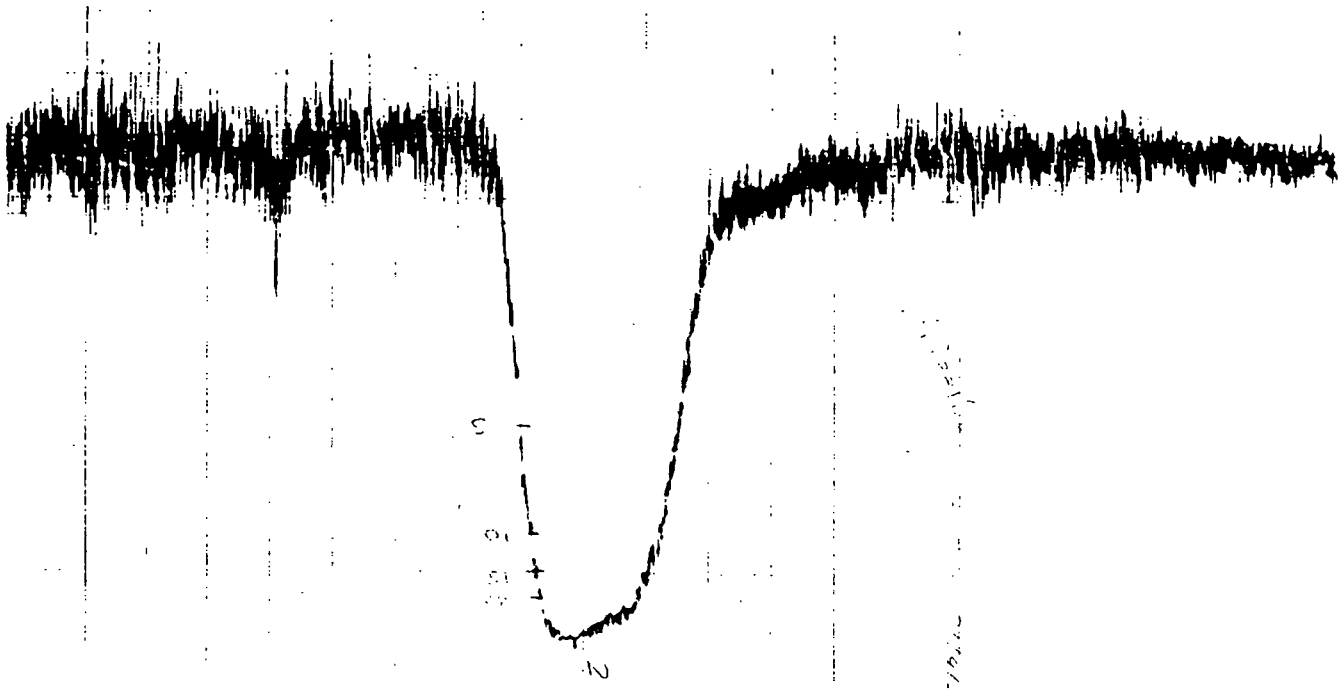

a) A fade of more than 20 dB.

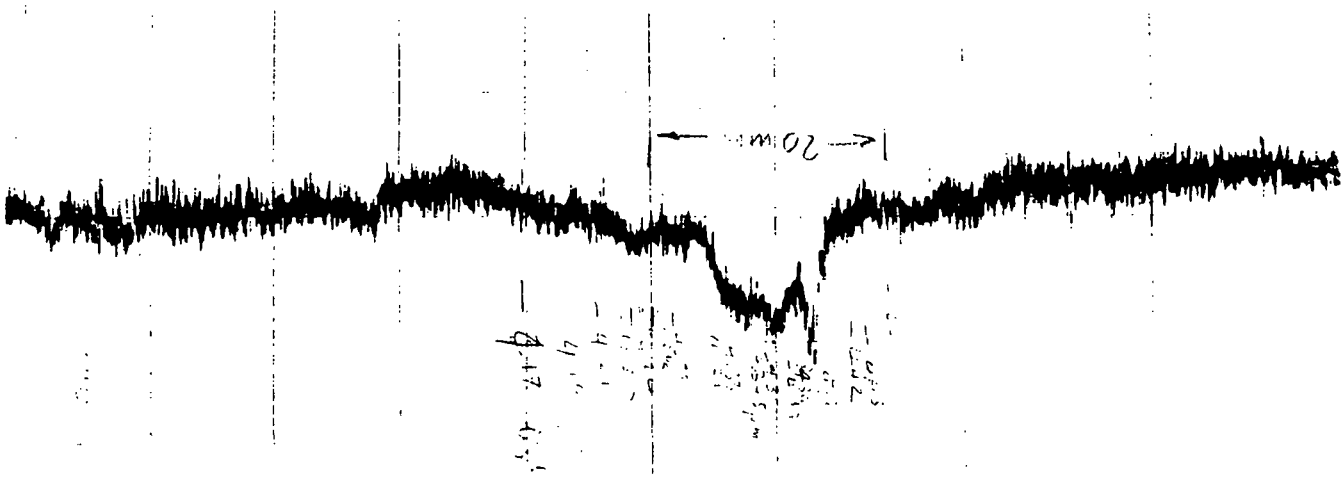

b) A subsequent fade of a few dB.

Figure 1. Beacon fades at 12.5 GHz for a rain event of April 21, 1990.

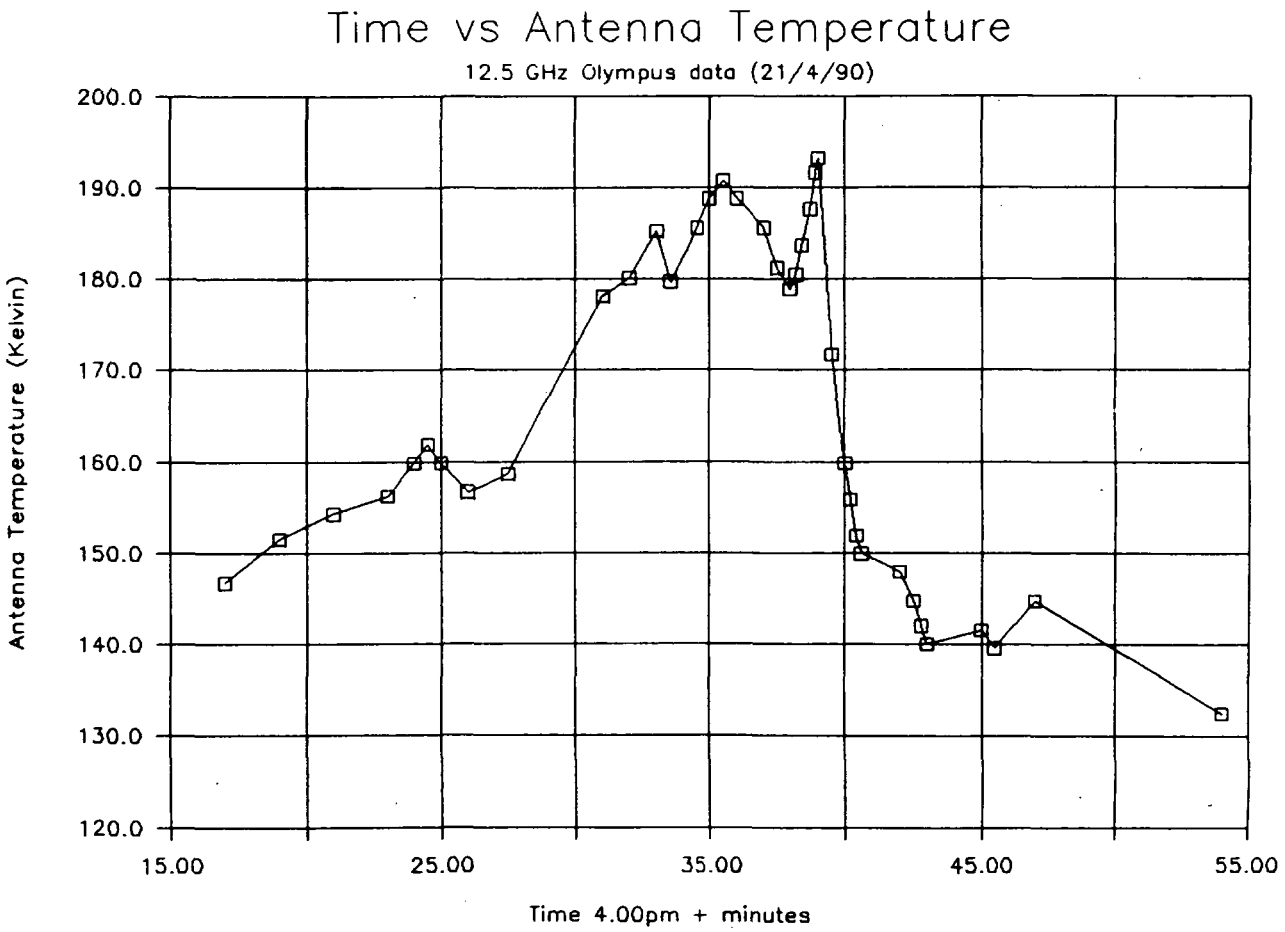

Figure 2. Radiometric temperature time history for the second event of Fig. 1.

N91-11959

OLYMPUS PROPAGATION STUDIES IN THE U.S. Receiver Development and the Data Acquisition System

John C. McKeeman
for the
Satellite Communications Group
Bradley Department of Electrical Engineering
Virginia Tech
Blacksburg, VA 24061-0111

Abstract - Virginia Tech has developed two types of receivers to monitor the OLYMPUS beacons, as well as a custom data acquisition system to store and display propagation data. Each of the receiver designs uses new hybrid analog/digital techniques. The data acquisition system uses a stand alone processor to collect and format the data for display and subsequent processing.

1. Introduction

The launch of the OLYMPUS satellite with its coherent beacons offers new opportunities to study propagation effects at 12.5, 20 and 30 GHz. At Virginia Tech, the satellite is at 14 degrees in elevation, which allows us to measure low elevation angle effects. However, to make these measurements, a very accurate and stable measurement system is required.

Virginia Tech has constructed a complex receiving system which monitors the OLYMPUS beacons and all parameters associated with propagation research. In our current configuration, we have developed a receiver which frequency locks to the less fade susceptible 12.5 GHz beacon. Since all beacons on the satellite are driven from a single master oscillator, drift in the 12.5 GHz beacon implies corresponding drifts in the 20 and 30 GHz beacons. The receivers for our 20 and 30 GHz systems derive their frequency locking information from the 12.5 GHz system. This widens the dynamic range of the receivers and allows our receivers to maintain lock in severe fade conditions.

In addition to monitoring the beacons, we also monitor the sky noise with radiometers at each frequency. The radiometer output is used to set the clear air level for each beacon measurement. We also measure the rain rate with several tipping bucket rain gauges placed along the propagation path. In the future, we hope to provide radar coverage of rain events. System temperature is continuously monitored at 22 points in the receiving system in an effort to obtain precise calibration of the receivers. Lastly,

wind speed and direction are monitored by the data acquisition system to keep a log of meteorological data.

In this paper, the details of the two receiver prototypes are first presented. An overview of the data acquisition system is then presented.

2. Receiver Development

Virginia Tech, with help from JPL personnel, has developed two receiving systems for use with OLYMPUS. Both systems input an IF of 70 MHz. The first system downconverts the IF to 10 kHz and then digitizes the signal to obtain the I and Q outputs. The second system downconverts the 70 MHz to 10 MHz, digitizes the 10 MHz IF, and then uses Fast Fourier Transform (FFT) techniques to obtain the I and Q outputs.

2.1 Hybrid Analog/Digital Receiver

Our 12.5 GHz receiving system is shown in Figure 1. The incoming microwave beacon signal is first converted to 1120 MHz and then to 70 MHz. Our microwave LO is controlled by the Frequency Locked Loop (FLL). The 70 MHz signal is then converted to 10 kHz. To reduce the possibility of false lock, the 69.98 MHz image is suppressed in an image cancelling mixer. The 10 kHz signal is passed through a limiter which removes amplitude variations to prevent the loop gain from varying with signal level. The output of the limiter is bandpass filtered and then input to the frequency detector. The loop dynamics are set by the loop filter that follows the frequency detector.

The frequency detector mixes the incoming 10 kHz IF signal with quadrature 10 kHz reference signals. The mixing products are low pass filtered and the result is the quadrature of the frequency difference between the reference and the IF signal. These quadratures are delayed in an R-C network and then cross multiplied. The filtered output is then used to control the VCXO so that the IF output to the A/D converter is always 10 kHz.

IQ detection is accomplished by multiplying the signal with quadratures of its carrier frequency using a sampling process. The I and Q samples are separated by demultiplexing and low pass filtering to produce the detected output.

As shown in Figure 1, our IQ detection system consists of a 12 bit analog to digital convertor (ADC), a programmable timer, an 80286 microprocessor, memory and a clock generation circuit. A 200 Hz wide, 10 kHz filter is placed before the A/D to ensure that the IF signal is sufficiently bandlimited. The ADC converts the input signal to a digital form and the microprocessor performs a digital low pass filter on the data. After performing the filtering operation, the microprocessor outputs the measured I and Q values

to a data acquisition and display system. Coordination of the sampling and filtering as well as handshaking to the data acquisition system is accomplished by the microprocessor.

The low pass filter used is a finite impulse response (FIR) filter which implements a Kaiser window 1116 points long. The Kaiser window forms a digital 3 Hz low pass filter to ensure that the detected signal is sufficiently bandlimited for the desired 10 Hz output rate. Although the detector was programmed to produce output at 10 Hz, the hardware design is flexible enough to implement other algorithms at varying sampling rates.

The software of the digital detector implements two low pass digital filters on the incoming IF data, one each for I and Q. The use of integer mathematics allows the system to operate without the complexity and cost of a math co-processor chip.

During normal operation, the hardware continuously collects I and Q data from the ADC and stores them in two buffers. These buffers are somewhat larger than the size of a complete filter set to allow samples to be collected while the processor concurrently performs a filter calculation.

2.2 Digital Receiver

Our digital receiver design is shown in Figure 2. In our design, the 10 MHz IF is sampled at 8 MHz to yield the I, Q, -I, -Q sample stream. The resulting samples are then decimated and sign corrected to yield a complex sample stream of 500 kHz. These data are stored in a dual ported random access memory (RAM) as the real and imaginary inputs for a complex FFT.

Once 1024 samples have been received, the DSP processor (TRW TMC 2310) retrieves the samples and applies a Hamming window to the data. These data are then input to a 1024 point complex FFT and the results are stored in the dual ported RAM. The DSP, which is controlled by an INTEL EPLD, then computes the power in each frequency bin by summing the squares of the real and imaginary components. At this point, the frequency "resolution" of each bin is 500 kHz/1024 = 488 Hz.

As the power associated with each bin is computed, (i.e. $I^2 + Q^2$) a simple comparator circuit compares the power of each bin until the bin with the greatest power is located. This bin is assumed to contain the carrier signal.

The contents of the single FFT bin corresponding to the bin with the largest energy is then stored in a second bank of dual ported RAM. Thus, one pair of IQ samples which correspond to the carrier power is stored for each of the first stage FFTs. When 1024 of these samples accumulate, a second FFT is performed. In a manner similar to the first FFT, a Hamming window is applied to the data and these data are again input to a 1024 pt FFT. The output of

this FFT is then stored in the second set of dual ported RAMs. At this point, the frequency "resolution" per bin is 488 Hz/1024 or 0.477 Hz.

After the second FFT is performed, the frequency components are squared and summed to determine the magnitude (squared) in each bin. The bins are then sorted to find the bin with the largest power. The I and Q components of that bin form the I and Q outputs for the beacon. The frequency of the carrier is then computed using an Intel 8085 processor and displayed along with the power on an LCD display.

The frequency information from the second FFT output is used to adjust the 48.45 MHz VCXO. This keeps the beacon signal within the bandwidth of one 488 Hz wide bin from the first FFT. Although the output of the second FFT is updated at approximately 500 Hz, the VCXO is only corrected at a 0.1 Hz rate to avoid instability. A flowchart of the FFT processing is shown in Figure 3. Figure 4 shows a block diagram of the FFT processing hardware.

The current version of the digital receiver is undergoing test and we expect to have a production version operational by 15 June 1990.

3. Data Acquisition System

The major components of the data acquisition system (DAS) are shown in Figure 5. The DAS is comprised of two units: the control rack and the personal computer.

The control rack is a standard 19" chassis unit whose function is to collect all data, format the data and transmit the data to the personal computer. In its minimum configuration, it is comprised of an electrical backplane, a power supply, a central processing card, 2 IQ detection cards, a radiometer card, a digital input card and one temperature card. The control rack is built around a standard (STD) bus electrical backplane.

Using a standard backplane allows the experimenter to easily modify the collection system by adding or removing boards as needed. The control card, which contains a stand alone 80286 system, was designed to sample the IQ outputs of the IQ card, the radiometer card outputs, the digital input card and the temperature outputs. The sampling rate is variable, however, we will be sampling at 10 Hz.

The IQ detection card performs the IF sampling and low pass filtering for two receivers. In our configuration, the 12.5 and 20 GHz IF signals are input to one IQ detection card, the 30 GHz and 20 GHz diversity IF signals are input to another. To keep the IQ detection synchronized, one common 40 kHz clock source is used for all IQ sampling cards as well as to set the system-wide 10 Hz sampling interval.

The radiometer card receives one output from each of the four radiometers. This output is a square wave whose frequency corresponds to the noise power in each radiometer band. The radiometer card converts these signals to digital noise values and provides them to the central processing card when polled every second.

The temperature card receives separate analog signals which represent the temperature at 22 locations in the experiment system. One temperature value is sampled in sequence at each 0.1 second interval.

4. Acknowledgements

The authors acknowledge the support of the Jet Propulsion Laboratory, and the technical assistance of Dr. Faramaz Davarian, Dr. Timothy Pratt, P. Willmann Remaklus, D.G. Sweeney and Frank Pergal. Further, we gratefully acknowledge the assistance of A.M. Kim and C.P. Marshall in typing this manuscript.

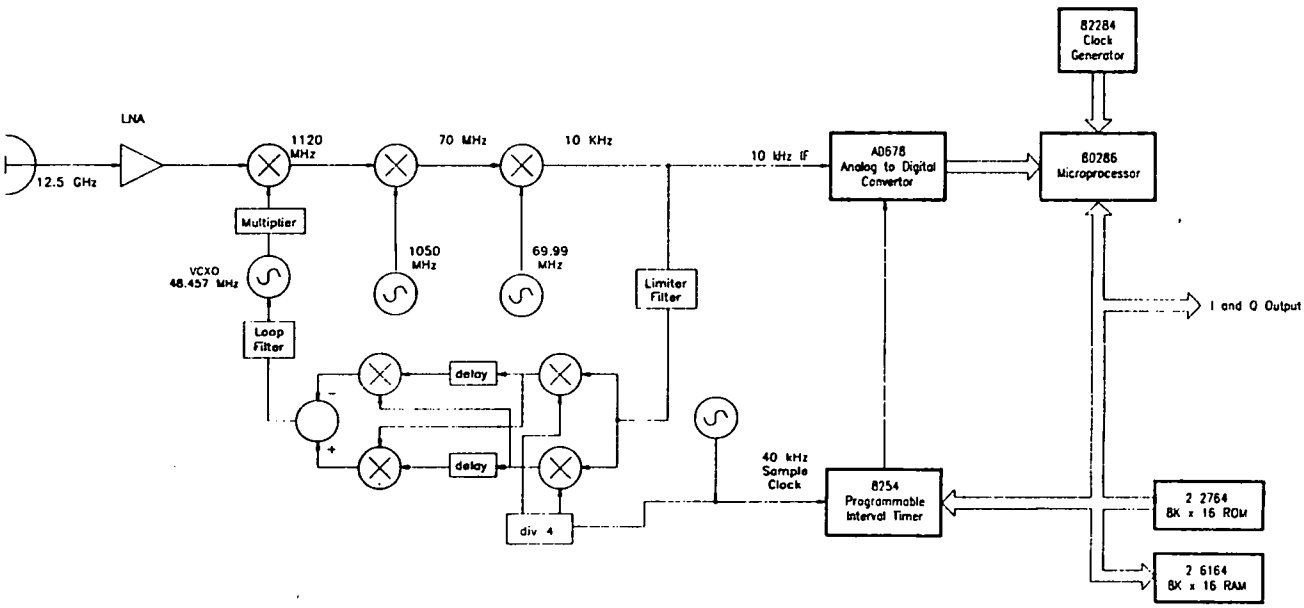

Figure 1. Block diagram of the hybrid analog/digital receiver

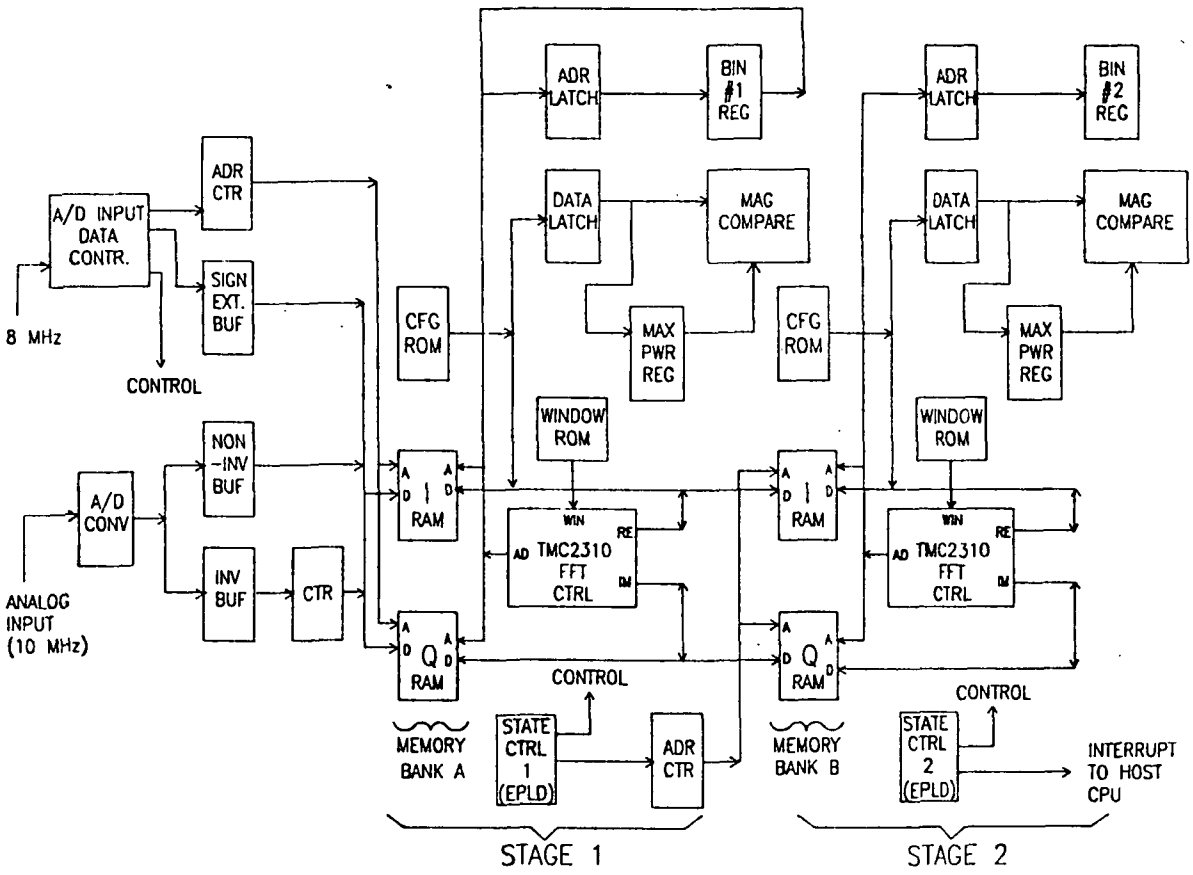

Figure 2. Block diagram of the digital receiver

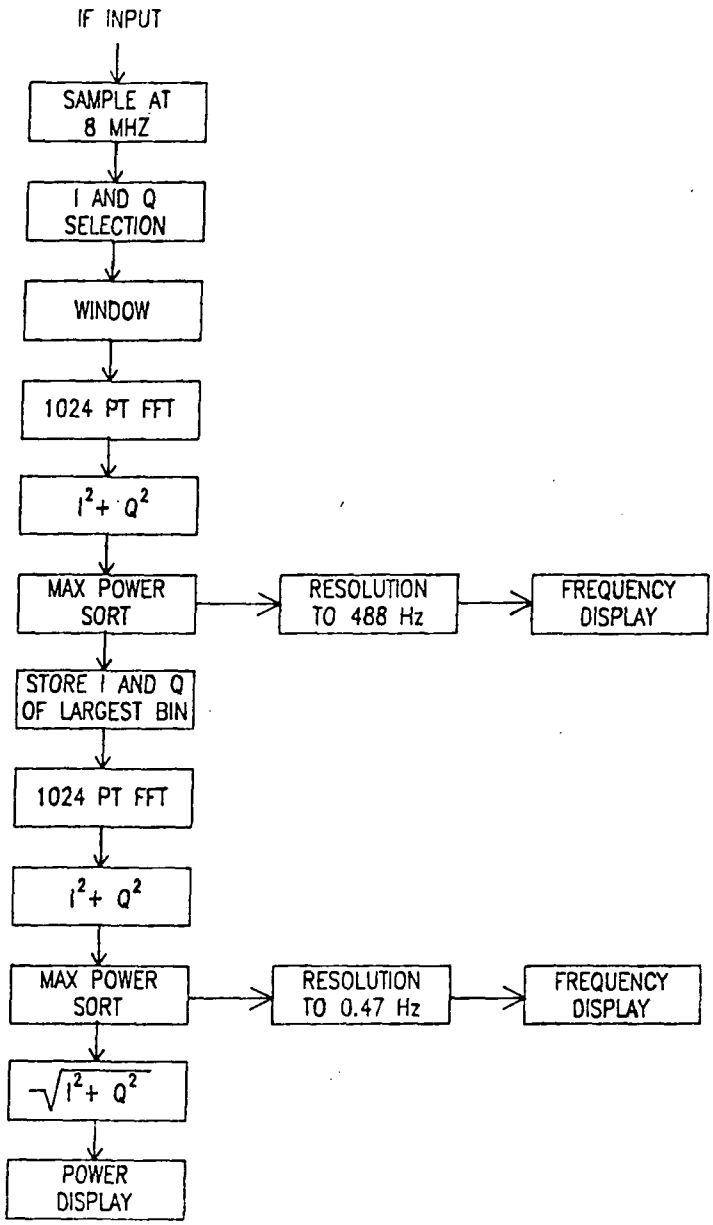

Figure 3. Flowchart of FFT processing

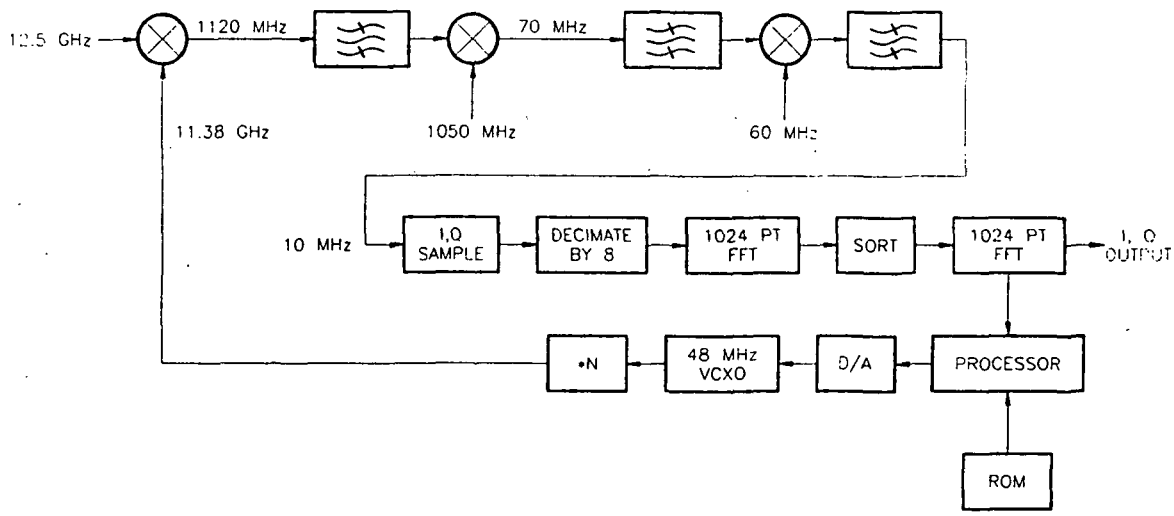

Figure 4. Hardware block diagram

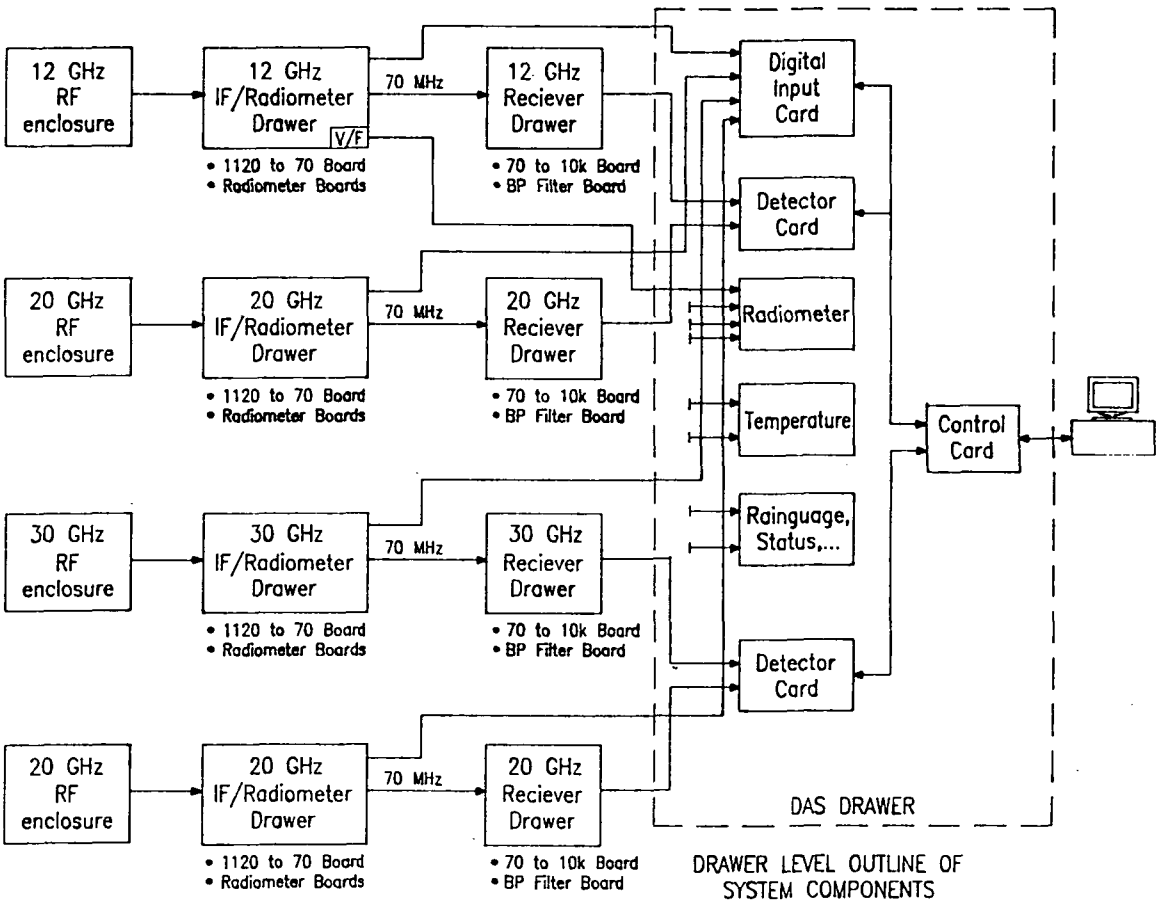

Figure 5. Overview of Data Acquisition System

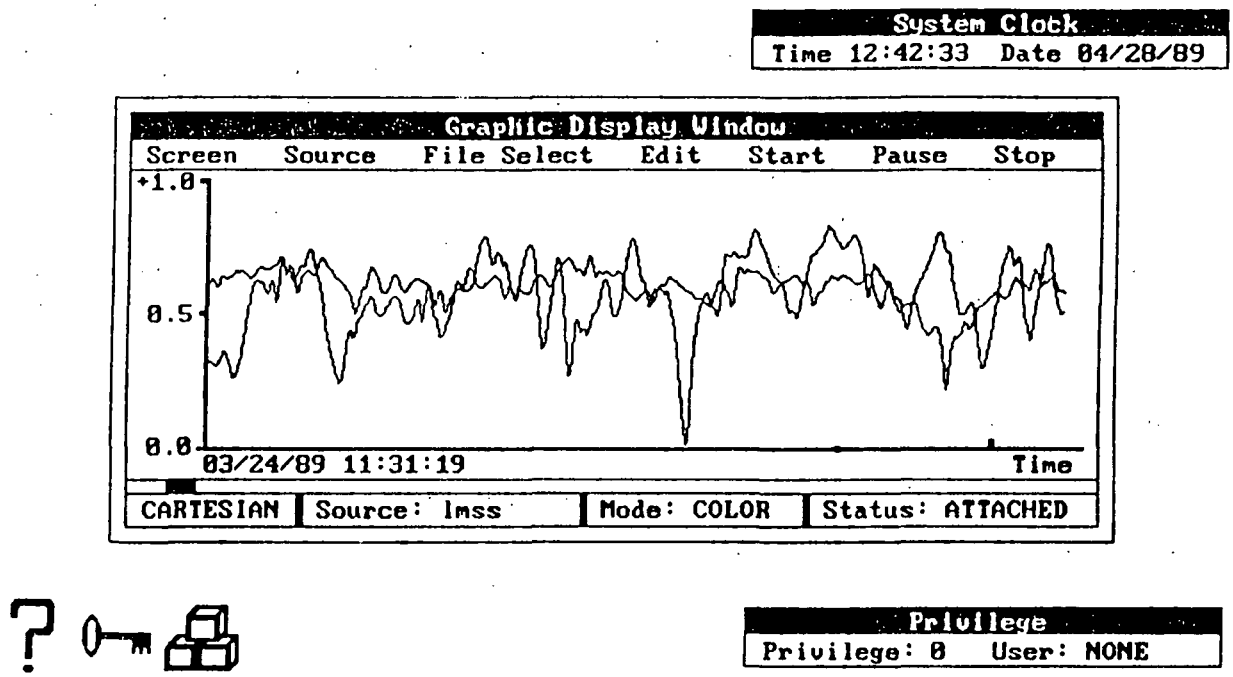

Figure 6. DAS Software Display

OLYMPUS RECEIVER EVALUATION AND PHASE NOISE MEASUREMENTS

Richard L. Campbell and Huailiang Wang
Sensing and Signal Processing Laboratory
Department of Electrical Engineering
Michigan Technological University
Houghton, MI 49931

Dennis Sweeney
Satellite Communications Group
Department of Electrical Engineering
VPI and State University
Blacksburg, VA 24061

This paper describes a set of measurements performed by the Michigan Tech Sensing and Signal Processing Group on the analog receiver built by VPI and JPL for propagation measurements using the Olympus Satellite. Measurements of local oscillator (LO) phase noise were performed for all of the LOs supplied by JPL. In order to obtain the most useful set of measurements, LO phase noise measurements were made using the complete VPI receiver front end. This set of measurements demonstrates the performance of the receiver from the RF input through the high IF output. Three different measurements were made: LO phase noise with DC on the VCXO port; LO phase noise with the 11.381 GHz LO locked to the Reference signal generator; and a reference measurement with the JPL LOs out of the system.

INTRODUCTION

The Olympus satellite has three beacon frequencies, all derived from a common high stability oscillator. If an earth station receiver is phase or frequency locked to any one of the beacons, the local oscillator frequencies for the other two beacons may be obtained. In the Virginia Tech Olympus receiver, the 12.5 GHz receiver frequency locks to the Olympus 12.5 GHz beacon. The local oscillator signals for the 20 and 30 GHz beacon receivers are then derived from the locked 12.5 GHz receiver. In this way, the 20 and 30 GHz receivers can remain locked even during deep fades of the 20 and 30 GHz signals. Phase noise on the earth station local oscillators is important for three reasons: the frequency locked loop (FLL) will be unstable if the phase noise is poor; received signals are modulated by the local oscillator phase noise; and the minimum receiver predetection bandwidth and hence sensitivity is limited by the short term fluctuations of the receiver local oscillator.

PREPARATION

The measurements were made at Virginia Tech the week of January 22 to 27, 1990. During the week before the trip, the 1296 IF system, Reference and PCM audio recorder were set up and calibrated at Michigan Tech. The system was then broken down and packed for shipping, along with a set of adapters and cables to connect the Michigan Tech and Virginia Tech systems.

TRAVEL TO VPI

The 1296 IF system, Reference oscillator and other critical components were taken as carry on baggage. The PCM recorder (Toshiba DX 900) was too large to be carried on, so it was packed in its shipping box and checked.

SET UP AT VPI

Tuesday, January 23, the 1296 IF system was connected to the VPI receiver with the assistance of Dennis Sweeney, as shown in Figure 1. The system was allowed to stabilize overnight while Dennis reviewed the current status of the receiver system.

JANUARY 1990 STATUS OF OLYMPUS RECEIVER

As of the end of January 1990, the analog receiver was working in breadboard form. Dennis was still working on minor modifications to the frequency locked loop dynamics before committing the design to a PC board layout. The system was capable of receiving the 12 GHz Olympus beacon signal, but an on-the-air test was not practical due to the high feedline loss between the outdoor antenna and the bench where the breadboard receiver was located. In final form, the receiver front end will be located in an outdoor cabinet near the dish feed.

Dennis demonstrated capture, lock and tracking of a weak CW signal from the HP 8673 signal generator. The system is capable of tracking any changes in beacon frequency over the life of the satellite. Since day to day variations will be much smaller, it is possible to improve loop stability by reducing the range of the tracking loop and providing a front panel manual adjustment with a zero center meter to compensate for long term variations.

PHASE NOISE MEASUREMENTS

Three different types of measurements were made:

1. Measurements of downconverted LO phase noise, using the apparatus shown in Figure 1. These measurements were made on all three analog receiver front ends, using both the primary and spare LOs. The VCXO frequency change terminal was grounded for these measurements. In order to insure that the dynamic range of the measurement system was not exceeded, two measurements were made on each LO: the first measurement was made with the signal level adjusted 10 dB lower than the maximum input to the digital audio recorder; and the second measurement was made with the signal level 20 dB lower than the maximum to the digital audio recorder. Since the dynamic range of the digital record is 86 dB, this provides two records, one with the signal 76 dB above the digital tape recorder noise floor and one with the signal 66 dB above the noise floor. The no signal receiver output was adjusted so that it just indicated on the recorder output. Either of these measurements has sufficient dynamic range to see the close-in phase noise on the LO and verify that it is within specifications at 100 Hz separation.

2. A measurement of the phase noise of the 11.381 GHz LO was made with the LO locked to the HP 8673 signal. This measurement was made with the signal downconverted to 10 kHz using the breadboard VPI receiver system. The downconverted signal was recorded on the right channel of the digital audio recorder, and the 10 kHz reference was recorded on the left channel. This permits not only a phase noise analysis of the locked LO, but a measurement of loop behavior by doing a cross-spectrum between the locked LO and the reference. This measurement also demonstrates direct digital audio recording of the 10 kHz IF signal which can be used to obtain data during propagation events with rapid fluctuations, as in thunderstorms.

3. The third measurement was made to determine the phase noise of the measurement system itself. As shown in Figure 2, the 576 MHz reference from the 1296 MHz IF receiver (derived from a 5 MHz Vectron CO-203 oscillator) is multiplied by 4 in a Campbell multiplier board. The 2304 MHz signal is then multiplied by 5 in a harmonic mixer (Mini-Circuits ZFM-4212) to 11.520 GHz. The HP 8673 is adjusted to 11.6641 GHz. The output of the harmonic mixer is then 144.1 MHz, which is downconverted to 1024 Hz using the low IF receiver as in the first set of measurements.

Table 1 shows the time, frequencies, levels and tape counter indications for all the measurements.

PROCESSING OF PHASE NOISE DATA AT MICHIGAN TECH

The lab was set up to process the recorded IF signal as shown in Figure 3. All of the data at 1024 Hz IF was processed, but the 10 kHz data (measurement "a" in Table 1) has not been processed.

The power spectra for the JPL LOs were obtained by playing the 1024 Hz recorded IF signals as analog audio into the HP 5451C Fourier analyzer. For each spectrum plot, 100 sequential 1024 sample time records were Hanning windowed, Fourier transformed, converted to a power spectrum and averaged to obtain a 500 Hz wide spectrum with 1.5 Hz noise bandwidth and 1 Hz spacing between frequency domain points.

The JPL LO phase noise plots are shown as Figures 5-14. All of these plots have phase noise at the 100 Hz points that are very close to the Olympus LO specification shown schematically in Figure 4. These LOs meet the specifications set at the beginning of the receiver development program. The $\pm$ N x 60 Hz noise sidebands are discussed in the next section.

PHASE NOISE MEASUREMENT SYSTEM CALIBRATION

In order to prove that the phase noise being measured was actually that of the JPL LOs rather than the measurement system, a measurement was made of a very low phase noise microwave LO built by R. Campbell. Unfortunately, the output of the Campbell LO was contaminated by 60 Hz noise on the bench at Virginia Tech. This may have been 60 Hz noise transmitted over the power supply lines

or it may have been magnetically coupled from a nearby power transformer into the ovenized crystal oscillator in the Campbell LO. It would have been easy to remove the 60 Hz noise from the reference LO by running it on a different power supply and moving it away from any nearby magnetic AC devices, but the 60 Hz contamination was not suspected at the time of the measurements.

In any case, Figure 15 demonstrates that the phase noise measurement system used to measure the JPL LOs has a phase noise floor at least 10 dB below the best JPL LO within 50 Hz of the carrier and at least 5 dB better at + 100 Hz from the carrier.

APRIL 1990 STATUS OF THE OLYMPUS RECEIVER AT VIRGINIA TECH

As of April, 1990, the 12.5 GHz beacon receiver and radiometer are on the air at Virginia Tech, as discussed in the companion paper by Warren Stutzman. The signal was first received with a carrier to noise ratio of 30 dB in March 1990. The FLL locks from -115 to -150 dBm. Three additional IF systems are now under construction for the 20 and 30 GHz receivers.

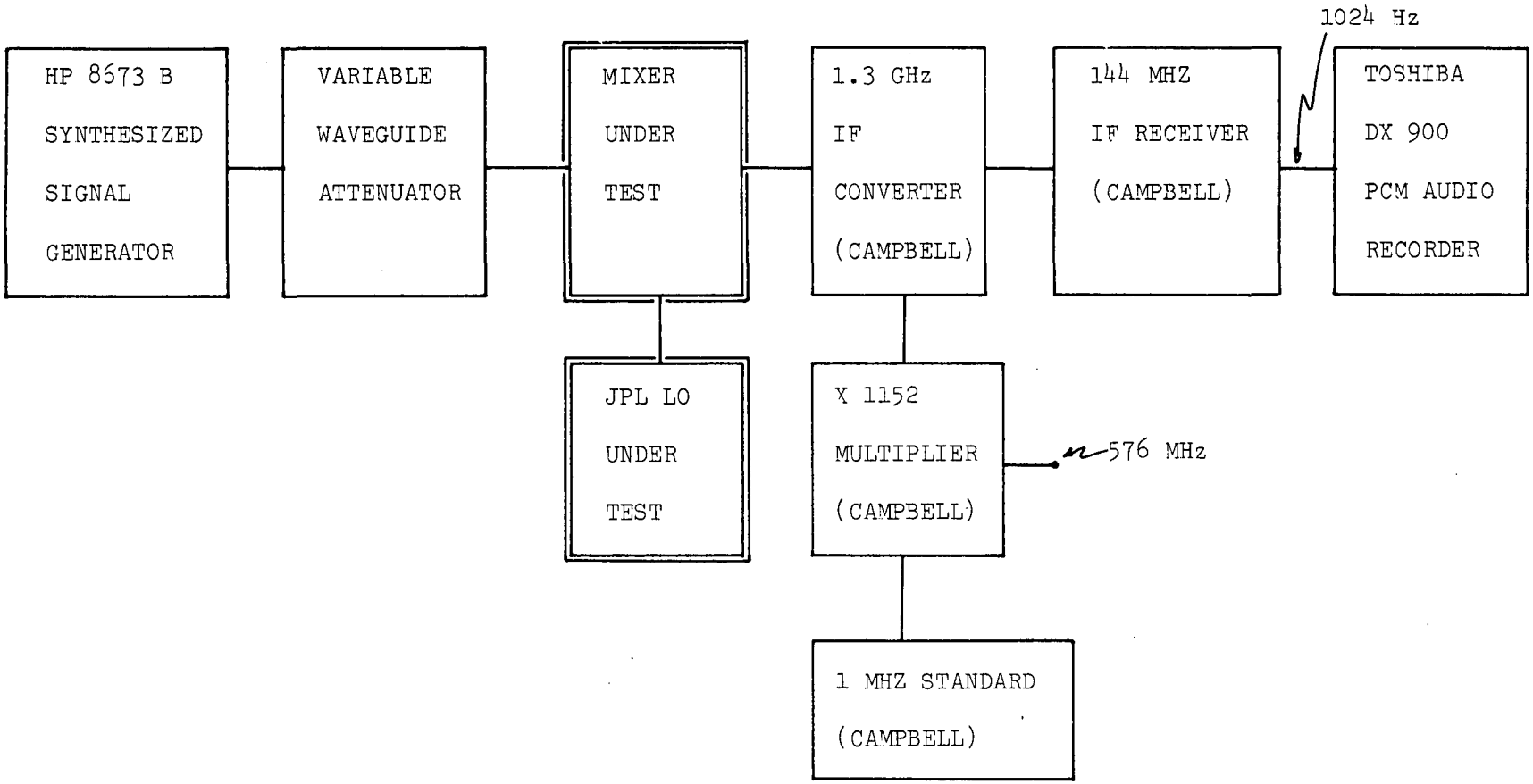

PHASE NOISE TEST

FIGURE 1

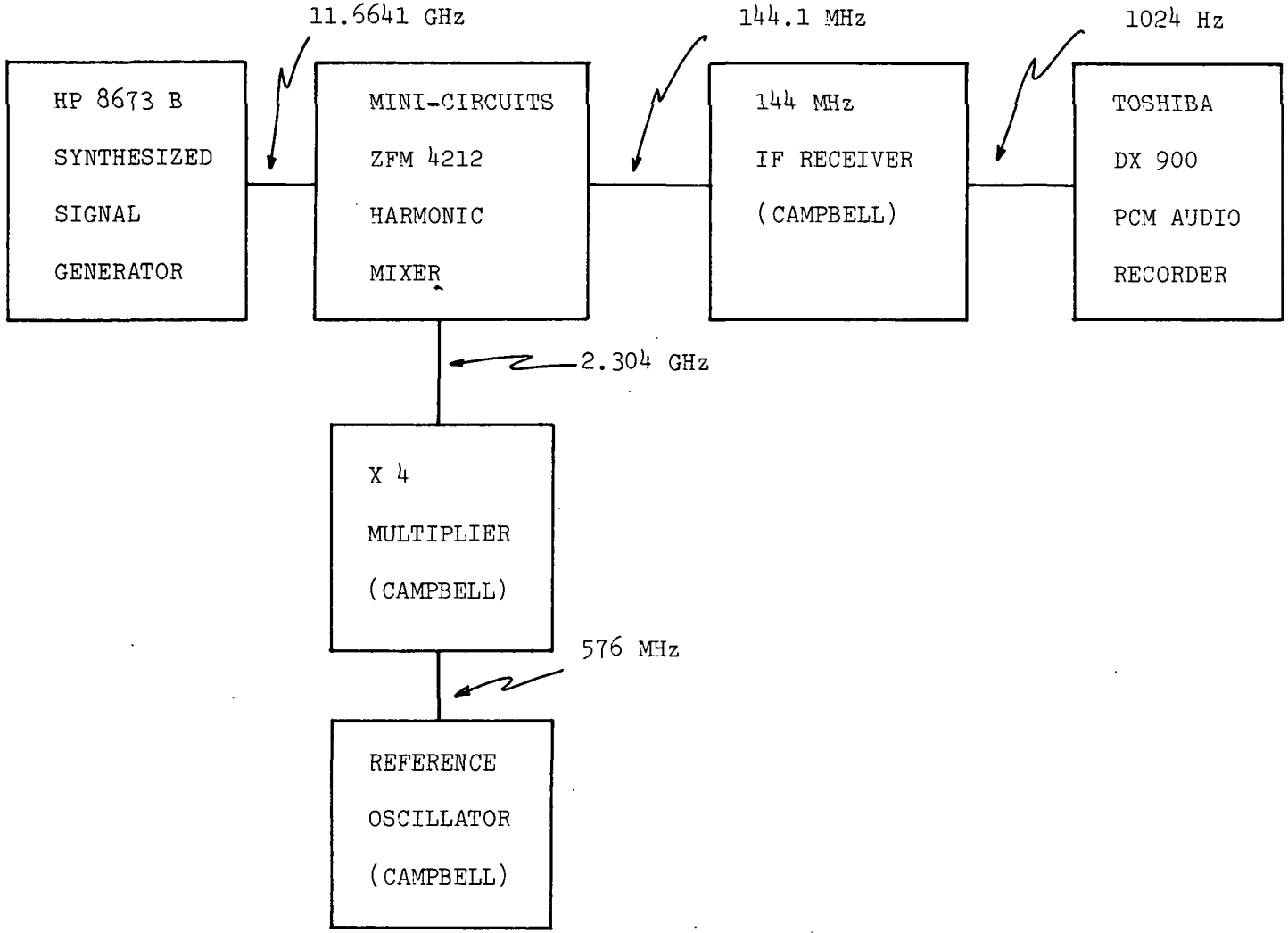

REFERENCE TEST

FIGURE 2

TABLE 1

Run #	LO Freq. and SN	HP 8673 freq. GHz	HP 8673 level dBm	Record level dB	Start time EST	Start count	Stop time EST	Stop Count	Notes
1	--	--	--	--	--	--	--	--	
2	10.3819 SN 35267	12.678006							1
3	same	same	-40	-15	11:21	0615	11:36	1665	2
4	same	same	-30	0	2:51	1670		1713	3
5	same	same	-30	0	2:54	1713	3:04	2290	
6	same	same	-40	-15	3:08	2290	3:16	2714	4
7	10.3819 SN 35268	same	-40	-15	3:20	2716	3:25	2926	
8	same	same	-30	0	3:26	2926		3219	
9	4.4640 RLC LO	5.7601	-80	0	3:42	3219	3:45	3367	5
a	10.3819 SN 35268	12.5019		0	4:03	3365	4:09	3629	6
b	28.535684 SN 35270	29.831784		-10	4:45	3633	5:00	4237	
c	same	same		0	5:02	4240	5:12	4620	
d	18.650456 SN 35273	19.946492	-64	0	9:57	4619	10:07	4945	
e	same	same	-74	-10	10:09	4945	10:14	5121	
f	18.650456 SN 35272	same	-64	0	10:30	5121	10:30	5464	
g	same	same	-74	-10	10:41	5464	10:46	5632	
h	11.520 reference	11.66410		0	11:11	5640			7
Tape # 2	same	same		0	11:37	0020	1:00		8

Notes:
1. Data is at 1024 Hz unless otherwise noted.
2. Runs 1, 2 and 3 were setup runs. Don't use.
3. Aborted run 4 to ground VCXO terminal.
4. "0" and "-15" on recorder are approximate from LED bar graph
5. Diagnostic measurement of free running 5th OT Butler oscillator
6. Measurement of locked 11.381 GHz LO. Data is at 10 kHz
7. Run h aborted -- end of VHS tape.
8. Tape #2 is 1.5 hours of 1024 Hz reference sine wave downconverted from 11.6641 GHz

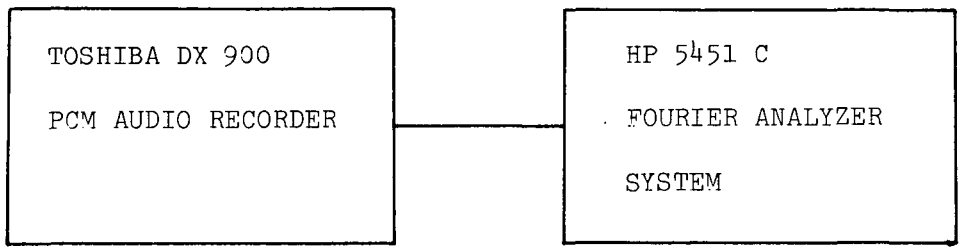

1024 HZ IF SIGNAL PROCESSING

FIGURE 3

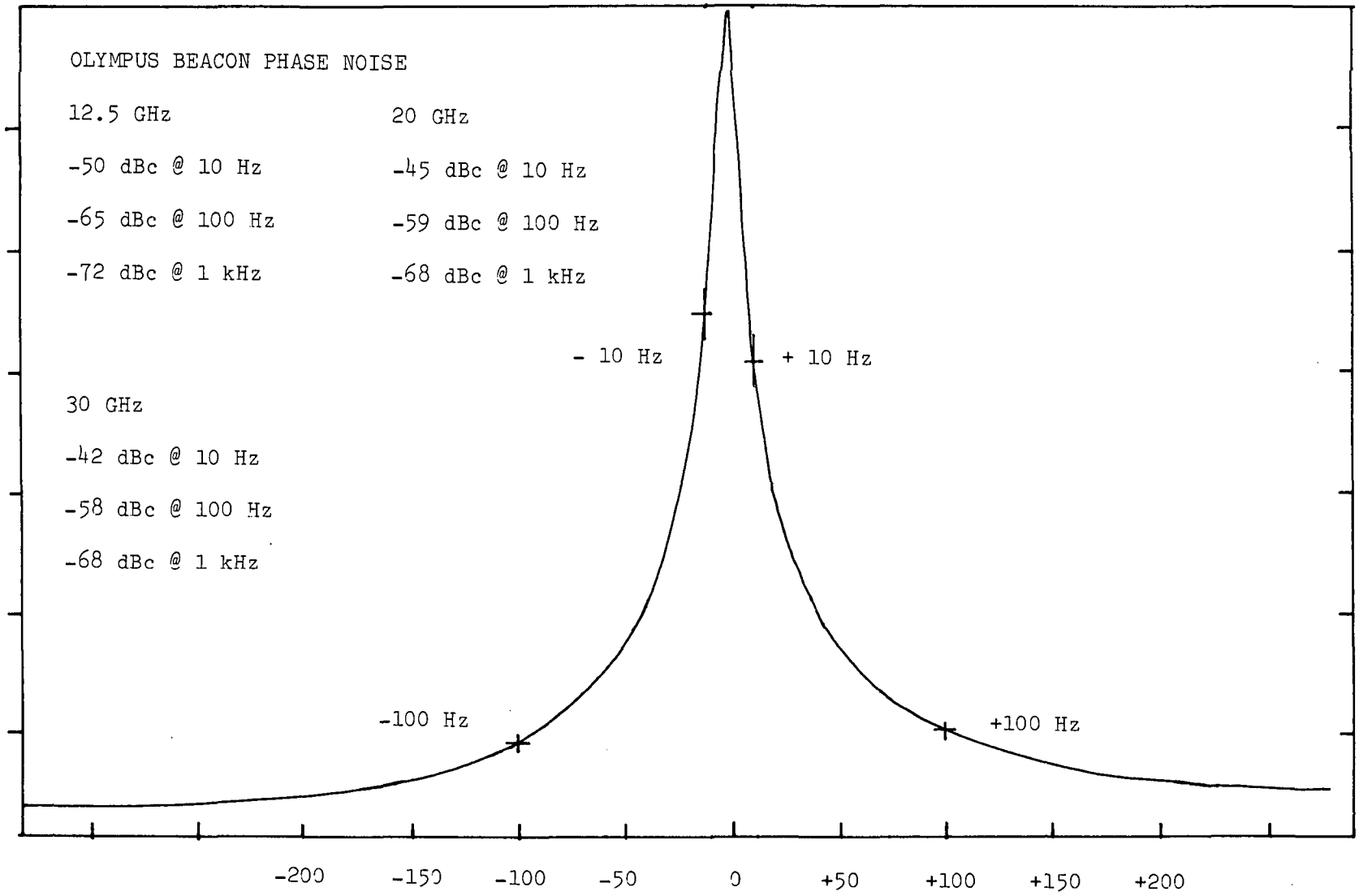

OLYMPUS BEACON PHASE NOISE

FIGURE 4

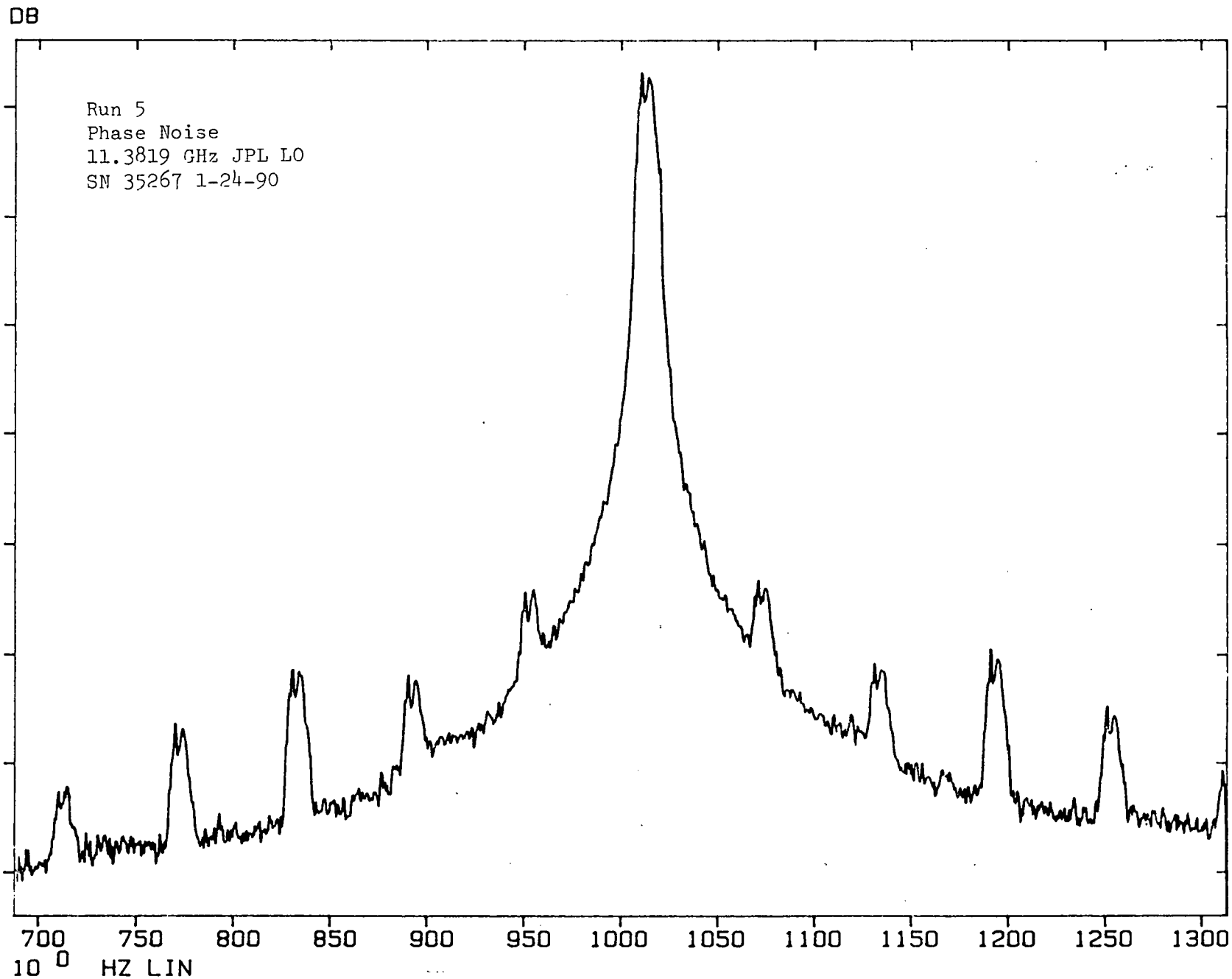

FIGURE 5

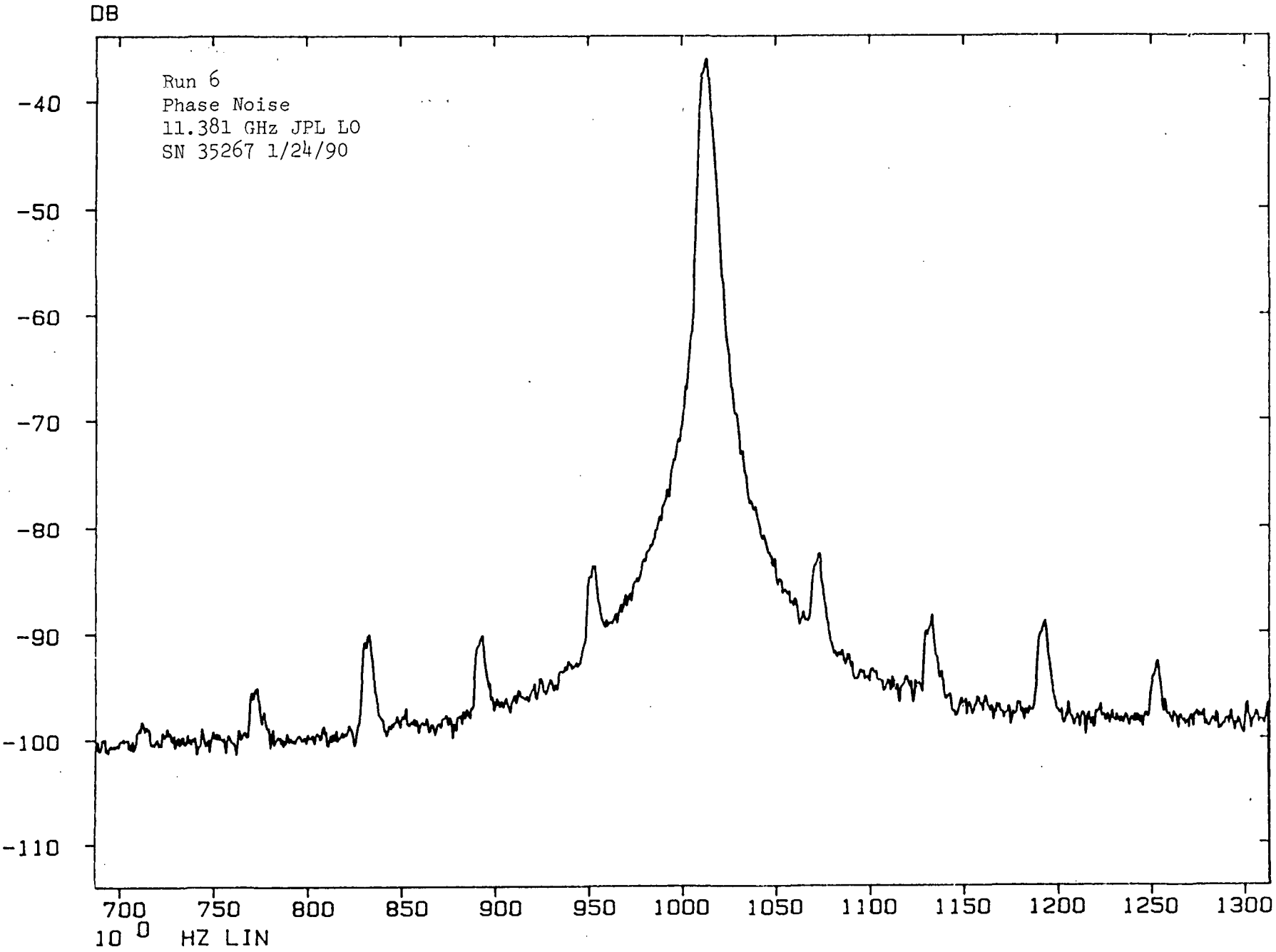
DB
Run 6
Phase Noise
11.381 GHz JPL LO
SN 35267 1/24/90
-40
-50
-60
-70
-80
-90
-100
-110
700
750
800
850
900
950
1000
1050
1100
1150
1200
1250
1300
10 0 HZ LIN

Figure 6

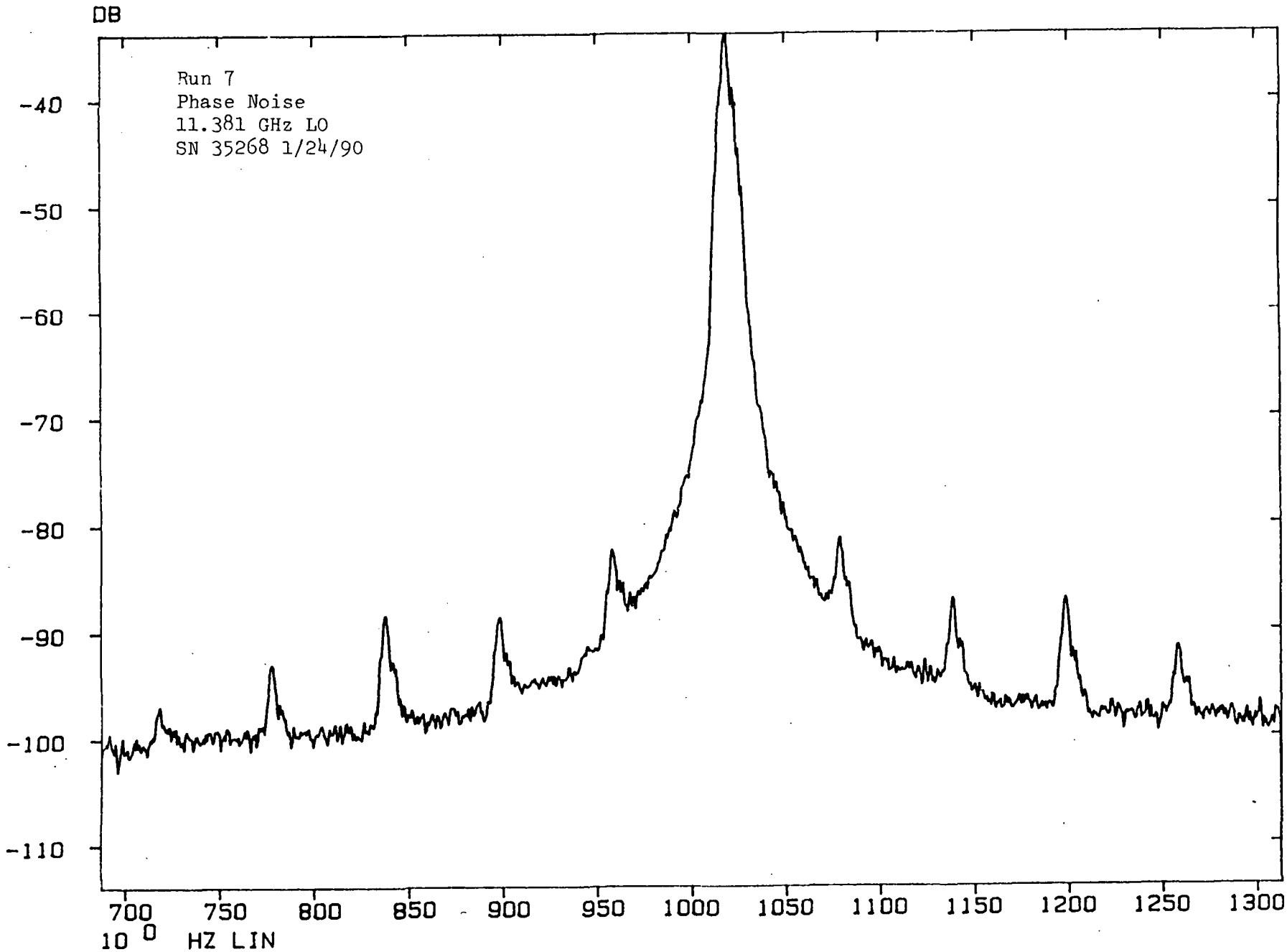
DB
Run 7
Phase Noise
11.381 GHz LO
SN 35268 1/24/90
-40
-50
-60
-70
-80
-90
-100
-110
700
750
800
850
900
950
1000
1050
1100
1150
1200
1250
1300
10 0 HZ LIN

Figure 7

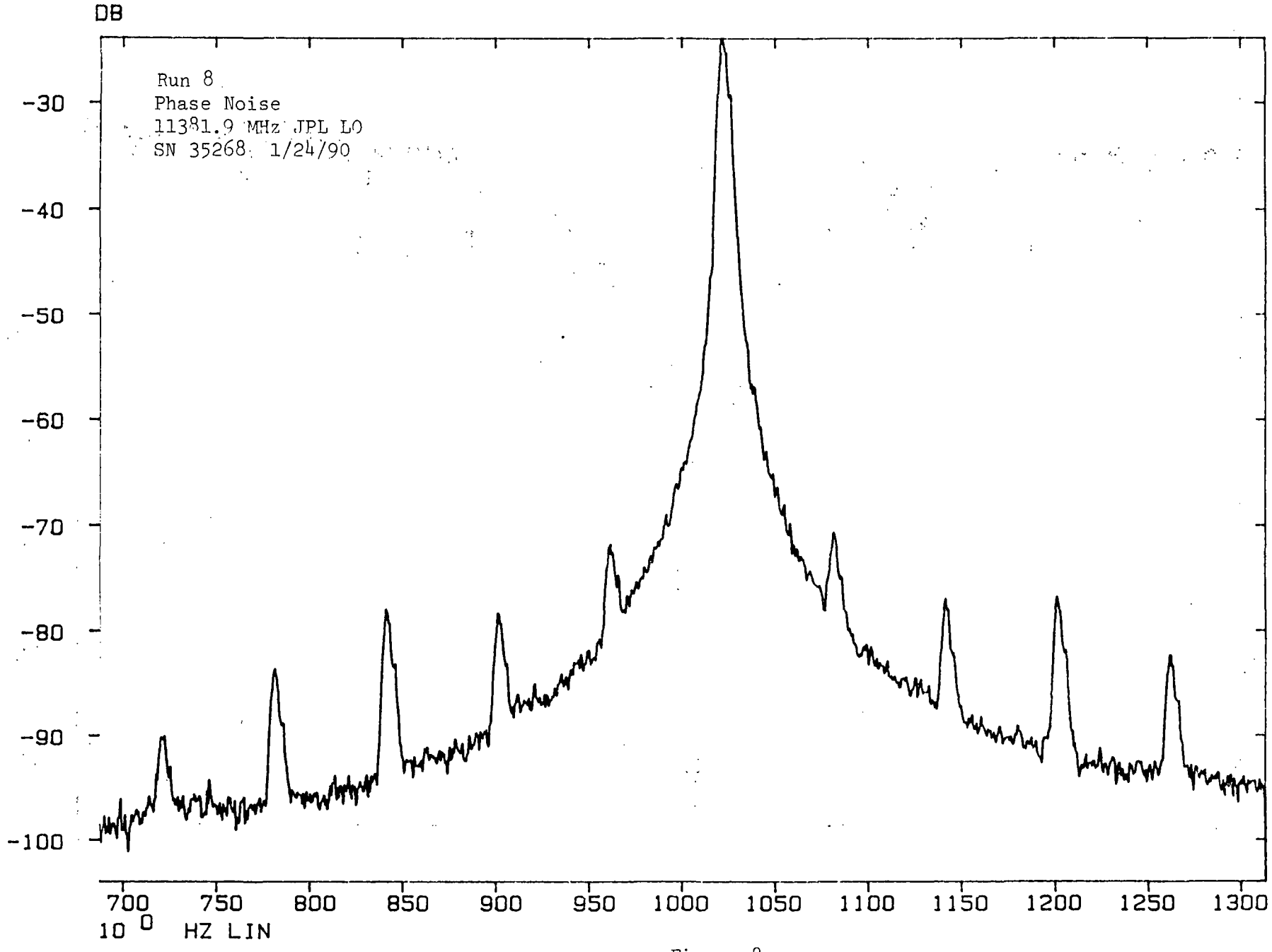
DB
Run 8
Phase Noise
11381.9 MHz JPL LO
SN 35268 1/24/90
-30
-40
-50
-60
-70
-80
-90
-100
700
750
800
850
900
950
1000
1050
1100
1150
1200
1250
1300
10 0 HZ LIN

Figure 8

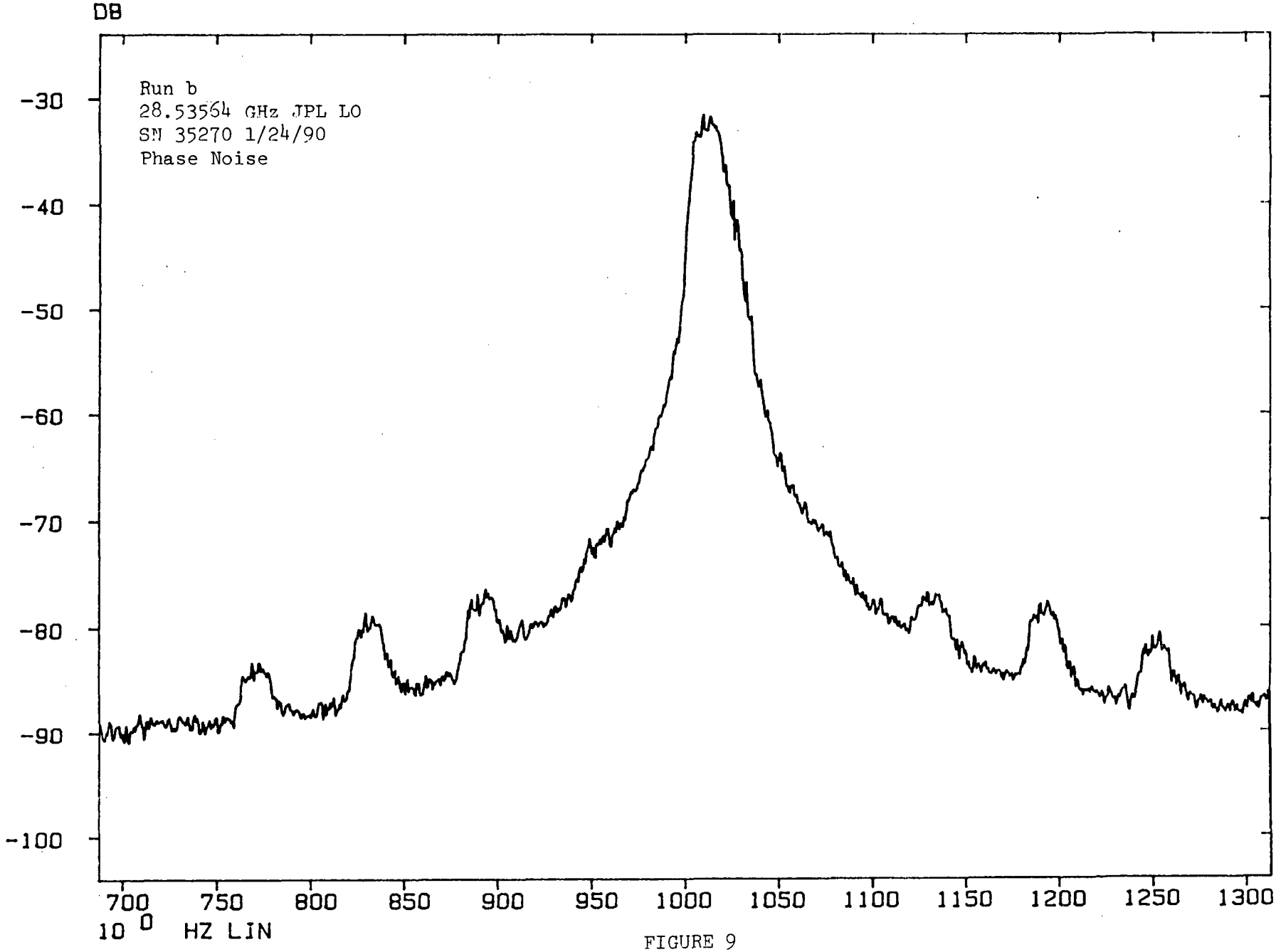
DB
Run b
28.53564 GHz JPL LO
SN 35270 1/24/90
Phase Noise
-30
-40
-50
-60
-70
-80
-90
-100
700
750
800
850
900
950
1000
1050
1100
1150
1200
1250
1300
10 0 HZ LIN

FIGURE 9

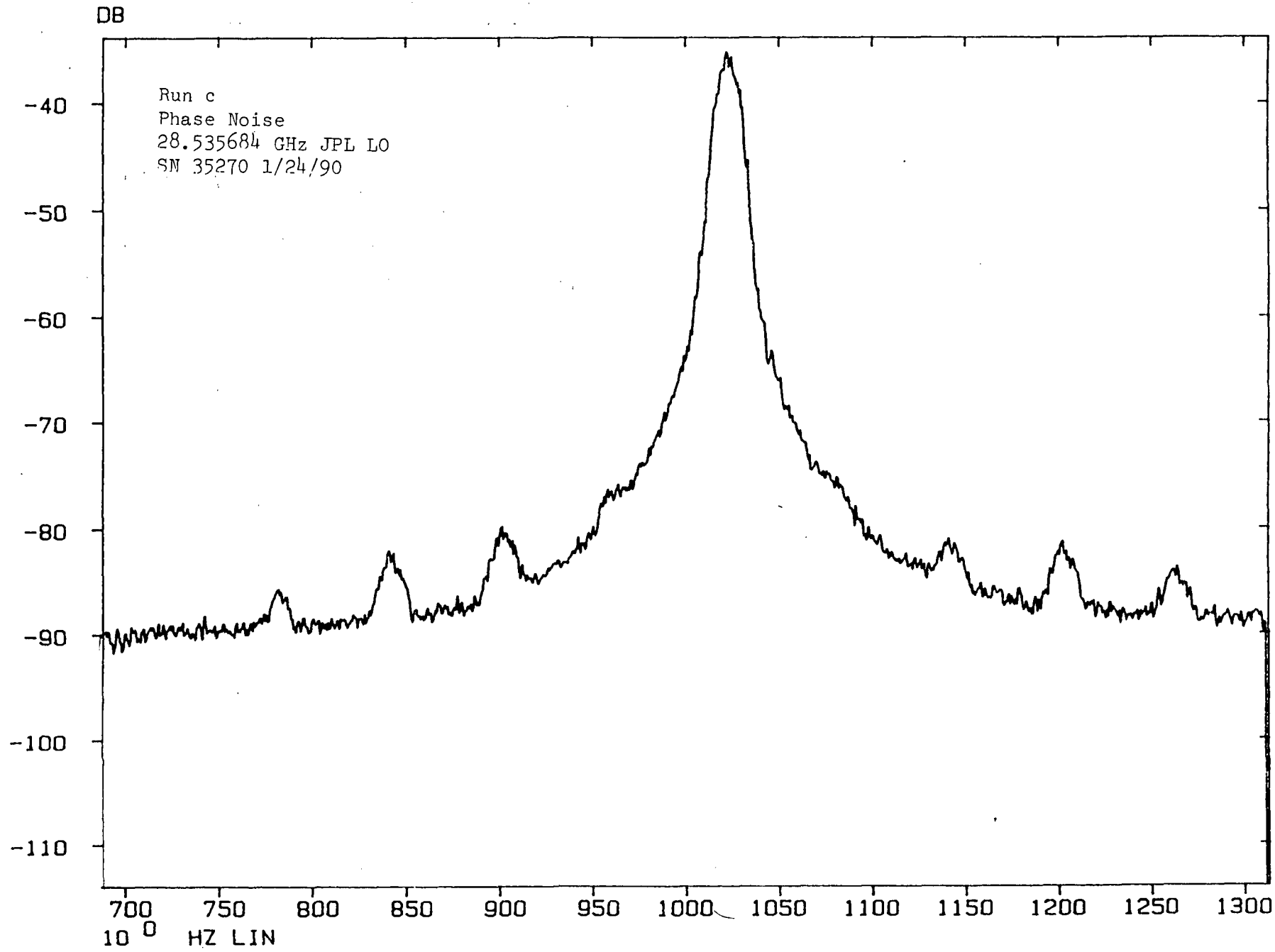
DB
Run c
Phase Noise
28.535684 GHz JPL LO
SN 35270 1/24/90
-40
-50
-60
-70
-80
-90
-100
-110
700
750
800
850
900
950
1000
1050
1100
1150
1200
1250
1300
10 0 HZ LIN

Figure 10

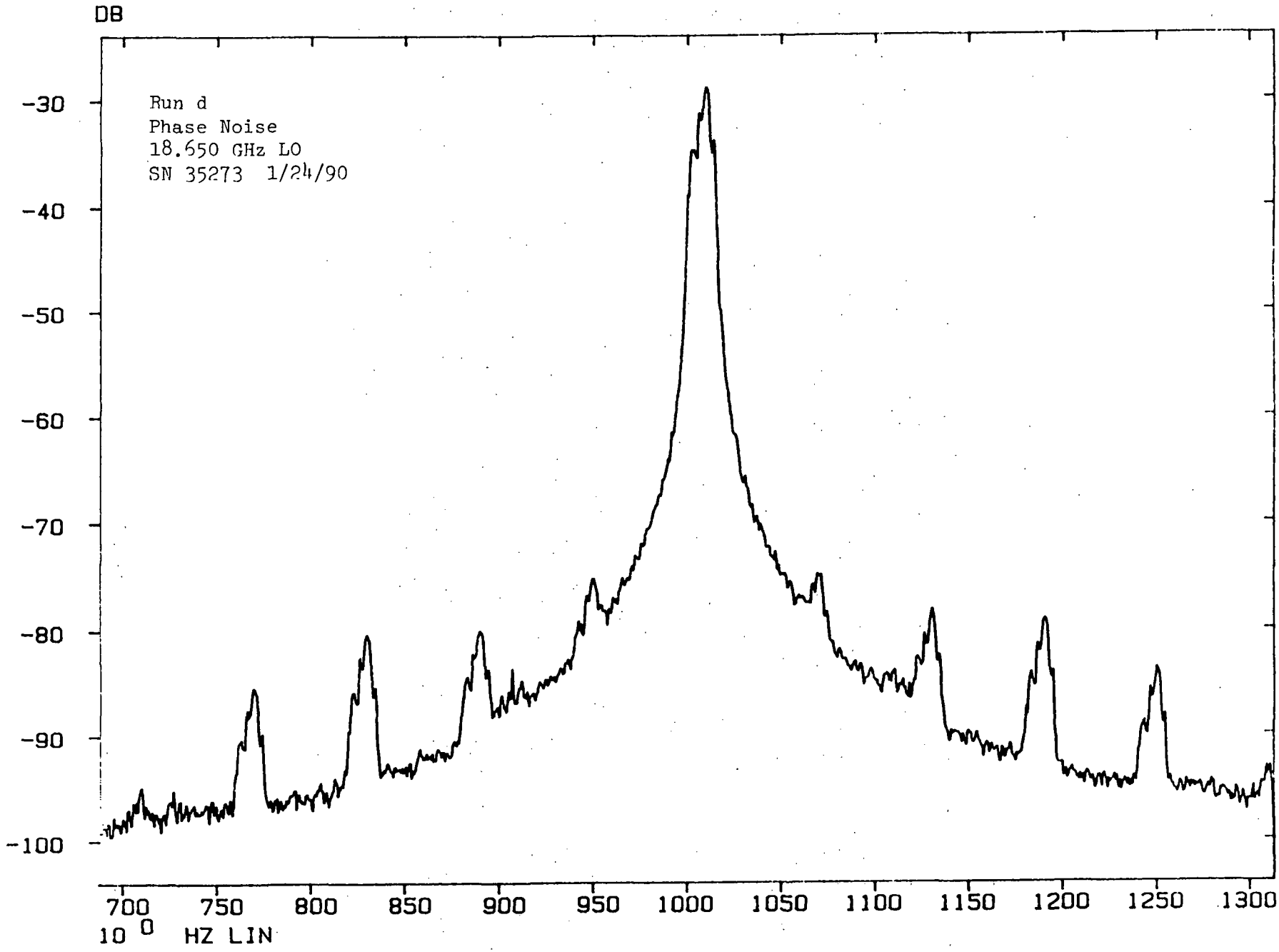
DB
Run d
Phase Noise
18.650 GHz LO
SN 35273 1/24/90
-30
-40
-50
-60
-70
-80
-90
-100
700
750
800
850
900
950
1000
1050
1100
1150
1200
1250
1300
10 0 HZ LIN

FIGURE 11

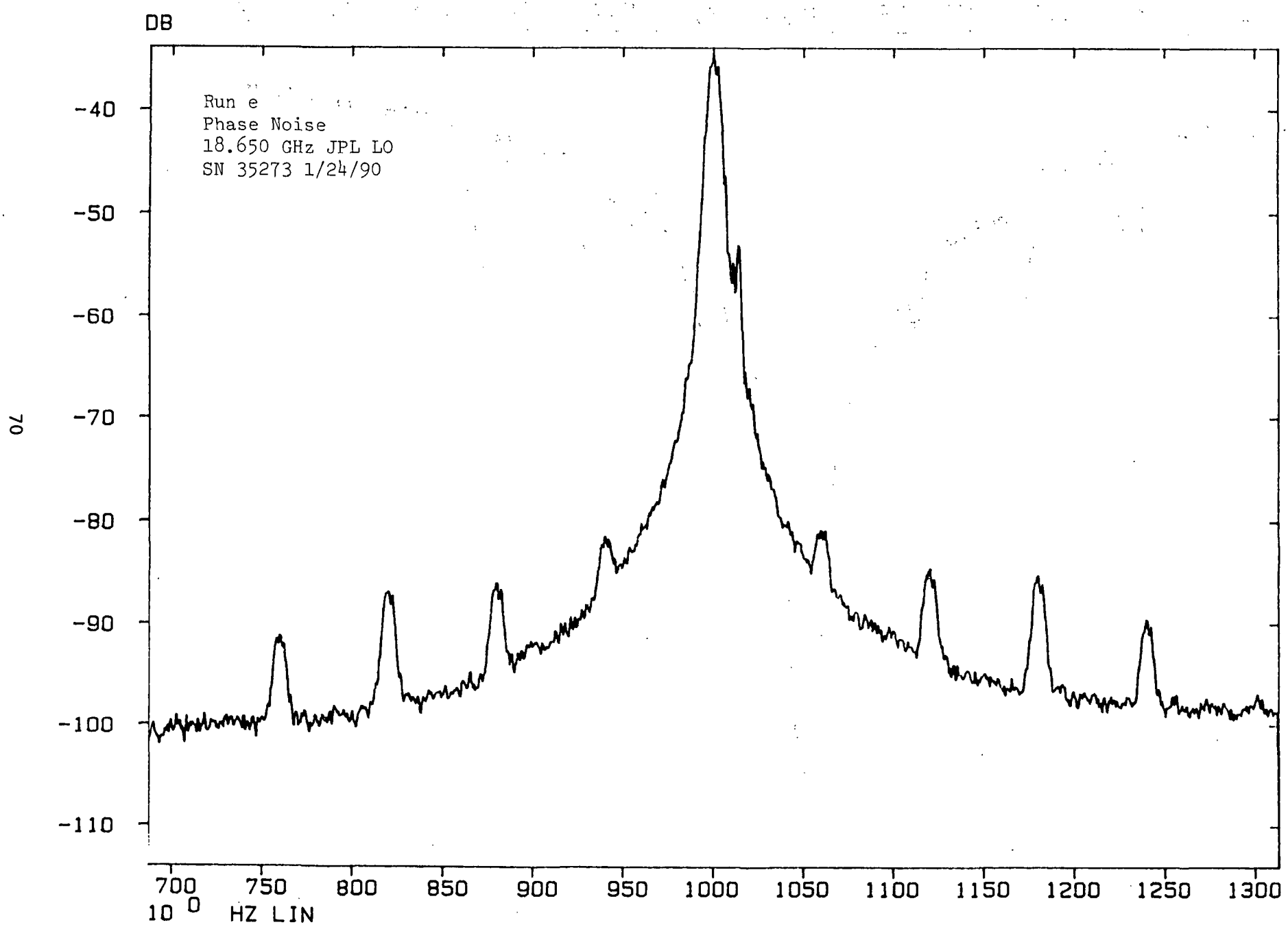
DB
Run e
Phase Noise
18.650 GHz JPL LO
SN 35273 1/24/90
-40
-50
-60
-70
-80
-90
-100
-110
70
700
750
800
850
900
950
1000
1050
1100
1150
1200
1250
1300
10 0 HZ LIN

FIGURE 12

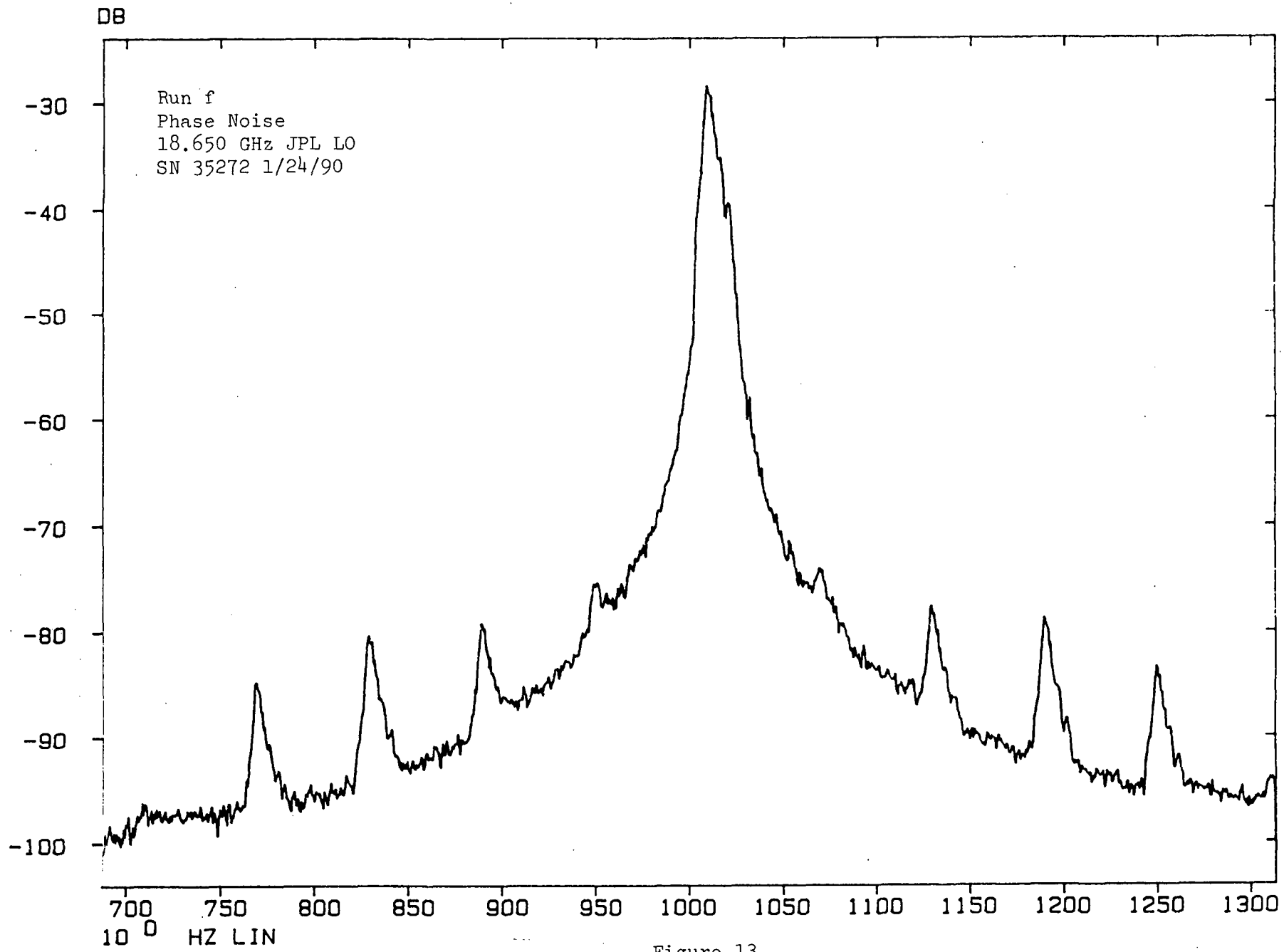
DB
Run f
Phase Noise
18.650 GHz JPL LO
SN 35272 1/24/90
-30
-40
-50
-60
-70
-80
-90
-100
700
750
800
850
900
950
1000
1050
1100
1150
1200
1250
1300
10 0 HZ LIN

Figure 13

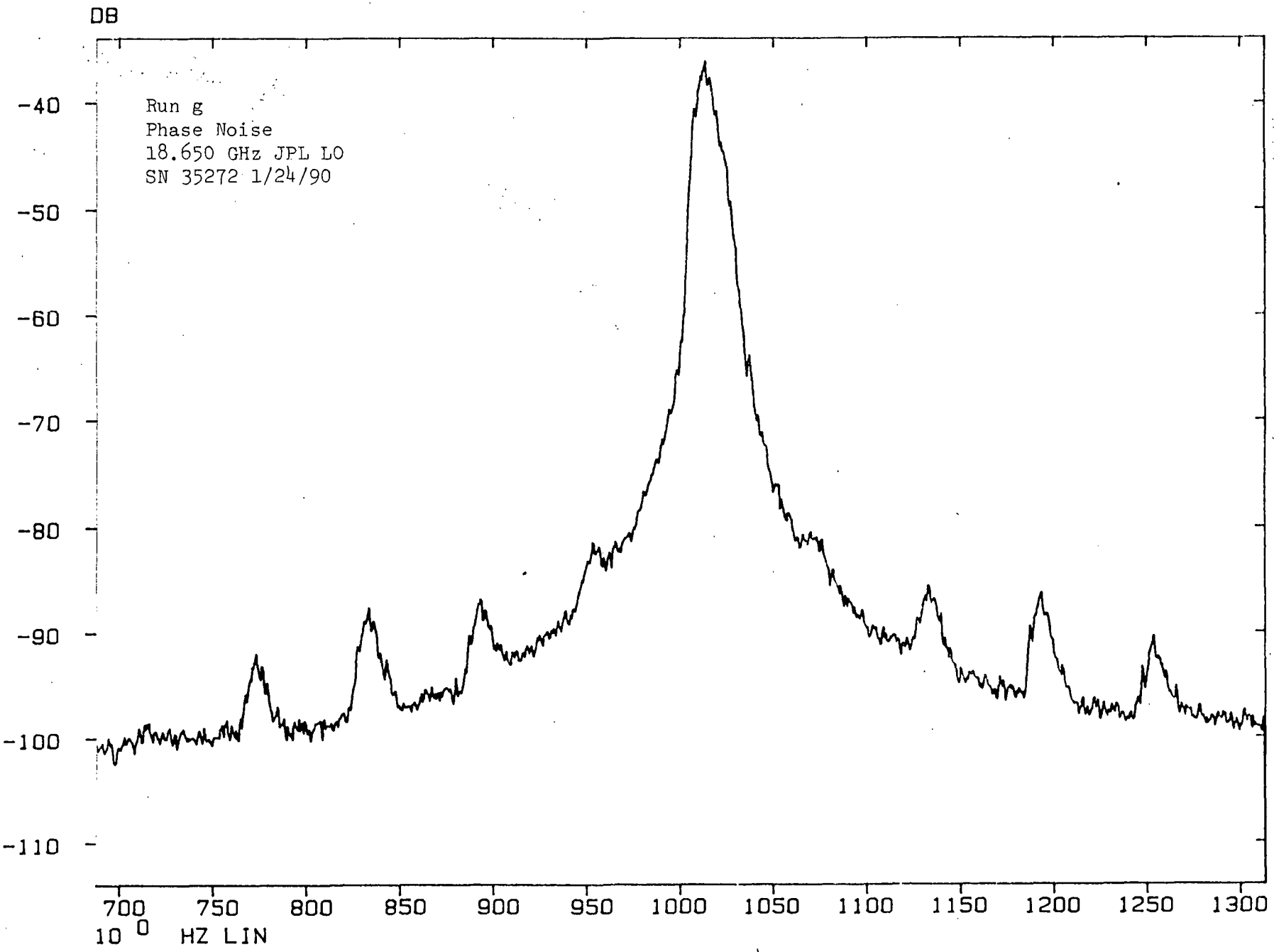
DB
Run g
Phase Noise
18.650 GHz JPL LO
SN 35272 1/24/90
-40
-50
-60
-70
-80
-90
-100
-110
700
750
800
850
900
950
1000
1050
1100
1150
1200
1250
1300
10 0 HZ LIN

FIGURE 14

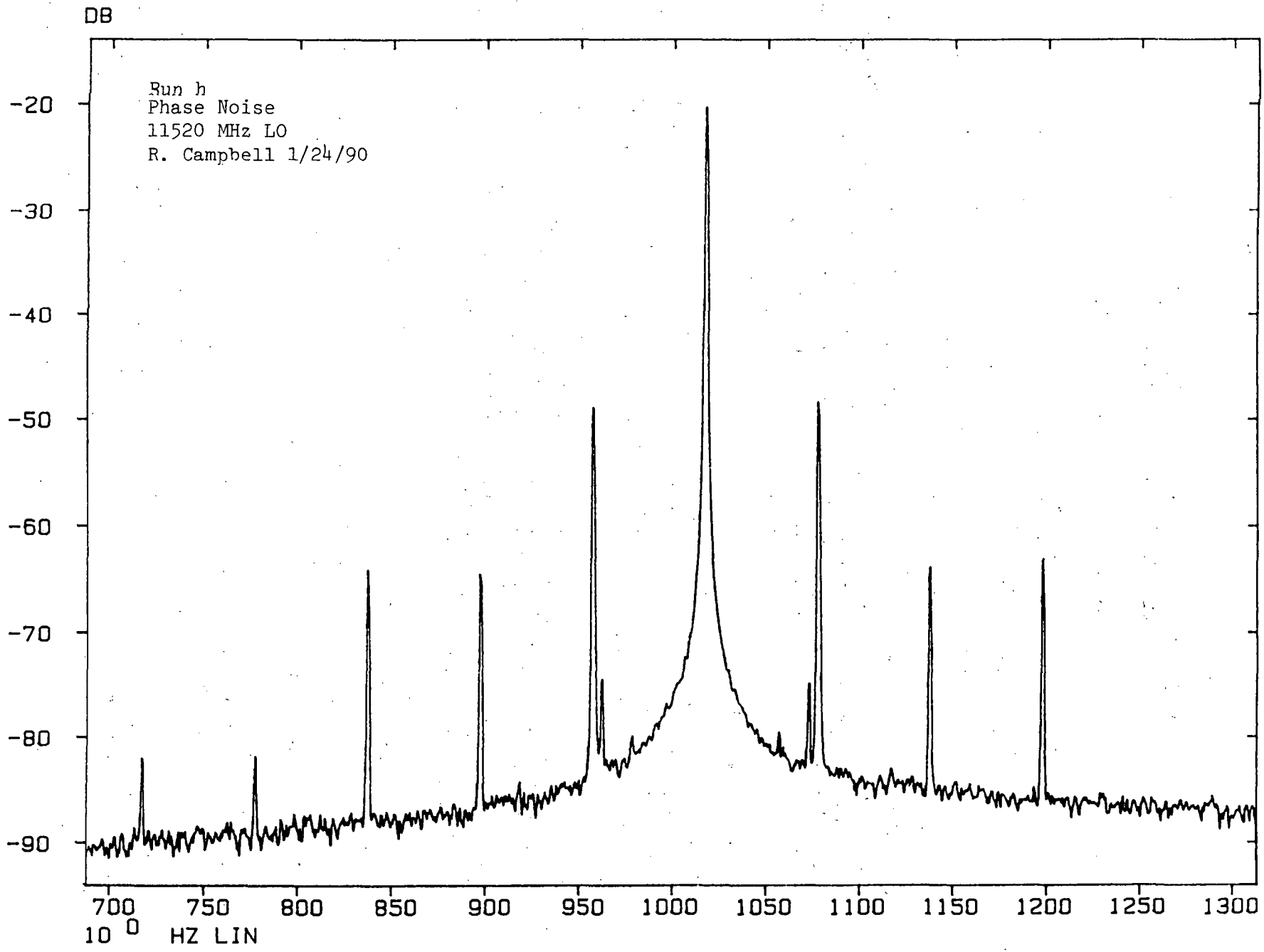
DB
Run h
Phase Noise
11520 MHz LO
R. Campbell 1/24/90
-20
-30
-40
-50
-60
-70
-80
-90
700
750
800
850
900
950
1000
1050
1100
1150
1200
1250
1300
10 0 HZ LIN

FIGURE 15

EXPERIMENTS FOR KA-BAND MOBILE APPLICATIONS — THE ACTS MOBILE TERMINAL

Polly Estabrook, Khaled Dessouky, and Thomas Jedrey

Jet Propulsion Laboratory
California Institute of Technology
4800 Oak Grove Dr.
Pasadena, California, 91109

Abstract

To explore the potential of Ka-band to support mobile satellite services, JPL has initiated the design and development of a Ka-band land-mobile terminal to be used with the Advanced Communications Technology Satellite (ACTS). The planned experimental setup with ACTS is described. Brief functional descriptions of the mobile and fixed terminals are provided. The inputs required from the propagation community to support the design activities and the planned experiments are also discussed.

1 Introduction

JPL is embarking on the design of a mobile terminal to be used in conjunction with the Advanced Communications Technology Satellite (ACTS) to explore the potential of Ka-band to meet the needs of future mobile satellite services. Mobile service providers have the desire to provide a greater number of services to mobile users and to support a larger user base. In view of the congestion and small bandwidth available at L-band, and of the existence of prior allocations at C- and Ku-band, Ka-band may be the next band available to the mobile community, whether for land, aeronautical or maritime mobile users. The goals of the ACTS Mobile Terminal (AMT) project are to develop link technologies necessary for operation in Ka-band and the characterization of the land-mobile channel in that band. Thus, the key system and technology challenges confronting mobile communications at Ka- band will be identified and solutions proposed. Once the experiments have been carried out and the data analyzed, issues such as the differences between operation in L-band and Ka-band, the need for and performance of various channel compensation techniques, and the tradeoffs of system availability versus terminal complexity will be better understood.

2 Overview of AMT Project

The AMT project began in May 1990 and will continue through the various phases of analysis, design, development, test and subsequent data analysis until late 1993. The following tasks will be performed in support of this project. First, the system challenges arising from mobile operation in the Ka-band channel: rain attenuation, shadowing, Doppler, and multipath, will be identified, quantified as best as possible, and algorithms will be designed to compensate for the channel. Second, the mobile terminal will be designed to develop the enabling technologies for a land-mobile satellite demonstration and will incorporate the channel compensation algorithms. The terminal will have a modular architecture to support future hardware developments and future experiments and demonstrations. It will also possess extensive recording and analysis equipment to permit real-time and post-experiment analysis of the mobile channel. The individual terminal components will be built by July 1992; they will be integrated into the mobile and fixed terminals and undergo system tests from July until December 1992. Third, a series of experiments, beginning in January 1993 and lasting through June 1993, will be carried out to characterize the land-mobile channel and to verify the terminal performance. Fourth, the data obtained from these experiments will be analyzed in order to improve understanding of the Ka-band channel impairments, to identify the performance of the

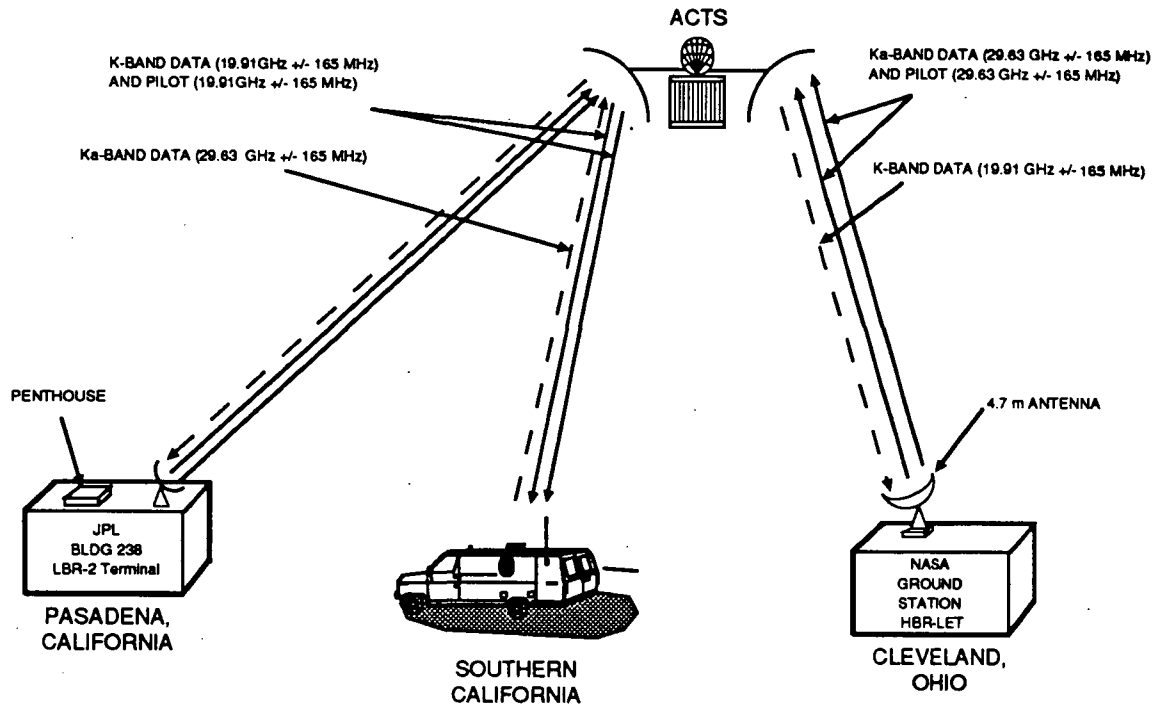

Figure 1: The AMT experimental setup using ACTS.

proposed compensation schemes, and to assess the measure of terminal performance improvement versus ensuing terminal complexity. Last, a series of recommendations for mobile service operation in this band will be released.

3 Experimental Setup

Figure 1 shows the experimental setup for the AMT testing using ACTS. ACTS will be used in the microwave switch matrix (MSM) mode to connect the mobile hub station with the mobile unit. The NASA ground station known as the High Burst Rate - Link Evaluation Terminal (HBR-LET) will be used to simulate a mobile hub station. This terminal is located at the NASA Lewis Research Center (LeRC) in Cleveland, Ohio. In the AMT experiment, only the 4.7 meter antenna and up- and down-conversion electronics of the HBR-LET will be utilized. Baseband equipment specific to the AMT will be designed to interface to the HBR-LET at an IF of 3.373 GHz. This terminal has a $G/T \approx 27$ dB/K and transmits at an EIRP varying from 68 dBW to 76 dBW, depending on the drive level to the travelling wave tube amplifier (TWTA).

The mobile terminal will be located in Southern California; this allows access to the satellite via its Los Angeles/San Diego uplink and downlink beams. Block diagrams for the fixed and mobile equipment will be given in Section 4. To facilitate debugging of the mobile to hub station communication link, the possibility of obtaining a second fixed terminal for installation at JPL is being investigated. This 'JPL' terminal would have three uses: (1) as a testbed for the mobile terminal hardware being developed at JPL; (2) as a local hub station in lieu of the HBR-LET for initial system operation; and (3) as a second 'mobile' terminal for network tests should network protocols be tested rather than simulated.

The forward link is depicted by the solid lines in Figure 1. Two signals are transmitted from the HBR-LET terminal: one is the data stream that would be sent from the hub station; the other is the pilot signal

that would be sent from the Network Management Control center of the network. The data stream is currently modelled as being a 96 kbps time domain multiplexed signal containing information for users in the Los Angeles/San Diego beam from the hub station. The pilot signal will be used by the mobile terminal for antenna acquisition and tracking, as a frequency reference to permit time and frequency acquisition, and finally to acquire rain fade information about the Cleveland beam.

This information for the Cleveland beam is generated in Cleveland by the HBR-LET and by the NASA ground station (NGS), which is collocated with the HBR-LET. The NGS receives three ACTS generated beacons: a vertically polarized beacon at 20.185 GHz, a horizontally polarized beacon at 20.195 GHz, and a vertically polarized beacon at 27.505 GHz. The first two beacons are fade and unified telemetry beacons. The latter is a rain fade beacon only. Rain fade information at both 20 GHz and 27 GHz is received by the NGS and passed along to the HBR-LET. In addition the HBR-LET possesses its own 20 GHz beacon receivers. This rain fade information will be communicated to the mobile terminal, possibly by modulating the pilot, and thus notifying it of the rain attenuation in the Cleveland beam. This data is necessary so that the mobile terminal, upon reception of the Cleveland transmitted pilot, can distinguish between rain fades in the uplink beam and those in the downlink beam.

In the forward link, ACTS is commanded by the NGS to receive signals on the fixed Cleveland beam and to translate these signals to one of four possible transponders, e.g. transponder #1.[1] The MSM will connect the output of receiver #1 to the high power amplifier #1 and to the Los Angeles/San Diego feed of the ACTS downlink scanning beam. The scanning beam will be kept fixed over the LA/San Diego area for the duration of the experiment. Two signals, namely the data and the pilot, will be received by the ACTS transponder. The effects of the limiter in the MSM ACTS transponder have be taken into account to obtain the correct link margins. A preliminary clear-weather link budget for the forward link from Cleveland to LA/San Diego is shown in Table 1. Conservative numbers have been used in conjunction with the transponder and the HBR-LET. The available $C/No_{overall}$ is 67.4 dB-Hz; the required C/No for 96 Kbps operation is 58.3 dB-Hz. This corresponds to a required E_b/N_o of 4 dB for differentially coherent BPSK in an AWGN channel at a BER of 10^{-3}, a convolutional code with $r = 1/2$ and $K = 7$, a modem implementation loss of 1.5 dB_r and an overall fade allowance for light vegetative shadowing of 3.0 dB. The clear weather forward link margin is 9.1 dB.

The return link is depicted in Figure 1 by the dotted lines. The mobile terminal transmits a single signal, the data channel signal (voice or data messages), to the hub station. Its data rate varies according to the rain fade conditions in the uplink beam (LA/San Diego) and the downlink beam (Cleveland). ACTS is commanded by the NGS to receive signals on the LA/San Diego beam feed of the ACTS uplink scanning beam and to translate these signals to one of four possible transponders, e.g. transponder #2. The microwave switch matrix will connect the output of receiver #2 to the high power amplifier #2 and hence to the Cleveland fixed beam feed. The uplink scanning beam will be kept fixed over the LA/San Diego area for the duration of the experiment.

A preliminary clear weather link budget for the return link from LA/San Diego to Cleveland is shown in Table 2. Again, conservative characteristics for the transponder and HBR-LET are assumed. The available $C/No_{overall}$ is calculated to be 50.87 dB-Hz; the required C/No is 48.32 dB-Hz. The latter corresponds to requirements similar to those of the forward link with the exception of the data rate. The return link clear-weather margin is 2.55 dB.

When the 'JPL' terminal is used as the hub station in JPL to JPL tests, the two uplink signals from the 'JPL' terminal and the one uplink signal from the mobile terminal will be received by the uplink LA/San Diego beam feed and transmitted to the downlink LA/ San Diego beam feed via the same ACTS transponder. Thus signals with very different power levels will be present in the transponder; the effect of the limiter differs from that of the two previous cases. The clear weather forward link margin is then calculated to be 8.4 dB at 96 Kbps. The clear weather return link margin is calculated to be 1.6 dB at 4.8 Kbps. The return link can not support the full 9.6 Kbps link.

In later experiments, signals from both the mobile terminal and the 'JPL' terminal may be transmitted

[1] ACTS possesses four wideband transponders of which three can be used at any one time as one is saved for redundancy.

Table 1: Forward Link Calculation for the Cleveland to LA/San Diego beam

Uplink Supplier to Satellite 30 GHz		Downlink Satellite to AMT 20 GHz	
HBR-LET at LeRC:		Satellite:	
f_{center} (uplink)	29.63 GHz	f_{center} (downlink)	19.91 GHz
Antenna Gain (4.7m)	61 dBi	Antenna Gain (3.3m)	48.1 dBi
TX Polarization	HP	TX Polarization	VP
EIRP	65 dBW	EIRP (61.7 dBW max)	56.22 dBW
$L_{pointing}$	-0.39 dB	$L_{pointing}$	0 dB
Propagation Losses (Clear Weather):		Propagation Losses (Clear Weather):	
$L_{Atmosphere}$	-0.92 dB	$L_{Atmosphere}$	-0.61 dB
L_{Space} (Clev. to ACTS)	-213.48 dB	L_{Space} (ACTS to LA)	-209.89 dB
$L_{Polarization}$	-0.5 dB	$L_{Polarization}$	-0.5 dB
Satellite:		ACTS Mobile Terminal in LA:	
$L_{Pointing}$	0 dB	$L_{Pointing}$	-0.5 dB
G/T (Clev. Fixed Beam)	19.6 dB/K	G/T	-5.91 dB/K
C/T	-130.69 dBW/Hz	C/T	-161.19 dBW/Hz
C/No_{up}	97.91 dB-Hz	C/No_{down}	67.41 dB-Hz
B_T (900 MHz)	89.54 dB-Hz		
SNR_{in}	8.37 dB		
Limiter Suppression Factor, Γ	3.8		
Hard Lim. Eff. SNR_{out}	4.57 dB		
Overall Link Performance:			
$C/No_{overall}$		67.40 dB-Hz	
$C/No_{required}$ (for 96 kbps operation)		58.32 dB-Hz	
Link Margin		9.08 dB	

Table 2: Return Link Calculation for the LA/San Diego to Cleveland Beam

Uplink AMT to Satellite 30 GHz		Downlink Satellite to Supplier 20 GHz	
ACTS Mobile Terminal in LA:		Satellite:	
f_{center} (uplink)	29.63 GHz	f_{center} (downlink)	19.91 GHz
Antenna Gain	24.7 dBi	Antenna Gain (3.3m)	51.3 dBi
TX Polarization	HP	TX Polarization	VP
EIRP	21.0 dBW	EIRP (64.8 dBW max)	28.85 dBW
$L_{pointing}$	-0.5 dB	$L_{pointing}$	0 dB
Propagation Losses (Clear Weather):		Propagation Losses (Clear Weather):	
$L_{Atmosphere}$	-0.61 dB	$L_{Atmosphere}$	-0.92 dB
L_{Space} (LA to ACTS)	-213.34 dB	L_{Space} (ACTS to Clev.)	-210.03 dB
$L_{Polarization}$	-0.5 dB	$L_{Polarization}$	-0.5 dB
Satellite:		HBR-LET at LeRC:	
$L_{Pointing}$	0 dB	$L_{Pointing}$	-0.5 dB
G/T (LA/SD Spot Beam)	17.3 dB/K	G/T	27.3 dB/K
C/T	-176.65 dBW/Hz	C/T	-155.80 dBW/Hz
C/No_{up}	51.95 dB-Hz	C/No_{down}	72.80 dB-Hz
B_T (900 MHz)	89.54 dB-Hz		
SNR_{in}	-37.60 dB		
Limiter Suppression Factor, Γ	$\pi/4$		
Overall Link Performance:			
$C/No_{overall}$		50.87 dB-Hz	
$C/No_{required}$ (for 9.6 kbps operation)		48.32 dB-Hz	
Link Margin		2.55 dB	

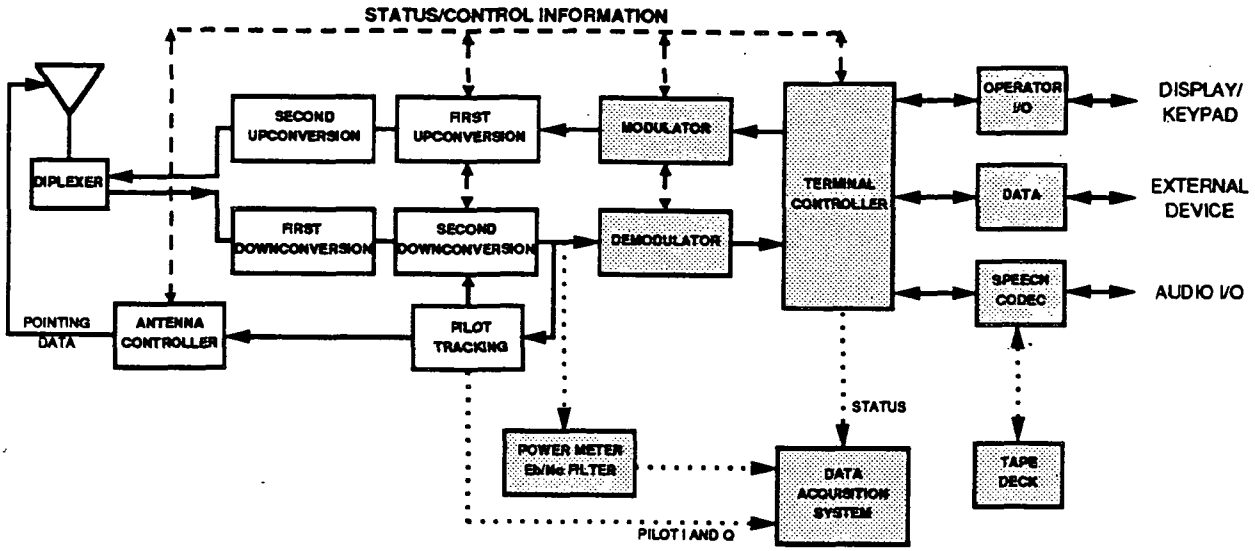

Figure 2: Block diagram of the mobile terminal.

simultaneously to the hub station in Cleveland to simulate network operation. The effect of several uplink signals sharing the limiting ACTS transponders will have to be taken into account in this case as well.

4 Mobile and Fixed Terminal Design

4.1 The Mobile Terminal

The block diagram for the mobile terminal is shown in Figure 2. The terminal is conveniently divided into a microwave and a baseband processor. The elements belonging to the baseband processor are shown shaded. They include auxiliary components required for experimentation.

The antenna under design is a low profile, high gain, mechanically steered array. The antenna controller will allow the antenna to acquire and track the HBR-LET generated pilot signal. The RF up- and down-converters will translate their respective input signals at 3.373 GHz and 19.91 GHz to output frequencies of 29.63 GHz and 3.373 GHz, 3.373 GHz being the specified IF for interfacing to the HBR-LET. The IF up- and down-converters will translate between the modem output IF, most likely 70 MHz, and 3.373 GHz. Pilot tracking, where needed, will be performed in the IF down-converter.

The modem must be power efficient and utilize robust modulation and demodulation schemes that allow it to freewheel through vegetative shadowing. It will operate at variable data rates - from 9.6 Kbps to 2.4 Kbps - to compensate for rain fading as will the speech codec. The latter will utilize different vocoder algorithms depending on the output symbol rate so as to maximize speech quality for a given data rate.

These variable rate modems and codecs will be used in both the mobile and fixed terminals. The hub station will command a data rate change in the forward link if it is notified by the mobile terminal that rain exists in the mobile terminal's downlink beam. The data rate from the mobile terminal will be decreased if rain attenuation is found in either the mobile terminal's uplink beam or in the downlink beam to the hub station. The algorithm for data rate change is envisioned as operating without network coordination. The modem, therefore, must be able to sense or command a data rate change without receiving information from the network or notifying it.

The design of the algorithm used to control the data rate will depend on the time variation of the rain fade. These second order rain statistics will depend on the location in CONUS and on the time of year; they

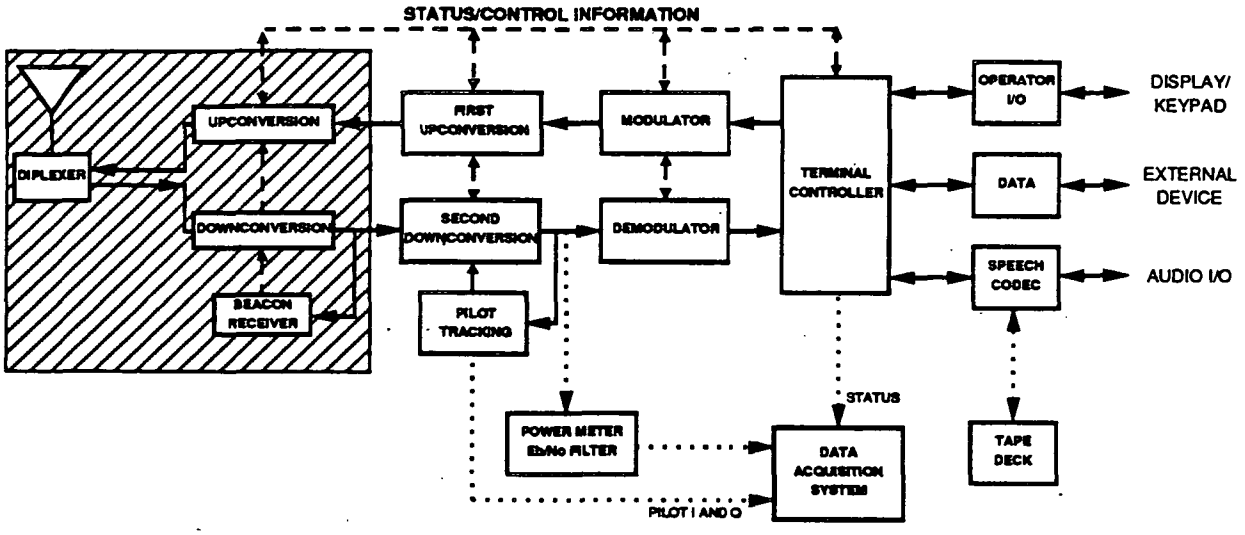

Figure 3: Block diagram of the fixed terminal.

will be obtained from the propagation community based on the results obtained from the OLYMPUS-1 and ACTS beacons. The data will be used to determine the thresholds at which the data rate should be changed and the number of data rate levels necessary to compensate for rain fades. It will also be used to determine whether changes in the data rate should be ordered apriori or aposteriori to the measurement of these rain fade threshold levels. The design of the algorithm and its implementation must also take into account the level of BER improvement expected, the increased signal delay, and the implementation cost in the modem. The ensuing system availability (for various data rates and voice qualities) will then be assessed.

The terminal controller governs the interface between the various types of inputs to the terminal, i.e. from the codec, the keyboard, or any other external device, and the modem. It monitors and controls the operation of all of the terminal's components and is responsible for executing the rate control algorithms. The terminal controller will also perform various diagnostic tests on the terminal and will pass status data on to the data acquisition system.

The data acquisition system will record the operation of many of the terminal's components. It will provide for real time display of various signal levels and bit-error-rate information. Channel characterization in terms of vegetative shadowing, rain fades, Doppler and multipath depend on accurately recording and time-tagging the performance of the link and on being able to correlate this with the correct mobile environment.

4.2 The Fixed Terminal

The block diagram for the fixed terminal is given in Figure 3. Shown is the equipment that will be necessary for the hub station whether it is located at NASA LeRC or at JPL. The equipment shown in the hatched box belongs to the HBR-LET terminal located at LeRC or to the loaned equipment for the 'JPL' terminal. The remaining equipment is identical to that used in the mobile terminal. It should be noted that the pilot tracking circuit is not necessary for the operation of the fixed terminal.

All components function as in the mobile terminal with the exception of the terminal controller which performs an additional task. It monitors the rain fade condition at 27 GHz from the NGS's beacon receivers in order to control the drive level of the HBR-LET's TWTA. Algorithms for uplink power control will be developed for use only by the hub station to compensate for rain in its beam. Due to transmit power limitations, the mobile terminal cannot compensate for uplink rain fades in this manner.

5 Planned Experiments

Planned experiments include both stationary and mobile clear-weather link tests of the mobile terminal. The objectives for these tests will be to: (1) verify the analyses performed prior to terminal design; (2) permit the refinement of the Ka-band channel characterization; (3) determine system and subsystem performances under true field conditions; (4) support terminal design refinements and enhancements; and (5) demonstrate the technologies and system concepts to potential end-users and manufacturers.

Antenna acquisition and tracking functions will be demonstrated and quantified. Modem and codec performance will be ascertained at various data rates. Performance of the chosen modulation and coding schemes and modem and speech codec implementations will be evaluated in terms of compensating for Doppler and frequency offsets, minimizing any effects due to multipath, and permitting freewheeling through shadowing with quick recovery from voice outages.

The performance of the power and data rate control rain compensation algorithms will be measured, first, by simulating rain attenuation, and, then by testing during various rainy conditions. The variable rate modem will be tested to assess its response time, optimum setting of threshold levels, number of data rate steps, and to determine the achieved system availability. The data rate control algorithms for the modulator and the speech coder will be implemented in software so that they can be refined in accordance with experimental results and retested. The ensuing system availability will then be assessed in light of the increased terminal complexity required to implement these algorithms. The appropriate tradeoff analysis will be performed and conclusions will be derived.

This baseline experimentation plan will provide a foundation upon which other Ka-band mobile, aeronautical or maritime, and micro-terminal experiments can be based.

6 Inputs from the Propagation Community

Information about the Ka-band channel is necessary for the AMT project in order to guide the development of the rain compensation algorithms and to aid in the selection of the modulation and coding schemes. Second order rain statistics at Ka-band are required to determine how useful changing the data rate is in preserving the link. Investigations are under way to determine the most useful format for such statistics. Decisions have to be made on whether simply the time variations of the rain attenuation would be sufficient, or if the channel model requires conditional expectations or the autocorrelation of the rain fade process. Both rain statistics and inputs regarding channel modeling are required from the propagation community.

Channel characterization in terms of shadowing and multipath are also necessary. Issues such as the shadowing and scattering characteristics due to tree tops, the duration and depth of tree shadowing as a function of the mobile terminal elevation angle, and multipath as a function of elevation angle and beamwidth for high gain mobile antennas must be studied.

7 Conclusion

JPL is initiating the design of a mobile terminal and developing plans for a series of mobile communication link experiments at Ka-band in order to explore the potential of Ka-band to meet the needs of future mobile satellite services. The two main technical challenges foreseen are those of maintaining the link in a severe propagation environment and of developing the enabling Ka-band technologies. The first challenge consists of developing the power and data rate control algorithms to compensate for rain fade, the modulation and coding techniques to combat Doppler and multipath, a modem implementation that freewheels through shadowing events, and high performance antenna tracking algorithms. The second technical challenge involves developing of Ka-band components, packaging techniques and active antennas.

The land-mobile ACTS experiments are centered around the goal of providing a more accurate characterization of the Ka-band channel and its potential to support mobile communications. The planned baseline

experimentation plan will serve as a starting point for other mobile and micro-terminal experiments at Ka-band. Although the experimental phase of the AMT project is currently scheduled to occur from January to June 1993, it is hoped that other experiments involving advanced land mobile terminal hardware, maritime or aeronautical applications, testing of hybrid satellite and land based networks, or demonstration of truly personal micro-terminals will occur throughout the lifetime of ACTS.

Acknowledgement

This work was performed at the Jet Propulsion Laboratory, California Institute of Technology, under a contract with the National Aeronautics and Space Administration.

NAPEX XIV

Session 2

FIXED AND MOBILE SATELLITE PROPAGATION STUDIES AND EXPERIMENTS

Chairmen:

Part A:
Faramaz Davarian
Jet Propulsion Laboratory

Part B:
John Kiebler
Public Service Satellite Consortium

N91-11962

DEEP SPACE PROPAGATION EXPERIMENTS AT K_a-BAND

Stanley A. Butman
Jet Propulsion Laboratory
California Institute of Technology
Pasadena, California 91109

ABSTRACT

This presentation discusses propagation experiments as essential components of the general plan to develop an operational deep space telecommunications and navigation capability at K_a-band (32-35 GHz) by the end of the 20th century. Significant benefits of K_a-band over the current deep space standard X-band (8.4 GHz) are an improvement of 4 to 10 dB in telemetry capacity and a similar increase in radio navigation accuracy. Propagation experiments are planned on the Mars Observer Mission in 1992 in preparation for the Cassini Mission to Saturn in 1996, which will use K_a-band in the search for gravity waves as well as to enhance telemetry and navigation at Saturn in 2002. Subsequent uses of K_a-band are planned for the Solar Probe Mission and the Mars Program.

DEEP SPACE PROPAGATION EXPERIMENTS AT K_a-BAND

JPL

Presentation To
Fourteenth NASA Propagation Experimenters Meeting
Austin, Texas

by

Stanley A. Butman

Jet Propulsion Laboratory
California Institute of Technology
Pasadena, California

May 11, 1990

JPL

CONTENTS

JPL

K_a-BAND RATIONALE

- K_a-BAND OFFERS SIGNIFICANT BENEFITS
  - TELEMETRY
    - EXPECTED x4 TO x10 IMPROVEMENT IN CHANNEL CAPACITY OVER X-BAND
  - NAVIGATION AND RADIO SCIENCE
    - REDUCED PLASMA SENSITIVITY ENABLES MORE PRECISE NAVIGATION AND HIGHER PRECISION GRAVITATIONAL EXPERIMENTS THAN X-BAND
    - 500 MHz BANDWIDTH INCREASES RADIO METRIC ACCURACY AND FACILITATES ACCURATE RELATIVITY MEASUREMENTS
  - REDUCED FLIGHT RADIO SYSTEM COSTS
    - PERMITS REDUCTION IN ANTENNA SIZE FOR EQUIVALENT PERFORMANCE AT X-BAND
    - PERMITS REDUCTION IN POWER REQUIREMENTS FOR EQUIVALENT PERFORMANCE AT X-BAND
  - REDUCED DSN TRACKING TIME vs EQUIVALENT DATA VOLUME AT X-BAND

DEEP SPACE DOWNLINK PERFORMANCE EVOLUTION AT X-BAND AND K_a-BAND

30 DEG ELEVATION, 90% WEATHER, GOLDSTONE, CA

COMPONENT		X-BAND (8.4 GHz)		K_a-BAND (32 GHz)	
		1990	1995	1995	2000+
SPACECRAFT					
TRANSMITTER	dBm	40.0	40.0	37.0	40.0
3.66 M ANT. GAIN	dBi	48.3	48.3	59.3	59.3
POINTING LOSS	dB	-1.0	-0.1	-1.0	-0.2
SPACE LOSS	dB	-294.6	-294.6	-306.2	-306.2
GROUND					
ATMO. ATTEN.	dB	-0.1	-0.1	-0.4	-0.4
70M ANT. GAIN	dBi	74.2	74.4	84.0	85.8
POINTING LOSS	dB	-0.3	-0.1	-0.3	-0.1
NOISE SPECTRUM	dBm/Hz	-184.6	-185.9	-182.6	-182.6
SNR	dB-Hz	51.1	* 53.7	55.0	** 60.8

* X-BAND IMPROVES BY 2.6 dB FROM NOISE REDUCTION (1.3 dB) AND 1.3 dB ANTENNA AND POINTING IMPROVEMENTS REQUIRED FOR K_a-BAND

** K_a-BAND IMPROVES BY 5.8 dB FROM POWER INCREASE (3 dB) AND FURTHER TOLERANCE TIGHTENING ON ANTENNAS AND POINTING SYSTEMS

JPL

MISSIONS WITH K_a-BAND LINKS

MARS OBSERVER – SEPT 16, 1992

- **IMPLEMENTING 10 mWatt BEACON TO EVALUATE PERFORMANCE OF LINK RELATIVE TO X-BAND BASELINE**

CASSINI (SATURN) – APRIL 8, 1996

- **DESIGNING A 5 Watt TELEMETRY LINK AS A MISSION ENHANCEMENT TO AUGMENT X-BAND BASELINE**

SOLAR PROBE – ABOUT THE YEAR 2000

- **PLANNING ON K_a-BAND AS THE BASELINE**

MARS PROGRAM

- **SIGNIFICANT USE OF K_a-BAND**

90

OVERVIEW K_a-BAND SCHEDULE

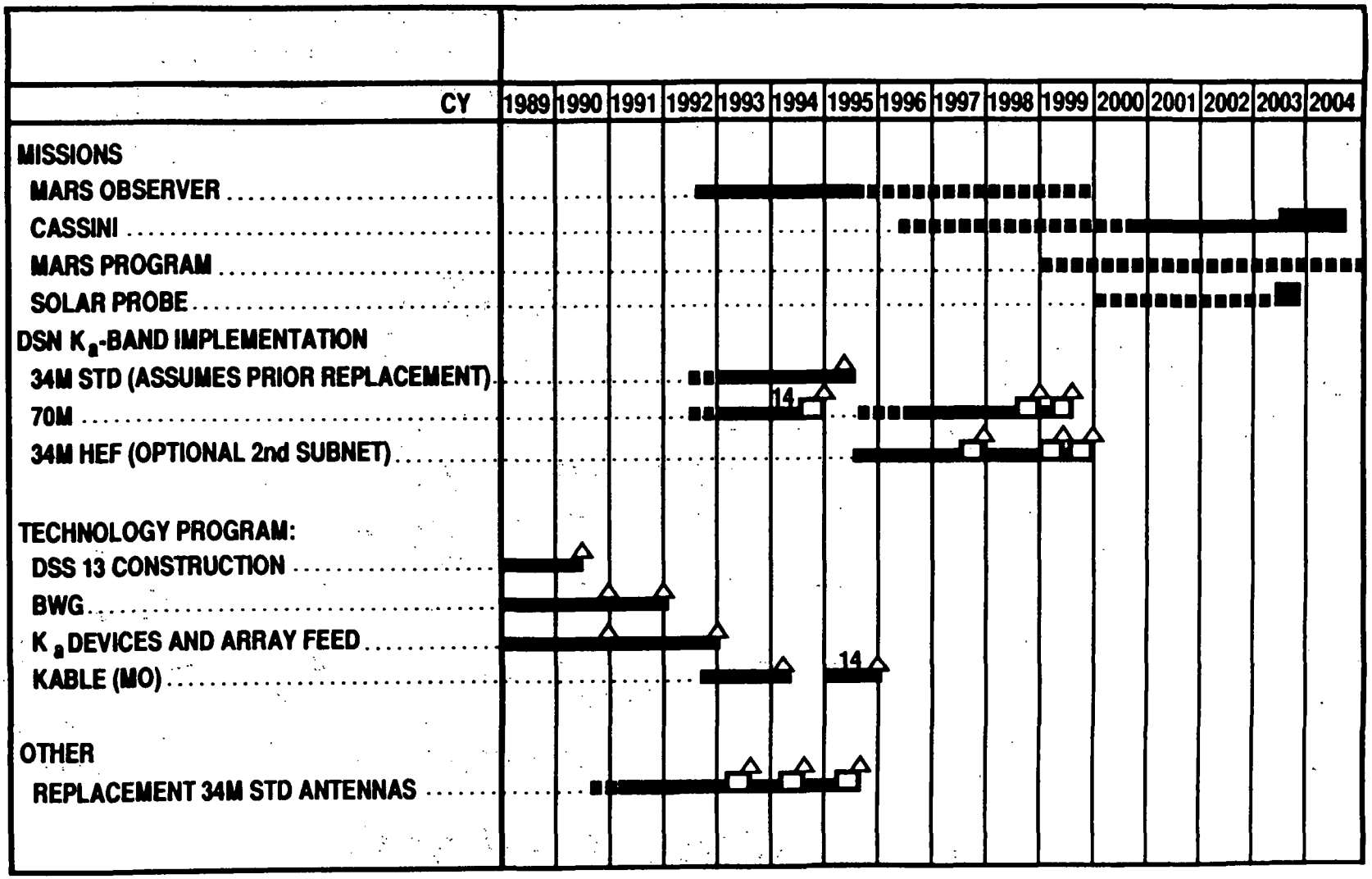

MARS OBSERVER K_a-BAND LINK EXPERIMENT (KABLE)

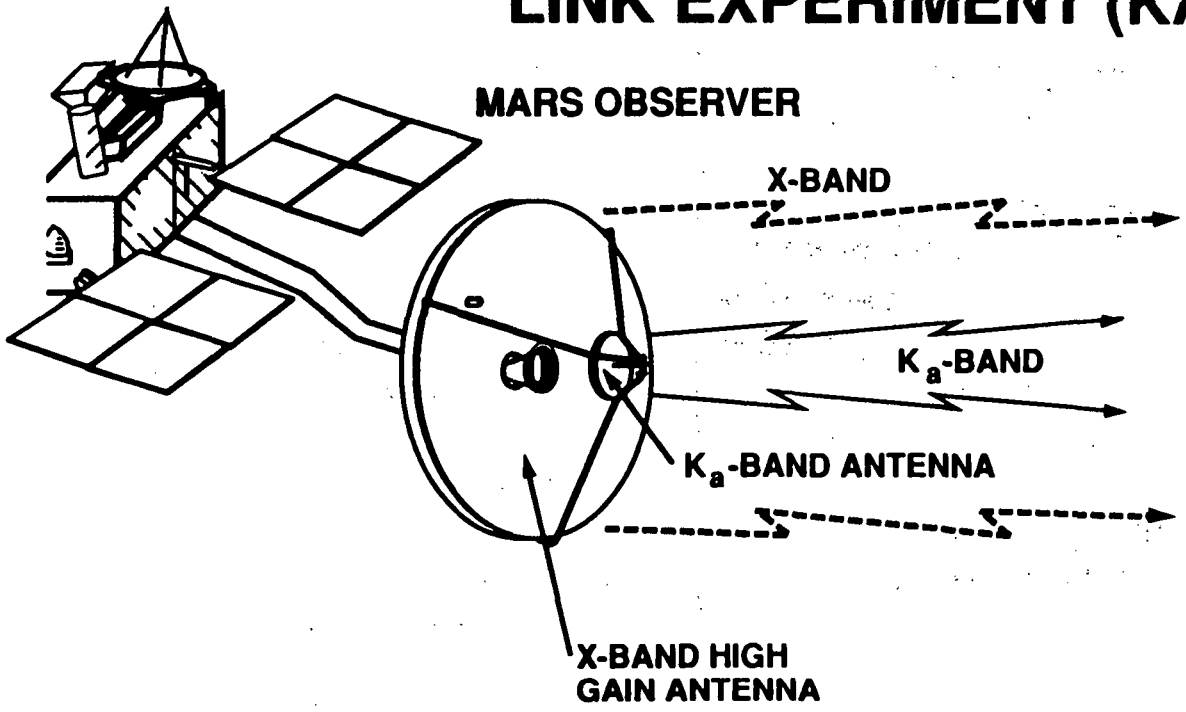

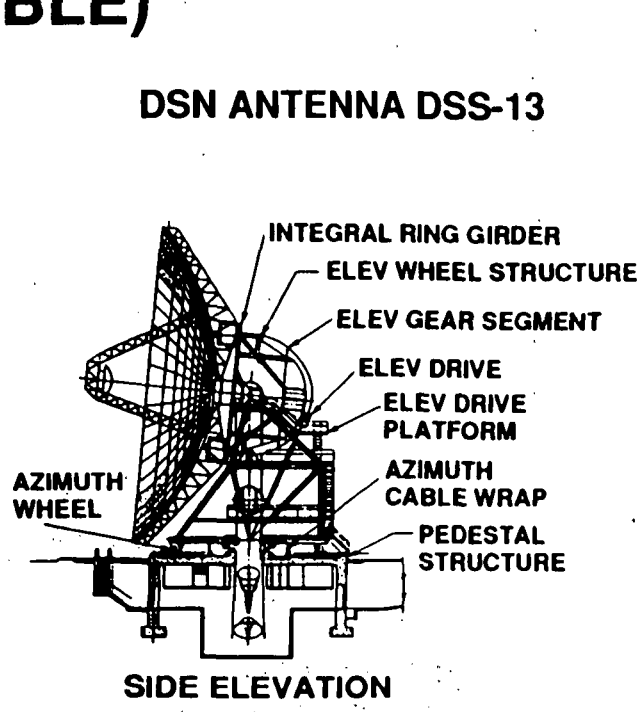

OBJECTIVE

- EVALUATE K_a-BAND LINK PERFORMANCE RELATIVE TO X-BAND OVER THE SAME PATH AND OVER THE DURATION OF THE MISSION

ENHANCEMENT OPPORTUNITY

- DEMONSTRATE ABILITY TO RECEIVE TELEMETRY AT K_a-BAND (EARLY OUTER CRUISE PHASE OF MISSION)
- EVALUATE DOPPLER AND INTERFEROMETRIC NAVIGATION USING K_a-BAND AND X-BAND

MARS OBSERVER
MISSION SCENARIO

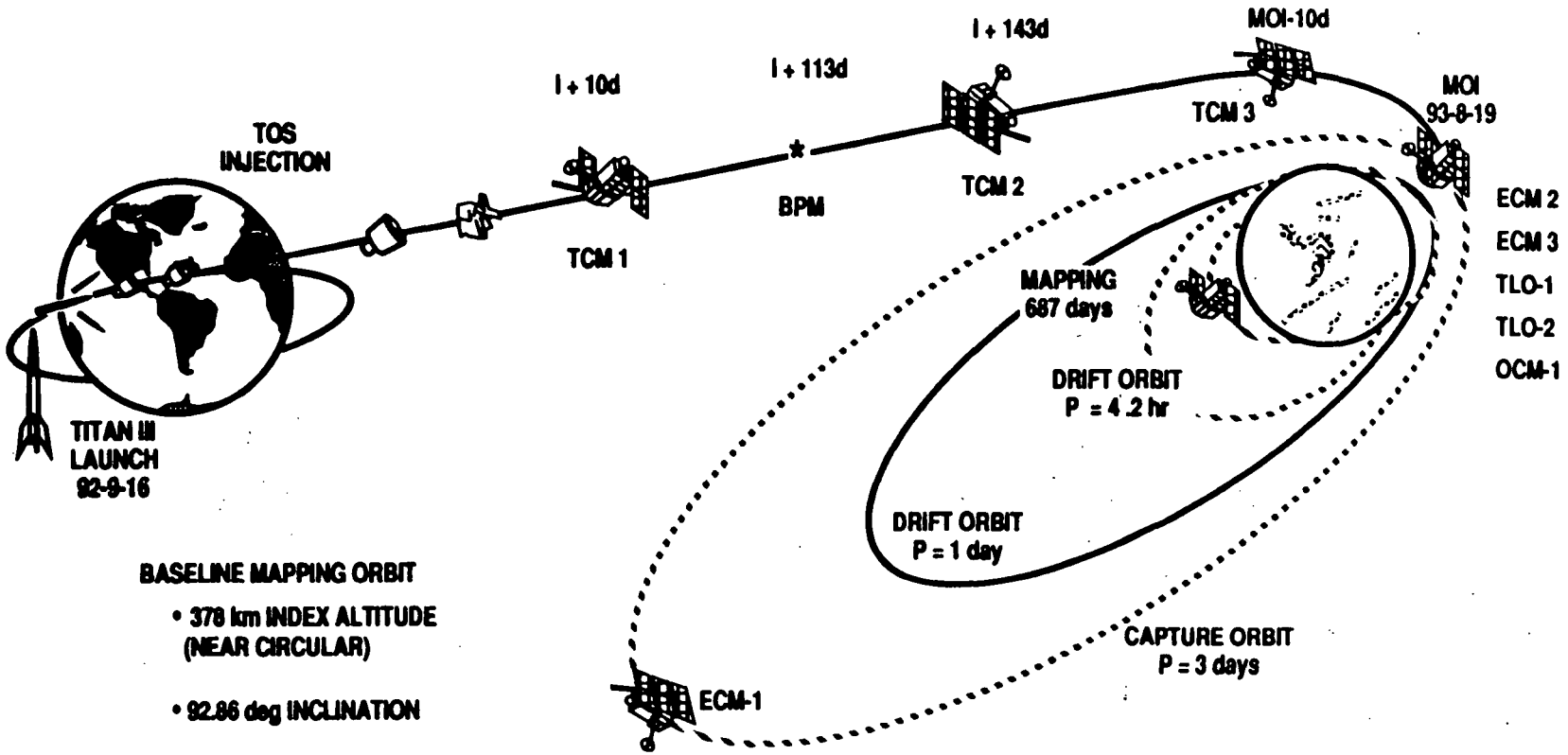

BASELINE MAPPING ORBIT

- 378 km INDEX ALTITUDE (NEAR CIRCULAR)
- 92.86 deg INCLINATION
- SUN SYNCHRONOUS (2 PM DESC NODE)
- 117.5 m PERIOD
- FROZEN (APSIDES)

JPL

MARS OBSERVER
SPACECRAFT CONFIGURATIONS

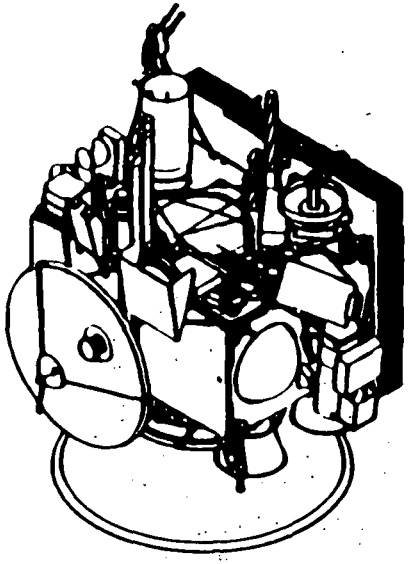

LAUNCH CONFIGURATION

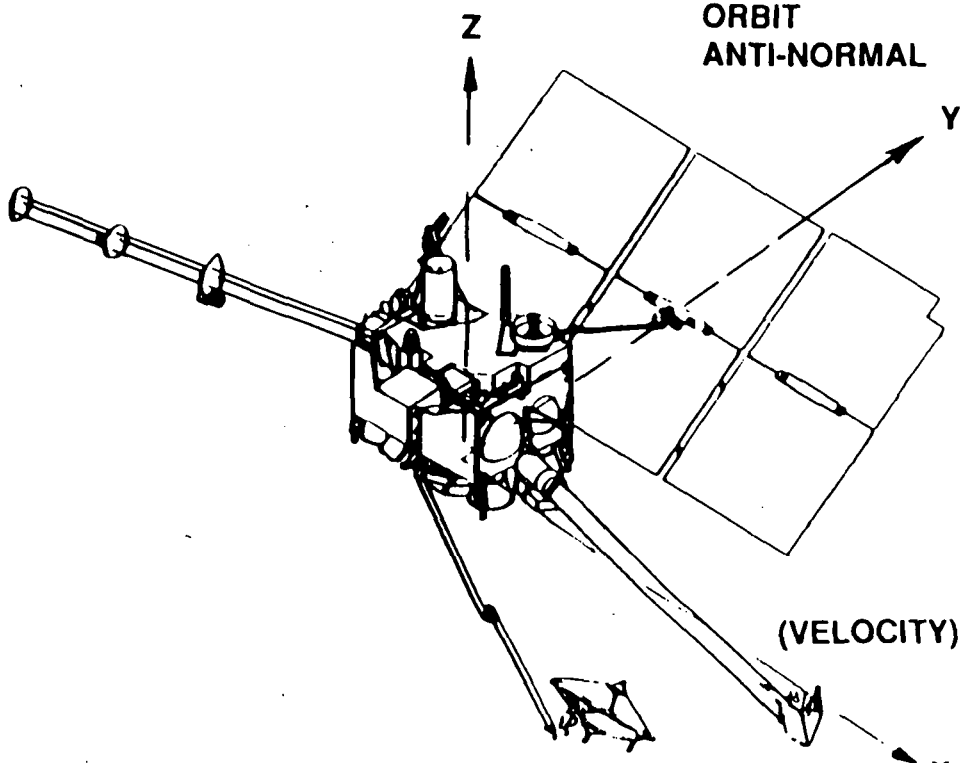

MAPPING CONFIGURATION

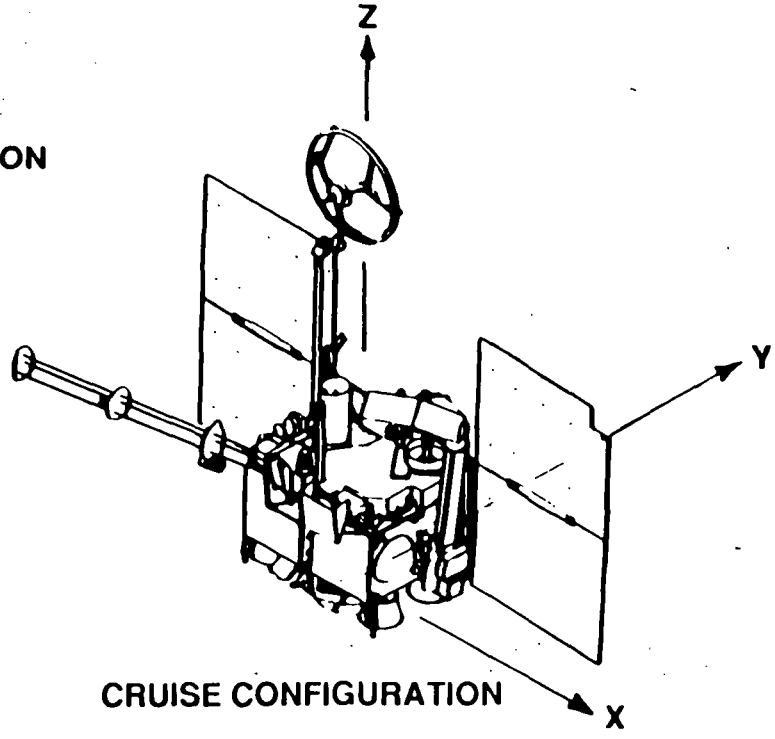

CRUISE CONFIGURATION

MARS OBSERVER

K_a-BAND BEACON PERFORMANCE, 90% WEATHER AT GOLDSTONE, CA

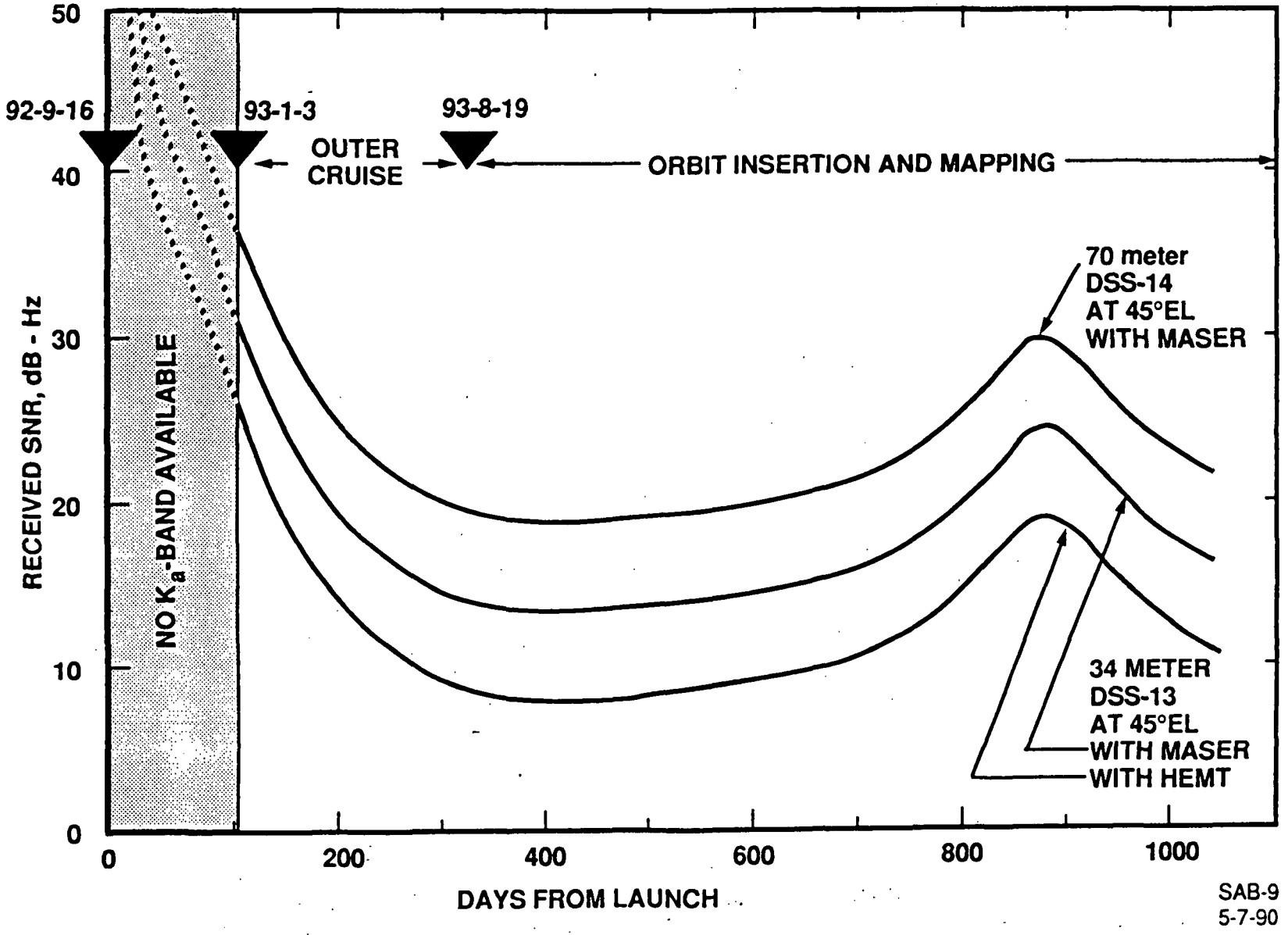

SAB-9
5-7-90

DOWNLINK BUDGETS FOR MARS OBSERVER TO DSN 34M ANTENNA AT GOLDSTONE CA
FOR 90% WEATHER AT 30 DEG ELEVATION

MISSION, DISTANCE AND DATE		MARS OBSERVER AT 2.45 AU, 1994	
SPACECRAFT SYSTEM		X-BAND	K_a-BAND
FREQUENCY	(GHz)	8.42	33.7
XMTR. PWR.	(dBm)	43.0	10.0
ANT. GAIN	(dBi)	40.0	37.0
POINTING LOSS	(dB)	-0.8	-0.5
EIRP	(dBm)	82.2	46.5
SPACE LOSS		-282.4	-294.4
GROUND SYSTEM			
* ATMO. ATTEN.	(dB)	-0.1	-0.4
ANT. GAIN	(dBi)	67.8	78.0
POINTING LOSS	(dB)	-0.1	-0.2
* NOISE	(dBm/Hz)	-184.6	-182.6
SIGNAL/NOISE	(dB-Hz)	52.1	12.1

* VARIES WITH ANTENNA ELEVATION ANGLE AND ATMOSPHERIC CONDITIONS. PROBABILITY IS 90% THAT VALUES WILL NOT BE EXCEEDED

JPL

CASSINI
INTERPLANETARY TRAJECTORY

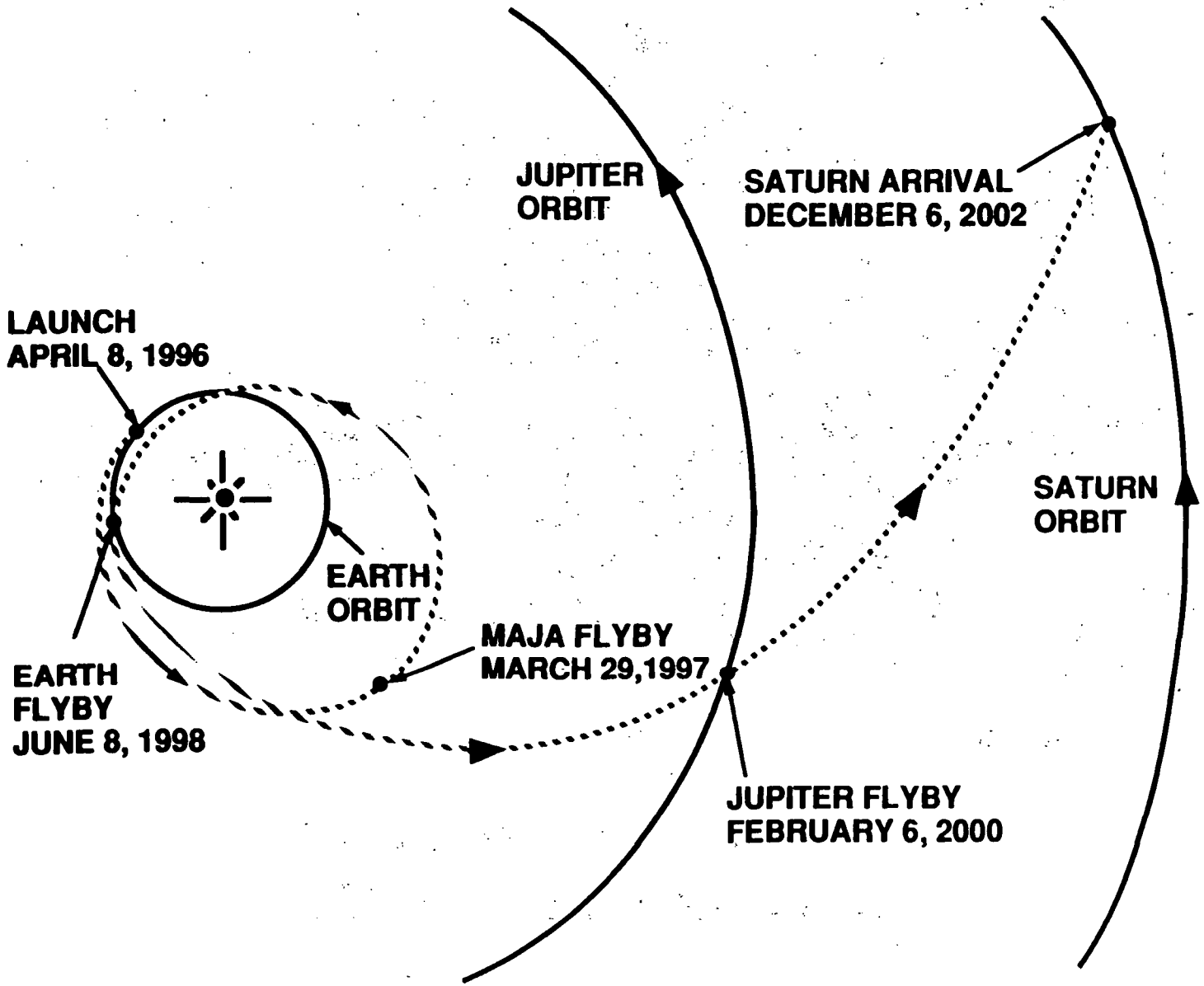

SAB-11
5-7-90

JPL

CASSINI SPACECRAFT
DEPLOYED FRONT ISO VIEW

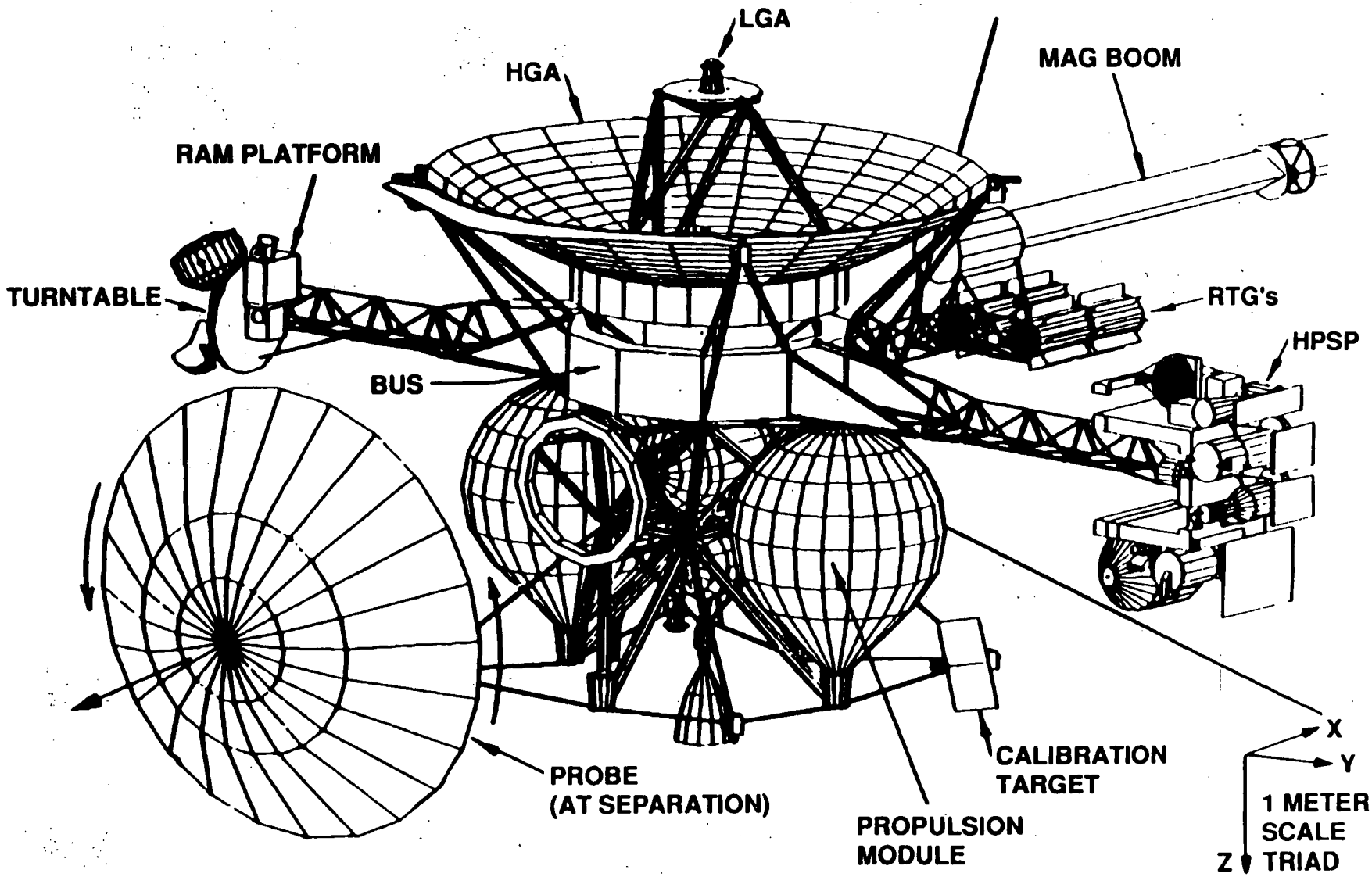

SAB-12
5-7-90

JPL

K_a-BAND ADVANTAGES FOR THE CASSINI MISSION

- REDUCED SPACECRAFT DC POWER (16 Watts) FOR TELEMETRY
- ENHANCED TELEMETRY
  - HIGHER TELEMETRY RATES AT LESS POWER
  - AVOID TAPE RECORDER CAPACITY CONSTRAINT
- IMPROVED RADIO SCIENCE
  - REDUCED PLASMA NOISE
  - IMPROVED SMALL BODY MASS DETERMINATIONS
  - GRAVITATIONAL WAVE DETECTION
- IMPROVED NAVIGATIONAL ACCURACY
  - 4 TO 6 dB REDUCED THERMAL NOISE FOR DOPPLER
  - WIDER BANDWIDTH FOR VLBI

CASSINI K_a-BAND DOWNLINK SYSTEM ASSESSMENT

PARAMETER	BASELINE X-BAND	K_a-BAND
• CLASS	A	A
• FREQUENCY (GHz)	8.4	32.0
• ANTENNA GAIN (DB)	48.3	59.3
• POINTING ACCURACY REQUIREMENT (MRAD, 3σ)	2.0	0.87
• RF POWER OUT (W)	10.6	5.0
• POWER REQUIREMENT DURING DOWNLINK (W)		
• TRANSMITTER DC POWER INPUT	40.0	20.0
• K_a EXCITER	–	3.5
• SUN SENSOR	1.4	2.0
• TOTAL	41.4	25.5
• MAGNETIC TAPE RECORDER	HIGH DUTY CYCLE	LOWER DUTY CYCLE
• MASS (KG)		
• MASS DELTA (REDUNDANT EXC, PWR COND, TWT)	–	16.0
• SUN SENSOR	0.5	1.0
• TOTAL	0.5	17.0
• BENEFITS		
• ACHIEVABLE DATA VOLUME @ 10 AU ON 70M G & M WITH 2 RATES PER PASS (GBITS/DAY)	3.6	8.3
• RADIO SCIENCE	HIGH	HIGHER
• NAVIGATIONAL ACCURACY	HIGH	HIGHER

JPL

SUMMARY

- K_a-BAND OFFERS SIGNIFICANT BENEFITS TO NASA FOR FUTURE MISSION SCIENCE RETURN
- A DEVELOPMENT ROADMAP IS IN PLACE AND BEING FOLLOWED
- PROPAGATION EXPERIMENTS WILL PLAY A KEY ROLE

ATTENUATION STATISTICS DERIVED FROM EMISSION MEASUREMENTS BY A NETWORK OF GROUND-BASED MICROWAVE RADIOMETERS

E. R. Westwater J. B. Snider M. J. Falls
NOAA/ERL/WPL, Boulder, CO.

E. Fionda
Fondazione Ugo Bordoni, Rome, Italy.

Abstract--Two seasons (1987: December through 1988 February; and 1988: June through August) of thermal emission measurements, taken by a multi-channel, ground-based microwave radiometer, are used to derive single-station zenith attenuation statistics at 20.6 and 31.65 GHz. For the summer period, statistics are also derived for 52.85 GHz. In addition, data from two dual-channel radiometers, separated from Denver by baseline distances of 49 and 168 km, are used to derive two-station attenuation diversity statistics at 20.6 and 31.65 GHz. The multi-channel radiometer operated at Denver, Colorado; the dual-channel devices operated at Platteville and Flagler, Colorado. The diversity statistics are presented by cumulative distributions of maximum and minimum attenuation.

I. Introduction

With the deployment of communication satellites such as OLYMPUS, (Brussard, 1988) ITALSAT, (Paraboni, 1989) and ACTS, (Davarian, 1989) there is an increased need to know atmospheric attenuation at frequencies higher than 20 GHz. At these frequencies, attenuation is strongly influenced by water vapor, oxygen and clouds. Currently, there is a lack of information on cloud attenuation and its temporal and spatial variability. Although they are not widely available, dual-frequency microwave radiometers are unique in deriving integrated cloud liquid from attenuation measured during cloudy conditions. In this paper, radiometer data from three locations have been processed to derive both single- and two-station cumulative attenuation distributions. The data given here provide information both on frequency scaling and on-site diversity. Separation distances of 49 and 168 km are examined.

II. Instrumentation

Over the past decade, the Wave Propagation Laboratory (WPL) has designed, constructed, and field-tested several ground-based microwave radiometers to observe the atmosphere (Hogg, et al, 1983). These instruments were designed to run continuously, to provide unattended observations, and to operate in almost all weather conditions. A prototype six-channel radiometer, having channels at 20.6, 31.65, 52.85, 53.85, 55.45, and 58.8 GHz, operates at Stapleton International Airport in Denver, Colorado, USA. All channels point in the zenith direction from the same location and have equal beamwidths of 2.5°. After data processing,

the instrument provides 2-min-average measurements of temperature, precipitable water vapor, and integrated cloud liquid. The radiometer is about 10 m from a U.S. National Weather Service rawinsonde launch facility; hence, ground-truth meteorological data from balloon soundings of temperature, water vapor, and pressure are available twice daily. These radiometers are well known for their meteorological capability (Askne et al., 1986); they are also useful in radio communication studies (Westwater and Snider, 1989). In addition to the currently operating six-channel instrument in Denver (Den), from 1985 to 1988 WPL operated a network of three zenith-viewing dual-channel radiometers in the plains of eastern Colorado. Data from two of the stations, Platteville (Plt) and Flagler (Flg) are analyzed here. The Plt station is separated from Den by 49 km; the distance between Flg and Den is 168 km. Both stations differ in altitude from Den (1.612 km MSL) by less than 150 m. These radiometers operated at 20.6 and 31.65 GHz, and differed from the Denver radiometer by having 5.0° beamwidths. We have experimentally studied the effects of different beamwidths by operating a transportable radiometer that has a 2.5 beam along side each of the network radiometers. The correlation coefficients describing the data taken by the transportable and by the Plt and Flg radiometers were 0.99 and 0.90 (Snider, 1988). For the Den system, we do not derive attenuation from 53.85, 55.45, and 58.8 GHz channels because, even in the clear air, the ambient brightness temperatures from these channels are near saturation. These upper three channels were chosen to measure lower atmospheric temperature profiles.

The dual-channel radiometers are calibrated using the "tipping curve" method (Hogg et al., 1983); emission measurements as a function of elevation angle are required for this method. The 52.85-GHz channel is calibrated by comparing emission measurements with values calculated from radiosondes. Both methods of calibration require clear-sky conditions. The absolute accuracy of brightness temperature measurements is estimated to be about 1 kelvin (K). For an ambient signal level of 100 K, this accuracy is roughly equivalent to an attenuation error of 0.05 dB, or a relative accuracy of 2.4%. By using a well-known relationship derived from the radiative transfer equation, the radiometer output at each operating frequency is related to the atmospheric brightness temperature T_b and total absorption τ (in nepers) by (Westwater, 1978)

$$T_b = 2.75\ e^{-\tau} + T_{mr}(1 - e^{-\tau}) \qquad (1)$$

where T_{mr} is a mean radiating temperature of the atmosphere and 2.75 is the cosmic background brightness temperature (both in kelvins). We further approximate the profile-dependent variable T_{mr} by a constant that is calculated from climatological radiosonde data Westwater, 1978). We solve (1) for τ and compute total absorption (in decibels) from measured T_b by

$$\tau(\mathrm{dB}) = 4.34 \ln \frac{(T_{mr} - 2.75)}{(T_{mr} - T_b)}. \qquad (2)$$

Typical time series of three-frequency data from Den and two-frequency data from Plt are shown in Fig. 1. The sharp maxima in T_b's are due to liquid-bearing clouds; note the different response to clouds for each observing frequency. Generally speaking, the liquid contribution to absorption (and hence to emission) increases as the square of the frequency. The water vapor response is more significant near the 22.235 GHz rotational spectral line. As inferred from the dual-channel radiometers, the precipitable water vapor for this day was about 2.0 cm at each station. However, the onset of continuous liquid-bearing clouds began in Plt at around 1100 UTC and at Den at around 1600 UTC. Isolated clouds occurred at both stations before these times.

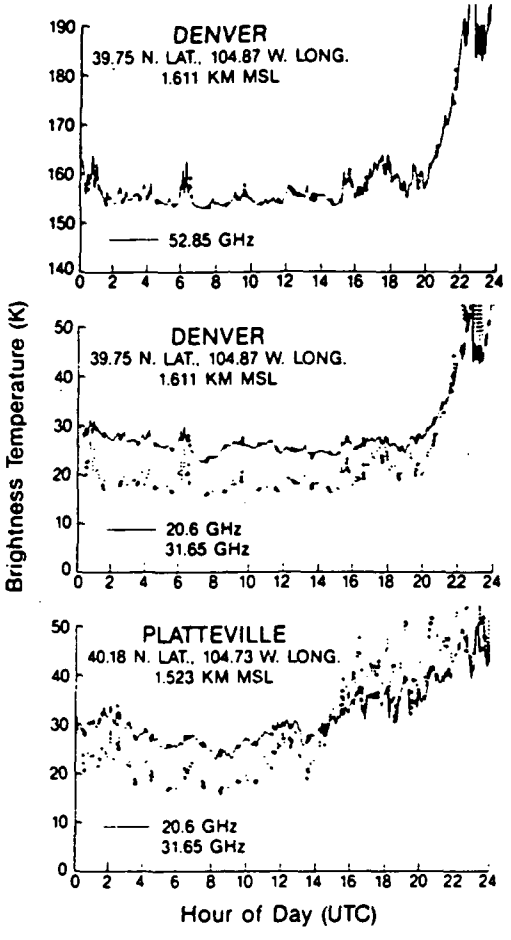

Fig. 1. Time series of zenith brightness temperatures at 20.6, 31.65, and 52.85 GHz. Denver and Platteville, Colorado. 13 September 1988.

III. Attenuation Statistic

Preliminary screening of data was done by visual inspection of 24-h time series. For example, outliers arising from occasional non-zenith observations were eliminated this way. Additional editing required scatter plots displaying the 20.6 and 31.65 GHz data. Outliers detected by this method included those arising from melting snow on antennas or from rain. Roughly, about 15% of the theoretical maximum number of data for both seasons were not available. This percentage also includes power outages and problems associated with communications. To derive joint-station statistics, we placed both the Plt and Flg data into one-on-one correspondence with Den, within a time uncertainty of +/- 1 minute. Then, at each 2-min time interval, if both samples of data from station pairs passed editing, both were included in the statistics; otherwise, both were deleted.

A. Denver-Platteville Statistics

For the Den and Plt locations, we derived summer (July, August,and September) and winter (December, January, and February) statistics; the 52.85 GHz radiometer did not operate during the winter of 1987-1988. The single-station cumulative distributions for Den and Plt are shown in Fig. 2. We note that, in the winter, 2.5 dB is exceeded less than 0.01% of the time. These low values of attenuation are due to the limited amount of cloud liquid water that cold winter clouds can contain. For summer conditions, the presence of greater amounts of precipitable water vapor, as well as of clouds with higher liquid content, gives rise to higher values of attenuation. At 31.65 GHz, for example, values of 5 dB are exceeded about 0.1% of the time. Note that only small differences occur between the statistics for the two locations. Also note the much higher attenuation at 52.85 GHz; this is caused both by the increased oxygen absorption and by the higher attenuation from water vapor and clouds. Based on Den data, a regression analysis using measured attenuations at 20.6 and 31.65 GHz to predict attenuation at 52.85 GHz gave a correlation coefficient of 0.957 and a residual rms prediction error of 0.21 dB.

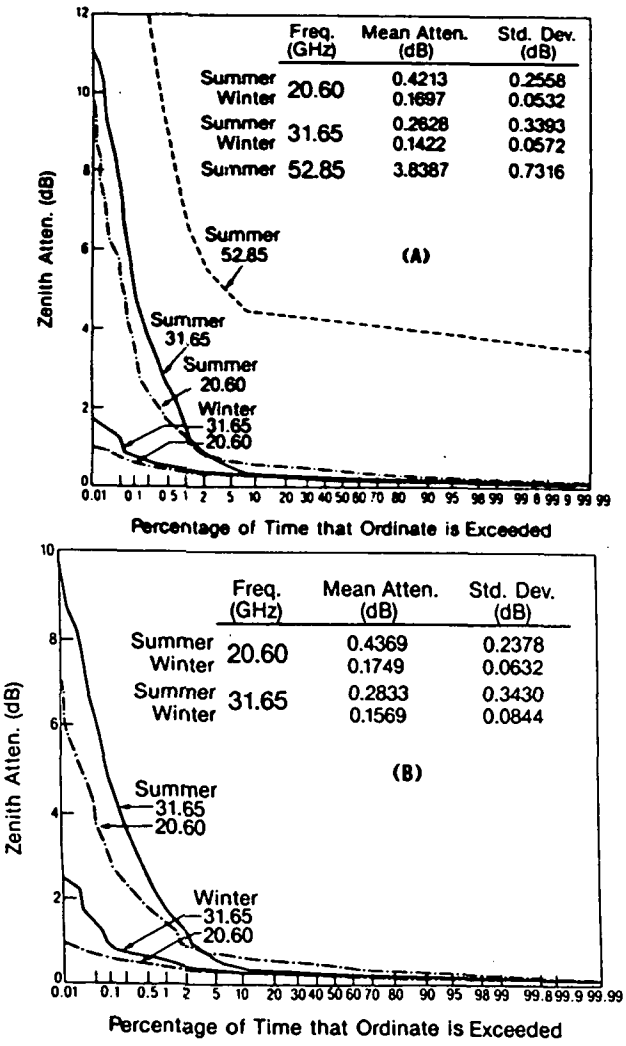

Fig. 2. Single station cumulative distributions of zenith attenuation for (A) Denver, Colorado, and (B) Platteville, Colorado. Sample size: summer-46539; winter-41298.

For the 20.6 and 31.65 GHz channels, we also determined joint-station attenuation diversity statistics for Den and Plt for both the summer and winter seasons. We first constructed time series of the Den and Plt data. Next, for each 2 min time interval, we determined the maximum and the minimum of the two attenuation values. Then, we constructed two additional time series of the minimum and maximum values. From these derived time series, we constructed cumulative distributions for the winter and summer seasons (Fig. 3). We note that, at the 0.01% level, only 1-2 dB is gained by the difference in maximum and minimum attenuation during winter conditions. However, in summer, when significant attenuation from clouds can occur, a margin of 8 dB is gained at 31.65 GHz.

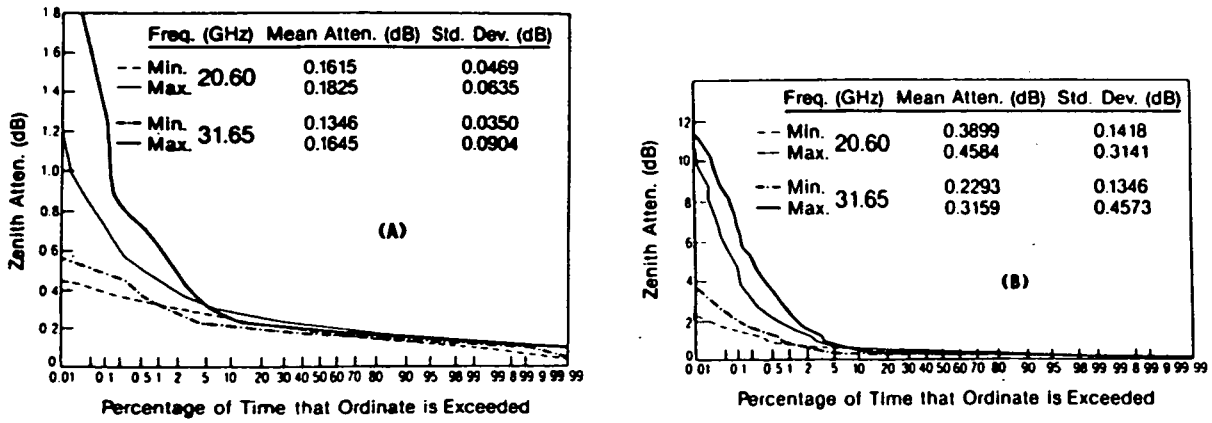

Fig. 3. Joint station cumulative distribution of maximum and minimum zenith attenuation measured at Denver and Platteville, Colorado. (A) Winter 1987/1988; (B) Summer 1988. Sample sizes given in the caption of Fig. 2.

We also determined the percentages of time that measurable cloud liquid ($L \geq 0.04$ mm) was present at Den, at Plt, or at both locations. These results, shown in Table 1, indicate that only slight differences exist between Den and Plt for either of the two seasons. Clouds exist at both stations simultaneously roughly about 6% of the time; conversely, this means that either one or both stations are clear about 94% of the time.

TABLE 1. Percentage of time that measured cloud liquid exceeded threshold of 0.04 mm.

Season	Single Station	$L \geq 0.04$ (mm)
Winter	Den	10.4 %
	Plt	12.2 %
Summer	Den	9.5 %
	Plt	10.6 %

Season	Clouds at both Stations $L \geq 0.04$ (mm)
Winter	5.8 %
Summer	6.0 %

B. Denver-Flagler Statistics

Because of the low values of observed attenuation during the winter (~ < 2 dB), we only derived statistics for Den-Flg during the summer. The single station cumulative distributions at 20.6 and 31.65 GHz are shown in Fig. 4. Note that, because of different sample sizes for the summer period, the Den statistics differ somewhat from those shown in Fig. 2A. The different sample sizes arise because there is a difference in times at which valid data were obtainable at Den-Plt and at Den-Flg. We also show cumulative distributions for the minimum and maximum of the 2-station data in Fig. 5. These results again show a ~ 9 dB diversity gain at 31.65 GHz, and that minimum attenuations of the order of 1 dB are obtainable with diversity at this separation.

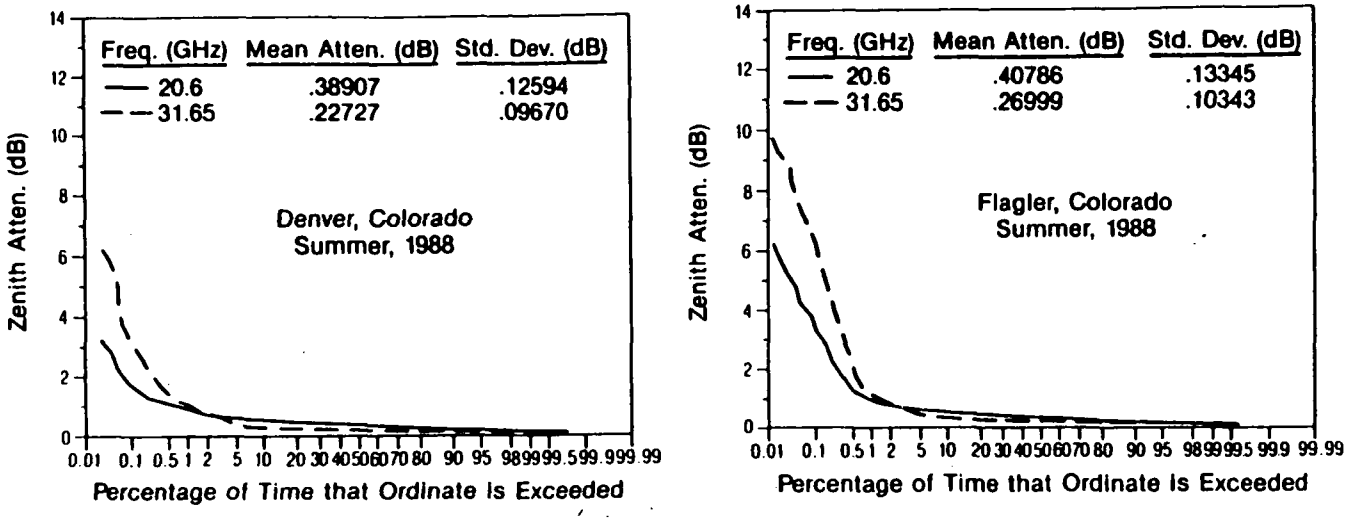

Fig. 4. Single station cumulative distributions of zenith attenuation for (A) Denver, Colorado and (B) Flagler, Colorado. Sample size-40283.

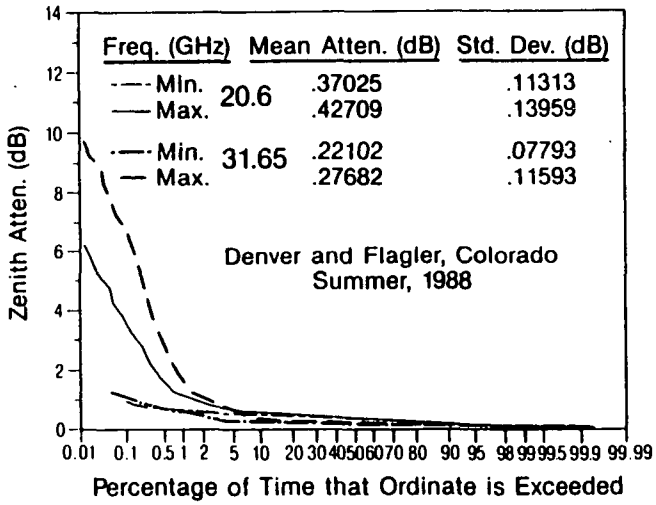

Fig. 5. Joint station cumulative distribution of maximum and minimum zenith attenuation measured at Denver and Flagler, Colorado. Sample size given in caption of Fig. 4.

IV. Summary

In summary, we used ground-based radiometer data to derive both single-station and two-station attenuation statistics for the attenuation range 0 to 12 dB. These statistics were derived at 20.6 and 31.65 GHz in Denver and Platteville, Colorado, for 3-month winter and summer seasons in 1988. In the winter, when integrated amounts of water vapor and clouds are low, attenuations were generally less than 2 dB. In the summer, attenuations of 10-12 dB were exceeded at the 0.01% level. For summer, as much as 8 dB was gained with site diversity (the two stations were 50 km apart). For summer data at stations separated by ~ 170 km again about 8 dB was gained by site diversity. For our data, as shown in Table 1, the effects of liquid bearing clouds could be reduced by about 50% by site diversity. Also, for the summer data at Denver, cumulative attenuation distributions at 52.85 GHz were also derived; 12 dB was exceeded at the 0.5% level. At the same percentage of time level,

0.5%, the attenuation at 31.65 GHz was 2.8 dB and at 20.6 GHz about 1.8 dB. The channel at 52.85 GHz would not ordinarily be chosen as a communication beacon because of the high background of oxygen attenuation; however, the data we present should be useful in estimating 50 GHz attenuation.

In general, radiometric data such as we have presented should be useful in determining the effects of clouds on next-generation communication systems that use frequencies above 20 GHz.

V. Status of Experimental Observations and Data Analysis

Attenuation data were recorded at several locations and frequencies (listed in Table 2) during 1989 and 1990. These data are currently being processed to derive clear and cloudy attenuation statistics, frequency scaling of attenuation, and, where radiosonde data are available, to compare observed clear-air attenuation measurements with absorption calculated from models. Analysis of the Wallops Island data set is nearly complete. Comparisons of measured and calculated absorptions had to be repeated due to errors in the original radiosonde data supplied by NASA/Wallops. However, preliminary results from Wallops (Snider et al., 1989) are still valid.

Table 2. Radiometric Observations of Attenuation during 1989 and 1990.

Location	Time Period	Frequencies (GHz)	Radiosonde Data
Wallops Island, VA	4/11 - 5/8/89	20.6, 31.65, 90.0	Yes
Boulder, CO	9/5 - 10/4/89	20.6, 31.65, 90.0	No
Lacona, NY	12/15/89 - 2/28/90	20.6, 31.65, 90.0	Note 1
Elbert, CO	1/15 - 2/28/90	20.6, 31.65	Note 2

Note 1: Radiosonde observations were made only during storm periods.

Note 2: A limited number of radiosonde observations were made during clear weather; most soundings were obtained during storms.

The dual-channel radiometer employed at Elbert, CO, will be installed near Erie, CO, during June, 1990. Data from this system combined with data from Den and Plt will provide joint attenuation statistics for a new range of spacings as follows:

Erie - Platteville	27 km
Denver - Erie	41 km
Denver - Platteville	49 km.

It is planned to make measurements until approximately 1 December 1990 when the Erie system will be relocated to Elbert, CO, for additional aircraft icing measurements during early 1991.

The three-channel radiometer with steerable antenna will be moved to Virginia Polytechnic Institute and State University (VPI), Blacksburg, VA, in late summer of 1990. The radiometer will be operated for approximately 4 weeks to assist in the calibration of the VPI 20 and 30 GHz radiometers and beacon receivers observing the Olympus satellite. Individual and joint attenuation statistics will be calculated for the two data sets.

References

BRUSSARD, G.: 'Opex-Olympus propagation experiment', Proc. NAPEX XII, 1988, JPL Publ. **88-22**, pp. 140-145.

PARABONI, A.: 'The ITALSAT experiment', Proc. NAPEX XIII, 1989, JPL Publ. **89-26**, pp. 169-188.

DAVARIAN, F.: 'ACTS propagation concerns, issues, and plans', Proc. NAPEX XIII, 1989, JPL Publ. **89-26**, pp. 216-221.

HOGG, D.C., DECKER, M.T., GUIRAUD, F.O., EARNSHAW, K.B., MERRITT, D.A., MORAN, K.P., SWEEZY, W.B., STRAUCH, R.G., WESTWATER, E.R., & LITTLE, C.G. : 'An automatic profiler of the temperature, wind, and humidity in the troposphere', J. Appl. Meteor, 1983, 22, pp. 807-831.

ASKNE, J.I.H., & WESTWATER, E.R.: 'A review of ground-based remote sensing of temperature and moisture by passive microwave radiometers ,' IEEE Trans., 1986, **GE-2A**, pp. 340-352.

WESTWATER, E.R. & SNIDER, J.B.,: 'Applications of Ground-based Radiometric Observations of millimeter wave radiation', Alta Frequenz, Vol. LVIII, N. 5-6, Sept-Dec. 1989, pp. 467-474.

SNIDER, J.B. : 'Verification of the accuracy of a network of water-vapor radiometers', Proc. IGARSS '88 Symposium, Edinburgh, Scotland, 13-16 September, 1988. pp. 19-20.

WESTWATER, E.R.: 'The accuracy of water vapor and cloud liquid determination by dual frequency ground-based microwave radiometry', Radio Sci., 1978, **13**, pp. 677-685.

SNIDER, J.B., JACOBSON, M.D., & BEELER, R.H.: 'Observations of attenuation at 20.6, 31.65 and 90 GHz - Preliminary Results from Wallops Island, VA', Proceedings of the Thirteenth NASA Propagation Experimenters Meeting (NAPEX XIII), 1989, pp. 138-144.

SATELLITE SOUND BROADCAST PROPAGATION STUDIES AND MEASUREMENTS

Wolfhard J. Vogel and Geoffrey W. Torrence

Electrical Engineering Research Laboratory
The University of Texas at Austin
10100 Burnet Rd., Austin, TX, 78758

Abstract--Satellite Sound Broadcasting is an attractive satellite application. Before regulatory decisions can be made in 1992, the propagation effects encountered have to be characterized. The Electrical Engineering Research Laboratory has nearly completed a system which will allow amplitude measurements to be made over 10 MHz bandwidths in the 800 to 1800 MHz frequency range. The system uses transmissions from a transportable tower, and reception inside buildings or in the shadow of trees or utility poles. The goal is to derive propagation models for use by systems engineers who are about to design satellite broadcast systems.

1. Introduction

The advance of fiber-optics technology has helped to focus future development of satellite services into areas where satellites are uniquely competitive. One of these preferred satellite applications is the broadcasting of high-quality sound for stationary or mobile reception by listeners using low-cost, consumer-grade receivers. Before such services can be provided, however, the political hurdles of spectrum allocation have to be surmounted and the technical questions of standardization for world-wide compatibility have to be resolved. In order to arrive at an optimal system design, efficient in the use of our scarce spectral resources, affordable both to the broadcaster and the listener, and providing predictable performance, the propagation effects to which the service is subjected have to be characterized.

Consequently, the objective of the research project described in this contribution is to make basic propagation measurements for direct Satellite Sound Broadcasting Service (henceforth referred to as SSBS). The data obtained should allow the development of propagation models to be used by communications engineers designing the operational systems. Such models shall describe the effects of shadowing and multipath propagation on SSBS receivers operating in a specified environment, such as inside commercial or residential buildings of various construction and also in the shadow of trees or utility poles as might be encountered by transporting or mobile listeners.

Many studies have already been undertaken, concentrating on digital techniques (Miller, 1988; Levey,1988) and estimation propagation effects (Golshan and Vaisnys, 1990) for a hypothetical SSBS system.

The current window of potential SSBS frequencies was opened at the World Administrative Radio Conference dealing with the geostationary satellite orbit (WARC/ORB-88, non-geostationary orbits for SSBS are also under consideration) to include frequencies from 500 MHz to 3 GHz; a definite allocation will probably be made on the same forum in 1992. The study of propagation effects presented here is limited in the sense that (1) measurements will be performed in the frequency sub-range from 800 MHz to 1800 MHz, (2) amplitude characteristics only will be obtained, and (3) for the lack of a suitable satellite the transmitter will be mounted atop a transportable tower.

2. Experiment Description

In the following we give a description of our measurement plans for SSBS. Included are a sketch of a typical measurement setup, a block diagram of the measurement system, specifications of the measurement system, an explanation of our measurement strategy, and a description of typical measurement locations.

2.1 The Measurement Setup

The measurement system is self-contained and based around our LMSS van. The mobility of this design allows us to measure at any location of our choice, as depicted in Figure 1. Visible are (a) the van, (b) a transmitter tower which is mounted to the van and which supports the transmitter amplifier and antenna, (c) an obstacle, such as a tree or building, the effects of which on the propagation of the signal are to be determined, and (d) the receiver antenna, which connects to the receiver and data acquisition equipment in the van through a long cable.

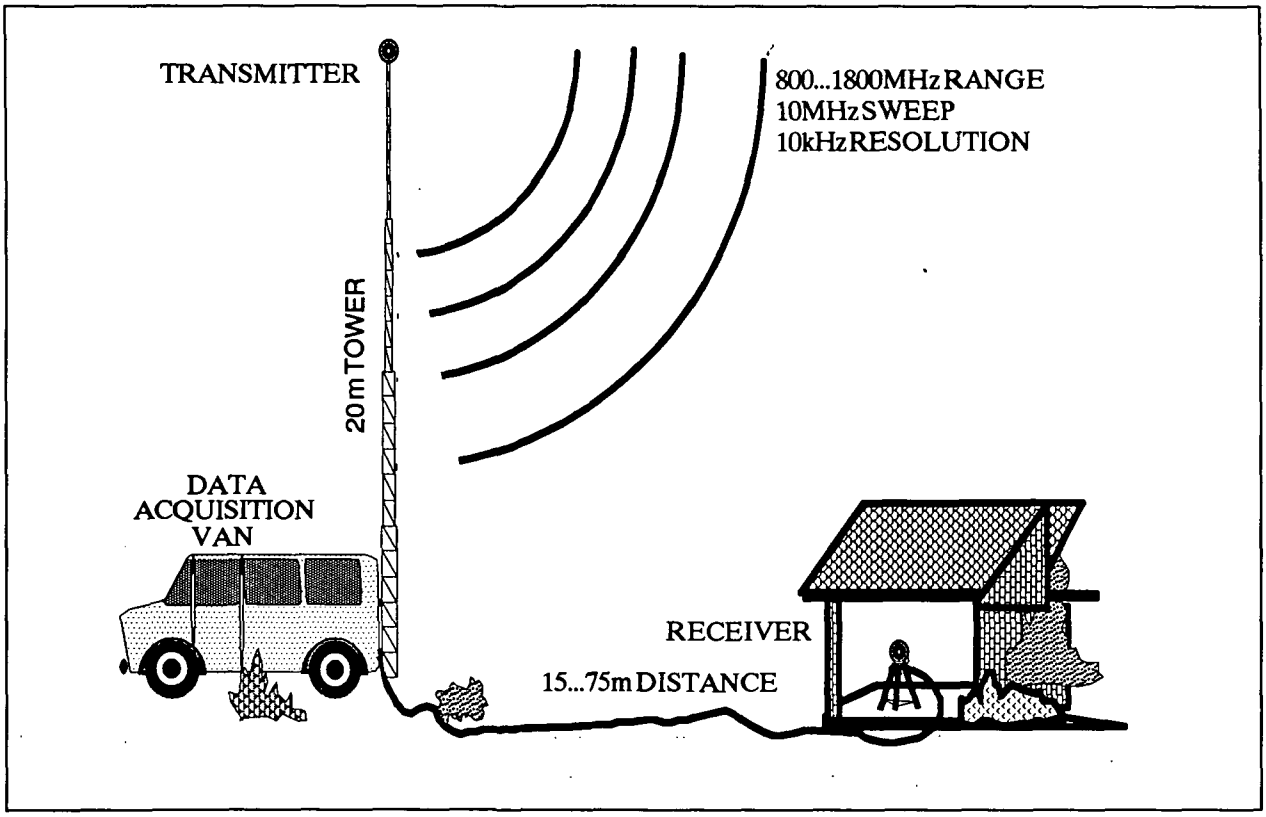

Figure 1: A typical scenario of SSBS propagation measurements in a building.

A typical scenario has the van parked outside of a building or in front of a tree. The tower is cranked up, elevating the circularly polarized transmitter antenna (140° half-power beamwidth) to a height of 20 m above ground. The antenna is pointed with a 30° to 45° depression angle towards the receiver area to be examined. In order to eliminate reflections from the aluminum tower, an absorbing shield is installed just below the antenna. The signal from the transmitter in the van is fed through a cable to the top of the tower, amplified to about 10 mW, and radiated towards the receiver. The receiver front end consists of an antenna and a low-noise amplifier. It is connected to the van through a cable

of about 75 m length. At the measurement location, the receiving front end is mounted to a non-conducting linear positioner which allows the antenna to be moved in small increments over about a 1 m range. The positioner can be adjusted for movement along any direction.

2.2 The Measurement System

Major components of the measurement system shown in Figure 2 are a Tektronix 2756P spectrum analyzer, a Hewlett-Packard 8662A synthesized signal generator, a PC with an IEEE-488 interface controlled by National Instruments LabWindows software, and a frequency converter built by EERL. The PC controls the instruments and displays and stores the data taken. The spectrum analyzer is set to a center frequency between 800 and 1800 MHz with a total frequency span of 10 MHz and a resolution bandwidth of 10 kHz. In this mode, one sweep takes about 5 seconds from the time it has started to the time the 1000 data points are stored on disk. The transmitter frequency is generated by mixing with the first local oscillator of the spectrum analyzer, thus slaving the transmitter to the spectrum analyzer as a tracking generator. The frequency conversion utilizes the synthesized signal generator.

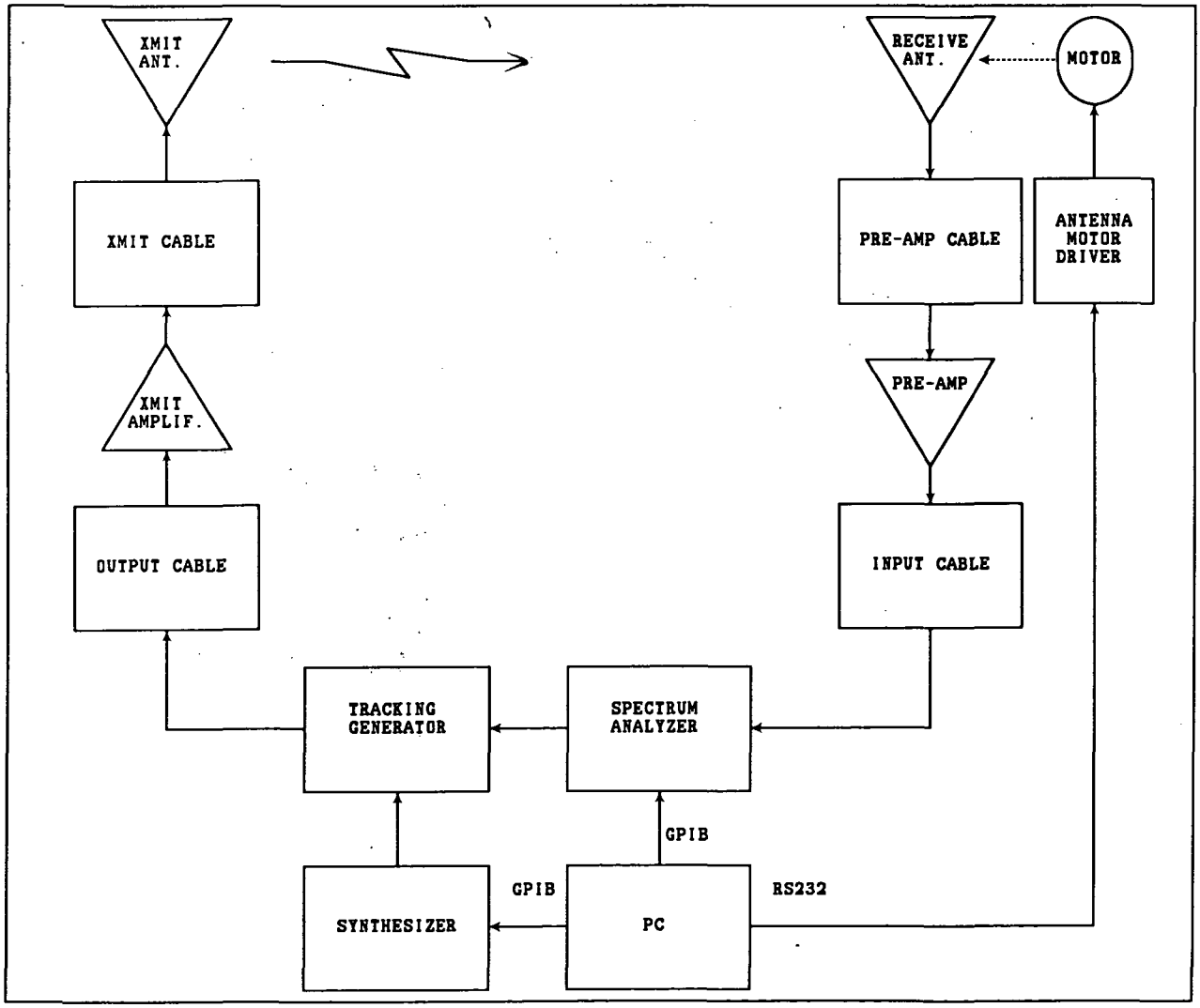

Figure 2: A block diagram of the SSBS measurement system.

2.3 Specifications

The pertinent specifications of the measurement system have been summarized in Table 1. Several different receiving antennas will be used in order to explore the sensitivity of the received signal levels to polarization and antenna size.

Frequency Coverage:	800 to 1800 MHz
Frequency Span:	10 MHz or 0 Hz
Frequency Resolution:	10 kHz
Trmt. Polarization:	RHCP Cavity Backed Spiral
Recv. Polarization:	RHCP Cavity Backed Spiral LHCP Cavity Backed Spiral Disk Cone (Linear Pol.) additional t.b.d.
Typical SNR:	45 dB at 1.5 GHz
Elevation angle range:	15° to 60°

Table 1: SSBS Propagation Measurement System Specifications

2.4 Measurement Strategy and Software

The measurement strategy is concerned with how the data are to be taken. One relevant concern is the presence of radio interference from transmitters within the test window of the spectrum analyzer. The severity of the interference depends very much on the location of the measurements (i.e. city or rural area), the time of day, and the particular center frequency chosen. Spectral surveying has shown that many frequencies can be selected where interference would be of concern only intermittently. For this reason, after tuning to a relatively clear 10 MHz channel near a frequency of interest, each data scan will be preceded and followed by a scan with our transmitter turned off. Any 10 kHz channels with signals present in either of these scans will be marked as invalid for the bracketed scan.

The receiving antenna positioner will be placed in the area to be measured and oriented as desired. At each position of the receiving antenna, scans can be taken at several center frequencies across the coverage of the system (maybe about 200 MHz apart), then the experiment controller will move the receiving antenna about 2.5 cm and repeat the process. This will produce data of path loss as a function of frequency and of location. To get information about the temporal variation of the signal level, scans can either be repeated or the system can operate at a fixed frequency (non-scanning) without moving the receiver.

The software for the PC is designed to run in the National Instrument LabWindows program development environment, where small sub-programs, or modules, are written and debugged using graphical interfaces called panels. Also, extensive use is made of the LabWindows internal functions controlling the graphics display, file handling, array processing, and the IEEE-488 and RS232 interfaces.

The modules are logically arranged in a bottom-up approach, [Figure 3] starting with LabWindows internal functions. At the lowest accessible level are modules controlling a specific hardware instrument, followed by the mid-level module which implements data acquisition procedures, and finally the top-level module which controls the sequence of data acquisition. The top-(main-) module receives instructions and outputs data via a set of files. The instruction file is written by a separate small program which must easily interact with

the operator, and thus must be outside of the LabWindows environment. Each of these levels will now be explained in more detail.

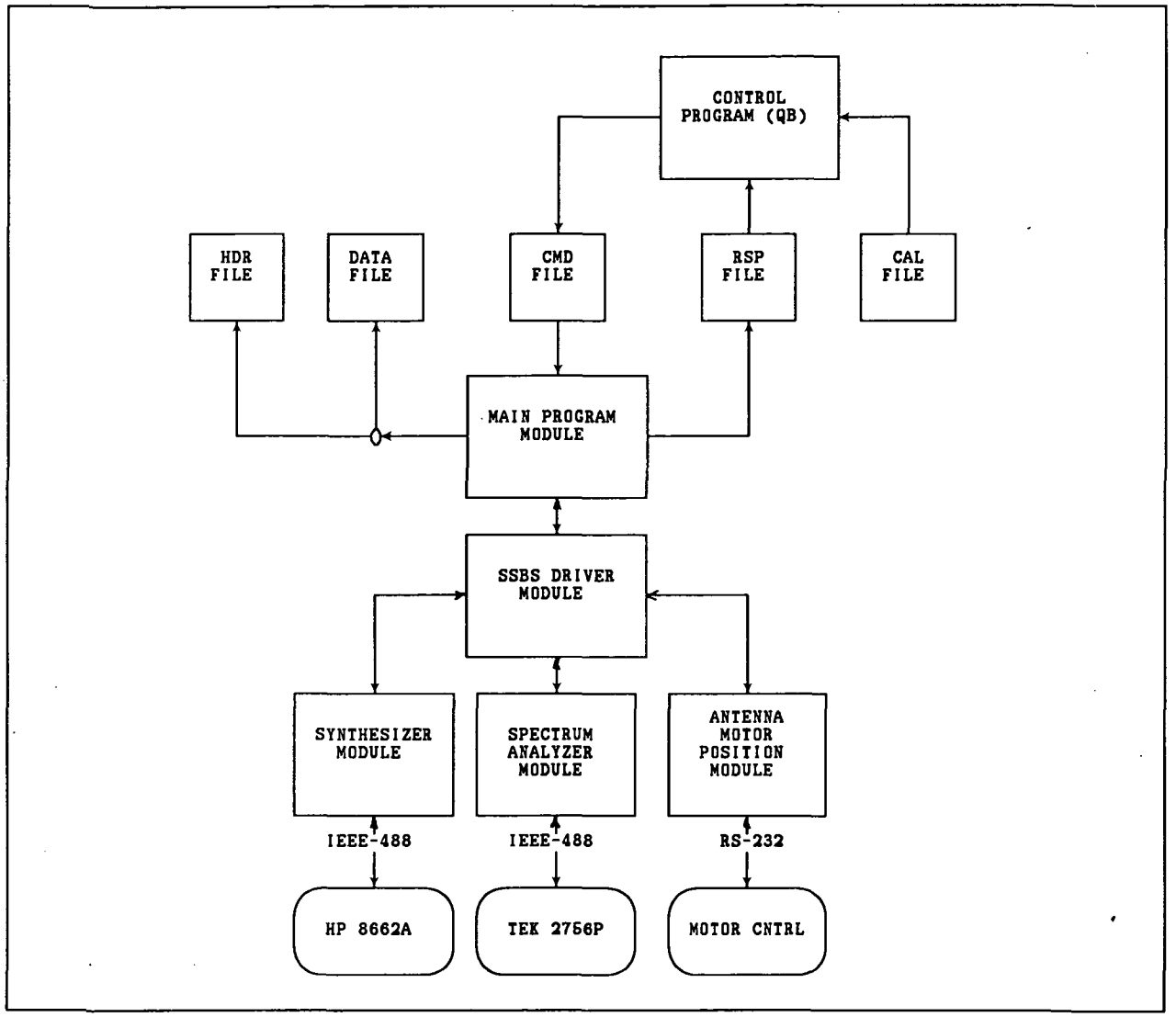

Figure 3: Software Organization for SSBS Measurements

LabWindows Functions: LabWindows implements a subset of the BASIC programming language which is upwardly compatible with Microsoft QuickBasic, which means that the final debugged program modules can all be compiled and linked with QuickBasic. In addition, LabWindows supplies as external libraries all the functions necessary to control the IEEE-488 and RS-232 interfaces, the graphics display and file handling on the PC, and many formatting and array processing functions. All of these libraries, as well as the LabWindows programming conventions and style were used as much as possible as the foundation of the data acquisition program.

HP 8662A Synthesizer Module: Only the basic frequency and amplitude control functions have been implemented as subroutines. The initialization routine does extensive checking to make sure the instrument is responding properly. Because software/hardware interactions are prone to many problems, all of the subroutines include many checks on proper operation.

TEK 2756P Spectrum Analyzer Module: A majority of the functions have been implemented as subroutines. As with the Synthesizer module, the initialization routine does extensive error checking. Control functions, such as frequency range and pre-detection bandwidth, are available. The data is retrieved as a 1000 element integer array scaled to the x-y display coordinates, and a set of conversion factors which are used to transform the array into real numbers scaled to dBm vs. MHz.

Antenna Positioner Module: The antenna positioner, although quite simple compared to either of the above, is implemented as a separate instrument module for programming consistency. It is connected to the PC via the RS232 interface, so initializing the "instrument" is really opening a serial port. Motor motion is controlled by sending single ASCII characters which are decoded as in/out and start/stop. The "instrument" responds with single ASCII character decoded to represent revolutions of the drive screw or hitting one of the end of travel switches. As an example, calling the subroutine AntMotor.advance(3) will send the character for start-forward, wait until three revolution characters have been received, and then send the motor stop character. Receiving an end of travel character would be an error.

SSBS Driver Module: This mid-level module lumps together many of the lower level functions from the above modules into sequences useful for our specific SSBS experiment, in contrast to the above modules which were written to be as general as possible. For example, calling the subroutine GPIB.init not only initializes the three instruments but also sets them into the configuration for this experiment. As another example, calling the subroutine DSSB.err.check checks all of the error flags of all the instruments and libraries and halts the program gracefully with a diagnostic message if an error occurs.

A secondary purpose of this module is to convey parameters to the various instruments and to the display. When a program consists of a number of modules, passing variables from module to module is easy, but must be done very carefully. This program has subroutines specifically for this purpose, although most of them are quite simple.

The main purpose of this module is to implement the procedures, or sequences of functions, used in data acquisition. The two elementary procedures are:

F-Sweep: a single sweep in frequency over an arbitrary 10 MHz, resulting in 1000 samples at 10 kHz spacing.

F-Mono: at an arbitrary time, sample in time for 10 seconds, resulting in 1000 samples at 10 milliseconds per sample.

In both cases, a) the video filter is OFF, b) all samples are average value, c) the vertical scale is 10 dB per division, and d) the tracking generator is ON.

A variation, or special case, of the two basic procedures are 'Pre-' and 'Post-', where the tracking generator is OFF, and the sample is taken with PEAK values. Thus, for example, an F-Sweep measures the strength of the signal received from the tracking generator, and a Post-F-Sweep measures the background noise or RFI level. Also a Pre-F-Mono plus a Post-F-Mono total 10 seconds.

The next two higher level procedures are a combination of the above basic procedures. They accomplish the RFI excised frequency sweep and the temporal stability assessment, respectively.

Frequency Sweep: a three step procedure of

1) Pre-F-Sweep
2) F-Sweep
3) Post-F-Sweep.

If any points in either Pre- or Post- F-Sweeps are above the value of threshold, then the corresponding point in the F-Sweep is blanked (set to an illegal value). Only the F-Sweep array (step 2) is saved to a file.

F-Mono Sweep: a four step procedure of

1) Pre-F-Sweep
2) Pre-F-Mono
3) F-Mono
4) Post-F-Mono.

After step 1, the point of lowest RFI is chosen, based on a sliding 10 pixel average. Steps 2 and 4 give the baseline noise, and peak values over a threshold value indicate RFI. Finally, step 3 gives the peak, RMS, and average values of signal stability. Only the statistics are saved to a file.

The reading of the command file and the writing of the data files are also implemented in subroutines.

Main Program Module: The data acquisition is orchestrated in this module, and is the only module where the procedures are not fixed. The main procedures are as follows.

Frequency Scan: a set of Frequency Sweeps taken in the range of 0.8 to 1.8 GHz. The number of scans and the frequency of each scan are determined from a study of the local RFI environment, and are loaded from the command file and are recorded with the data.

P-Scan: a set of Frequency Scans taken at intervals along the mechanical arm. The number of positions and the spacing between positions are loaded from the command file and are recorded with the data.

Position Scan: a two, four, or six step procedure of

1) F-Mono-Sweep
2) X-axis P-Scan
3) F-Mono-Sweep
4) Y-axis P-Scan
5) F-Mono-Sweep
6) Z-axis P-Scan

A Position Scan results in a set of data files containing a header, statistics, and all the F-Sweep data. If all three axes are done, it takes approximately 1 hour to complete.

Control Program: The Control program is the operator interface. The operator will input the position of the receive antenna relative to the transmit antenna (X,Y,Z), the polarization of the receive antenna, and a comment. The other experiment parameters such as number of frequencies, number of positions, etc., will probably remain unchanged from nominal; but, as an option, everything can be set. For a given position (X,Y,Z), the control program will interpolate from the table and find the free space loss. This value in turn will

be used to normalize the path loss measured by the main program. When all is set, the Command File is written, and the main program is run. After the main program completes, a Response file is written, and the Control program is again run. This time, the results are first displayed, and if all is okay, the process starts over again.

2.5 Measurement Locations

In order to calibrate the system, measurements will be made in an open field of the received line-of-sight signal level as a function of distance from the transmitter over the full range of center frequencies. All the measurements through trees and into buildings will be referred to this reference level. The stability of the system should allow absolute calibration to within about 1 dB, with much better relative calibration. It will be of importance, therefore, to accurately determine the transmitter-receiver distance during the experiment. Prospective measurement sites are:

a) Our laboratory building (single story concrete block exterior, wood frame interior, concrete on steel roof construction),
b) A modern concrete tilt-wall office building,
c) A multi-level parking garage (concrete/steel),
d) Trees at Balcones Research Center (Oak, Pecan, etc.) and at a nearby State Park (Pine),
e) Houses of varying construction (with/without aluminum heat shield, mobile home).

3 Analysis

The data will be analyzed to determine the spectral, spatial, and temporal variations of signal levels due to multi-path propagation and shadowing. Measurement parameters will be the type of receiving antenna used, the presence or not of a person near the receiving antenna, the measurement location and type of shadowing obstacle. Results will include the mean and variance of the signal attenuation as well as correlation distances in the spectral, spatial, and temporal domain.

4 RFI Tests

The RFI environment at our laboratory was tested over the full frequency range from 800 to 1800 MHz and with a 1 MHz bandwidth, in a maximum-hold mode for 20 seconds, 120 seconds and 45 minutes integration time, respectively. Comparing the spectra, it was found that the proposed mode of operation, i.e. acquisition of each 5 second data sweep sandwiched into transmissionless sweeps and excision of any active interference, will be successful in most of the band most of the time.

References

Golshan, N. and Vaisnys, A., "Satellite Sound Broadcasting System, Portable Reception," in Proc. of 13th AIAA ICSSC, Los Angeles, CA, Part 1, pp. 186- 204, March 11-15

Miller, J. E., "Application of Coding and Diversity to UHF Satellite Sound Broadcasting Systems"' IEEE Transactions on Broadcasting, Vol. 34, No. 4, pp.465-475, December 1988

Levey, R. J. (Ed.), "Advanced Digital Techniques for UHF Satellite Sound Broadcasting"' Published by the EBU Technical Center, Bruxelles, Belgium, August 1988

SATELLITE SOUND BROADCAST RESEARCH ASPECT IN CRL

Yoshihiro Hase, Kimio Kondo and Shingo Ohmori
Communications Research Laboratory
893-1, Hirai, Kashima, Ibaraki 314, Japan

Abstract -- Researches on Satellite Sound Broadcasting Services (SSBS) have become active for recent few years. In this paper, activities of the CCIR and WARC, especially about digital systems proposed in the CCIR report, are briefly reviewed. After that, CRL's future plan of SSBS research, stressing propagation rather than communications aspects, is described.

1. Introduction

Researches on Satellite Sound Broadcasting Services (SSBS) have become active for recent few years. The WARC'79 and WARC-ORB'88 issued the recommendation of research on SSBS in 0.5 to 3GHz band to the CCIR. The first report of the CCIR concerning SSBS appeared few years later. The report-955 of Study Group 10/11s is the only one report on SSBS, and includes precise description of communication systems and techniques which may be adopted in future operating systems.

In Japan, SSBS will be operational in Ku-band with broadcasting satellites and/or communications satellites probably in 1990. Though these systems are only for fixed receivers, it is natural that many people will be interested in mobile reception services after fixed reception services have been introduced.

In the following, we review the communication system for SSBS proposed in the CCIR report-955. Subsequently, our plan of SSBS research, especially on propagation, is described.

2. SSBS System in CCIR Report[1]

Some communication systems are proposed in the CCIR report-955 as shown in Table 1. The Advanced Digital II (AD II), which is the most complicated system in the table, must be the final target system. European Broadcasting Union (EBU) made a large

contribution to the development of the AD II system and is pushing its realization.

A highlight of the AD II system is a frequency multiplexing technique called OFDM[2] (Orthogonal Frequency Division Multiplex). Though the total bit rate of stereo sound programs is thought to be several Mbps, the high-rate data stream is distributed into many low-rate narrow-band carriers using the OFDM technique. For example, 16 programs, each of which consists of 16 low-rate QPSK carriers, are transmitted with 256 narrow band carriers as shown in Figure 1. As the frequency difference between each adjacent channels equals the symbol rate of the modulator, the spectral energy of each carrier becomes zero at any other carrier's position. This is why the term "orthogonal" is used.

An advantage of this technique is that it is robust to selective fading because each carrier has narrow bandwidth. Second advantage is the availability of FFT technique for signal demodulation. Only partial calculation in the FFT process is necessary since each program includes only several carriers out of many. Transmitted signal has a sharp and compact spectrum as there are no guard bands. The total required bandwidth for 16 programs is about 4MHz.

This technique also has some disadvantages. One of them is a large inter-modulation effect in on-board transponders. In order to avoid this effect, larger back-off of the on-board transponder may be inevitable.

MASCAM[3] (Masking-pattern Adapted Sub-band Coding and Multiplexing) is a strong source coding technique to reduce the bit rate with almost no degradation of sound quality. Concatenated code (a combination of convolutional code and Reed-Solomon code) is a good candidate of the channel coding technique. Deep interleaving is also considered to be adopted for overcoming shadowing.

3. Some Comments to CCIR Report

The most significantly different aspect of the SSBS link from the LMSS voice or data communication link is the wide-band high-data-rate transmission. Until now, a lot of researches on

propagation and communications have been conducted for LMSS. Most of them, however, were carried out from the viewpoint of narrow-band low-rate communication channels. Though the CCIR report describes also about propagation, most data and descriptions for propagation are obtained from papers on above mentioned LMSS links. We may need to obtain somewhat different propagation data from the viewpoint of high-speed wide-band transmissions.

The OFDM system in the report is rather complex and has been developed to overcome selective fading in low elevation area such as Europe. Selective fading may not be serious in Japan and United States because fairly high elevation angles can be expected. Hence we may be able to adopt a much simpler system.

Antenna size and output power of the satellite depend on the frequency and beam size of the system. Since there are few descriptions about these in the report, we should give more consideration to the feasibility of satellite antennas and transponders.

Anyway, we need more information and data to decide the final system configuration. Analysis of propagation data is a basic strategy for designing new systems.

4. Research Aspect in CRL

The research of SSBS in CRL has just started. In this section, CRL's plan of propagation measurement is discussed. These data should be obtained using low gain omni-directional antennas, because such economical antennas are expected for SSBS.

4.1. Delay Spread

As the elevation angle obtained in Japan is more than 35 degrees, multi-path effect in satellite systems must be much less than that in terrestrial systems. But the delay spread should be measured in order to assess selective fading channel characteristics for high speed wide frequency bandwidth transmissions of SSBS. We can obtain the delay spread data in L-band with ETS-V and an SS(Spread Spectrum) mobile terminal which has been developed for ETS-V communication experiment, though the bandwidth (3MHz) may not be enough for fine resolution.

4.2. Coherent Bandwidth

Though the coherent bandwidth for wide-band transmissions can be calculated from the delay spread data, we may be able to measure more directly and simply by the two carriers method. In this method, receiving levels of two CW carriers with different frequencies are measured simultaneously by a measuring van moving in various areas, especially in cities. Calculation of the cross correlation coefficient of two carriers makes it possible to evaluate the coherent bandwidth. Figure 2 shows an example of raw data of two carrier received levels. Some different variation patterns can be found in this data.

4.3. Fade Duration

Interleaving may become the most powerful technique for SSBS to overcome fading or shadowing, since long delay due to deep interleaving can be permitted in broadcasting services. In order to assess the improvement factor of interleaving, we should analyze fade durations[4] which are thought to be the most suitable data for grasping shadowing channel characteristics. We have a plan to carry out fade duration measurement by not only receiving radio waves but also using optical sensors. The optical sensor consists of a small telescope and a photo diode and it recognizes obstacles by discriminating shadows of obstacles from the background skylight. The resolution of the sensor is to be 5 centimeters at 5 meter distance from the sensor. These values represent the size of leaves of trees and an average distance between mobile antennas and roadside trees, respectively. An advantage of this method is that we can obtain data in any elevation angle without an actual satellite.

4.4. High S/N Measurement

Though it is true that deep interleaving and concatenated code are powerful techniques for overcoming fading and shadowing, enough link margins are still basic strategy. In the CCIR report 955, the link margin is expected to be 10dB or more. It may be better for us to investigate propagation characteristics at around threshold level (ie. 10dB less than the line-of-sight signal level). We have a plan to obtain precise data in shadowed area

with high Signal to Noise ratio measuring equipments. We will have to use very narrow band receiver, which can be realized by audio frequency filter banks or FFT processors. The data will be collected with the measuring van moving very slowly. Phase variation can also be analyzed by complex FFT technique.

5. Summary

Systems proposed in the CCIR report have been reviewed and CRL's plan for SSBS research has been described putting stress on propagation. CRL will also carry out researches on communications and system performances simultaneously. We may be able to make some contributions to the CCIR and WARC in near future.

The most attractive feature of SSBS is that long delay is permissible because of one way transmission. The SSBS may be a suitable service for satellite systems, since shadowing which is the dominant problem in LMSS may be reduced in the case of SSBS by deep interleaving of transmission.

6. References

[1] "Satellite sound broadcasting with portable receivers and receivers in automobiles", CCIR Report 955-1, Study Group X and XI,1989.

[2] M.Alard and R.Lassalle, "Principles of modulation and channel coding for digital broadcasting for mobile receivers", EBU Review, Technical No.224, 1987.

[3] G.Theile, G.Stoll and M.Link, "Low bit-rate coding of high-quality audio signals - An introduction to the MASCAM system", EBU Review, Technical No.230, 1988.

[4] Y.Hase, W.J.Vogel and G.Goldhirsh, "Fade-durations derived from land-mobile-satellite measurements in Australia", IEEE Trans. Communications (to be published).

Table 1. Systems in CCIR Report

System	Simple Digital	Advanced Digital I	Advanced Digital II
Audio BW	15kHz	15kHz	15kHz
Quantization	32kHz/14bits	32kHz/14bits	32kHz/16bits
Codec	---	ADM	MASCAM
Channel coding	yes	yes Convolutional	yes Concatenated
Interleave	---	yes	yes
Modulation/MPX	VSB 2-PSK	QPSK	QPSK/OFDM
Total bit rate	364kbps/mono	408kbps/mono	336kbps/stereo
RF bandwidth	---	400kHz/prog.	4MHz/16 prog.
Link margin	15dB	10dB	10dB

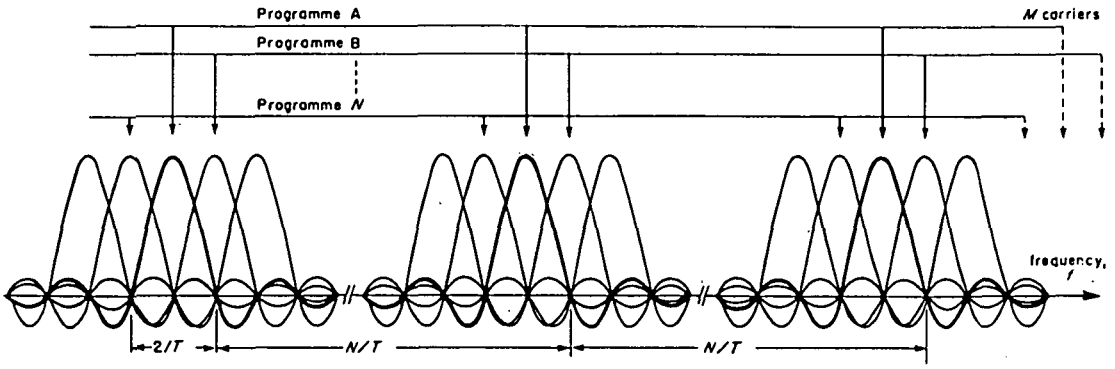

Figure 1. Principle of OFDM

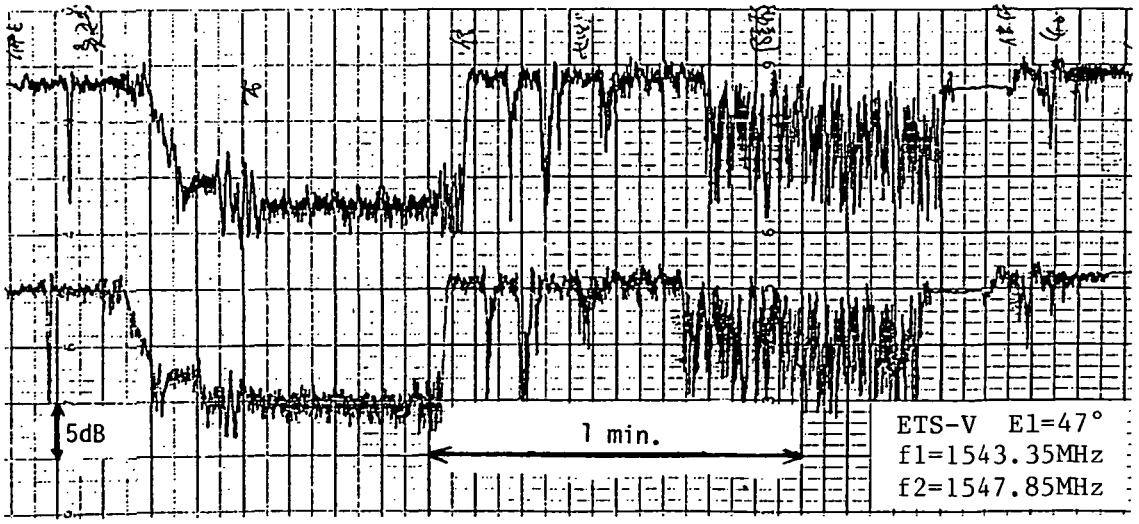

Figure 2. Example data of two carrier receiving

A DESCRIPTION OF RESULTS FROM THE "HANDBOOK ON SIGNAL FADE DEGRADATION FOR THE LAND MOBILE SATELLITE SERVICE"

Julius Goldhirsh *, **Wolfhard J. Vogel** +
* The Johns Hopkins University, APL, Laurel MD
+ The University of Texas at Austin, TX

ABSTRACT During the period 1983-88 a series of experiments were undertaken by the Electrical Engineering Research Laboratory of the University of Texas and the Applied Physics Laboratory of The Johns Hopkins University in which propagation impairment effects were investigated for the Land Mobile Satellite Service (LMSS). The results of these efforts have appeared in a number of publications, technical reports, and conference proceedings (see references). The rationale for the development of a "handbook" was to locate the salient and useful results in one single document for use by communications engineers, designers of planned LMSS communications systems, and modelers of propagation effects. Where applicable, the authors have also drawn from the results of other related investigations. We present here a description of sample results contained in this handbook which should be available in the latter part of 1990.

1. Introduction

The propagation measurement campaigns were performed in the Southern United States (New Mexico to Alabama), Virginia, Maryland, Colorado, and South-Eastern Australia. These experiments were implemented with transmitters on stratospheric balloons, remotely piloted aircraft, helicopters, and geostationary satellites (INMARSAT-B2, Japanese ETS-V, and INMARSAT Pacific). The earlier experiments were performed at UHF (870 MHz), followed by measurements at both L Band (1.5 GHz) and UHF. The satellite measurements were performed at L Band only. The general objectives of the above tests were to assess the various types of impairments to propagation caused by trees and terrain for predominantly suburban and rural regions where terrestrial cellular communication services are impractical. During these campaigns, the receiver system was located on a van outfitted with UHF (870 MHz) and L Band (1.5 GHz) antennas on its roof, and receivers and data acquisition equipment in its interior.

The major LMSS related topics reviewed in the "handbook" are: [1] Attenuation due to individual trees - static case, [2] Attenuation due to roadside trees-mobile case, [3] Signal degradation for line of sight communications, [4] Fade, non-fade duration and phase spread, and [5] Cross polarization, antenna directivity, and space diversity effects. In the following paragraphs we present an overview of results for items [2] and [5] in order to provide a "flavor" of the handbook contents and to examine material not detailed previously.

2. Attenuation Due to Roadside Trees - Dynamic Case

2.1 Empirical Roadside Shadowing Model

Cumulative fade distributions were systematically derived from helicopter-mobile [Goldhirsh and Vogel; 1987, 1989] and satellite-mobile measurements [Vogel and Goldhirsh, 1990] in the Central Maryland region. This formulation is referred to as the "Empirical Roadside Shadowing (ERS)" model. It may be described as follows for P = 1 to 20%

$$F(P,\theta) = -M(\theta)\ln P + B(\theta) \tag{1}$$

where F(P,θ) is the fade in dB, P is the percentage of distance (or time) the fade is exceeded, and θ is the path elevation angle to the satellite. Least square fits of second and first order polynomials in elevation angle θ (deg) generated for M and B, respectively, result in

$$M(\theta) = a + b\theta + c\theta^2 \tag{2}$$

$$B(\theta) = d\theta + e \tag{3}$$

where

$$\begin{cases} a = 3.44 \quad b = .0975 \\ c = -0.002 \quad d = -0.443 \quad e = 34.76 \end{cases} \tag{4}$$

In Figure 1 are given a family of cumulative distributions (percentage versus fade exceeded) for the indicated path elevation angles.

2.2 L-Band Versus UHF Attenuation Scaling Factor–Dynamic Case

Simultaneous mobile fade measurements by Goldhirsh and Vogel [1987, 1989] at L-Band (1.5 GHz) and UHF (870 MHz) have demonstrated that the ratio of fades at equal probability levels is approximately consistent with the square root of the ratio of frequencies over this frequency interval. More specifically, we observed that for f_L = 1.5 GHz and f_{UHF} = 870 MHz

$$F(f_L) \approx 1.31F(f_{UHF}) \tag{5}$$

where the multiplying coefficient 1.31 was shown to have an rms deviation of +/- 0.1 over a fade exceedance range from 1% to 30%.

2.3 Seasonal Effects–Dynamic Case

Seasonal measurements were performed by the authors for the dynamic case in which the vehicle was traveling along a tree-lined highway in Central Maryland (Route 295) along which the propagation path was shadowed over approximately 75% of the road distance [Goldhirsh and Vogel;1987, 1989]. Cumulative fade distributions were derived for March 1986 during which the deciduous trees were totally without foliage. These were compared with similar distributions acquired in October 1985 and June 1987, during which the trees were approximately in 80% and full blossom stages, respectively. For the frequency f = 870 MHz and P = 1% to 30%

$$F(\text{full foliage}) = 1.24F(\text{no foliage}) \tag{6}$$

3. Cross Polarization

By making repeated measurements at co- and cross-polarization for selected runs during the Australian campaign, equi-probability "cross-polar isolation levels, CPI" were determined. The CPI is defined by

$$\mathrm{CPI(P)} = \frac{\mathrm{COPS(P)}}{\mathrm{CRPS(P)}} \tag{7}$$

where COPS and CRPS represent the co-polarization and cross-polarization signal levels at the equi-probability level of fade exceedance, P. The CPI (in dB) was found to follow the linear relation,

$$\mathrm{CPI} = -1.605\mathrm{F} + 18.94 \tag{8}$$

where F is the co-pol fade (in dB).

The rms deviation between the "best fit linear" relation (8) and the data points for the corresponding runs was 0.4 dB. We note from the plot in Figure 2 that the isolation severely degrades as a function of fade level. Hence, the simultaneous employment of co- and cross-polarized transmissions in a "frequency re-use" system is implausible because of poor isolation caused by multi-path scattering into the cross-polarized channel.

4. Effect of Antenna Directivity on Fade Distributions

During the Australian campaign, a number of repeated runs were implemented in which high and low gain antennas were employed. The characteristics of these antennas are given in Table 1. Figure 3 shows a plot of the high gain receiver fade versus the low gain fade over the low gain fade interval of 1 to 15 dB. The data points were found to follow the linear relation

$$\mathrm{F(HG)} = 1.133 * \mathrm{F(LG)} + 0.51 \tag{9}$$

where F(HG) and F(LG) represent the high and low gain fades (in dB), respectively. Agreement between the relation (9) and the data points for F(HG) were within 0.2 dB rms.

We note that the high gain system experiences consistently more fading than the low gain case. For example at 3 and 14.5 dB (of low gain fades), the high gain fades are 4 and 17 dB, respectively, which represent 33% and 17% increases. This slight increase in attenuation for the high gain case occurs because less average power is received via multi-path through the associated narrower antenna beam. On the other hand, the azimuthally omni-directional low gain antenna receives more scattered multi-path contributions resulting in an enhanced averaged received power. It is important to note that because the more directive antenna has a 10 dB higher gain associated with it, the net power received by it is still significantly higher than that received for the less directive antenna. Even at the 15 dB fade level (low gain receiver system), the net received power for the more directive antenna system is larger by 7.5 dB.

5. Diversity Operation

A space diversity simulation has been carried out employing the data base corresponding to approximately 400 km of roadside tree shadowing measurements taken during the Australian campaign [Vogel, Goldhirsh, and Hase; 1989]. Space diversity operation for the LMSS may be envisaged by the scenario of two spaced antennas mounted atop a vehicle where each antenna is fed to a separate receiver system. Because the signal levels at the two separated antennas are likely to be different at any instant of time, rapid switching between the two receiver outputs followed by subsequent processing enable the larger signal to be accessed. Such a dual antenna system should therefore require smaller fade margins for the same driving distance than single terminal operation.

5.1 Joint Probabilities

In Figure 4 are depicted a family of cumulative fade distribution functions derived from the above mentioned simulation. The curve labeled d = 0 represents the single terminal cumulative fade distribution corresponding to the data base described above. The curves labeled d = 1 to 10 m represent the individual joint probability cumulative fade distribution for the indicated antenna separations. Such a distribution represents "the joint probability that two antennas spaced a distance d mutually exceed the abscissa value of fade." We note that the joint probabilities tend to coalesce with increasing antenna separation. That is, the fade distributions for 8 m and 10 m separation show insignificant differences.

5.2 Diversity Improvement Factor

A convenient descriptor for characterizing the improvement in communications for a space diversity configuration is the "Diversity Improvement Factor, DIF" defined by

$$\mathrm{DIF}(F,d) = \frac{P_o(F)}{P_d(F)} \tag{10}$$

where $P_o(F)$ represents the single terminal probability distribution at the fade depth F, and $P_d(F)$ represents the joint probability distribution for an antenna spacing d assuming the same attenuation F is exceeded. We note from Figure 4 that DIF(8,1) $\approx$ 3, which implies that when the antennas are separated 1 m, the equivalent time over which the fade margin of 8 dB is exceeded is three times greater for the single terminal system as compared to diversity pair operation. Hence, assuming an 8 dB fade margin and a 6 minute "down time" for the single terminal case, the outage for the diversity system would only be 2 minutes.

A least square estimate of DIF was derived given by,

$$\mathrm{DIF}(d,F) = 1 + [0.2 \times \ln(d) + 0.23] \times F \tag{11}$$

where d is the antenna separation expressed in m and F is the fade depth in dB. In Figure 5 are plotted a family of curves depicting DIF as a function of fade depth for antenna separations between 1 and 10 m. We note that at the larger separations for any given fade depth, the rate at which DIF increases diminishes rapidly.

5.3 Diversity Gain

The "diversity gain, DG" is a concept defined by Hodge [1978] for an earth- satellite communications system involving two spaced antennas operating in a diversity mode in the presence of precipitation. This concept may also be applied to space diversity operation for the LMSS case as described above. The diversity gain is defined as the fade reduction experienced while operating in the diversity mode at a given exceedance. It is equal to the difference in fades between the single terminal and joint probability distributions at a fixed exceedance level. For example, gleaning Figure 4, we note that the diversity gain at an exceedance of 1% for a 1 m antenna separation is 4 dB. Hence, while the single terminal operation at a 1% exceedance will experience a 12 dB fade, the fade for diversity operation with a 1 m antenna separation is only 8 dB.

In Figure 6 is plotted the diversity gain versus antenna separation for a family of single terminal fade levels. Each single terminal fade uniquely defines an exceedance level. For example, an 8 dB fade occurs at an exceedance level of 3% as is noted from Figure 4. Figure 6 shows that the effect of the antenna separation is dramatic the first 2 meters, beyond which relatively little fade reduction ensues for larger spacings.

5.4 Caveats

Although the above results pertaining to space diversity operation appears inviting, two major caveats must be borne in mind. One, signal fluctuations normally occur rapidly. For example, fade duration statistics derived by Hase, Vogel, and Goldhirsh [1990] have demonstrated that at a fade threshold of 5 dB, the median fade duration distance is 0.5 m. Assuming a nominal driving speed of 25 m/s, a typical switching rate of 20 ms is required. Secondly, there is the added cost for an additional antenna-receiver-processor system.

References

Goldhirsh, J. and W. J. Vogel, "Roadside Tree Attenuation Measurements at UHF for Land-Mobile Satellite Systems," *IEEE Trans. Antennas Propagat.*, AP-35, pp 589–596, 1987.

Goldhirsh, J. and W. J. Vogel., "Mobile Satellite System Fade Statistics for Shadowing and Multipath from Roadside Trees at UHF and L-band," *IEEE Trans. Antennas Propagat.*, AP–37, pp 489–498, 1989.

Hase, Y. W. J. Vogel, and J. Goldhirsh, "Fade-Durations Derived from Land-Mobile Satellite Measurements in Australia," *IEEE Trans. on Commun.*, (in press), 1990.

Hodge, D. B., "Path Diversity for Earth-Space Communication Links,"*Radio Sci.*, Vol 13, No 3, pp. 481–487, 1978.

Vogel, W. J., and J. Goldhirsh, "Tree Attenuation at 869 MHz Derived from Remotely Piloted Aircraft Measurements," *IEEE Trans. Antennas Propagat.*, AP-34, pp 1460–1464, 1986.

Vogel, W. J., and J. Goldhirsh, "Mobile Satellite System Propagation Measurements at L-Band Using MARECS-B2," *IEEE Trans. Antennas Propagat.*, AP–38, pp 259–264, 1990.

Vogel, W. J., and J. Goldhirsh ., "Fade Measurements at L-band and UHF in Mountainous Terrain for Land Mobile Satellite Systems," *IEEE Trans. Antennas Propagat.*, vol. AP-36, pp 104–113, 1988.

Vogel, W. J., J. Goldhirsh, and Y. Hase., "Land-Mobile-Satellite Propagation Measurements in Australia Using ETS-V and INMARSAT-Pacific," *APL/JHU Tech. Rep. S1R89U-037*, 1989 (Laurel, MD; The Johns Hopkins University, Applied Physics Laboratory).

Table 1: Summary of pertinent characteristics for high and low gain receiver antennas used during the Australian campaign [Vogel, Goldhirsh, and Hase: 1989].

Characteristics	Low Gain	High Gain
Type	Crossed Drooping Dipoles	Helix
Gain(dB)	4	14
Nominal Pattern (El)	15° - 70° (fixed)	45° (Principal Planes)
Nominal Pattern (Az)	omni-directional	45°
Polarization	RHCP or LHCP	RHCP or LHCP

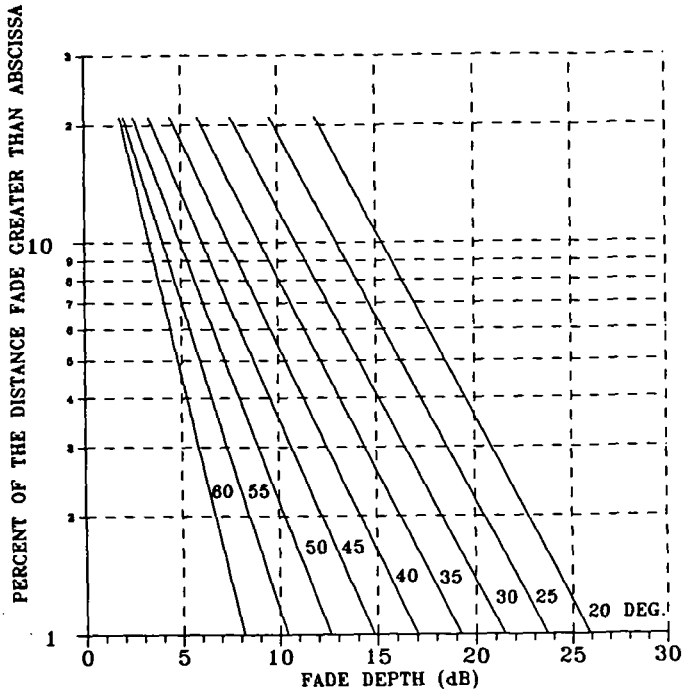

Figure 1: Empirical Roadside Shadowing (ERS) model giving cumulative fade distributions for a family of path elevation angles.

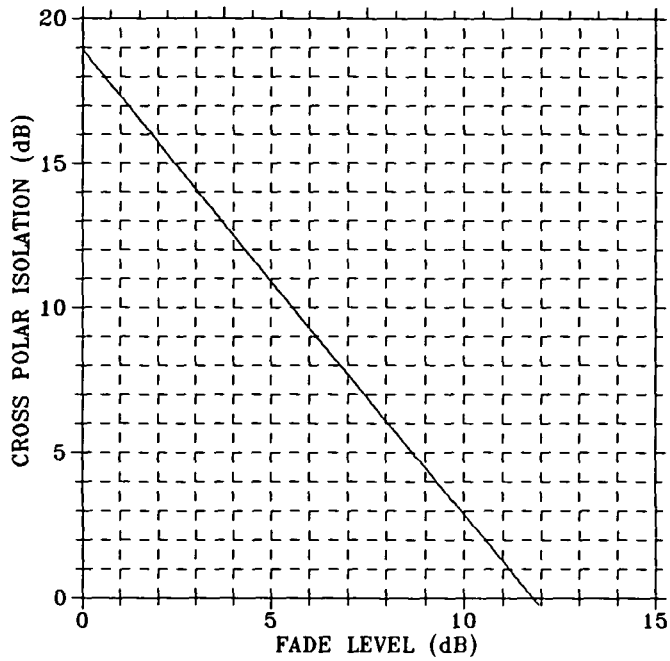

Figure 2: Cross-Polarization Isolation (CPI) as a function of fade depth.

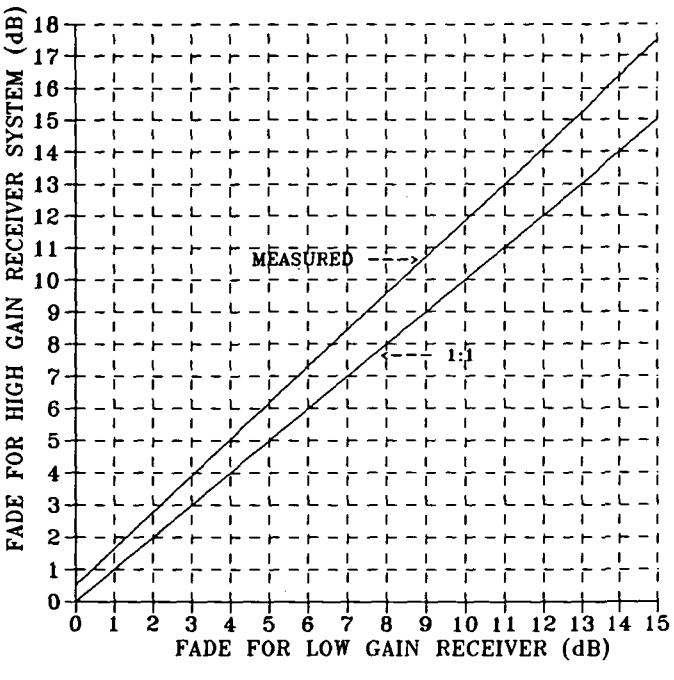

Figure 3: Fades derived from high gain versus low gain antenna systems for roadside shadowing.

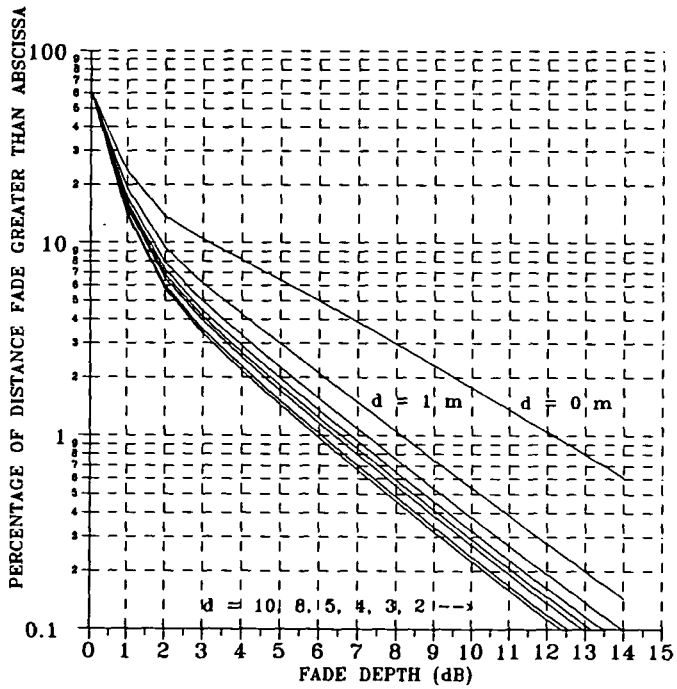

Figure 4: Family of joint probability distributions for various antenna separations corresponding to roadside shadowing.

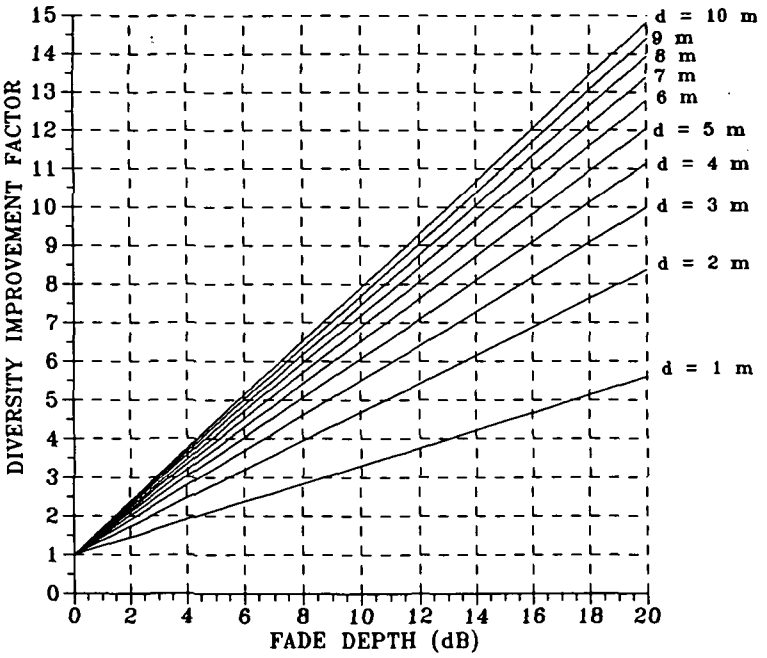

Figure 5: Family of Diversity Improvement Factors (DIF) as a function of fade for various antenna separations.

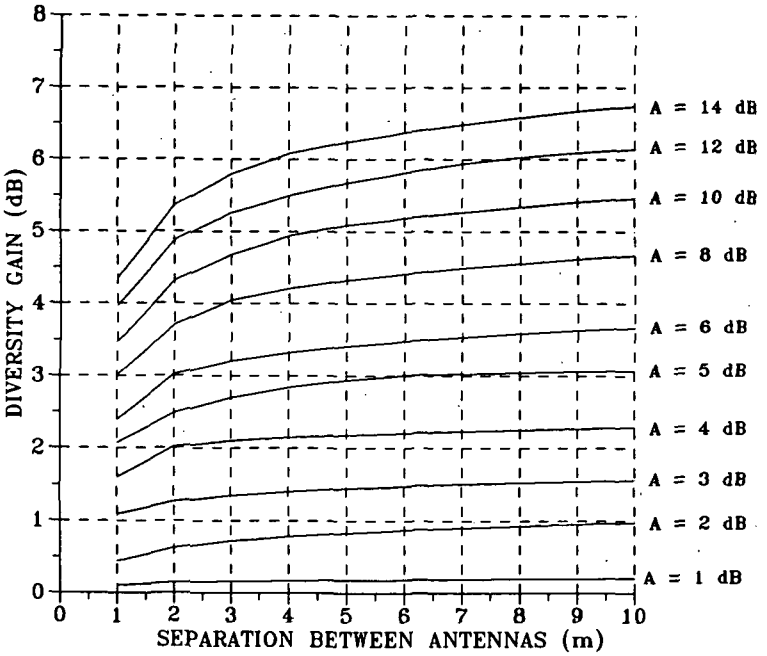

Figure 6: Family of Diversity Gains (DG) versus antenna separations for various single terminal fade depths.

N91-11967

CODELESS GPS APPLICATIONS TO MULTI-PATH: CGAMP

P.F. MacDoran, CCAR, University of Colorado
R.B. Miller and D. Jenkins, Z Systems, Arcadia, CA,
J. Lemmon, Institute for Telecommunication Sciences, NTIA
CU Graduate Students: K. Gold, W. Schreiner and G. Snyder

Summary

CGAMP is meeting the challenge of exploiting the L-band signals from the Global Positioning System (GPS) satellites for the measurement of the impulse response of radio transmission channels over space-Earth paths. This approach was originally suggested by E.K. Smith and has been pursued by J. Lemmon, without an affordable implementation being identifiable (ref. 1). In addition to the high cost of a suitable P code correlating GPS receiver, there is also the major impediment of the often announced Department of Defense SA/AS policy of selective availability /anti-spoof that clouds reliable access to the wideband (20 MHz) P channel of the GPS signals without cryptographic access. A technique proposed by MacDoran utilizes codeless methods for exploiting the P channel signals implemented by the use of a pair of antennas and cross correlation signal detection.

CGAMP System

Figure 1 illustrates the overall configuration of the CGAMP system. The antenna at the upper left in the diagram serves as the system reference with relatively high gain (22 dB) pointed at a selected space vehicle (SV). Because of the reference antenna gain, there is small multipath contamination relative to a broad beamed antenna desired in mobile communications. The second channel of the CGAMP system contains the antenna under test (AUT) with its upper hemispherical response resulting from low gain (e.g., 3 dB gain) and is shown in the upper right of the diagram.

The reference channel utilizes a hybrid digital/analog approach for recovering the P channel digital sequence and controlling its delay without a priori knowledge of the P code sequence. These codeless techniques are contained in references 2 and 3. The P channel is selected from the QPSK modulation using a Doppler shift compensated coherent conversion to baseband to achieve a stationary phase replica of the P code sequence arriving at the reference and AUT antennas at any instant in time.

Although the P code is a priori unknown in the CGAMP system, the system design extracts the direct sequence code chipping at 10.23 MHz, with its associated Doppler shift. It is that digital sequence which is used to suppress and spread the 1575.42 MHz L1 carrier in the GPS satellites. The recovered P code sequence is digitally delayed under computer control in increments of 456 nsec,

the approximate width of the 48 complex channel cross correlation processor, see Figure 2. The delayed digital sequence is then modulated onto the recovered carrier at an intermediate frequency stage of 35.42 MHz. This delayed replica of the P code channel serves as the reference channel for the cross correlation processor. Thus, no matter what pseudo random noise digital sequence is transmitted in the P channel, the signal derived from the reference antenna becomes essentially an exact replica of the signal from the selected SV but can be delayed by desired amounts up to 22.5 usec. That nearly exact replica then serves as the local code reference for correlating with the output of the AUT which contains all GPS satellites in view and is contaminated by multipath.

Because the GPS codes are of the code division multiple access type, the inter-code cross correlation products are very low. Thus, the cross correlation processor is able to select out only the AUT multipath signals caused by the SV in the beam of the reference antenna.

The cross correlation processor (Figure 2) operates with an active mixer, analog multiplier at the 35.42 MHz I.F. with a 500 Hz low pass filter playing the role of the integrator in the cross correlation function. Because the P code is actually available to that portion of the processor, the benefits from spread spectrum process gain are obtained. Specifically, the double sideband P channel chipping rate of 10.23 MHz creates a 20.46 MHz wide signal received at 1575.42 MHz which is coherently converted to an I.F. of 35.42 MHz. The process gain is the ratio of the 20.46 MHz modulation width to the 500 Hz width of the low pass filter following the multiplication operation. Further digital processing will decrease the effective detection bandwidth to even smaller values which will increase the processing gain. Thus, the process gain will be at least 46 dB.

As seen in Figure 3, the CGAMP design incorporates a calibration subsystem which is capable of synthesizing the combination of direct signal arrivals at the two antennas as well as creating a multipath-like signal delayed up to 22 microseconds from the direct signal and of weaker level by 20 dB. The calibrator creates a spread spectrum signal by using a 9 stage shift register clocked at 10.23 MHz which is coherently related to the first local oscillator which is shared between the Reference and AUT channels. The spread spectrum generator sequence can be phased to simulate a multipath arrival out to a delay of 51 microseconds. The system design sensitivity has been set to measure multipath of 17 dB below the direct signal path with total delay spreads up to 20 usec, a delay resolution of 10 nsec and temporal sampling rates up to 100 Hz. Two transportable multi-path measurement systems are in the process of being developed, one for NASA and the other for the ESA.

The following section will deal with the analytical equivalence of the CGAMP approach with those of the more conventional channel probe methods.

Relationship between CGAMP and Conventional Channel Probe

The objective of the codeless GPS approach to multipath measurements is to measure the equivalent baseband impulse response of transmission channels over space-Earth paths using signals from the GPS satellites. It is therefore important to have a clear understanding of the correlator outputs in the proposed multipath measurement system and of their relation to the baseband impulse response.

In past channel probes designed and built at the Institute for Telecommunication Sciences the transmitted probe signal consists of a carrier which phase-modulated by a pseudonoise (PN) code; in the probe receiver the received signal is multiplied by locally generated probe signals which are in phase quadrature and in which the PN code is generated by a "slow" clock. Thus, the locally generated code is allowed to slip slowly in time relative to the received code. The resulting products of the received and locally generated signals are then bandpass filtered, so that for a given value τ of the time lag between the received and locally generated codes, the outputs of the in-phase and quadrature channels of the probe receiver can be written as

$$I=\int_0^T P(t-\tau)\cos\omega t[R_I(t)\cos\omega t+R_Q(t)\sin\omega t]\,dt$$

$$=\frac{1}{2}\int_0^T p(t-\tau)R_I(t)\,dt \propto h_I(\tau) \qquad (1)$$

and

$$Q=\int_0^T P(t-\tau)\sin\omega t[R_I(t)\cos\omega t+R_Q(t)\sin\omega t]\,dt$$

$$=\frac{1}{2}\int_0^T P(t-\tau)R_Q(t)\,dt \propto h_Q(\tau) \qquad (2)$$

where P(t) is the binary-valued (± 1) PN code, R_I and R_Q are the baseband in-phase and quadrature components of the received signal, respectively, and T is the integration time associated with the bandpass filters. Since the received signal is the convolution of the impulse response of the transmission channel with the transmitted signal, expressions (1) and (2) correspond to the convolution of the impulse response with the autocorrelation function of the PN code. Thus, for a sufficiently impulsive autocorrelation function (sufficiently high chip rate of the PN code), (1) and (2) correspond to h_I and h_Q, the in-phase and

quadrature components, respectively, of the complex baseband impulse response of the radio channel.

In the codeless GPS approach to channel probe measurements the signal from the high gain reference antenna is used in lieu of a locally generated signal. The reference signal is delayed relative to the signal from the antenna under test in two stages: a "coarse" time delay τ_c which takes place at baseband and a "fine" time delay τ_f which takes place at IF. The quad divider acts on the signal from the antenna under test. Thus, the I and Q channel outputs, analogous to (1) and (2) above, are

$$\begin{aligned} I &= \int_0^T P(t-\tau_c-\tau_f)\cos\omega(t-\tau_f)\,[R_I(t)\cos\omega t + R_Q(t)\sin\omega t]\,dt \\ &= \frac{1}{2}\int_0^T P(t-\tau_c-\tau_f)\,[R_I(t)\cos\omega\tau_f + R_Q(t)\sin\omega\tau_f]\,dt \\ &\propto h_I(\tau_c+\tau_f)\cos\omega\tau_f + h_Q(\tau_c+\tau_f)\sin\omega\tau_f \end{aligned} \tag{3}$$

and

$$\begin{aligned} Q &= \int_0^T P(t-\tau_c-\tau_f)\cos\omega(t-\tau_f)\,[-R_I(t)\sin\omega t + R_Q(t)\cos\omega t]\,dt \\ &= \frac{1}{2}\int_0^T P(t-\tau_c-\tau_f)\,[-R_I(t)\sin\omega\tau_f + R_Q(t)\cos\omega\tau_f]\,dt \\ &\propto -h_I(\tau_c+\tau_f)\sin\omega\tau_f + h_Q(\tau_c+\tau_f)\cos\omega\tau_f \end{aligned} \tag{4}$$

where P(t) is the GPS P-code, and R_I and R_Q are the baseband in-phase and quadrature components of the signal from the antenna under test. Although the I and Q channel outputs in (3) and (4) do not correspond to h_I and h_Q, it is easy to see that

$$I^2+Q^2 \;\propto\; h_I^2(\tau_c+\tau_f)+h_Q^2(\tau_c+\tau_f) \tag{5}$$

and that

$$h_I(\tau_c+\tau_f) \;\propto\; I\cos\omega\tau_f - Q\sin\omega\tau_f \tag{6}$$

and

$$h_Q(\tau_c + \tau_f) \propto I \sin \omega\tau_f + Q \cos \omega\tau_f. \quad (7)$$

The phase ϕ of the impulse response can therefore be obtained from I and Q by computing

$$\phi = \tan^{-1} \frac{h_Q}{h_I} = \tan^{-1} \frac{I \sin \omega\tau_f + Q \cos \omega\tau_f}{I \cos \omega\tau_f - Q \sin\omega\tau_f} \quad (8)$$

$$= \tan^{-1} \frac{Q}{I} + \omega\tau_f.$$

Thus, the correlator outputs in CGAMP yield the same information (amplitude and phase of the impulse response) as conventional channel probes.

REFERENCES

1. Lemmon, John J., "MULTIPATH MEASUREMENTS FOR LAND MOBILE SATELLITE SERVICE USING GLOBAL POSITIONING SYSTEM SIGNALS," Proceedings of the NAPEX, May 1988.

2. Spilker, J.J., Digital Communications by Satellite, Prentice-Hall, Inc., Englewood Cliffs, New Jersey, 1977

3. MacDoran, P.F., R.B. Miller, L.A. Buennagel, H.F. Fliegel, and L.Tanida, "Codeless GPS Systems for Positioning of Offshore Platforms and 3D Seismic Surveys", NAVIGATION: Journal of the Institute of Navigation, ION Vol. III on the Global Positioning System, Pgs 147 to 159, 1986.

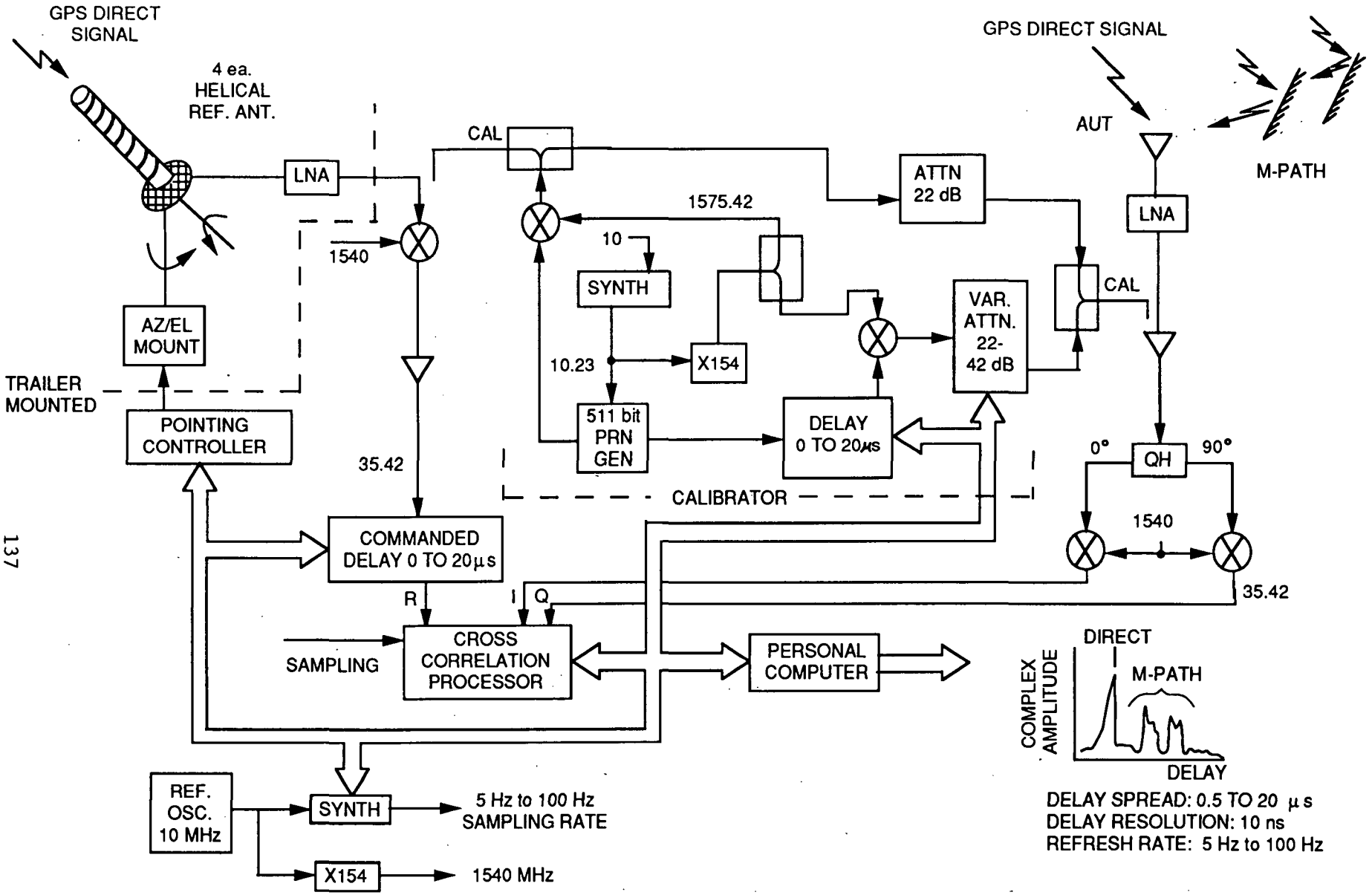

CODELESS GPS APPLICATIONS TO MULTI-PATH (CGAMP)

FIGURE 1

UNIVERSITY OF COLORADO

PFM
14MAY90

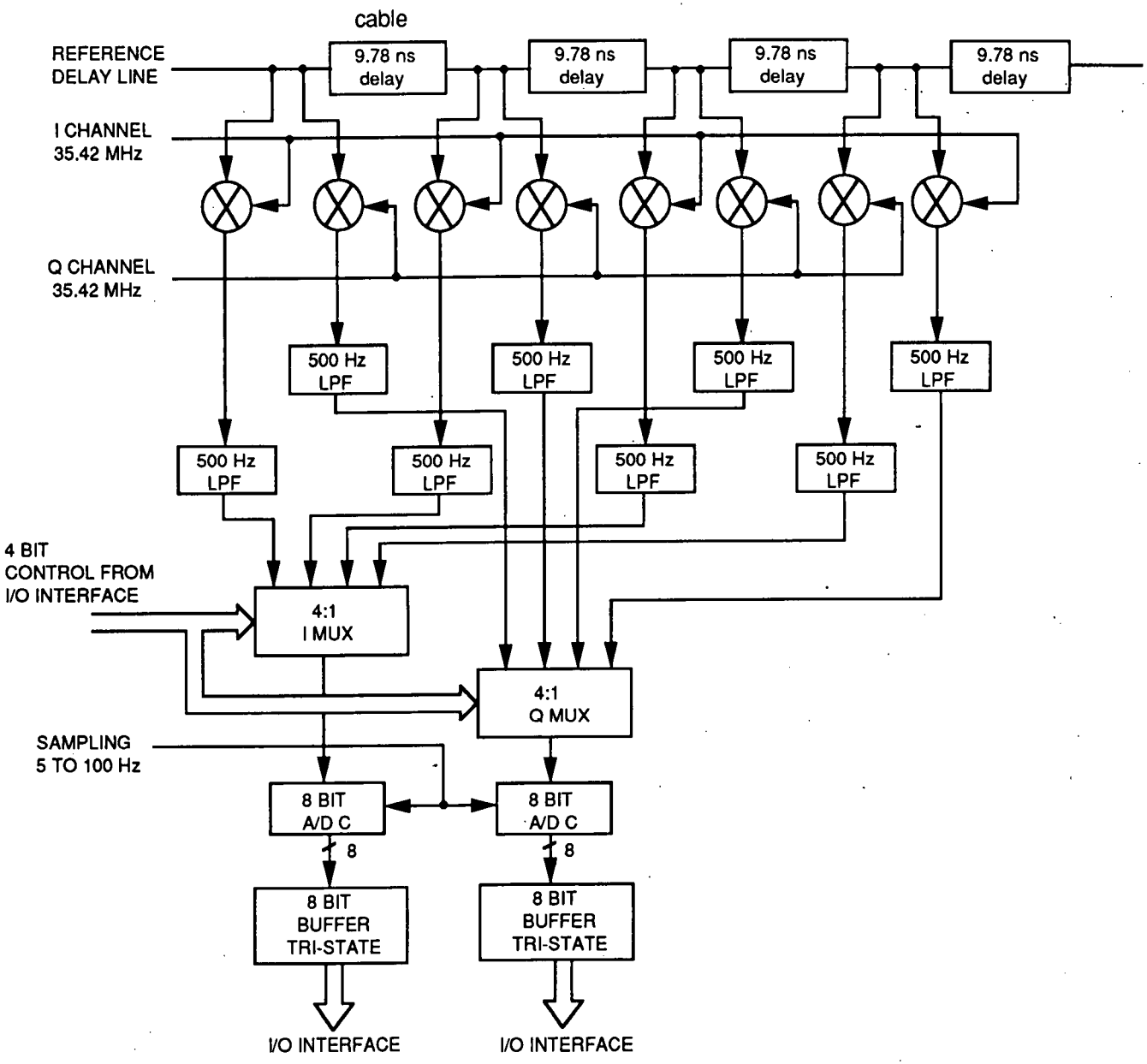

FOUR CHANNEL COMPLEX CORRELATOR BOARD (12 REQUIRED)

14MAY90

UNIVERSITY OF COLORADO

FIGURE 2

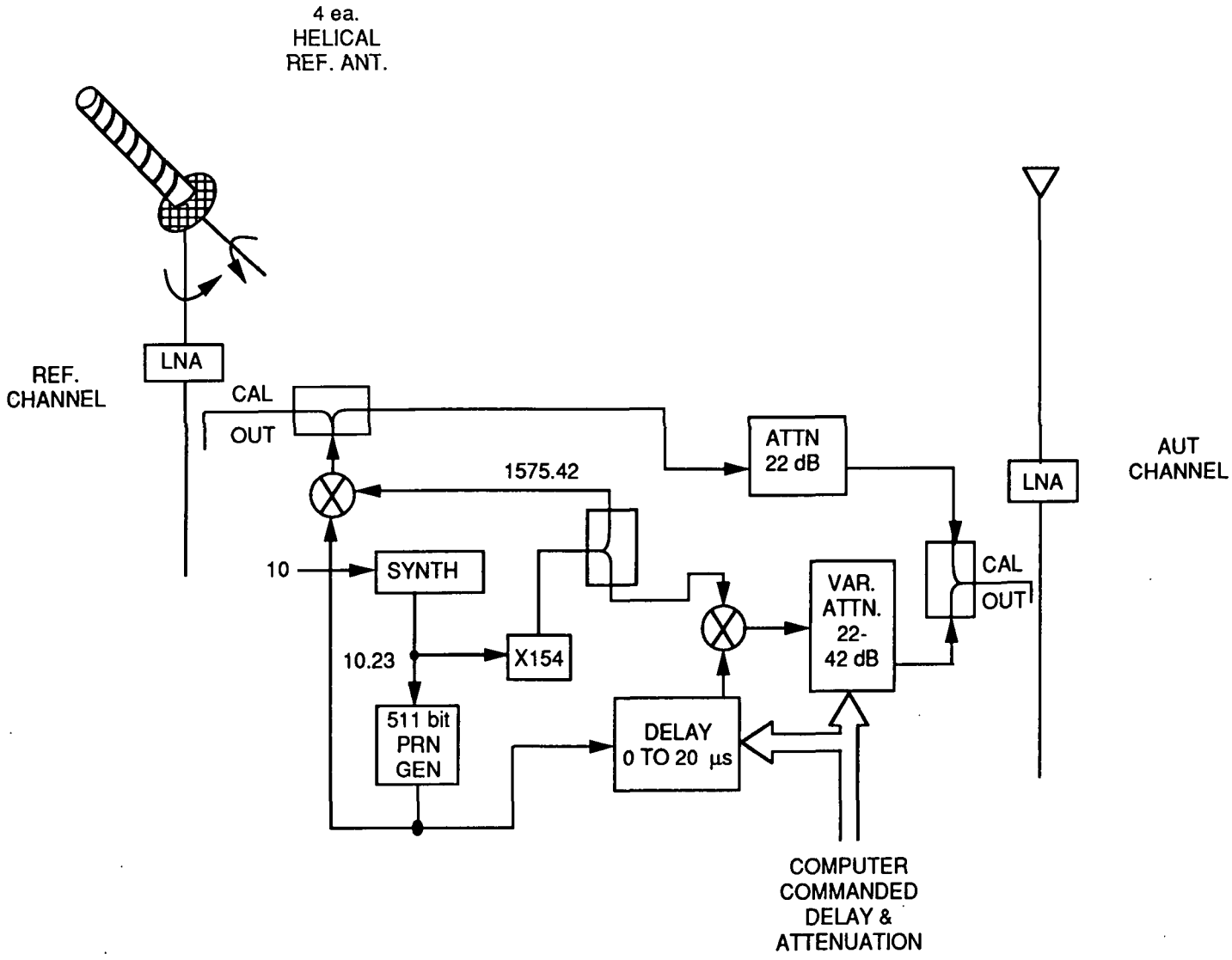

UNIVERSITY OF COLORADO

CALIBRATION SUB-SYSTEM BLOCK DIAGRAM

FIGURE 3

LAND-MOBILE FIELD EXPERIMENTS IN AUSTRALIA

Loretta G. L. Ho and Khaled Dessouky

Jet Propulsion Laboratory
4800 Oak Grove Drive
Pasadena, CA 91109

Abstract

The MSAT-X/AUSSAT experiment offered the first true land-mobile satellite configuration to evaluate the MSAT-X technologies and equipment. Both quantitative data tests and qualitative voice link demonstrations were successfully conducted. From the collected data, system performance in typical land-mobile conditions was extracted. A set of propagation characteristics corresponding to the wide range of environments encountered was also obtained. This article presents a brief description of the MSAT-X/AUSSAT experiment and a summary of its results analyzed to date.

1. Introduction

The Mobile Satellite Experiment (MSAT-X) has aimed to develop system concepts and high-risk technologies for land-mobile satellite communications. Pilot Field Experiments (PiFEx) have been conducted to meet the following objectives: 1) test and validate the subsystems of the MSAT-X mobile terminal; 2) characterize end-to-end system performance; 3) support design refinements and enhancements; and 4) demonstrate the viability of the system concept and technologies to users and manufacturers. The MSAT-X/AUSSAT experiment is the latest in the series of field trials. It was conducted in Australia between July 17 and August 2, 1989, and was the first field experiment where a true land-mobile satellite communications link was established.

2. PiFEx-- Background

Six field experiments have been conducted to date. The emphasis in the early experiments was on trouble-shouting and subsystem validation. The first three experiments: Tower 1 [1], Satellite 1a [2], and Tower 2 [3] took place in 1987. They were primarily aimed at validating the acquisition and tracking of the medium gain antennas developed in MSAT-X. Tower 3 was then conducted during the Summer of 1988 [4]. It was the first end-to-end test of the MSAT-X system in a simulated satellite environment. The MSAT-X/FAA/COMSAT/INMARSAT experiment was conducted in the winter of 1989. It successfully demonstrated both a fixed, ground and an aeronautical-mobile end-to-end satellite link [5]. Finally, the MSAT-X/AUSSAT experiment during the summer of 1989 offered the first true land-mobile satellite environment to test the MSAT-X technologies and equipment [6].

One further experiment is planned at this point. A Multipath Rejection Measurement Experiment (MRMEx) is scheduled for the summer of 1990. The ability of the directional antennas to discriminate against multipath signals, and thereby enhance system performance relative to an omni antenna, will be evaluated. Other experiments may be scheduled in the future as needed.

3. MSAT-X/AUSSAT Experiment Description

The experiment configuration is depicted in Figure 1. The set-up comprised a fixed hub station, the Japanese Experimental Technologies Satellite (ETS-V), and the mobile MSAT-X van. The hub station was located at the AUSSAT headquarters building in downtown Sydney. The van traveled between Sydney and Brisbane primarily along the coastline. This range of travel was dictated by the severe power limitations on the ETS-V satellite. During the experiment, the elevation angles at the van to the satellite varied between 51^{o} and 57^{o}.

Both data and voice tests were conducted. On the forward link, the hub station transmitted data at a frequency of 1646.70 MHz which the satellite translated to 1545.20 MHz for down-link transmission. On the return link, the van transmitted data at 1646.60 MHz which was retransmitted by the satellite at 1545.10 MHz. In either case, a pilot signal was also transmitted to the van at 1646.65 MHz which was then translated to 1545.15 MHz by the satellite. The pilot signal is required primarily for vehicle antenna tracking. It is also used to provided a reference for the receiver.

Both the hub station and van contained the basic communications terminal and other test and data acquisition equipment as appropriate to the site. The main components of the MSAT-X terminal are the speech codec, terminal processor, modem, transceiver, and directional antenna. Two directional antennas were tested. One is a low profile, mechanically steered tracking antenna developed at JPL and the other is an electronically steered phased array antenna developed for JPL by Teledyne Ryan Electronics (TRE). The directional antennas were used interchangeably on the van. In addition, an omni-directional antenna was placed on the van to provide some reference data during the experiment.

A data acquisition system (DAS) was provided in the van and the fixed station (hub). It recorded various system parameters and equipment outputs during the experiment. The data of primary interest is shown in Table 1 along with the sampling period and an indication of the site at which it was recorded. The power meter data are digital measurements of the received signal of the data channel. The Reference I and Q data are measurements of the pilot signal received through the omni-directional antenna. What is referred to as the Pilot I and Q data is the pilot signal received through either the JPL or TRE antenna. The terminal processor data contains information on the bit error rate (data link) tests performed. The compass X and Y data indicate the bearing (or direction) of the van. Unfortunately, the speed data was not recorded because the counter was inadvertently removed along with other unnecessary data acquisition equipment from previous experiments. Consequently, the propagation analysis presented here will cover signal probability densities and cumulative fade distributions, but will not include fade duration statistics.

4. Experiment Results

4.1 Propagation results

Although the primary focus of the experiment was on testing end-to-end system performance, typical propagation results were also obtained through post-experiment analysis.

Approximately 600 miles were covered by the van as it traveled from Sydney to Brisbane. Over this journey, a wide range of environmental conditions were encountered. There were periods with clear line-of-sight propagation to periods of moderate shadowing and to

heavy shadowing as well. The van traveled along terrain that ranged from flat to mountainous. The roads also varied from straight to winding. This mixture of environments provided typical mobile conditions; i.e., conditions which may be encountered under normal operation of a mobile satellite communication system. Experimentation was not restricted to well-defined paths or areas with pre-selected characteristics.

Three typical received pilot signal profiles were observed at the van. Figure 2 shows the received signal during a clear line-of-sight condition. The constant overall signal level resembles an additive white Gaussian noise (AWGN) channel. A received signal through light to moderate shadowing is shown in Figure 3. As this figure shows, the duration of attenuation can last for several seconds at a time. Finally, the signal profile displaying a condition of heavy shadowing/multipath is shown in Figure 4. The discrete levels of attenuation apparent in Figure 4 are due to a combination of the low signal level being received in this shadowed environment and quantization effects in the DAS.

The cumulative fade distribution for these clear, light shadowing, and heavy shadowing/multipath environments are shown in Figure 5. On the clear channel, a fade level of 2.2 dB is experienced 1% of the time. A good portion of the fade is believed to be due to the noise present on the signal. The lightly shadowed channel experiences a 5.9 dB fade level 1% of the time. The heavy shadowing/multipath channel experiences a 12.5 dB fade level 1% of the time. In the heavy shadowing situation, the received signal is already experiencing about 2.6 dB of fade 90% of the time. This is due to the fact that the overall signal level is already undergoing a degree of attenuation and scattering. This takes place, for example, when the van passes by a continuous row of trees.

The probability density function for the received pilot envelope in the clear and the light shadowing conditions are shown in Figure 6. Unfortunately, insufficient data is available to obtain a comparable density for the heavy shadowing case. Also shown in Figure 6 is an analytically-derived Rician density that was fitted to the clear channel. The Rician K-factor (ratio of direct to scattered power in a multipath environment) is 16.5 dB. As mentioned previously, there is noise present on the pilot (approximately 42 dB.Hz C/N_0) and there is noise inherent in the data acquisition system, this is believed to be limiting the K value. The actual K value may be even higher. At a K of 16.5 dB (and higher values), the Rician density is already seen to be converging to the Gaussian shape. This reiterates the observation that the clear mobile channel, with a medium gain vehicle antenna and at a sufficiently high elevation angle, approaches an AWGN link.

4.2 System Performance Results

Data tests were performed to characterize the end-to-end system performance. A typical test consisted of transmitting 4000 contiguous blocks of 512 bits each. The system performance for stationary tests on the return link with the JPL antenna is depicted in Figure 7. Bit error rate (BER) performance in the field suffered approximately a 0.6 dB degradation compared to laboratory performance. Given the host of possible imperfections on the satellite link, the observed performance is well within expectation.

The mobile data tests are not as straightforward in their analysis as the stationary case. Significant signal fluctuations due to the changing environment, particularly deep fades due to occasional blockage, must be taken into account. The effect of such fades is shown in Figure 8 for a forward link test (similar effects are seen on the return link). The top plot is of the cumulative bit errors during a test. The corresponding received data channel power is also shown below it. This figure shows how an episode of brief but deep signal attenuation can lead to a disproportionate accumulation of bit errors. In other words, the contribution of such an event to the increase in bit error rate (BER) is not proportional to

the resulting drop in signal-to-noise ratio averaged over the entire test. This phenomenon is natural in the mobile environment and arises often. Unfortunately, it complicates the extraction of system performance results.

Performance curves for mobile tests on the return link are shown in Figure 9. Curves for both the JPL and TRE antennas are shown. They show that link performance under generally clear conditions was approximately 8.5 to 9.3 dB E_b/N_0 to achieve a BER of 10^{-3}. Thus, performance in the field is within approximately 1 dB from the performance in the lab. This, again, is well within expectation.

4.3 Qualitative Observations

In addition to the essentially one-way data tests, two way voice communications were established and used often between the experimenters in the van and the hub. A variety of recorded standard voice test material was also used for post-experiment evaluation. As an example of outstanding system robustness, a two-way voice link was established and maintained for two hours through a variety of propagation environments. No loss of modem synchronization occurred and only occasional, brief periods of silence were experienced.

5. Conclusions

The MSAT-X/AUSSAT experiment was successfully completed. Characterization of the system performance under typical mobile conditions which are not rigidly controlled was achieved. A variety of land-mobile environments were encountered and characterized. With a medium gain antenna, and at 51^o - 57^o elevation angles, the clear condition closely resembles an AWGN channel. When deep fades are encountered, the errors induced by such events tend, as expected, to dominate the overall error rate performance.

The field performance of the data links under mobile and stationary conditions was less than 1 dB from laboratory (stationary) performance. Good voice quality and a high degree of robustness were also demonstrated on the voice links. In all, the MSAT-X terminals performed very well in the land-mobile environment.

References

1. MSAT-X Quarterly, No. 13 (Special Issue), JPL 410-13-13, January 1988.

2. J. B. Berner, "The Pifex Satellite 1a Experiment," MSAT-X Quarterly, No. 15, JPL 410-13-15, June 1988.

3. J. B. Berner, "The Tower 2 Experiment," MSAT-X Quarterly, No. 15, JPL 410-13-15, June 1988.

4. K. Dessouky, T. C. Jedrey, and L. Ho, "Summary of Results From The Tower 3 Experiment," MSAT-X Quarterly, No. 20, JPL 410-13-20, July 1989.

5. T. C. Jedrey, K. Dessouky, and N. E. Lay, "An Aeronautical Mobile Satellite Experiment," JPL report to be published Summer 1990.

6. T. C. Jedrey, and W. Rafferty, "The MSAT-X/AUSSAT Land-Mobile Satellite Experi- Experiment: An Overview," MSAT-X Quarterly, No. 22, JPL 410-13-22, Jan. 1990.

Table 1. Partial List of Recorded Data

ITEM	DESCRIPTION	SAMPLING PERIOD	VAN	HUB
1	TIME TAG	3.75 sec	X	X
2	POWER METER	3.75 sec	X	X
3	REFERENCE I & Q	1 msec	X	
4	PILOT I & Q	1 msec	X	
5	TERMINAL PROCESSOR	30 msec	X	X
6	COMPASS (Y)	30 msec	X	
7	COMPASS (X)	30 msec	X	
...	SEVERAL OTHER PARAMETERS ...	...	...	...

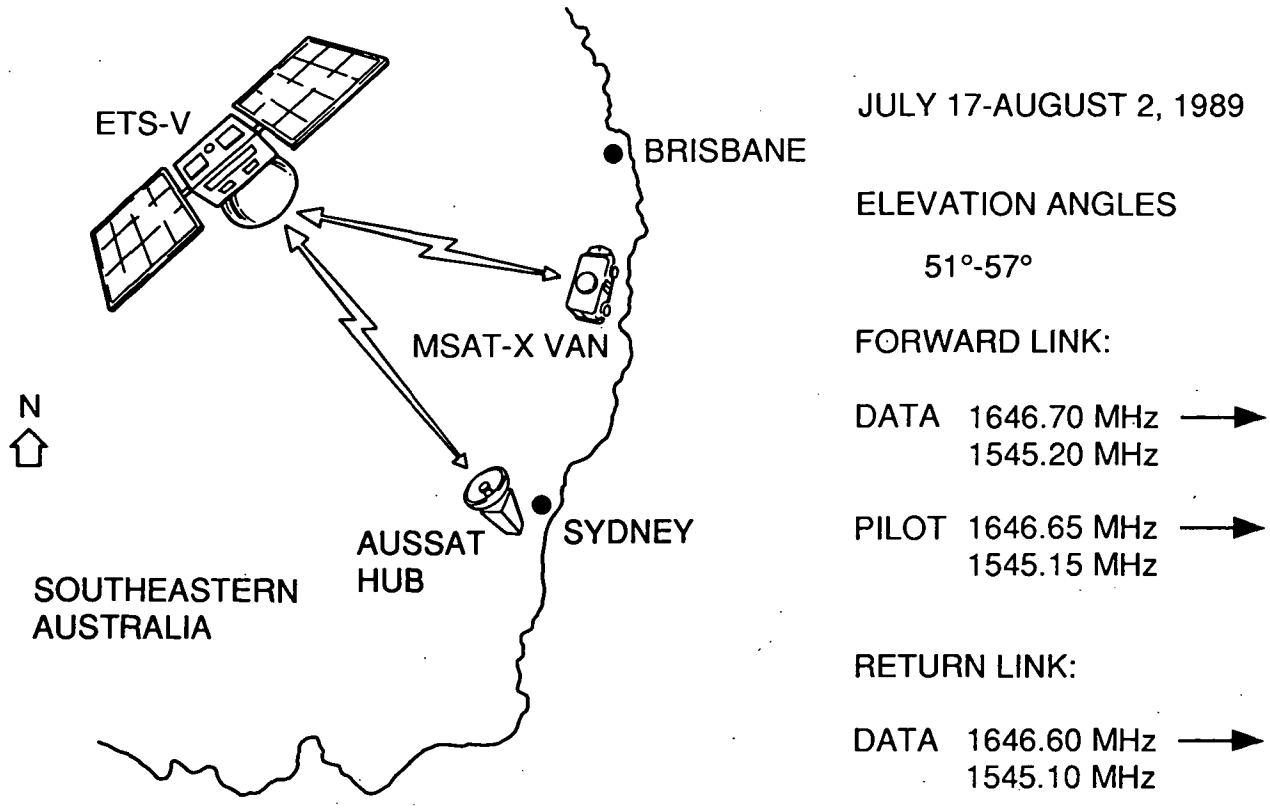

Figure 1. MSAT-X/AUSSAT Experiment Configuration

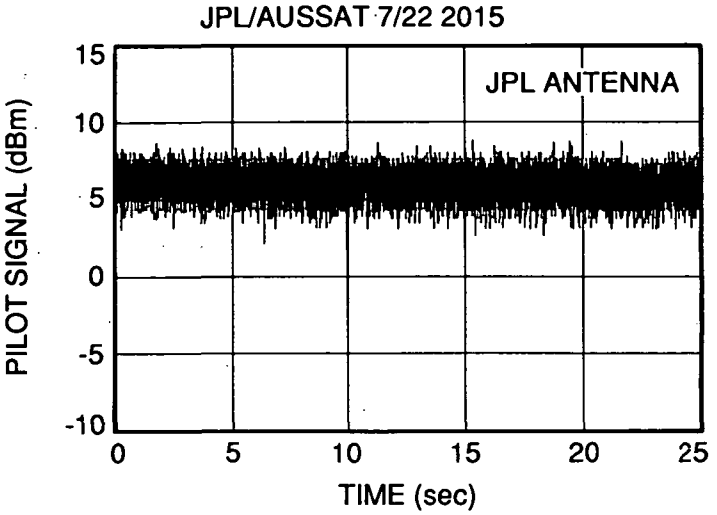

Figure 2. Received Pilot on a Clear Channel

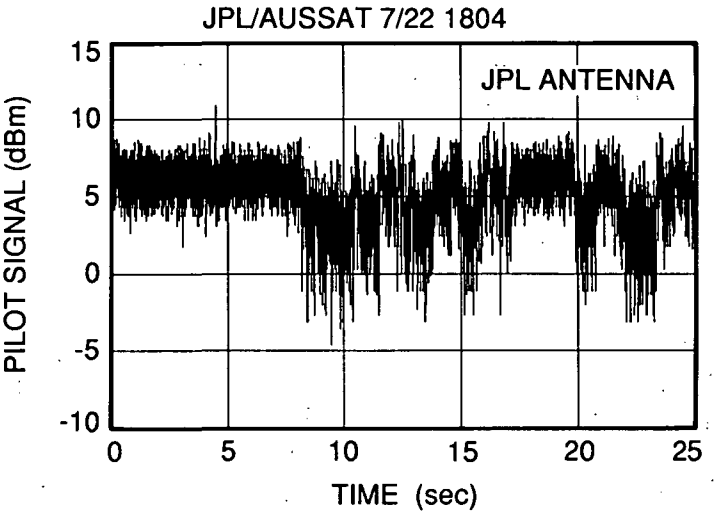

Figure 3. Received Pilot with Light/Moderate Shadowing

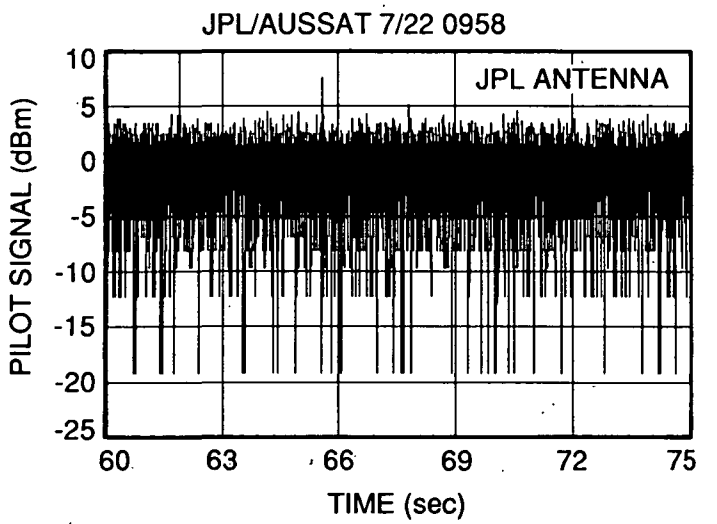

Figure 4. Received Pilot with Heavy Shadowing/Mulitpath

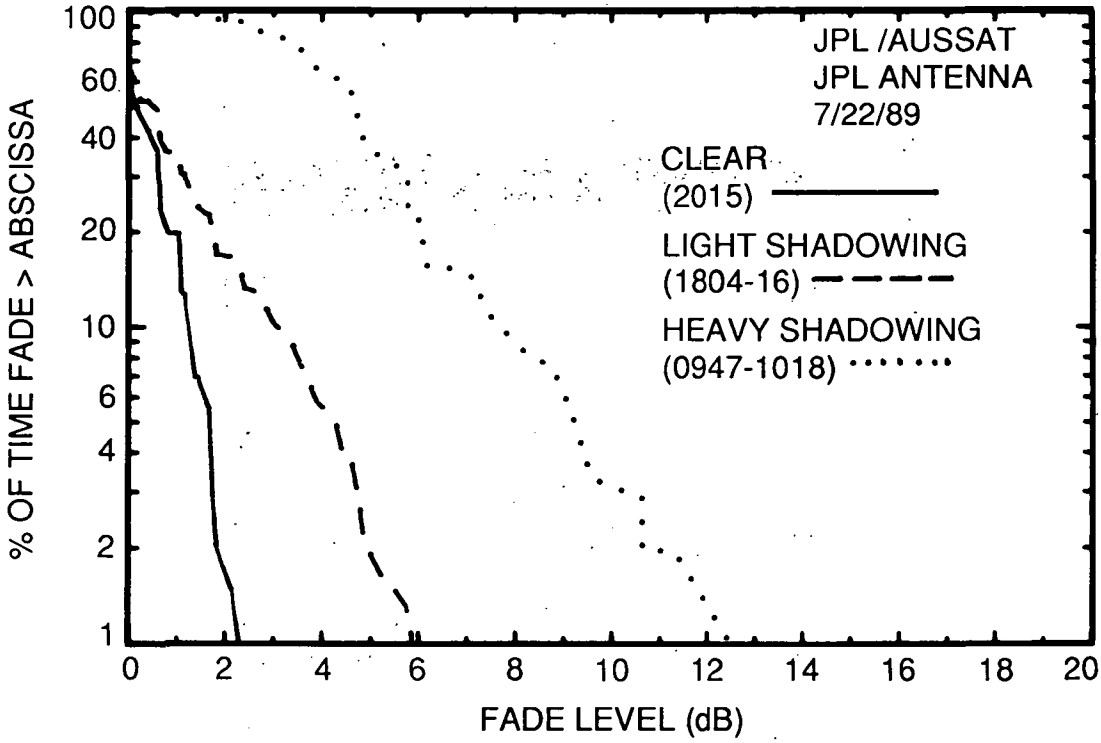

Figure 5. Cumulative Fade Distribution of Received Pilot in Different Environments

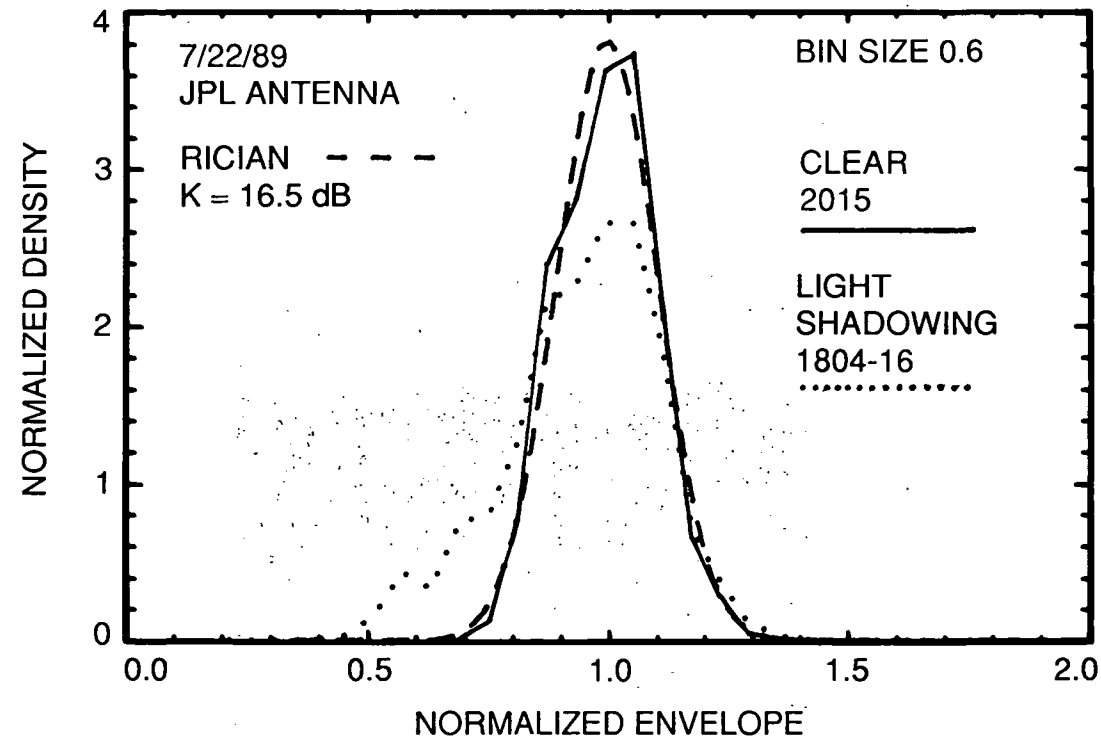

Figure 6. Probability Density Functions for Envelope of Received Pilot

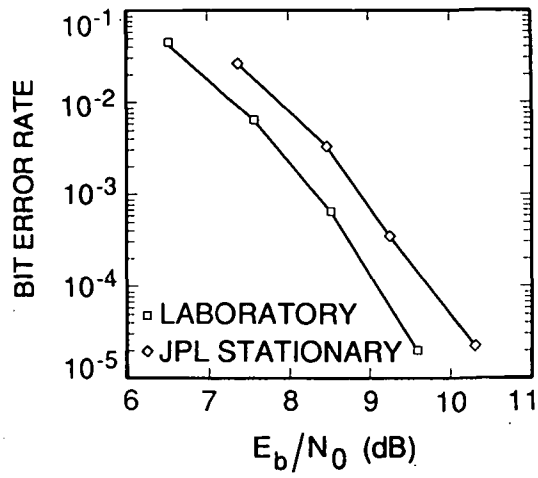

Figure 7. System Performance During Stationary Tests

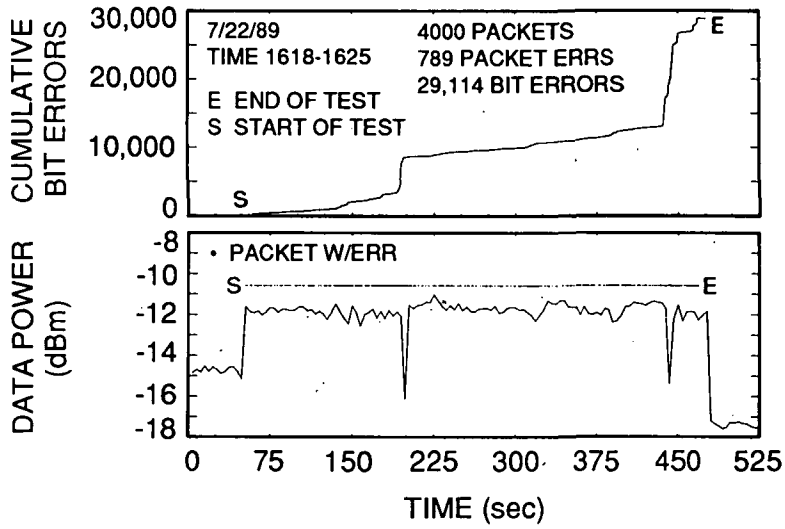

Figure 8. Cumulative Bit Errors and Received Data Channel Signal Power During a Mobile Test

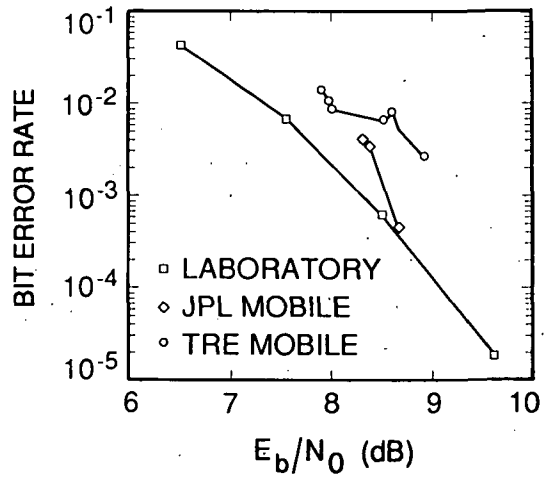

Figure 9. System Performance During Mobile Tests

N91-11969

NASA PROPAGATION INFORMATION CENTER

Ernest K. Smith and Warren L. Flock
University of Colorado at Boulder
Department of Electrical and Computer Engineering
Boulder, Colorado

Introduction

The NASA Propagation Information Center is a modest enterprise funded by NASA and is built around two semi-retired men: Professor Emeritus Warren Flock and Professor Adjunct Ernie Smith. It is congenially located in the Department of Electrical and Computer Engineering of the University of Colorado. Warren and Ernie both enjoy their association with the NASA Propagation Program to which they were previously connected. Flock is the author of the Earth-space Propagation Handbook for frequencies below 10 GHz, and Smith was JPL RTOP manager of the program. Both charge 14% of their time to the program which they spend on items clearly appropriate to the program, e.g. Flock on a Quarterly Newsletter and Smith on support of program management. Additional activities give visibility to and provide publicity for the program and help train graduate students in propagation. Lisa Leonard, research assistant, supports the program in a secretarial capacity, while Zhang Zengjun, a visiting scholar, assists in computer aspects. The Information Center became operational in July 1988.

The Center aims to be several things: a communications medium with the outside world, a mechanism for internal communication within the NASA Propagation Program and an aid to its management. To justify its position in the ECE Department it also offers graduate instruction in propagation and serves on thesis committees. Boulder has an illustrious history in radio wave propagation but it now lacks focus for the subject, at least with respect to communications. The Center attempts to provide this focus.

The impetus for the Center derives, in part, from recommendations of the NASA Science Review Panel in 1986, such as: increased cooperation with other organizations, enhanced monitoring of outside activities, harmonizing acquisition/processing standards, continued CCIR activities, continued handbook support, and continued NAPEX meetings.

Recent Activity

The Center has certain items of regular activity that have gone on since its inception. For example the Center has produced eight quarterly newsletters with an increased demand for each successive edition {Warren Flock, editor.}, supported preparations for NAPEX XIV and for the ACTS Propagation Workshops {E. K. Smith}, and maintains mailing lists for various Propagation Program distributions {Lisa Leonard}. Items of a more general nature which are felt to be in the general interests of the Propagation Program include

- serving as Associate Editor for Propagation for the IEEE Antennas and Propagation Magazine {E. K. Smith since November 1989}.
- During the Fall 1989 Term one of us {Ernie Smith} taught a first year graduate course with Dr. Kenneth Davies of NOAA on Fundamentals of Propagation, and in Spring Term 1990 {Ernie Smith again} taught Earth-Space Propagation with Dr. David Hogg, a course pioneered at the University of Colorado by Warren Flock. There were 16 students in each course.
- At the invitation of Dr. H. Kikuchi, chairman of URSI Commission E, Ernie Smith is serving as co-convener of two sessions at the URSI General Assembly in Prague in August 1990. At the urging of the US URSI Commission E chairman, Emil Soderberg, Ernie Smith has submitted his candidacy for international vice chairman of Commission E.
- Both Warren and Ernie continue to serve on the IEEE Wave Propagation Standards Committee where Warren continues as Mini-Review Editor.
- The Center is active in US-CCIR Study Groups 5 and 6 and is accorded special status by the two US chairmen, Dr. John Cavanagh (USSG 5) and Dr. Charles Rush (USSG 6) in that

preparatory document distribution is made to the Center to the same degree normally afforded subgroup chairmen.

- Foreign travel took Ernie Smith to Japan in August/September 1989 for the International Symposium on Antennas and Propagation (ISAP'89) and the URSI Symposium on Environmental and Space Electromagnetic, both held in Tokyo. During this trip he also visited the Advanced Telecommunications Research Laboratories (ATR) in Kyoto, the Communications Research Laboratories (CRL) in Kokubunji and its Radio Wave Observatory in Wakkannai. During the Japan leg of the journey he gave five lectures, one in each symposium, one at ARC, and one at Wakkannai. The fifth was a public lecture in downtown Tokyo sponsored by the International Satellite Communication Society, Dr. Kenichi Miya President. He then traveled on his own in September 1989 to spend 12 days in China.at the invitation of three organizations there: The Office of Spectrum Management in Beijing, the China Research Institute of Radiowave Propagation in Xinxiang, Hebei, and Xidian University in Xi'an. Warren Flock attended the AGARD Meeting in Copenhagen on Atmospheric Propagation in the UV, Visible, IR and MM-Wave Region and Related Aspects in October 1989. These trips were reported on in the AP-S Antennas and Propagation Magazine.

Foreign visitors to the Propagation Information Center included Prof. Fan Changxin of Xidian University in November 1989 (during which time an inter-university agreement was consummated), Dr Kiyoshi Igarashi from CRL Tokyo in April 1990, and Prof Lin Deyun of Tsinghua University in May 1990.

DISCUSSION AND CLOSING REMARKS

G. Brussaard
Advisory Panel Representative

It is gratifying to see that so much cross fertilization has been realized between the two programs. Active participation at OPEX and NAPEX by those responsible for the programs is the basis; as products we see coordinated experiments and efficient use of experience. The ACTS workshop is a commendable start for a coordinated effort in the USA. The digital receiver at Virginia Tech uses the experience of the development of the SPL receiver. The development of 9 identical terminals, placed at strategic locations in the USA, is a definite advantage of the USA program over Europe.

The research at WPL (Westwater) is an example of basic studies of atmospheric phenomena that was recommended by the Panel as a necessary addition to the application-driven empirical studies. In fact the SSBS studies are an example of such studies.

After the completion of the very commendable effort by Goldhirsh and Vogel to take stock of all that has been learned in the past in the way of land-mobile modelling, it may be time to take another good look at physical modelling of the land-mobile scene and combine satellite measurements with experiments directed towards cellular radio systems and attempt to provide an overall model combining the two scenes, where the first emphasizes blockage and the second emphasizes the multipath environment. The CGAMP receiver effort may be a very useful means to achieving that goal. I should also like to suggest at this stage that a basic theoretical modelling effort may be helpful to substantiate and explain some of the trends which were found empirically in the studies reported. Especially the modelling of the multipath environment, when the main signal is blocked or undergoing several attenuation, is important in this context.

My second recommendation is to start organizing collective data analysis for the ACTS program on a more timely basis so that potential problems can be ironed out in advance of the actual experiments. This is especially important in view of the short satellite lifetime.

In conclusion, I am impressed with the progress that has been made in forming a coherent program and the work by NASA/JPL in conducting this program. The NAPEX newsletter is a useful output of the Propagation Information Center, the activities of which are enthusiastically pursued by W.L. Flock and E.K. Smith.

ADVANCED COMMUNICATIONS TECHNOLOGY SATELLITE PROPAGATION STUDIES MINIWORKSHOP

Chairmen:

D. (Jack) Chakraborty
Jet Propulsion Laboratory

Faramaz Davarian
Jet Propulsion Laboratory

ADVANCED COMMUNICATIONS TECHNOLOGY SATELLITE
PROPAGATION STUDIES MINIWORKSHOP

PREFACE

Following the NAPEX XIV meeting, the ACTS Propagation Studies Miniworkshop was held on May 12, 1990, at the Hotel Driskill, Austin, Texas.

The purpose of the miniworkshop was to review the progress of the ACTS propagation study efforts that followed the First ACTS Propagation Studies Workshop (APSW I) held at the Miramar Sheraton Hotel, Santa Monica, California, during November 28-29, 1989.

Five papers were presented by contributors from government agencies, private industries, and research institutions that included the following topics:

(1) Status Report on the ACTS Propagation Experiments Program.

(2) ACTS Propagation Terminal Prototype Planning and Design.

(3) Spacecraft Beacon Characteristics Update.

(4) Low-Bit Rate (LBR) Earth Stations for the ACTS Program.

(5) Review of Fade Detection Techniques.

Lively discussions took place during and after the Session, which highlighted issues and answers pertinent to the prototype receive terminal design, including radiometers and baseband processors. Budgetary issues were discussed for support of prototype development, manufacture of 8-10 terminals, and data analysis.

The proposal to write a comprehensive document entitled "ACTS Propagation Experiments Handbook" was unanimously accepted by participants at large; an initial list of contributors was selected.

The miniworkshop was adjourned with the announcement that APSW II will be held in Santa Monica, California, during November 1990.

Faramaz Davarian
Workshop Chairman

Dayamoy (Jack) Chakraborty
Workshop Chairman

A STATUS REPORT ON THE ACTS PROPAGATION EXPERIMENTS PROGRAM

PART A - REVIEW OF RECOMMENDATIONS FROM THE FIRST ACTS PROPAGATION WORKSHOP

PART B - STATUS OF ACTS AND THE ACTS EXPERIMENTS PROGRAM

PRESENTED BY JOHN KIEBLER AND DEAN OLMSTEAD

MAY 12, 1990

SCIENCE GROUP RECOMMENDATIONS

EXPERIMENTS TO COMPLETE ATTENUATION MODEL DEVELOPMENT

* CURRENT SITUATION IN NORTH AMERICA
  - ALL BUT TWO U.S. MEASUREMENTS IN SINGLE RAIN CLIMATE ZONE
  - ONLY DATA FROM B1 & D2 HAVE STATISTICAL ERRORS < 15%
* NEED
  - NEED MINIMUM OF 3 YEARS DATA IN AT LEAST 7 LOCATIONS
* SUGGESTED LOCATIONS:

CLIMATE ZONE	LOCATION
B2	COLORADO
C	WESTERN WASHINGTON
D1	MICHIGAN
D1	NEW HAMPSHIRE
D3	TENNESSEE, NORTH CAROLINA
E	FLORIDA
F	CALIFORNIA

ATTENUATION MODEL (CONT.)

* GLOBAL SITUATION
    - CRITICAL NEED FOR DATA FROM THE ARCTIC (A) AND TROPICS (G & H)
* SUGGESTED LOCATIONS
    - ARCTIC:
        + ALASKA
        + ANTARCTIC
    - TROPICS:
        + NONE IDENTIFIED

SCIENCE GROUP RECOMMENDATIONS (CONT.)

EXPERIMENTS TO OBTAIN DATA IN THE 1% TO 10% OF A YEAR REGIME

* NO AVAILABLE DATA VALID IN THIS REGIME
* COMBINATION OF BEACON RECEIVER AND RADIOMETER NEEDED TO PRODUCE MEASUREMENTS WITH 15% ACCURACY OVER RANGE OF 0.2 TO 15 DB
  - BEACON RECEIVER REQUIRES DYNAMIC RANGE OF > 26 DB
* OBSERVATIONS TO EXTEND DYNAMIC RANGE NEEDED IN ALL CLIMATE ZONES IN NORTH AMERICA
  - ZONE D2 OBSERVATIONS SHOULD BE MADE FROM LOCATIONS REPRESENTED IN THE EXISTING DATA BASE

SCIENCE GROUP RECOMMENDATIONS (CONT.)

IDENTIFICATION OF THE PHYSICAL PROCESS

* **IN THE 1-10% REGIME SEVERAL PROCESSES WILL CAUSE SIGNIFICANT ATTENUATION:**

  CLOUDS
  WATER VAPOR VARIATIONS
  REFRACTION EFFECTS AT CLOUD EDGES
  REFRACTION EFFECTS AT LOW ELEVATION ANGLES
  LIGHT RAIN

* **EACH OF THESE PROCESSES HAS A DIFFERENT FREQUENCY DEPENDENCE**
* **CORRECT PROCESS MUST BE IDENTIFIED TO MODEL FADING AT HIGHER FREQUENCIES**
* **TWO FREQUENCY RADIOMETER MEASUREMENTS REQUIRED TO MEASURE PATH INTEGRATED LIQUID WATER CONTENT AND WATER VAPOR DENSITY STATISTICS**
  - **ABSOLUTE TEMPERATURE MEASUREMENT BETTER THAN 1 K REQUIRED**
  - **MEASUREMENT PRECISION OF BETTER THAN 0.2 K IN 10 SECONDS IS REQUIRED**
  - **DICKE RADIOMETER REQUIRED TO MEET ACCURACY AND PRECISION**
* **STATISTICS ON PATH INTEGRATED CLOUD WATER CONTENT NEEDED BY THE SATELLITE COMMUNICATIONS COMMUNITY AND FOR THE STUDY OF GLOBAL CLIMATE CHANGE**

SCIENCE GROUP RECOMMENDATIONS (CONT.)

MITIGATION TECHNIQUES

* DYNAMIC ADJUSTMENT OF FADE MARGIN REQUIRES DETECTION AND FORECAST OF RAIN FADE LEVELS
* MEASUREMENTS OF THE TEMPORAL STRUCTURE OF THE RAIN ATTENUATION PROCESS REQUIRED
* TIME SERIES OF FADING SIGNALS MUST BE RECORDED
* STATISTICS ON FADE DURATIONS, INTERFADE PERIODS, FADING RATES NEEDED
* SAMPLING RATE OF ONCE PER SECOND NEEDED FOR BEACON AND RADIOMETER IN ORDER TO TEST THE BEHAVIOR OF FADE DETECTION AND FORECAST SCHEMES

SCIENCE GROUP RECOMMENDATIONS (CONT.)

NEW SERVICES

* LAND MOBILE SATELLITE SERVICE
  - MEASUREMENT PROGRAM RECOMMENDED TO COMPLEMENT EXISTING DATA BASE AT UHF AND L BAND
    + PROPAGATION THROUGH TREES AND ROAD SIDE OBSTRUCTIONS
    + USE 20 AND 30 GHZ BEACONS AND ACTS STEERABLE ANTENNA
* DATA TRANSMISSION SERVICES TO REMOTE AREAS
  - MAKE MEASUREMENTS TO ANTARCTICA AT LOW ELEVATION ANGLES
    + USE THE ACTS STEERABLE ANTENNA
  - DEVELOP SAMPLING TECHNIQUES TO COMBINE OCCASIONAL SATELLITE DATA WITH RADIOMETER DATA

SCIENCE GROUP RECOMMENDATIONS (CONT.)

VERTICAL STRUCTURE

* RADIOMETER DATA CAN SUPPORT DEVELOPMENT OF ALGORITHMS FOR MEASUREMENT OF PRECIPITATION FROM SATELLITES
* RADIOMETER DATA WILL PERMIT REDUCTION OF KNOWN ELEVATION DEPENDENT MODELING ERRORS IN CONTEMPORARY RAIN ATTENUATION MODELS
* DEPLOYMENT OF NOAA/WPL MULTIPLE FREQUENCY, VERTICALLY POINTING RADIOMETERS TO EACH PROPAGATION TERMINAL SITE IS RECOMMENDED
  - OBTAIN DATA ON VERTICAL STRUCTURE OF CLOUDS AND LIGHT RAIN TO DEVELOP AND TEST REFINED MODELS

SCIENCE GROUP RECOMMENDATIONS (CONT.)

DATA ACQUISITION AND DATA PROCESSING

* **PROVIDE AN OPTICAL RAIN GAGE FOR EACH SITE**
  - **WIDE DYNAMIC RANGE**
  - **UNIFORM INTEGRATION TIME ACROSS DYNAMIC RANGE**
  - **MUCH GREATER RELIABILITY**
  - **CAN INDICATE THE PHASE OF THE PRECIPITATION**
* **TEMPERATURE, PRESSURE AND HUMIDITY SHOULD BE RECORDED**
* **ALL EXPERIMENTERS USE THE SAME RECORDING AND DATA PROCESSING SYSTEMS**
  - **USE SINGLE SET OF PROCESSING ALGORITHMS TO PROCESS DATA**
  - **USE UNIFORM FORMAT TO RECORD ALL DATA**
  - **OBTAIN RECORDING AND PROCESSING SOFTWARE FROM A SINGLE VENDOR**
  - **MAKE SOFTWARE AVAILABLE TO ALL EXPERIMENTERS BEFORE EXPERIMENTS BEGIN**

DATA ACQUISITION AND DATA PROCESSING (CONT.)

* ESTABLISH CALIBRATION PROCEDURES BEFORE EXPERIMENT BEGINS
    - ALL EXPERIMENTERS USE THE SAME PROCEDURES
    - INCORPORATE ALGORITHMS IN DATA COLLECTION SOFTWARE
* PROVIDE UNIFORM DOCUMENTATION FOR HARDWARE AND SOFTWARE
* EXPERIMENT RESULTS SHOULD BE PREPARED AND REPORTED IN A UNIFORM MANNER
* DEVELOP PROCEDURE TO HANDLE DOWN TIME DUE TO SYSTEM FAILURES
* PROVIDE A BACKUP POWER SYSTEM
    - A SYSTEM THAT FAILS WHEN IT RAINS IS USELESS

SYSTEMS GROUP RECOMMENDATIONS

SYSTEM NEEDS

* FADING RATES, DURATIONS, INTERFADE INTERVALS AT SPECIFIED THRESHOLDS AND CONTROL ALGORITHMS FOR DYNAMIC ALLOCATION OF COMMUNICATIONS RESOURCES
* DATA ABOUT GASEOUS ABSORPTION, CLOUD LOSSES, AND TROPOSPHERIC SCINTILLATION FOR ADAPTIVE DECISION MAKING AT LOW FADE LEVELS
* MULTIPATH AND SHADOWING/BLOCKAGE MEASUREMENTS FOR MOBILE APPLICATIONS
* DUAL-POLARIZATION STUDIES TO IDENTIFY EFFECTS OF POWER CONTROL ON CROSSPOLAR INTERFERENCE, NEED FOR JOINT CODING FOR FADING AND DEPOLARIZATION
* EFFECTS OF IMPORTANCE TO SMALL, TRANSPORTABLE TERMINALS SUCH AS PASS
* SITE DIVERSITY DATA FOR SMALL TERMINALS AT SMALL SEPARATIONS

SYSTEMS GROUP RECOMMENDATIONS (CONT.)

ACTS PROPAGATION TERMINAL MEASUREMENT PARAMETERS

* 20 GHZ BEACON RECEIVE SIGNAL LEVEL
* 30 GHZ BEACON RECEIVE SIGNAL LEVEL
* 20 GHZ RADIOMETRIC SKYNOISE TEMPERATURE
* 30 GHZ RADIOMETRIC SKYNOISE TEMPERATURE
* POINT RAIN RATE NEAR THE TERMINAL
* ATMOSPHERIC TEMPERATURE AT THE EARTH'S SURFACE
* ATMOSPHERIC HUMIDITY AT THE EARTH'S SURFACE
* AMBIENT TEMPERATURE OF SENSITIVE TERMINAL COMPONENTS

SYSTEMS GROUP RECOMMENDATIONS (CONT.)

ACTS PROPAGATION TERMINAL DESIGN REQUIREMENTS

* **SAMPLE RATES UP TO 100 HZ FOR BEACON RECEIVE SIGNALS**
* **VARIABLE DETECTION BANDWIDTH TO MATCH SAMPLING RATE**
* **SAMPLE RATES FOR RADIOMETERS SAME AS FOR RECEIVERS TO FACILITATE DATA HANDLING**
* **SAMPLE RATES OF ABOUT 1 PER 10 MINUTES FOR HUMIDITY AND TEMPERATURE**
* **RECORD UNIVERSAL TIME ACCURATE TO +/- 2 SECONDS**

SYSTEMS GROUP RECOMMENDATIONS (CONT.)

MITIGATION ALGORITHMS

* FIVE MAJOR AREAS RECOMMENDED FOR INVESTIGATION AND DEVELOPMENT
  - FADE DETECTION
  - PROPAGATION EFFECT IDENTIFICATION
  - BASELINE DETERMINATION AND EXTRACTION
  - ADAPTIVE FADE RESPONSE AND COMPENSATION
  - FREQUENCY SCALING

SYSTEMS GROUP RECOMMENDATIONS (CONT.)

TERMINAL DESIGN AND DATA ACQUISITION

* FOR BEACON MEASUREMENTS:
  - 0.1 DB RESOLUTION; 0.5 DB RMS ACCURACY
  - 10-15 DB DYNAMIC RANGE NEEDED
* CONTINUOUS MONITORING OF INJECTED SIGNAL FROM STABLE SOURCE DESIRED FOR CALIBRATION
* RAIN GAGE ESSENTIAL; TEMPERATURE AND HUMIDITY DATA DESIRABLE
* RELIABLE UNINTERRUPTABLE POWER SUPPLY ESSENTIAL
* SELF-TEST FEATURE HIGHLY DESIRABLE
* DATA COLLECTION:
  - 12 BIT ACCURACY FOR DATA STORAGE
  - BINARY STORAGE WITH TIME STAMP
  - PROVIDE REAL TIME DISPLAYS WITH VARIABLE TIME HISTORIES
* MODEM TO PHONE LINE REQUIRED FOR REMOTE MONITORING
* ALL TERMINALS SHOULD BE A STANDARD DESIGN AND PRODUCE STANDARDIZED DATA

SYSTEMS GROUP RECOMMENDATIONS (CONT.)

NOVEL EXPERIMENTS USING ACTS LBR AND HBR COMMUNICATIONS CHANNELS

* CHANNEL-PROBE EXPERIMENTS
  - IMPULSE-RESPONSE MEASUREMENTS
  - BIT ERROR RATE
  - PERFORMANCE DEGRADATION AS FUNCTION OF PROPAGATION IMPAIRMENT
* AERONAUTICAL MOBILE-SATELLITE MEASUREMENTS
  - SIGNAL FADING
  - ELEVATION-ANGLE DEPENDENCE
  - EFFECTS OF AIRCRAFT SURFACE MULTIPATH
  - SIGNAL-TO-NOISE AS FUNCTION OF AIRCRAFT ANTENNA GAIN
* LAND MOBILE-SATELLITE EXPERIMENTS
  - ESTABLISH FEASIBILITY AND REQUIREMENTS
  - ACQUIRE DATA BASE OF FADING DUE TO TREES AND TERRAIN
  - EVALUATE ADVANTAGE OF SPREAD SPECTRUM TECHNIQUES TO COMBAT TERRAIN MULTIPATH
* OUTER/INNER CODING TECHNIQUES
  - EVALUATE FOR ADAPTIVE COMPENSATION OF FADING

DISPOSITION OF RECOMMENDATIONS

STATUS

* ALL RECOMMENDATIONS BEING CONSIDERED AND EVALUATED
* FACTORS CONSIDERED IN EVALUATION
  - SCIENTIFIC MERIT
  - TECHNICAL MERIT
  - EFFECT ON RELIABILITY
  - SCHEDULE IMPACT
  - COST IMPLICATIONS
* REVIEW INCOMPLETE
* REVIEW WILL BE COMPLETED PRIOR TO NEXT ACTS PROPAGATION WORKSHOP

ADVANCED COMMUNICATIONS TECHNOLOGY SATELLITE (ACTS) PROGRAM

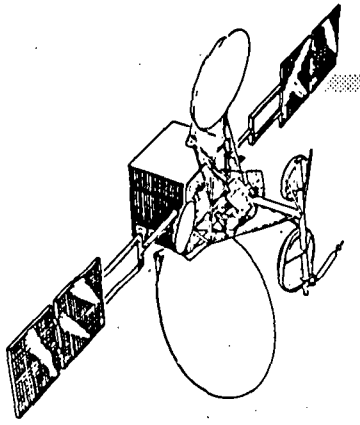

Presentation to
NAPEX WORKSHOP by

DEAN A. OLMSTEAD
May 12, 1990

ACTS

NASA

ACTS EXPERIMENTS PROGRAM

ACTS Propagation Experiments Program

- Obtain Propagation Data Base Over Wide Range of Climates for 20/30 GHz Data
- Collect Data on Fade Depths, Duration, and Rate of Change not Available from any Previous Program
- Support Large Number of Interested Experimenters
- Develop and Test Rain Attenuation Adaptive Compensation Protocol
- Collect Statistics on Simultaneous Rain Fades at Multiple Sites
- 8-10 Propagation Terminals

ACTS EXPERIMENTS PROGRAM
Experimenter Terminal Categories

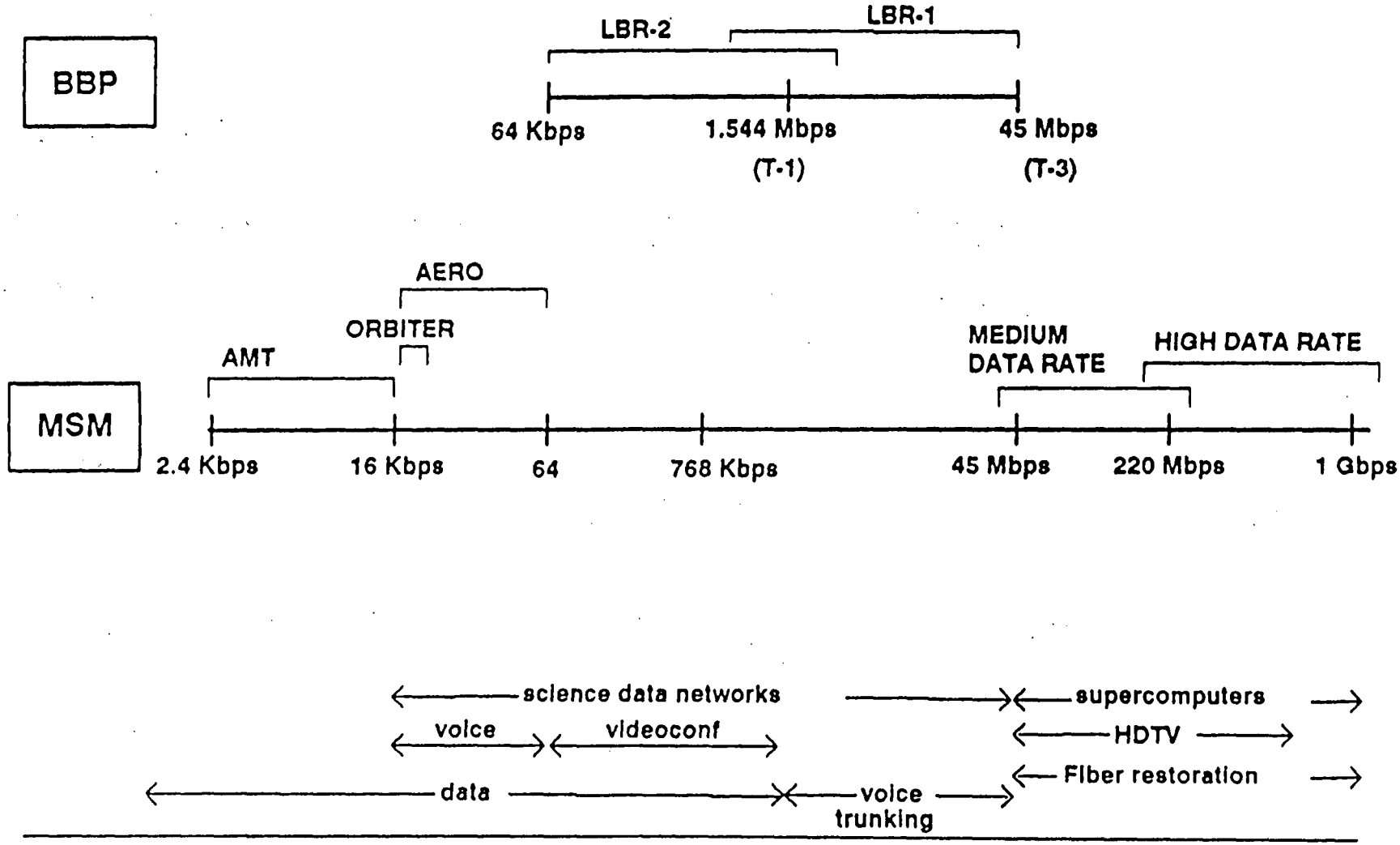

ACTS EXPERIMENTS PROGRAM
BUDGET OPTIONS
(DOLLARS IN MILLIONS)

	UNITS PROTO	UNITS BUILD	FY 91	FY 92	FY 93	FY 94	TOTAL
OPTION D							
PROPAGATION			.6	.6	.8	.5	2.5
GIGABIT	1	2	1.4	3.2	1.6		6.2
MOBILE	3		2.6	3.0	1.9		7.5
HDTV	1	1	1.3	2.4	.4		4.1
LBR-1	1	2	1.7	1.8			3.5
LBR-2		4	.2	.6			.8
INTERFACE			.5	.5	.2	.	1.2
SUBTOTAL			8.3	12.1	4.9	0.5	25.8
SPONSORED UTILIZATION			.5	2.1	2.4	2.4	7.4
CONTINGENCY			.5	1.0	.	.	1.5
TOTAL	6	9	9.3	15.2	7.3	2.9	34.7

ACTS EXPERIMENTS PROGRAM

SUMMARY SCHEDULES

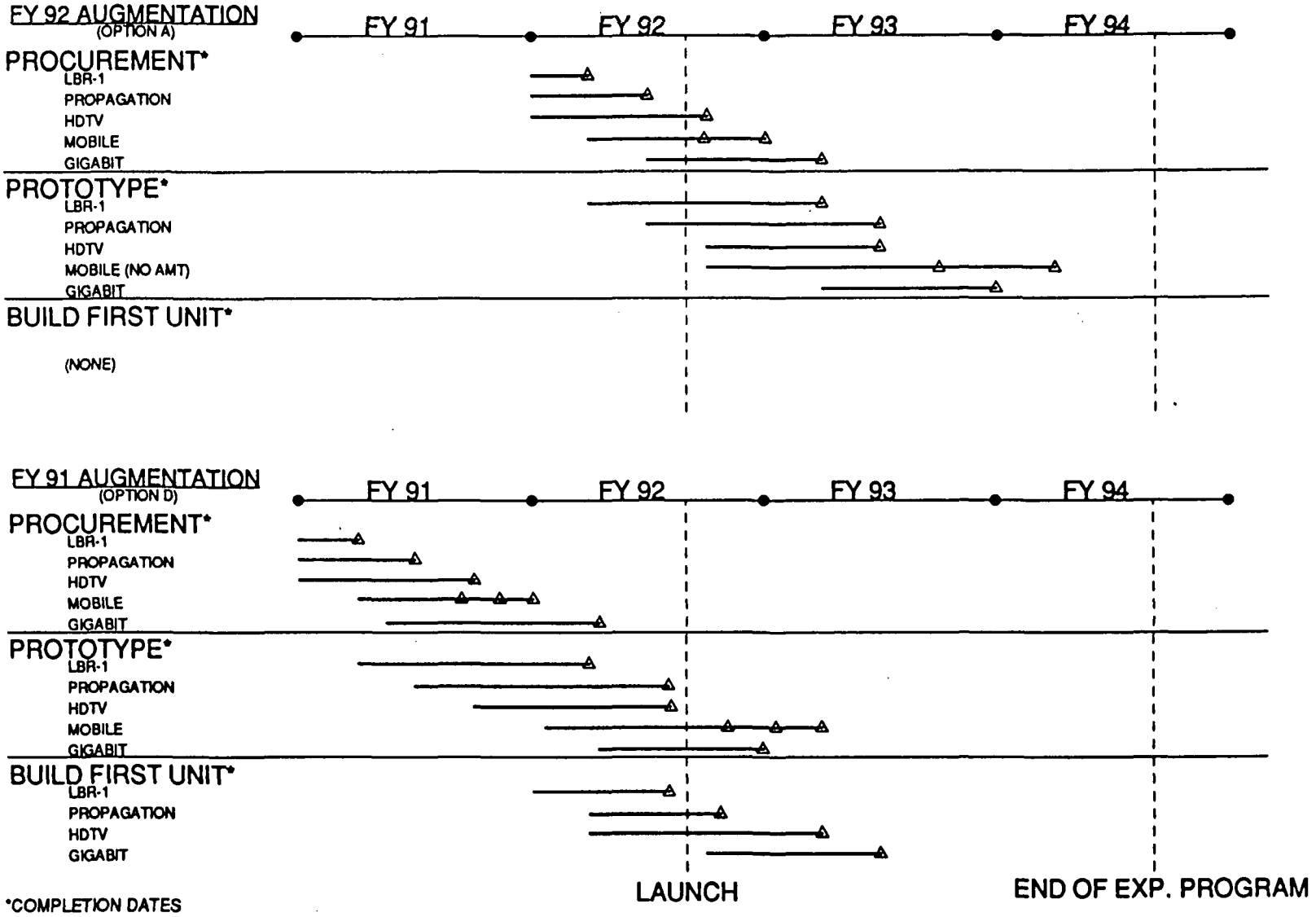

*COMPLETION DATES

ACTS EXPERIMENTS PROGRAM
BUDGET OPTIONS
(DOLLARS IN MILLIONS)

	JULY 1988	OPTION A	OPTION B	OPTION C	OPTION D
PROPAGATION	2.0	2.5	2.5	2.5	2.5
GIGABIT		3.2	2.8	6.2	6.2
MOBILE		6.2	6.2	7.9	7.5
HDTV		2.8	2.8	4.6	4.1
LBR-1	2.5	2.8	2.7	3.7	3.5
LBR-2	8.2			0.9	0.8
INTERFACE		1.3	1.3	1.2	1.2
SUBTOTAL	12.7	18.8	18.3	27.0	25.8
UTILIZATION	5.0	1.0	5.5	5.5	7.4
CONTINGENCY	1.7				1.5
TOTAL	19.4	19.8	23.8	32.5	34.7

ACTS Propagation Terminal Prototype Planning and Design

by

F. Davarian, F. Pergal and D. Chakraborty

Jet Propulsion Laboratory
California Institute of Technology
Pasadena, California

W. Stutzman

Virginia Tech, EE Department
Blacksburg, Virginia

Abstract

This paper examines the planning and design of a prototype propagation receive terminal for beacon signal at 27 and 20 GHz bands. The developmental plan is discussed first followed by technical design considerations including, a) ACTS system salient features and frequency plan, b) beacon signal parameters and specifications, c) system calculations, and d) terminal hardware design issues.

1. Introduction

The purpose of the Advanced Communications Technology Satellite (ACTS) is to demonstrate the feasibility of Ka-band (20/30 GHz) spectrum for Satellite Communications and to help maintain US leadership in Satellite Communications by incorporating innovative schemes such as advanced TDMA, microwave and baseband switching, onboard regeneration, and adaptive application of coding during rain fade conditions.

The success or failure of ACTS experiment will hinge upon one critical issue that is how accurately one could predict the rain fade statistics, fade dynamics and derive an appropriate algorithm to combat weather vagaries specifically for links with small terminals such as VSATs (Very Small Aperture Terminals) where the power margin is a premium.

Unlike terrestrial links, a satellite link has two elements in the same link such as the up-link and the down-link which may fade simultaneously or individually. Therefore, continuous measurements in the up-link (27 GHz) and in the down-link (20 GHz) have to be carried out to predict the rain attenuation. Furthermore, in addition to finite perturbation in receiver noise temperature, any attenuation process that involves energy absorption is associated with thermal noise emission to maintain thermal equilibrium. Signal absorption due to rain gives rise to an increased system noise temperature [1]. Therefore, in addition to rain attenuation measurements some radiometric measurements have to be carried out simultaneously to assess the

degradation caused by the increased system noise due to rain and finite perturbation in system noise temperature due to fluctuations in the receiving system.

This paper presents an outline of the process involved in generating a working plan for the ACTS propagation study and participation of experimenters and hardware designers to finalize the receive terminal design. It is anticipated that experimenters will be located throughout the rain rate regions for the Continental United States [2] and beyond.

2. Planning

Planning for the ACTS propagation terminal was initiated at the First ACTS Propagation Studies Workshop, November 28-29, 1989. The workshop was convened to develop the ACTS propagation studies program. At the end of two days, the participants delivered a set of recommendations regarding propagation studies and experiments using ACTS. These recommendations addressed a range of topics, from the need for propagation data to the configuration and the number of propagation terminals.

Some of these recommendations are:

- Complete models for the prediction of attenuation statistics in climate regions within the United States that have not been studied.
- Obtain a statistical description of attenuation in about 1 percent of a year regime.
- Obtain information needed for the evaluation of the schemes for attenuation compensation employed in the ACTS program.
- Provide additional data for the design of new mitigation techniques.
- Explore the use of 20 to 30 GHz for the development of new services.

The workshop participants also provided guidelines regarding measurement parameters and requirements. These guidelines require that the terminal should be configured to record the following propagation and meteorological parameters:

- 20-GHz beacon receive signal level
- 27-GHz beacon receive signal level
- 20-GHz radiometric sky noise temperature
- 27-GHz radiometric sky noise temperature
- Point rain rate near the terminal

- Atmospheric temperature at the earth surface, and
- Atmospheric humidity at the earth surface.

Due to the approaching spacecraft launch date and the satellite's short life span, it was strongly suggested that the work on the development of the terminals start without delay. The workshop participants agreed that it would be best to collect propagation data for a minimum of three years, an objective that can be achieved only if the terminal development effort starts immediately.

To respond to the workshop recommendations regarding propagation terminals, we have devised a two-phase plan. In phase 1, a terminal prototype will be developed, and in phase 2, a number of terminals (8 to 10) will be manufactured for distribution to ACTS propagation experimenters. Figure 1 shows our schedule for the terminal development effort. The cost of the prototype has been estimated at $400,000.00, which is jointly funded by the ACTS Project ($300K) and the Propagation Program ($100K). The task will be performed cooperatively by Jet Propulsion Laboratory, Virginia Polytechnic Institute, and Michigan Technology University.

An ACTS propagation receiver terminal will consist of a dual-channel receiver, a dual-channel radiometer, and a data acquisition system. The terminal will also be equipped with meteorological recorders for measuring the point rain rate, and the atmospheric temperature and humidity. Provisions will be provided for an HBR signal output at a convenient receiver I.F. Subsystem. HBR channel power when transmitted for example in a CW mode via the spacecraft steerable antenna will permit propagation measurements outside the CONUS. Therefore, this provision will facilitate experiments in the Arctic and the Tropics.

3. ACTS System Salient Features and Frequency Plan

ACTS uses three different beam connectivities as follows [3]:

- Electronically hopping spot beams for low capacity links
- Fixed spot beams for high capacity links
- Mechanically steered spot beam for experiments outside the normal CONUS coverage.

There are two hopping beams; one of these hopping beams can hop to six discrete locations, each encompassing a major metropolitan area, and also to anywhere within a contiguous area called the west sector. The second hopping beam can hop to seven discrete locations and to anywhere within a contiguous area called the east sector. There are three stationary beams, focused on Cleveland, Atlanta, and Tampa.

The half-power beamwidth for both the stationary and the hopping beam is approximately 0.3 degrees. For experimental purposes and to extend the

Schedule Name : ACTS Experimenter's Terminal Development
Responsible : JPL Section 339
As-of Date : 5-Mar-90 Schedule File : C:\TL3\DATA\ACTS00

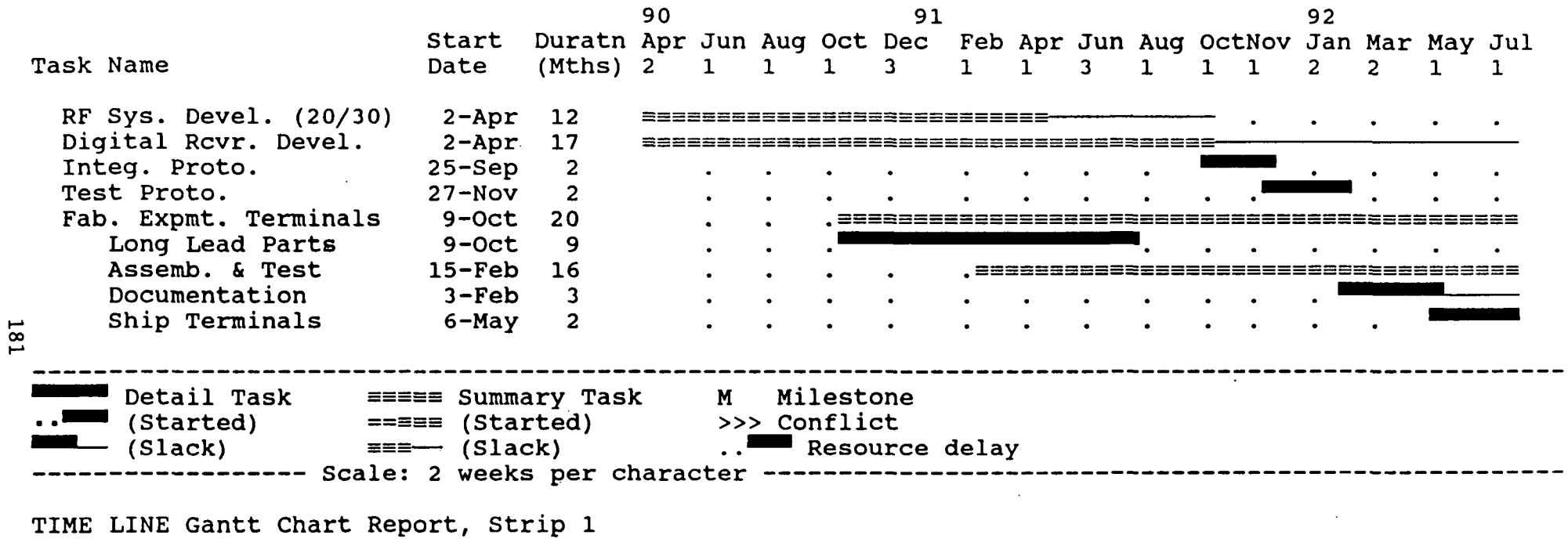

TIME LINE Gantt Chart Report, Strip 1

Figure 1. Schedule for Terminal Development

coverage beyond CONUS, a mechanically steerable antenna with 1.0-degree beamwidth is also incorporated.

ACTS operates in one of the two switching modes. For high-capacity trunk an IF matrix switch is used. For lower-volume traffic such as VSAT networks, a baseband processor provides the switching. In either case, the system access is provided by Time Division Multiple Access (TDMA) with Demand Assignment (DA) managed by the network's master control station.

The three stationary beams use the same frequency, but the Cleveland polarization is orthogonal to that of the other two beams. The two hopping beams also use the same frequency but employ opposite polarization.

ACTS EIRP, G/T and Burst Rate summary is shown below:

Table 1. ACTS EIRP, G/T and Burst Rate Summary

Beam	EIRP (dBw)*		Satellite G/T (dB/K)		Information Rate (Mbps)			
	Max	Min	Max	Min	Uncoded		Coded	
					Up-Link	Dn-Link	Up-Link	Dn-Link
Hopping (#1)	62.9	60	20	17.5	110[a] 27.5[b]	110[a] 110[b]	55[a] 13.75[b]	55[a] 55[b]
Hopping (#2)	63.1	57.6	17.4	14.7	110[a] 27.5[b]	110[a] 110[b]	55[a] 13.75[b]	55[a] 55[b]
Stationary	64.1	57.4	19.8	18.6	220	220	-	-
Steerable (Mechanical)	54.4	-	11.3	-	-	-	-	-

a) Single channel TDMA, b) FDM/TDMA mode (more than one TDMA carrier).

* Existing Ku-band domestic satellite EIRP range is 40-44 dBw. Therefore the excess EIRP of about 17 to 20 dB can be used as fade margins in existing Ku-band VSAT antennas if used in Ka-band.

3. Beacon Signal Parameters and Measured Data

The ACTS System envisions up-link power control during up-link fade and down-link fade compensation will be achieved by a combination of fixed margin plus adaptive application of coding. Beacons are provided at 27 GHz and 20 GHz bands. The up-link beacon is unmodulated whereas there are two beacons

in the down-link, each of these down-link beacons can be modulated by two subcarrier modulated telemetry data channels (PCM and FM). Occasionally, the down-link beacon will be used for ranging also. While ranging the 20 GHz beacon will handle one subcarrier telemetry channel only. The Composite Signal Spectrum including the two subcarrier modulated telemetry channels or the single telemetry channel plus the ranging channel linearly phase modulates the 20 GHz beacon transmitter. It is envisioned that when the spacecraft is on station, only one 20 GHz down-link beacon will be in use while the second beacon will be on a standby mode. Beacon signals are noncoherent.

The principal characteristics [3] of the beacons are shown in Table 2 and the ACTS·Frequency Plan is shown in Figure 2.

Table 2. Characteristics of the ACTS Beacons

Parameters	27 GHz Beacon	20 GHz Beacon
No. of beacons	1	2
Frequency/(polarization)	27.505 GHz ±0.5 MHz (V)	20·185 GHz ±0.5 MHz (V) 20·195 GHz ±0.5 MHz (H)
Function	Fade Measurement	Telemetry
Modulation	None	Yes (FM & PCM)
Nominal RF output (dBm)	20.0	23
Operating Temperature (°C)	-10 to +55	-10 to +55
Frequency Stability	±10 PPM over 2 years at constant temperature ±1.5 PPM over 24 hours for temperature range -10°C to 55°C	
Output Power Stability	±1.0 dB over 24 hours ±2.09 dB over full mission	
Phase Noise	-49 dBC/Hz @ 50 Hz -80 dBC @ 3000 Hz	-51 dBC/Hz @ 50 Hz -92 dBC/Hz @ 19kHz

Note: Most of the characteristics shown above have been met in actual spacecraft hardware measurements [4].

Measured beacon antenna gain contours [4] are shown in Figures 3, 4 and 5.

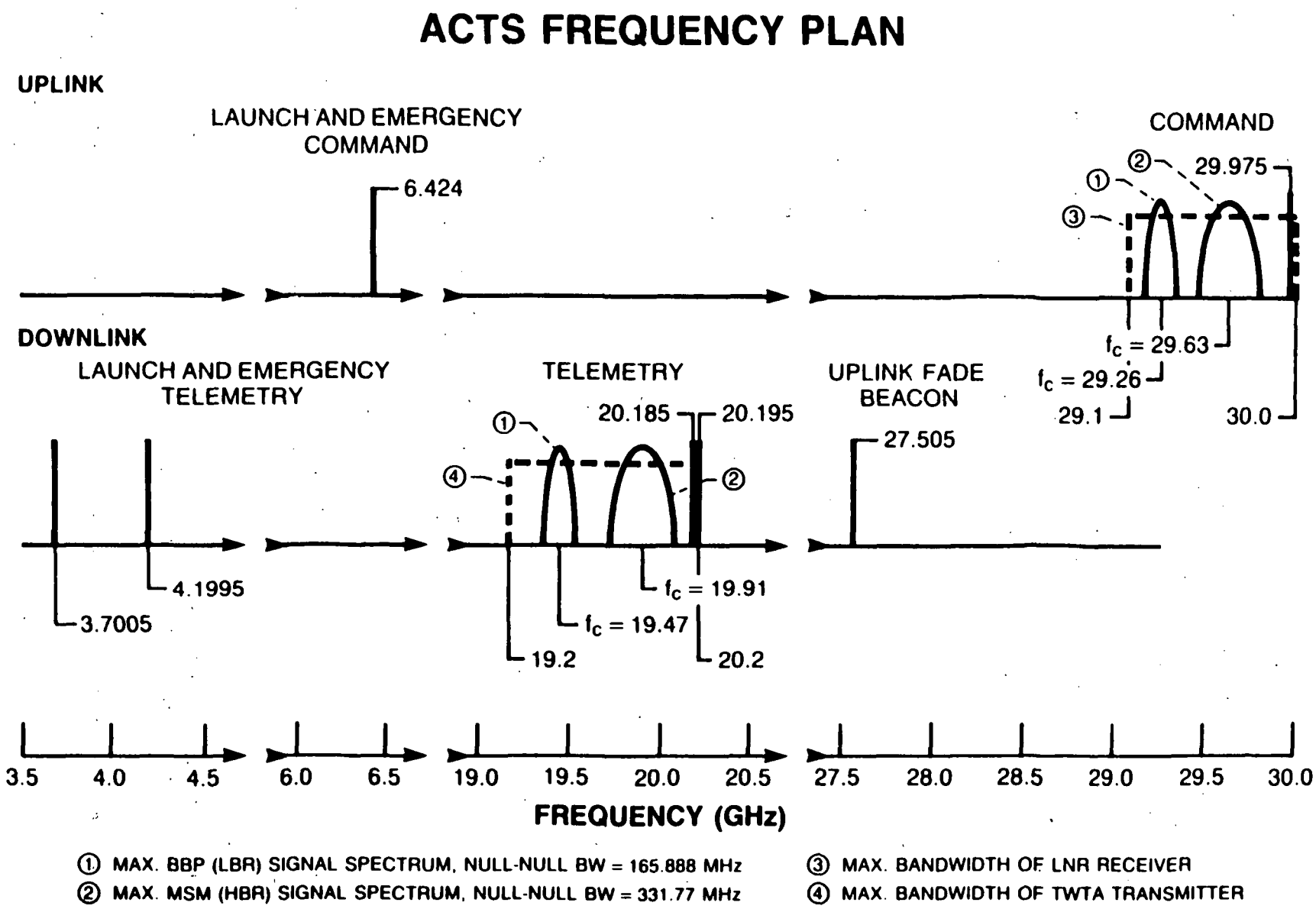
ACTS FREQUENCY PLAN
UPLINK
LAUNCH AND EMERGENCY COMMAND
6.424
COMMAND
29.975
f_c = 29.63
f_c = 29.26
29.1
30.0
DOWNLINK
LAUNCH AND EMERGENCY TELEMETRY
4.1995
3.7005
TELEMETRY
20.185
20.195
f_c = 19.91
f_c = 19.47
19.2
20.2
UPLINK FADE BEACON
27.505
3.5 4.0 4.5 6.0 6.5 19.0 19.5 20.0 20.5 27.5 28.0 28.5 29.0 29.5 30.0
FREQUENCY (GHz)
① MAX. BBP (LBR) SIGNAL SPECTRUM, NULL-NULL BW = 165.888 MHz
② MAX. MSM (HBR) SIGNAL SPECTRUM, NULL-NULL BW = 331.77 MHz
③ MAX. BANDWIDTH OF LNR RECEIVER
④ MAX. BANDWIDTH OF TWTA TRANSMITTER

Figure 2.

Ka-Band CR&T Antenna Assembly
V-POL Beacon Pattern—Measured 20.185 GHz

Figure 3.

Ka-Band CR&T Antenna Assembly
H-POL Beacon Pattern—Measured 20.195 GHz

Figure 4.

Ka-Band CR&T Antenna Assembly
Uplink Fade Beacon Pattern—Measured 27.505 GHz V-POL

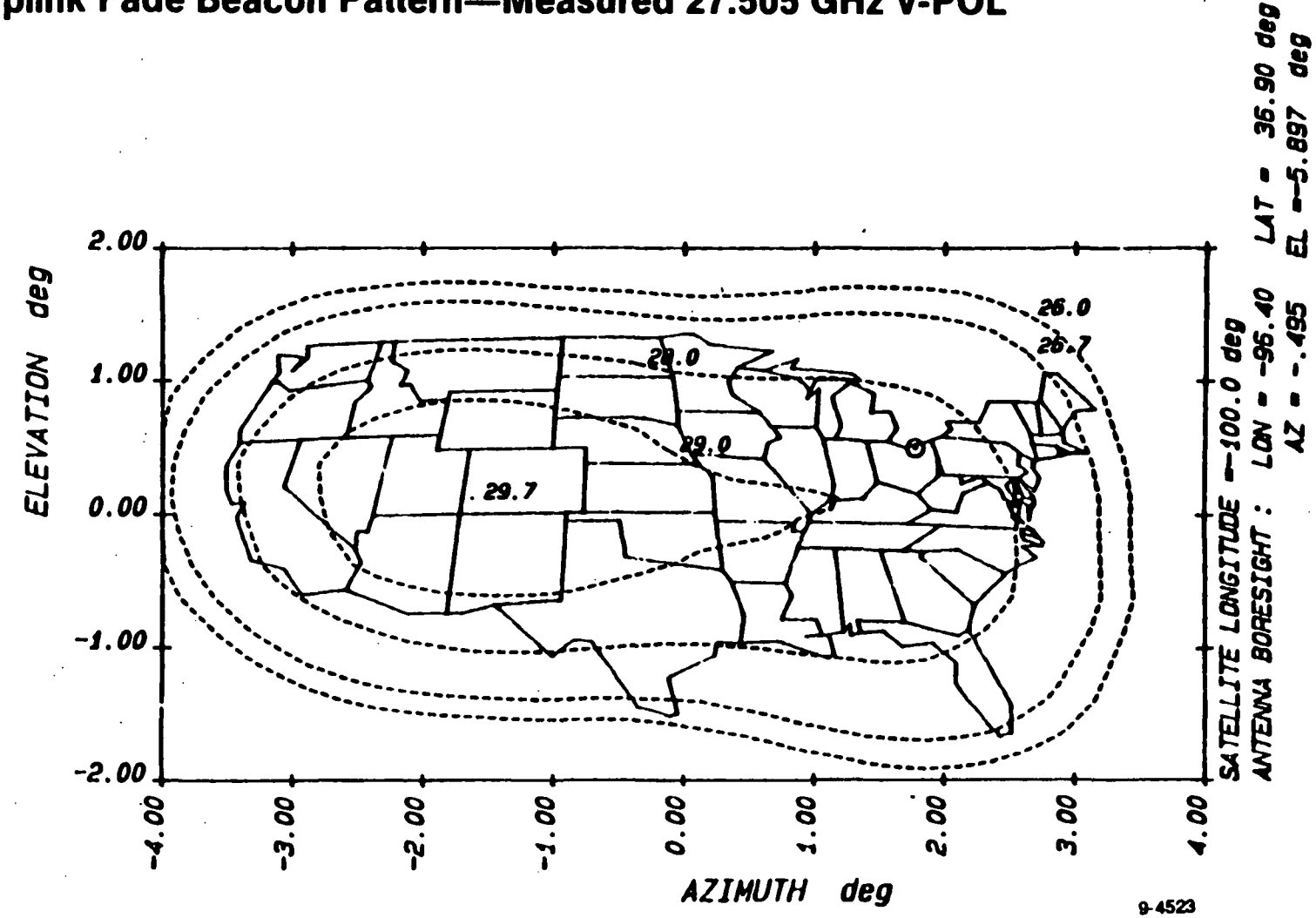

Figure 5.

4. System Calculations

4.1 Carrier-to-Noise Density

The carrier-to-noise density received on the ground is

$$C/N_o = EIRP \left(\frac{\lambda}{4\pi R}\right)^2 \frac{G}{kT} \frac{1}{L} \qquad (1)$$

where

C/N_o = Carrier-to-noise density
EIRP = Effective Isotropic Radiated Power of the beacon
λ = Wavelength of the beacon
R = Slant range between the satellite and the beacon receive terminal

$\left(\frac{\lambda}{4\pi R}\right)^2$ = Free Space Path Loss (PL) factor

G = Receive Antenna gain factor

k = Boltzmann's Constant (1.38×10^{-23} J/K)

T = Receive System Noise Temperature

L = System Loss factors

Expressing in dB, (1) can be written as

$$C/N_o \text{ (dB-Hz)} = EIRP \text{ (dBw)} - PL\text{(dB)} + G/T \text{ (dB/K)} + 228.6 \text{ (dBw/K-Hz)} - \text{Losses (dB)} \qquad (2)$$

4.2 System Losses

The principal sources of dry weather losses are considered as follows:

- Pointing error loss due to receive terminal and satellite antenna boresight to boresight misalignment
- Polarization loss due to rotation of the polarization vector with respect to the reference axis
- Atmospheric, cloud and scintillation loss

- Modulation loss of the carrier due to spreading of the CW carrier energy in modulated sidebands which is dependent on the modulation index chosen.

An estimate of the above losses is shown below:

Table 3. Estimation of System Losses

Source	Losses (dB)	
Frequency Band	27 GHz	20 GHz
Pointing Error (small aperture - no tracking)	1.5	1.2
Polarization Loss (XPD = 25 dB assumed)	0.2	0.2
Atmospheric and Cloud Attenuation	1.8	2.0
Scintillation* [5] (30° elevation)	0.2	0.1
Modulation Loss	-	2.3
Total	3.7	5.8

*Could be much higher for short duration under extreme conditions and at low elevation.

4.3 Receive G/T

The antenna gain-to-noise temperature ratio (G/T) is a trade-off between cost and the dynamic range (margin above threshold) of the receiving system. A common antenna with a dual polarized feed is the desired objective for cost effectiveness and operational considerations.

As a starting point we assume a 1-m dish with Cassegrain or Front Feed. We estimate the antenna efficiency as follows:

Parameter	Losses (dB)	
Frequency Band	27 GHz	20 GHz
Feed horn loss	0.2	0.15
Feed window loss	0.1	0.05
VSWR loss	0.2	0.2
Subreflector spill over loss	0.2	0.2
Main reflector spill over loss	0.1	0.1
Illumination loss	0.2	0.2
Blocking loss	0.6	0.5

Surface tolerance loss	1.0	0.8
Total	2.6	2.2
Expected Antenna Efficiency	55%	60%

The receive noise temperature under rain fade conditions can be written as

$$T_\gamma(a) = \frac{1}{abc}\left[T_s + T_a(a-1)\right] + \frac{T_o}{b}\left[(c-1) + (b-1)\right] + T_L + \frac{T_2}{G_A} \tag{3a}$$

where

$T_\gamma(a)$ = Receive noise temperature under rain fade
a = Down-link rain attenuation factor
b = Feed loss factor
c = Cloud attenuation factor
T_s = Sky noise temperature
T_a = Rain media temperature = 285°K
T_o = Environmental temperature = 293°K
T_L = LNA noise temperature
T_2 = Post Low-Noise Amplifier Noise Temperature
G_A = LNA gain

For a high-gain LNA, the last term in (3a) can be ignored for all practical purposes. Under dry weather conditions, a = 1 and (3a) simply becomes

$$T_\gamma = \frac{T_S}{bc} + \frac{T_o}{b}\left[(c-1) + (b-1)\right] + T_L + \frac{T_2}{G_A} \tag{3b}$$

For a given value of T_L, the excess noise temperature due to rain attenuation

$$\Delta T = \{T_\gamma(a) - T_\gamma\} = \left(\frac{a-1}{a}\right)\left(\frac{T_a - T_s}{bc}\right) \tag{3c}$$

We now estimate noise temperatures contribution at two frequency bands as follows:

Noise Source	Parameter Value	
Frequency Band	27 GHz	20 GHz
Sky (at 30° elevation) (T_s)	30°K	45°K
Rain attenuation (a)	TBD	TBD
Dual Polarized Feed Loss (b)	1 dB	0.8 dB
Cloud attenuation (Slobin Model; Cumulative Distribution >90%)	1.3 dB	1.6 dB
LNA Noise Temperature (T_L)	TBD	TBD
Post LNA Noise (T_2/G_A)	negligible	negligible

Using the above parameters we calculate the excess noise temperature as a function of rain attenuation via (3c) as shown in Figure 6 .

4.4 Radiometers

In order to detect the system noise degradation due to rain attenuation and finite perturbation in the system parameters a radiometric measurement method has to be incorporated. Either Dicke-switched radiometers [6] or total power radiometer with self calibration can be used. The Dicke-switch switches periodically at a high rate between the incoming signal (or noise) with a reference source. By this comparison method at a reasonably high rate the low frequency fluctuations in the receive amplifiers and the active devices can be eliminated. On the other hand, total power radiometers are simple in design where the gain and bandwidth fluctuations of the receiving device need compensation. With temperature control and improved circuit design total power radiometers are becoming popular. The advantage of total power radiometer is that its sensitivity is almost a factor of two better than Dicke radiometer.

For a Dicke radiometer with square wave demodulation the noise temperature sensitivity can be written as

$$\Delta T_{rms} = \frac{2(T_S + T_R)}{\sqrt{B\tau}} \qquad (4)$$

T_S = Sky noise temperature
T_R = Receiver noise temperature
B = RF Bandwidth of the receiver
τ = Integration time

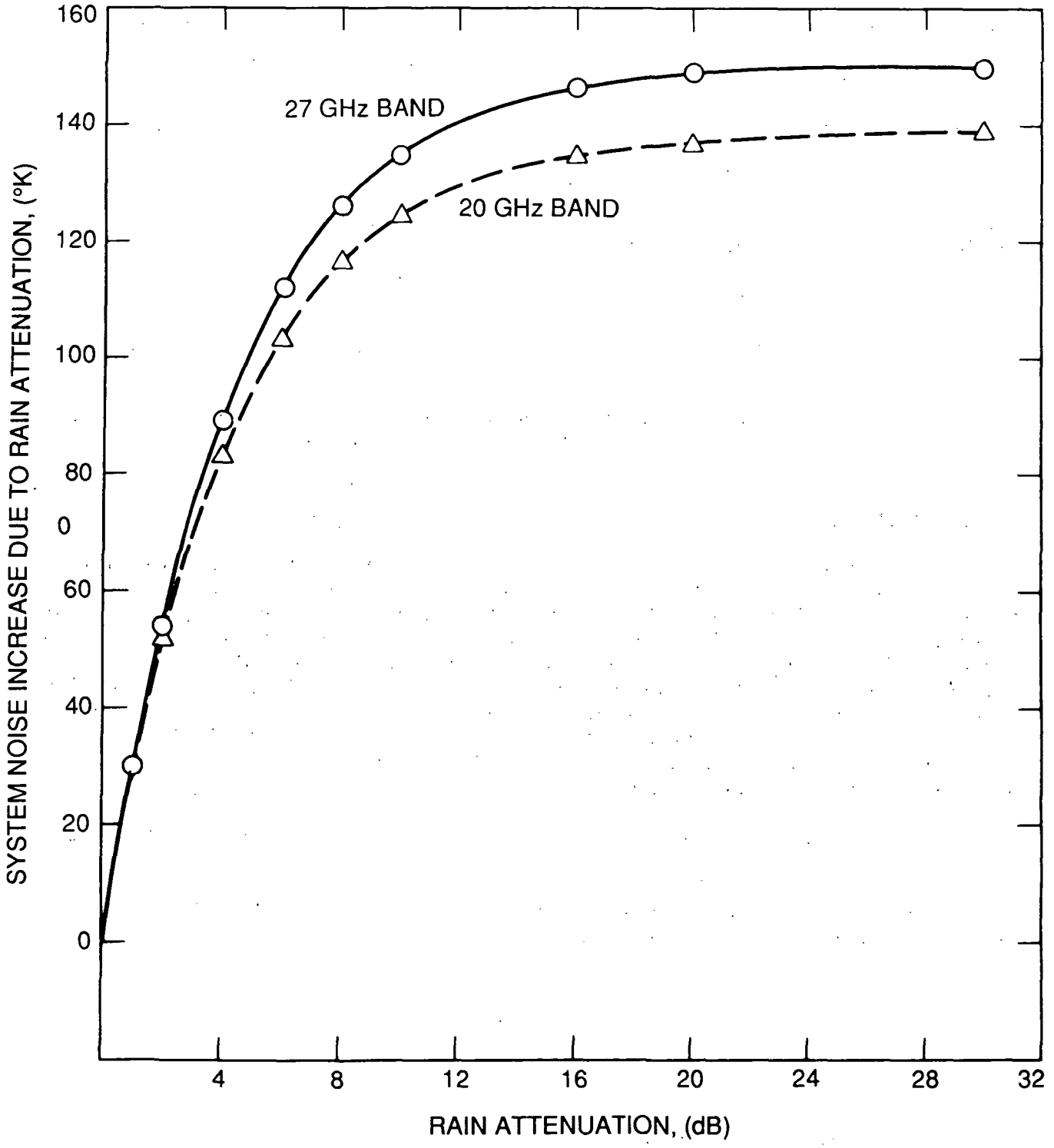

Figure 6. System Noise Increase Due Rain Attenuation

A typical sensitivity calculation for Dicke radiometer is shown below:

LNA maximum noise figure = 8-dB	$T_R \simeq 1550°K$ (max)
Sky noise temperature	$T_S \simeq 50°K$
RF Bandwidth	$B = 10$ MHz
Integration time	$\tau = 1$ sec
Sensitivity via (4)	$\Delta T_{rms} \simeq 1°K$

The proposed radiometer is a hybrid version of Dicke Switch and total power radiometer, hence, the sensitivity figure calculated above will be in the range of 0.5 to 1°K.

4.5 Example Link Calculations

We now perform some example link calculations using the concept of a common antenna, feed, and LNA for both 27 GHz and 20 GHz bands beacons as follows:

Parameters	Values	
Frequency band (GHz)	27.5	20
Common Antenna Size (m)	1	1
Antenna Efficiency (%)	55	60
Antenna Gain (dB)	46.5	44.2
Beam Width at -3 dB points (degree)	0.76	1.05
Beacon antenna gain over full CONUS (dBi)	26	26
Nominal beacon RF output (dBm)	20	23
Nominal beacon EIRP (dBw)	16	19
Path Loss at 30° elevation (dB)	213	210
Modulation Loss (dB)	-	2.3
System Losses including Modulation Loss (dB)	3.7	5.8
Max Dry Weather System Noise Temperature with 8-dB NF LNA (°K)	1750	1750
Dry Weather Receive G/T (dB/K) worst case	14.1	11.8
Boltzmann's Constant (dBw/K-Hz)	-228.6	-228.6
Receive Carrier-to-Noise Density, C/N_o (dB-Hz)	42	43.6
C/N in 10 Hz bandwidth (dB)	32	33.6
C/N Threshold Level (dB)	10	10
Dynamic range (margin over threshold) (dB)	22	23.6

Therefore, with a 1-m antenna, common feed and a worst case 8-dB noise figure LNA, the RF terminal will provide in excess of 20-dB dynamic range at both frequency bands. With 4-5 dB noise figure LNAs the dynamic range will be well in excess of 20-dB.

5. Hardware Design Considerations

ACTS beacon receive terminal design will perhaps be similar to the design of Olympus program [7]. However, logistically and technically, there are some differences [8, 9] which must be taken into consideration. In the Olympus program there are three beacons (12, 20, and 30 GHz bands) and three

separate antennas which simplified the RF system design. Economically, three separate antennas were perhaps justified for the Olympus experiment because only one experimenter was supported by NASA/JPL. On the other hand, a large number of participants (8-10) are envisioned in the ACTS propagation study. Therefore, two sets of antennas, and RF assemblies are not desirable economically and logistically. As a result, we examine two approaches as follows:

- Preferred Approach - Common antenna, dual polarized feed and two separate LNAs as shown in Figure 7.

- Alternate Approach - Two separate antennas and separate RF subsystems as shown in Figure 8 where the polarization of the 20 GHz terminal feed will be manually adjusted in the event the down-link beacon polarization is changed.

These two approaches are compared below:

Item	Common Antenna	Two Antennas
Antenna Cost	$XK	$2XK
Feed Cost	$YK	Nominal
(Antenna + Feed) Cost	$(X+Y)K	$2XK
Polarization Change	None	Yes
Operational Logistic	Simple	Difficult

Items mentioned above will be examined during the prototype development phase and the optimal design will be chosen for the manufacturing phase.

The proposed beacon receive terminal is comprised of three subsystems as follows:

- RF Subsystem - Out Door Unit (ODU), comprising the antenna, feed, radiometer, LNA and First IF Output (refer Figs. 7 and 8).

- IF Subsystem - In Door Unit (IDU), comprising second IF stage and distribution panel (refer Fig. 9).

- Fade detection unit comprising the digital signal processor and the computer interface unit which is discussed elsewhere.

5.1 RF Subsystem - Out Door Unit (ODU)

Two RF Subsystem (ODU) baseline block diagrams are shown in Figs. 7 and 8.

5.1.1 Antenna Functional Requirements

Size	1.0 m to 1.2 m
Type	Offset-fed or Cassegrain
Mount	Az/El
Feed Configuration	Dual Polarized

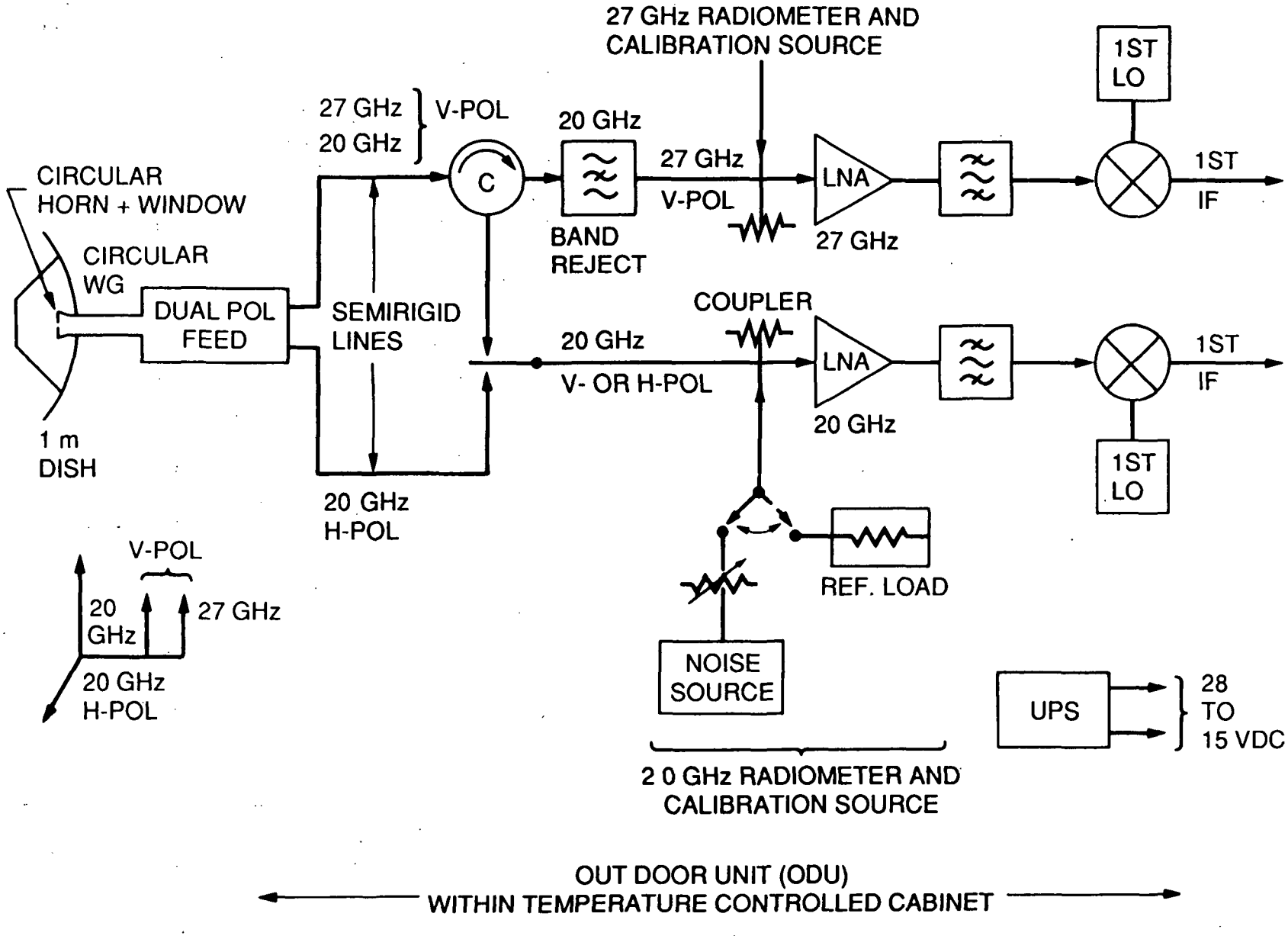

Figure 7. Scheme-1 Common Antenna: ACTS Beacon Receive RF Subsystem-Out Door Unit (ODU)

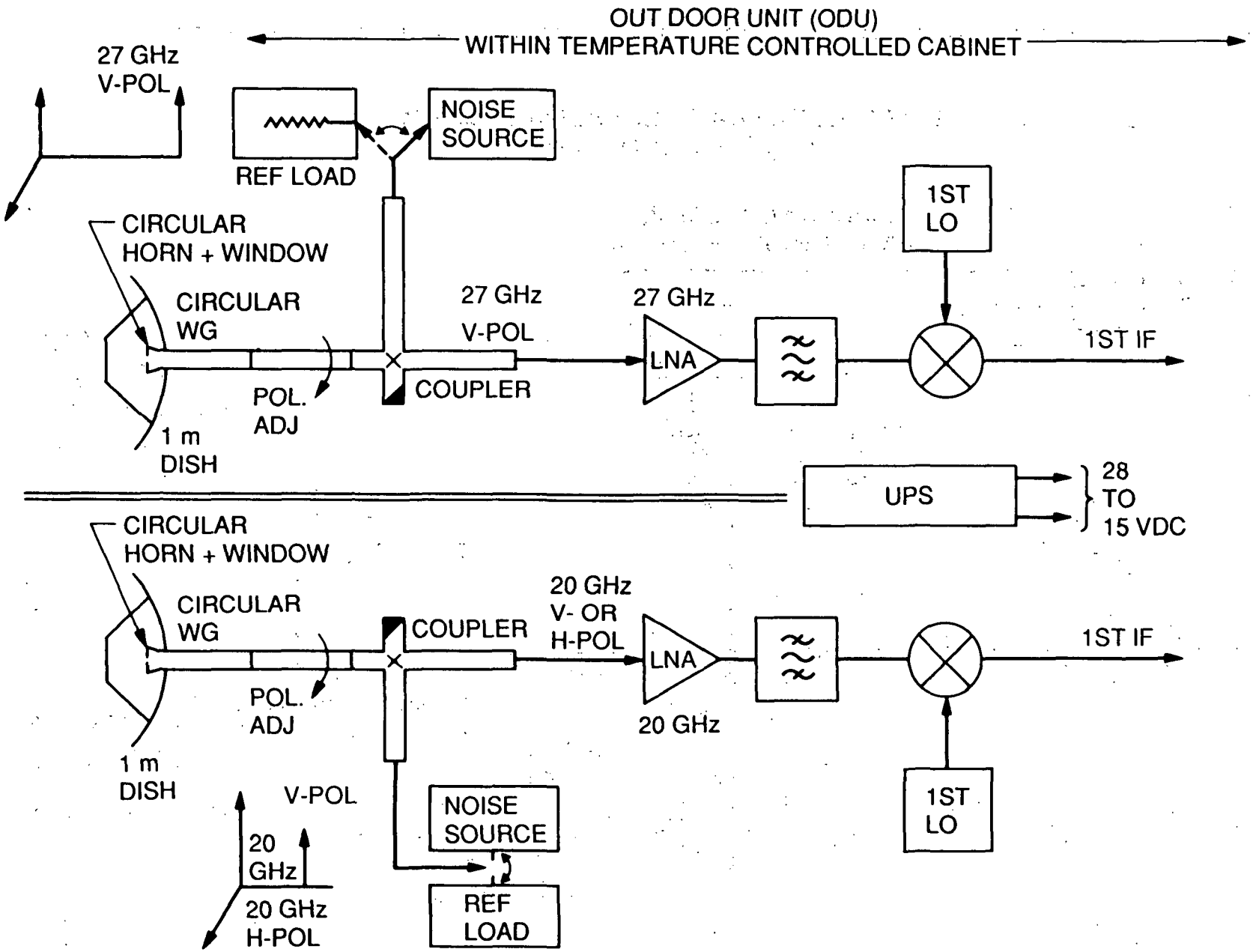

Figure 8. Scheme II Separate Antennas: ACTS Beacon Receive RF Subsystem-Out Door Unit (ODU)

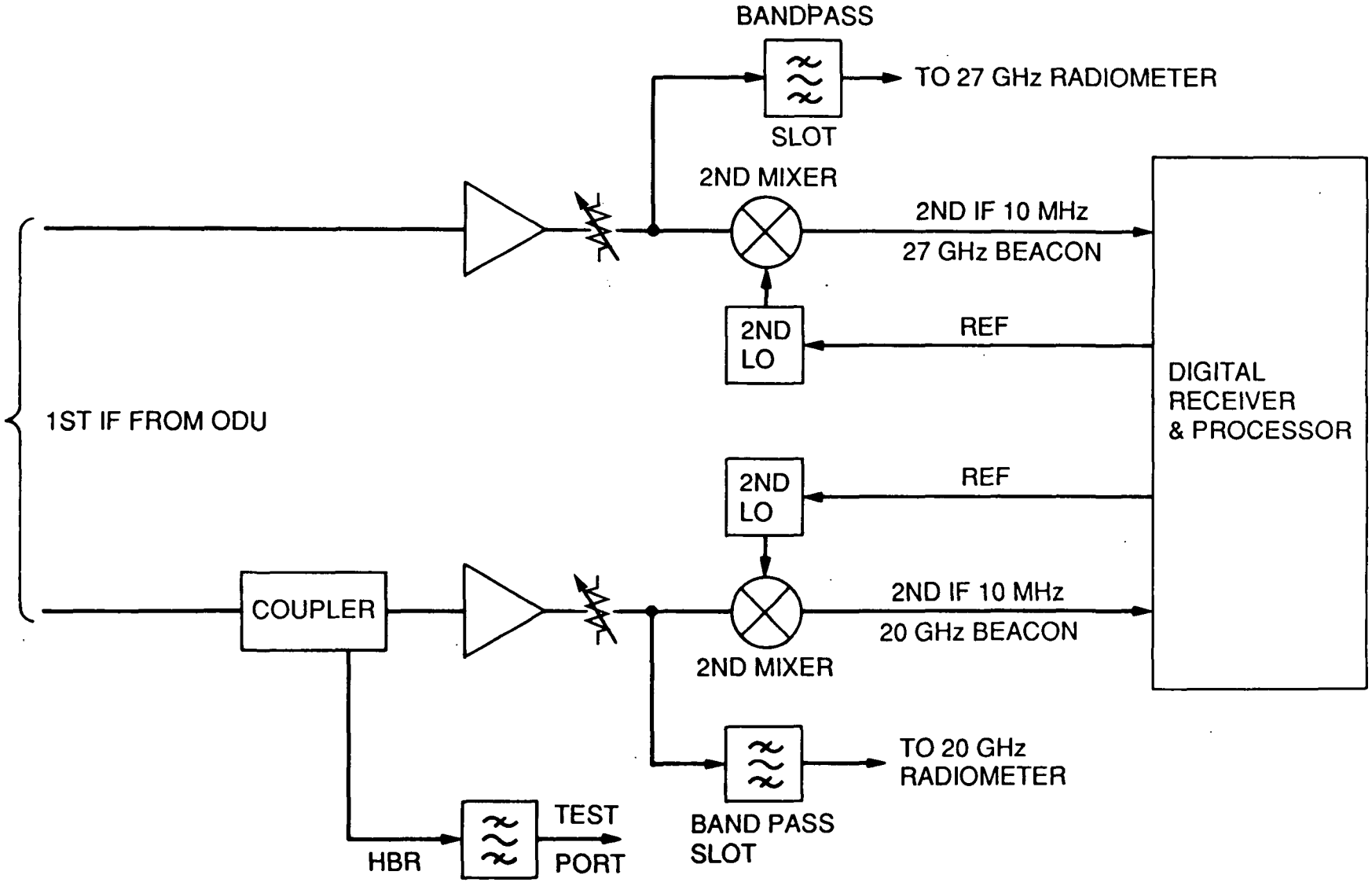

Figure 9. ACTS Beacon Receive IF Subsystem - In Door Unit IDU

Anti-Ice	Optional
Polarization	Orthogonal linear, mechanically adjustable (to 90°)
Receive Gain 1-m at 27.5 GHz	46.5 dBi
at 20 GHz	44.2 dBi
Cross-pol isolation	>25 dB
Waveguide interface	Circular (size TBD)
Operating temperature	-40° to +50°C
Operating wind speed	50 mph with 70 mph gusts
Survival wind speed	125 mph

5.1.2 Common Feed Unit

The principle of electric field distribution in a circular waveguide is utilized in separating two sets of orthogonal linear polarized signals [10] as shown in 10(a). The circular section of the feed excites both vertically polarized beacons when present in such a way that the TE_{11} Field vectors are perpendicular to the thin metallic septum (for initial alignment of the feed, the metal septum can be used as a reference plane) which transmits these vectors unperturbed to be coupled to the rectangular waveguide via a linear taper (circular-to-rectangular waveguide). The outputs are separated by a circulator and a 20 GHz band reject filter as shown in Fig. 7. Now if a coupling slot is cut across the broad side of a rectangular-circular waveguide junction as shown by the cross-sectional view (refer Fig. 10(b)) then the horizontally polarized beacon signal vector at 20.195 GHz when present will be coupled in the side rectangular waveguide exciting a TE_{10} mode. The septum will act as a reflector to the horizontal polarized vector. A mechanical switch will select the V- or H-Pol 20 GHz beacon as needed.

The slot dimensions, length (ℓ) and width (w) can be calculated [10] as follows:

$$\ell = \frac{\lambda o}{2} + 0.273\ w$$

or

$$1 = \frac{\lambda o}{2\ell} + 0.273\ \left(\frac{w}{\ell}\right) \qquad (5)$$

where

λ_o = Free space wavelength at 20.195 GHz
(w/ℓ) ratio ≤ 0.11

Thickness of the slot should not exceed (w/2)

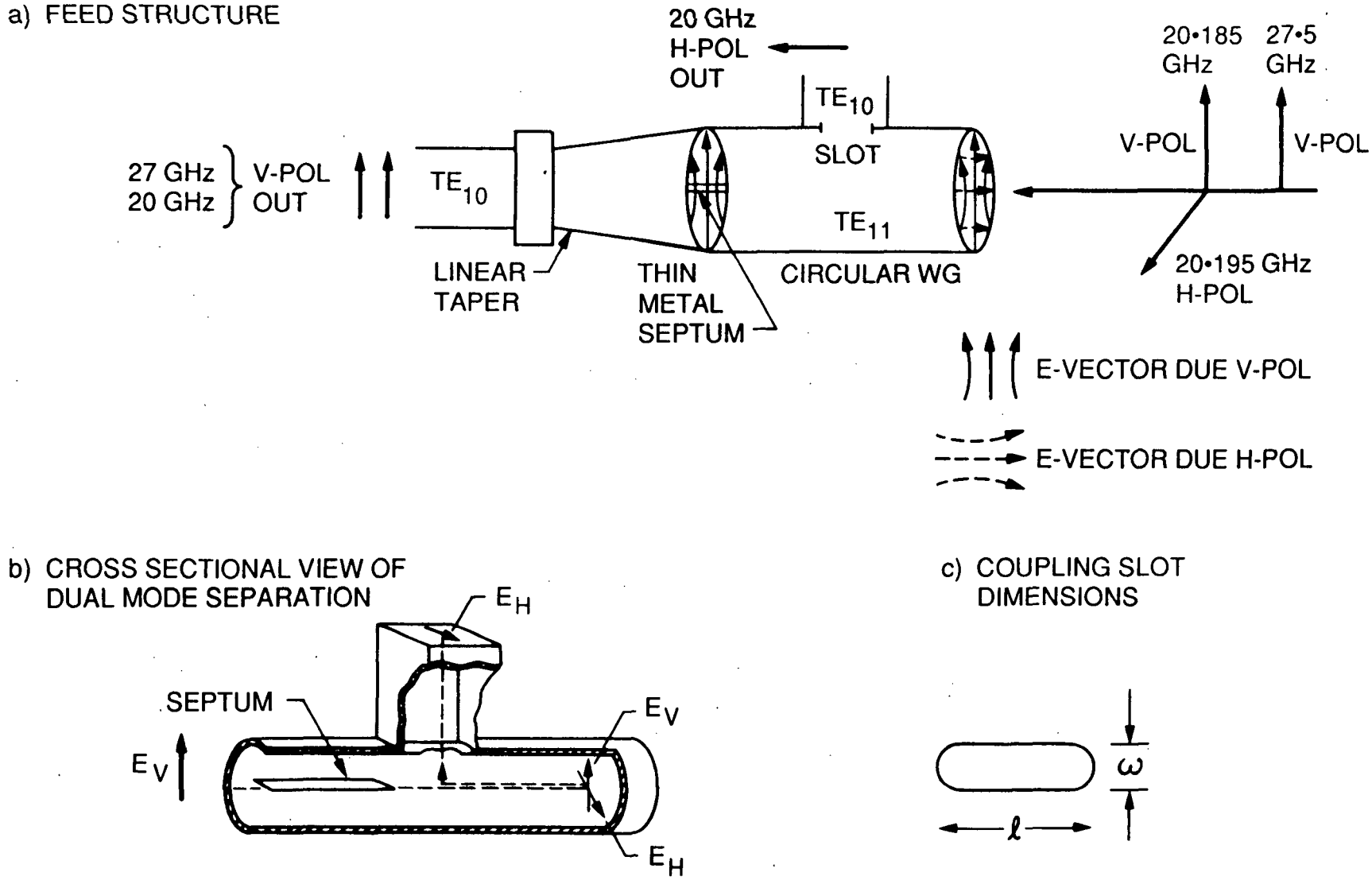

Figure 10. Common Feed Structure

5.1.3 LNA Characteristics

Typical characteristics of commercial LNAs are shown below:

Frequency Band	28 GHz	20 GHz
Gain	30 dB	30 dB
Noise Figure	4-dB	3.5 dB
Power Output @ 1-dB Compression	+10 dBm	+6 dBm
Gain Flatness	±0.5 dB	±0.75 dB
VSWR (In and Out)	2:1	2:1
Power Consumption	5.4-w @ +15 VDC	4.5-w @ +15 VDC
Operating Temperature	0-50°C	0-50°C
Connector	WR 28 (I/O)	SMA (I/O)

5.1.4 Excess Noise Source for Radiometer

As discussed before, a radiometer provision is essential to measure the excess noise temperature and to calibrate the system from slowly varying fluctuations of the system parameters such as gain/bandwidth of the receiver. The radiometer can be total power type or Dicke-switch type. A broadband saturated diode type noise source is provided with a precision attenuator for noise level setting which can be switched electronically by a motor drive. A reference ambient or cooled waveguide load or a combination of both can be provided for the noise source calibration at a regular interval.

5.1.5 First Down-Converter

After noise injection, the beacon signal in the presence of link noise and additional injected noise are split into two separate beacon paths in the Common Antenna Scheme as shown in Fig. 7. In the two-antenna scheme the RF paths are separate as shown in Fig. 8. The up-link fade beacon is filtered through a narrowband bandpass filter (±100 MHz) to eliminate spurious. On the other hand, the down-link beacon/s is filtered through a reasonably wideband filter, ±500 MHz bandwidth in order to accommodate the communication carrier band/s for experimental purposes to be discussed. Temperature controlled crystal oscillators provide two LO sources.

Functional requirements of the first down converter are shown below:

Input Level	-80 ±6 to -110 ±6 dBm
Output Level	-20 ±6 to -50 ±6 dBm
Nominal Frequency	TBD
Bandwidth	±500 MHz
Output Impedance	50 ohms
Return Loss	> 15 dB
Image Rejection	> 45 dB
Nominal LO Frequencies	TBD
Phase Noise	-80 dBC/Hz @ 10 KHz

5.2 IF Subsystem - In Door Unit (IDU)

The IF Subsystem as shown in Fig. 9 essentially provides two channel outputs for each receive beacon path. One channel feeds the radiometer and the second channel feeds the link fade detector. The nominal frequency of the second IF is 10 MHz. Two band pass slots are inserted in the radiometer path prior to the second mixer. The bandwidth of these slots determine the predetection bandwidth of the radiometer (B in equation 4).

The 20 GHz beacon path has an additional port which can allow the communication carrier say the HBR to be used for additional tests. An example of the additional test could be an attenuation measurement of the unmodulated HBR carrier power via the mechanically steered spot beam in region/s beyond CONUS coverage say Alaska, Polar Region or Hawaii where the beacon signal strength is very low.

6. Acknowledgements

Acknowledgement is made to R. Hughes of JPL and members of the EE Department of Virginia Polytechnique Institute for many useful discussions.

7. Conclusions

ACTS propagation experimenters' terminal hardware design issues have been identified and a practical design plan and specifications have been outlined.

8. References

1. D. V. Rogers, "Propagation Considerations for Satellite Broadcasting at Frequencies Near 10 GHz," IEEE J. Selected Areas Commun., January 1985.

2. R. K. Crane, "Prediction of Attenuation by Rain," IEEE Trans. Commun., Sept. 1980.

3. F. M. Naderi and S. J. Campanella, "NASA's Advanced Communications Technology satellite (ACTS): An Overview of the Satellite, the Network, and the Underlying Technologies," AIAA Proc., paper No. 88-0797.

4. F. Gargione, "Spacecraft Beacon Characteristics," Proc. First ACTS Propagation Studies Workshop (APSW1), November 28-29, 1989, Santa Monica, California.

5. L. J. Ippolito Jr., Radiowave Propagation in Satellite Communications, Van Nostrand Reinhold Co., New York, 1986.

6. J. D. Kraus, Radio Astronomy, McGraw Hill Book Co., 1966.

7. C. W. Bostian, W. L. Stutzman, T. Pratt, J. C. McKeeman, and T. S. Rappaport, "Communications and Propagation Experiments for the Olympus and ACTS Satellites," ICC, June 1989.

8. F. Davarian, "ACTS Propagation Workshop Opening Remarks," Proceeding First ACTS Propagation Studies Workshop, Santa Monica, California, November 28-29, 1989.

9. F. Pergal, "Development Plan for the ACTS Propagation Experimenters' Terminal," JPL Internal Memorandum, March 1990.

10. D. Chakraborty and G. F. D. Millward, "Circularly Polarized Diplexer," Int. Conf. on Satellite Communications, IEE, London, November 22-28, 1962.

Advanced Communications Technology Satellite (ACTS)
Propagation Workshop

Spacecraft Beacon Characteristics (Update)

May 12, 1990

Presented by

F. Gargione
GE

ACTS Spacecraft Beacon Characteristics

OVERVIEW

- Spacecraft Configuration
- CR&T Subsystem Block Diagram
- CR&T Antenna Characteristics
- Beacon Characteristics
- Expected Beacon Operational Temperatures
- Telemetry Modes
- Modulated Beacon Spectrum
- Conclusions

FLIGHT SYSTEM CONFIGURATION

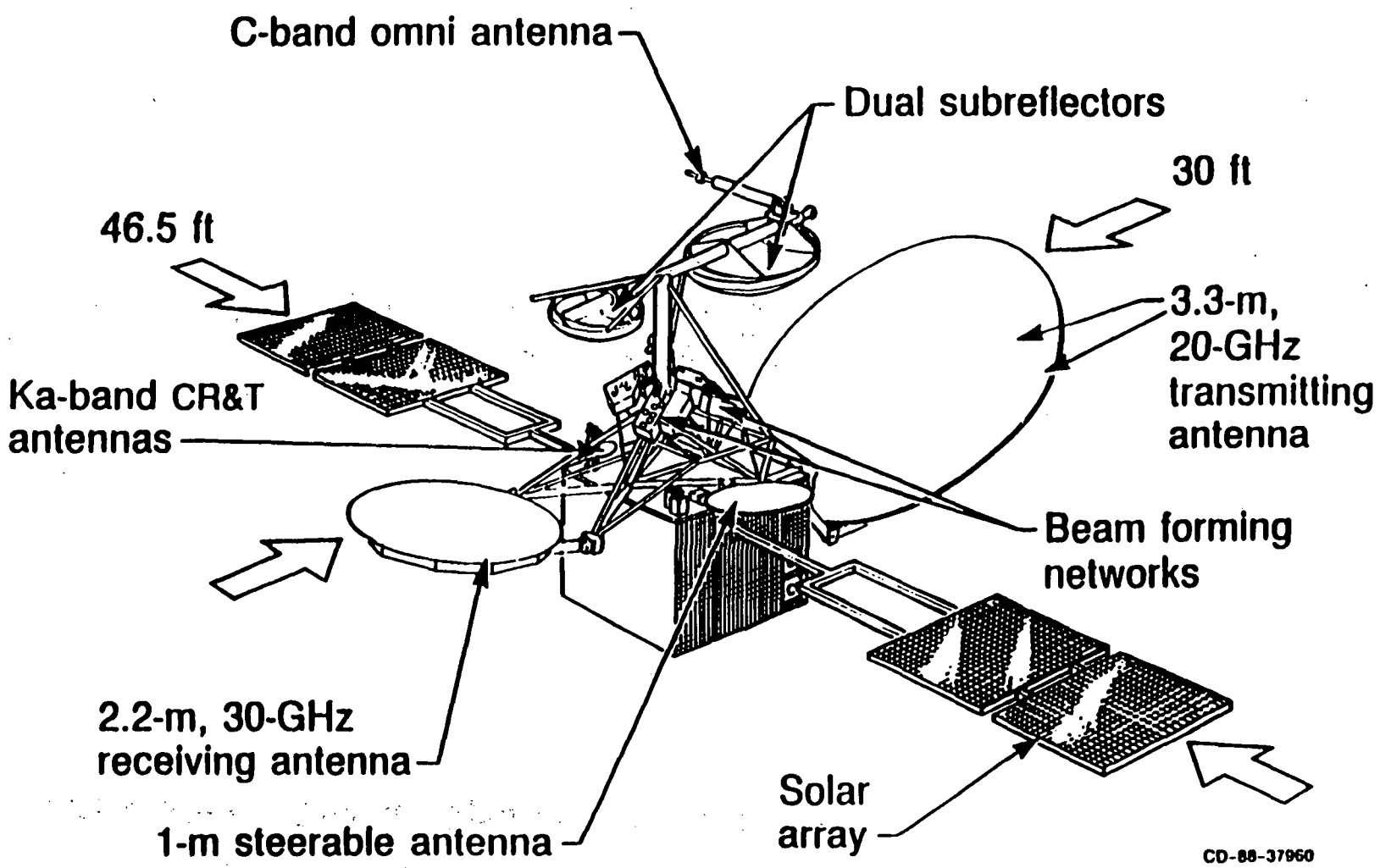

WFC-5/9/90

ACTS Spacecraft Beacon Characteristics

ACTS Flight System Operational Configuration

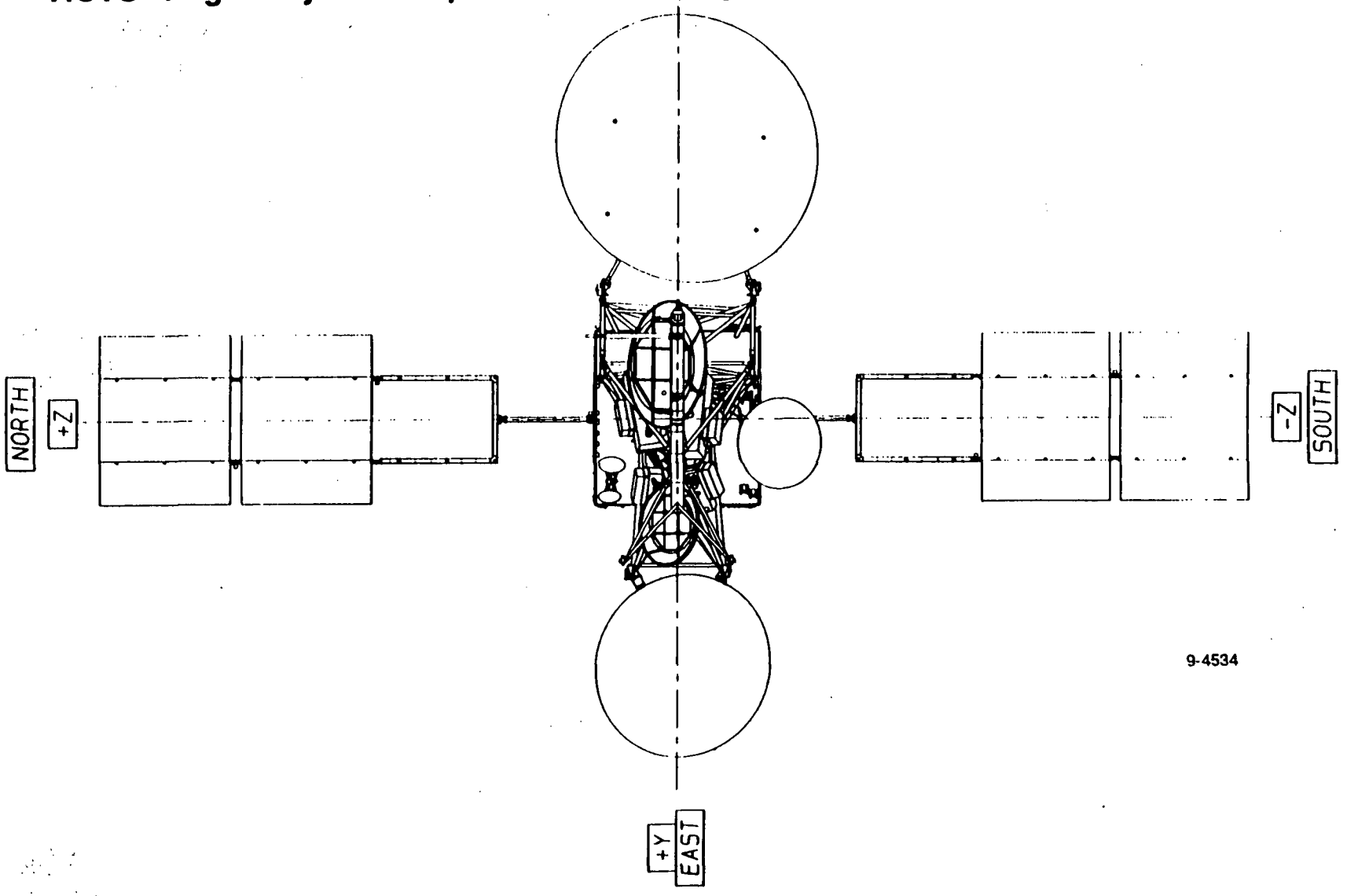

FLIGHT SYSTEM CHARACTERISTICS

WEIGHT: 5840 LBS IN GTO
3175 LBS ON STATION (BOL)

POWER: 1770 WATTS (BOL)

MISSION LIFE: 2 YEAR MINIMUM
(PROPELLANT AND POWER FOR 4 YEARS)

STABILIZATION: SPIN STABILIZED IN GTO
3-AXIS STABILIZED ON STATION

POINTING ACCURACY: 0.025 DEGREE WITH AUTOTRACK

LAUNCH VEHICLE: STS PLUS TOS UPPER STAGE

PAYLOAD: 3 KA-BAND CHANNELS
BANDWIDTH, 900 MHZ
G/T, 16 dB/K
EIRP, 59 dBW

WFC-5/9/90

ACTS Spacecraft Beacon Characteristics

Command, Ranging, and Telemetry Block Diagram

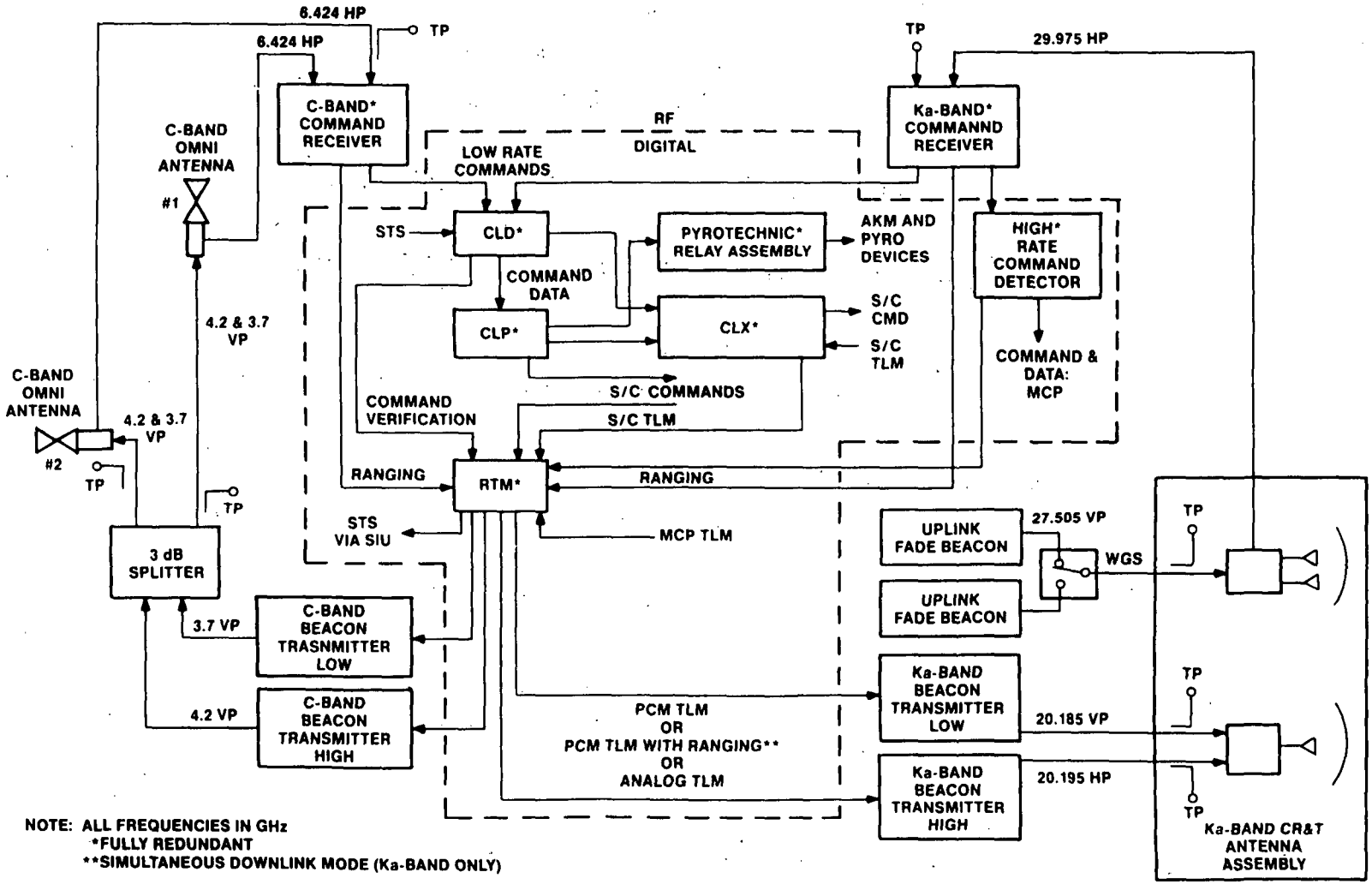

NOTE: ALL FREQUENCIES IN GHz
*FULLY REDUNDANT
**SIMULTANEOUS DOWNLINK MODE (Ka-BAND ONLY)

9-4502

ACTS Spacecraft Beacon Characteristics

Antenna Assembly (Plan View)

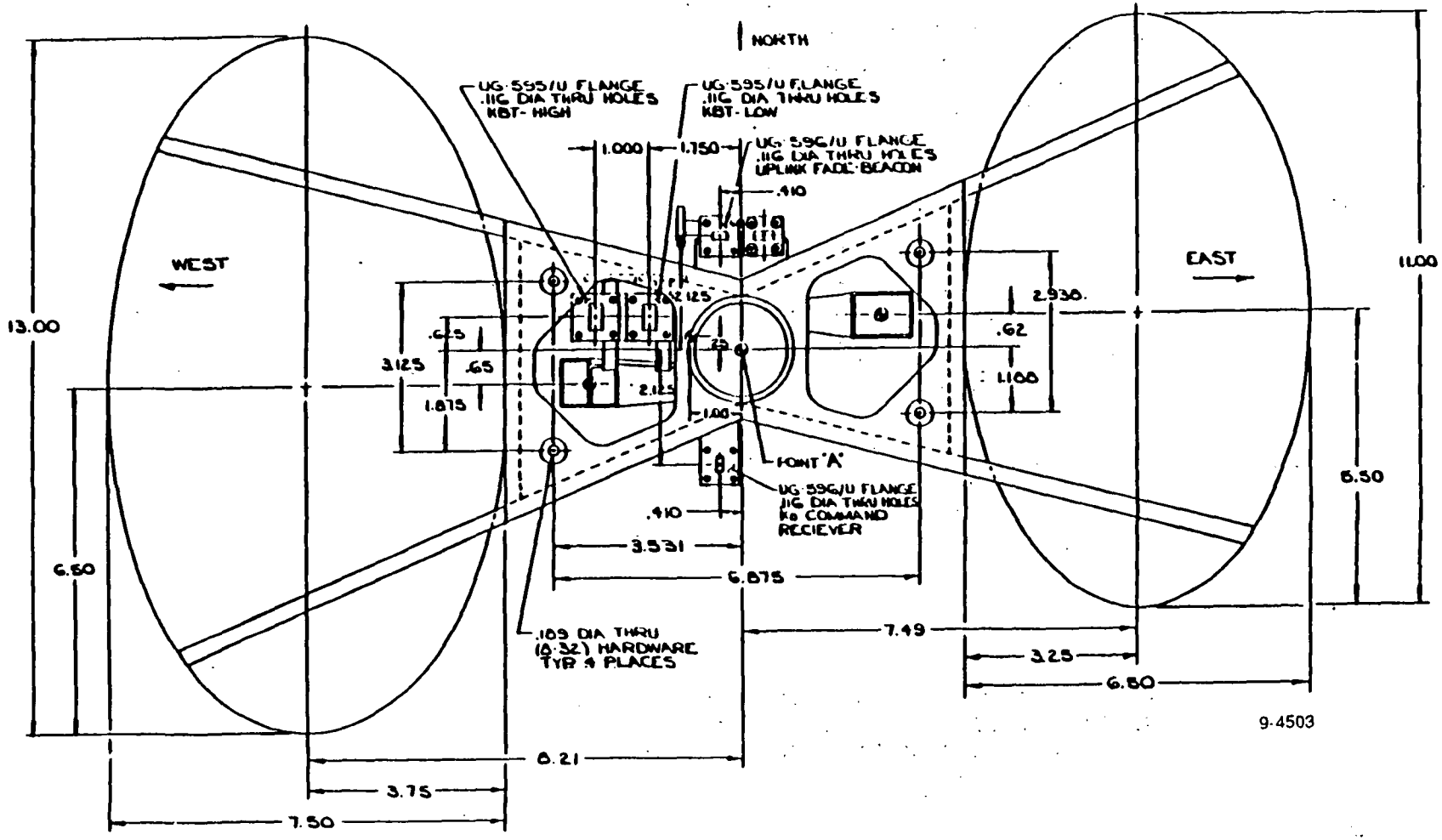

ACTS Spacecraft Beacon Characteristics

CR&T Ka-Band Antenna Diagrams

F_1 — FILTER WITH 40 dB SUPPRESSION OF 27.5-30.6 GHz
F_2 — FILTER WITH 35 dB REJECTION OF 27.5-27.510 GHz AND 60 dB SUPPRESSION OF 34.803 GHz RELATIVE TO 29.975 GHz

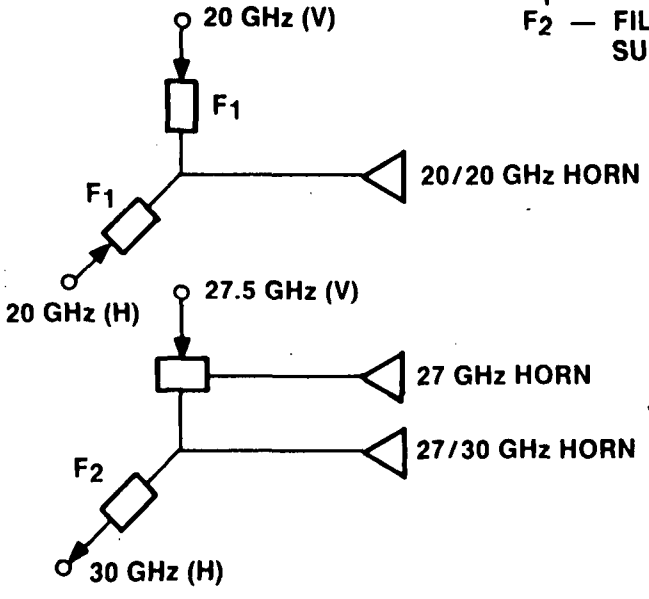

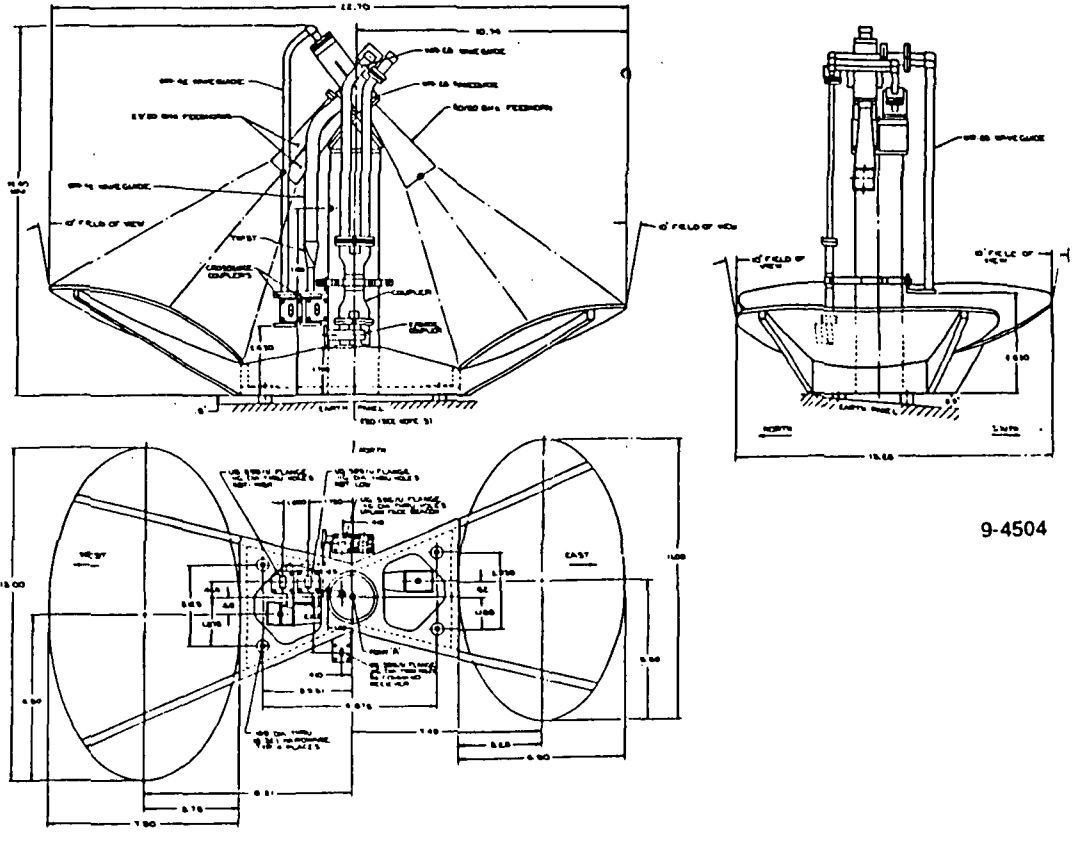

9-4504

ACTS Spacecraft Beacon Characteristics

Ka-Band Antennas Spec Summary

- 2 INDEPENDENT ANTENNAS
  - — 27/30 ANTENNA SIGNALS (TWO-HORN CONFIGURATION)
    - UPLINK FADE BEACON, 27.505 GHz, VERTICAL POLARIZATION
      - GAIN = 26.7 dBi (CONUS)
    - COMMAND RECEIVER, 29.975 GHz, HORIZONTAL POLARIZATION
      - GAIN = 29.7 dBi (CLEVELAND, OH)
  - — 20/20 ANTENNA SIGNALS
    - TELEMETRY BEACON, 20.185 GHz, VERTICAL POLARIZATION
      - GAIN = 25.9 dBi (CONUS)
      - GAIN = 28.4 dBi (CLEVELAND, OH)
    - TELEMETRY BEACON, 20.195 GHz, HORIZONTAL POLARIZATION
      - GAIN = 25.9 dBi (CONUS)
      - GAIN = 28.4 dBi (CLEVELAND, OH)
  - — ISOLATION REQUIREMENTS
    - ALL BEACONS (3) TO COMMAND RECEIVER — 70 dB
    - BOTH 20 GHz BEACONS TO 27/30 GHz ANTENNA — 50 dB
  - — WEIGHT APPROXIMATELY 2.5 LBS.

ACTS Spacecraft Beacon Characteristics

Antenna Block Diagram
20 GHz System

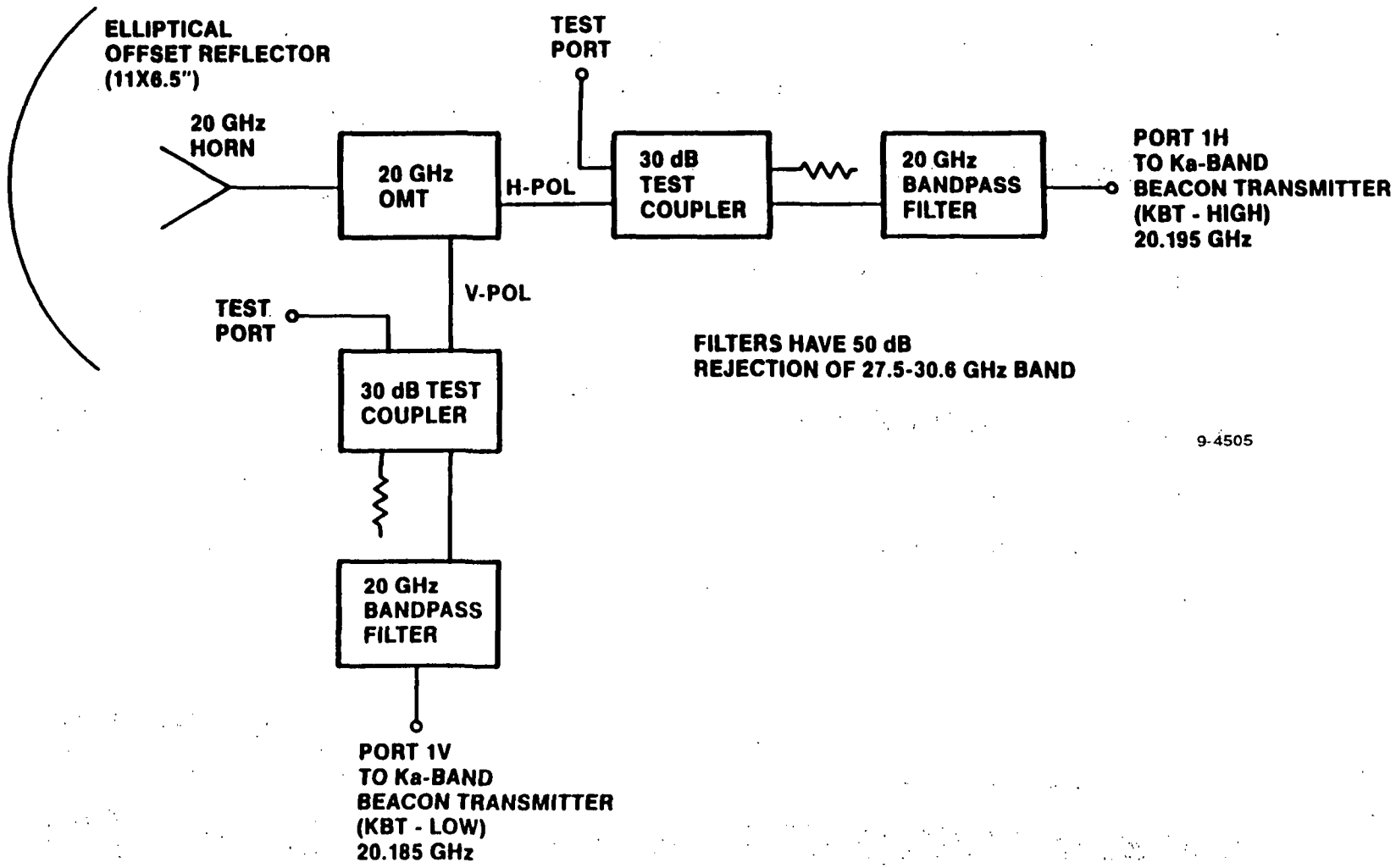

ACTS Spacecraft Beacon Characteristics

Ka-Band CR&T Antenna Assembly
V-POL Beacon Pattern—Measured 20.185 GHz

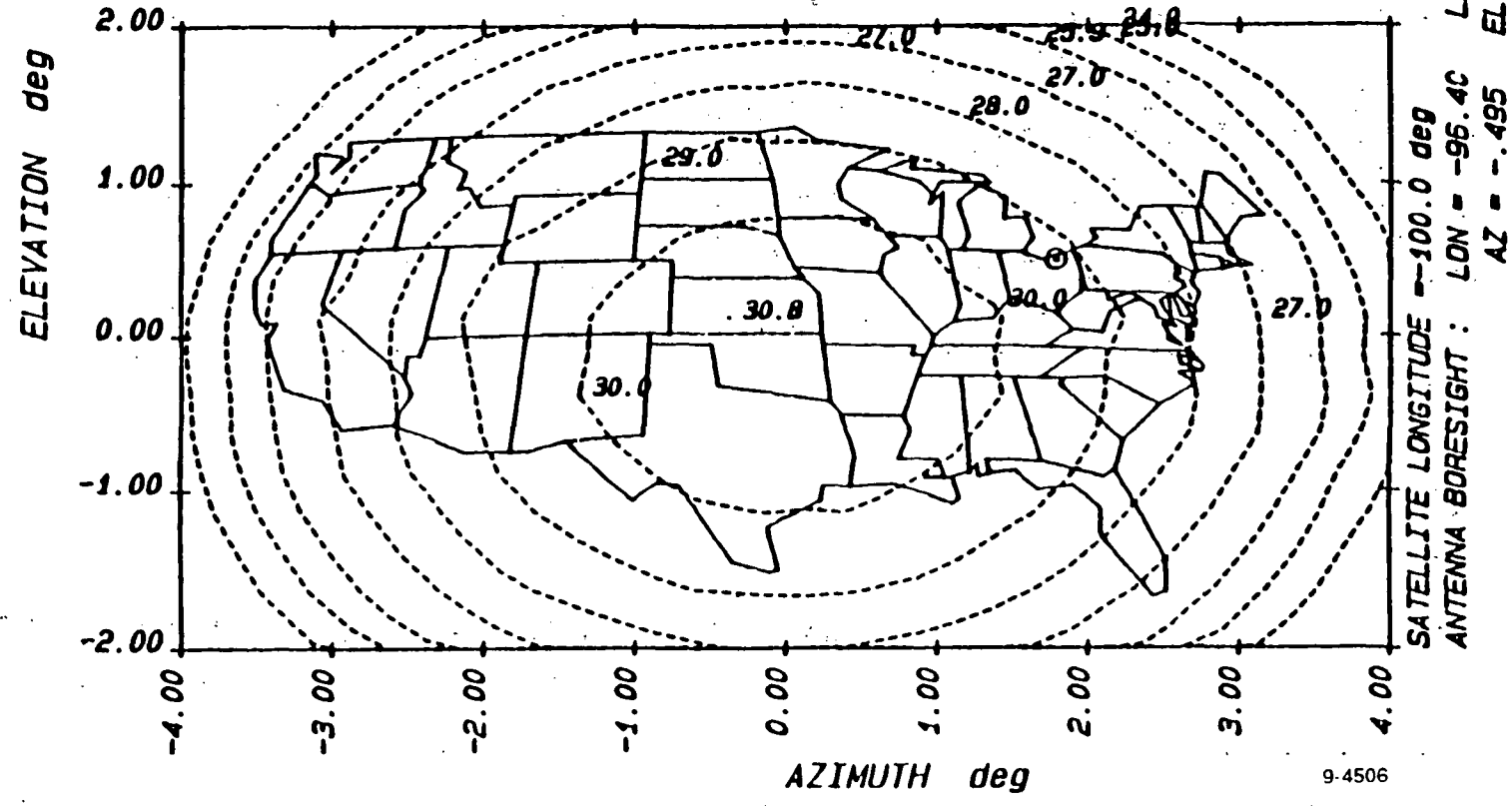

ACTS Spacecraft Beacon Characteristics

Ka-Band CR&T Antenna Assembly
H-POL Beacon Pattern—Measured 20.195 GHz

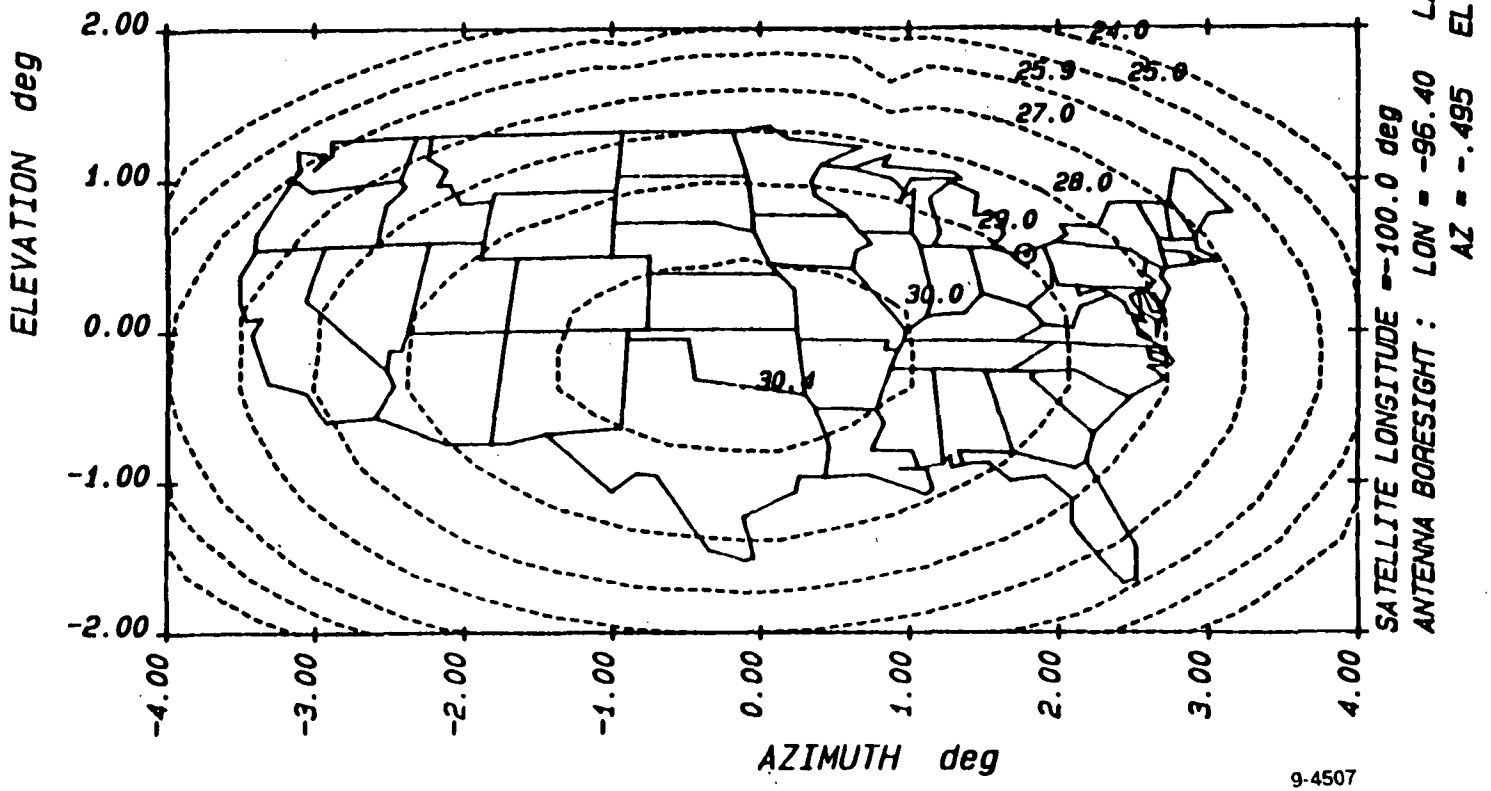

ACTS Spacecraft Beacon Characteristics

Antenna Block Diagram
27.5/30 GHz System

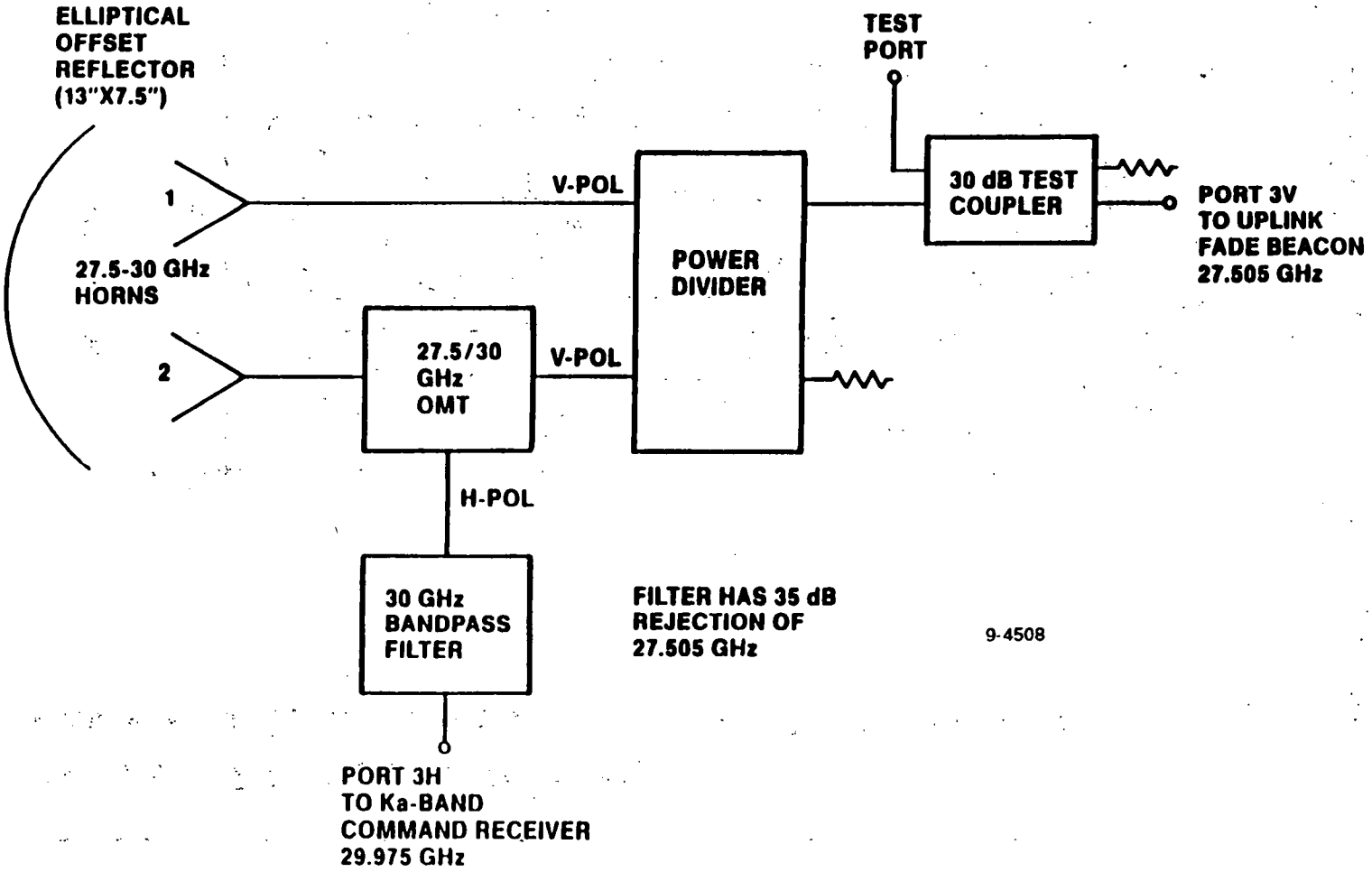

ACTS Spacecraft Beacon Characteristics

Ka-Band CR&T Antenna Assembly
Uplink Fade Beacon Pattern—Measured 27.505 GHz V-POL

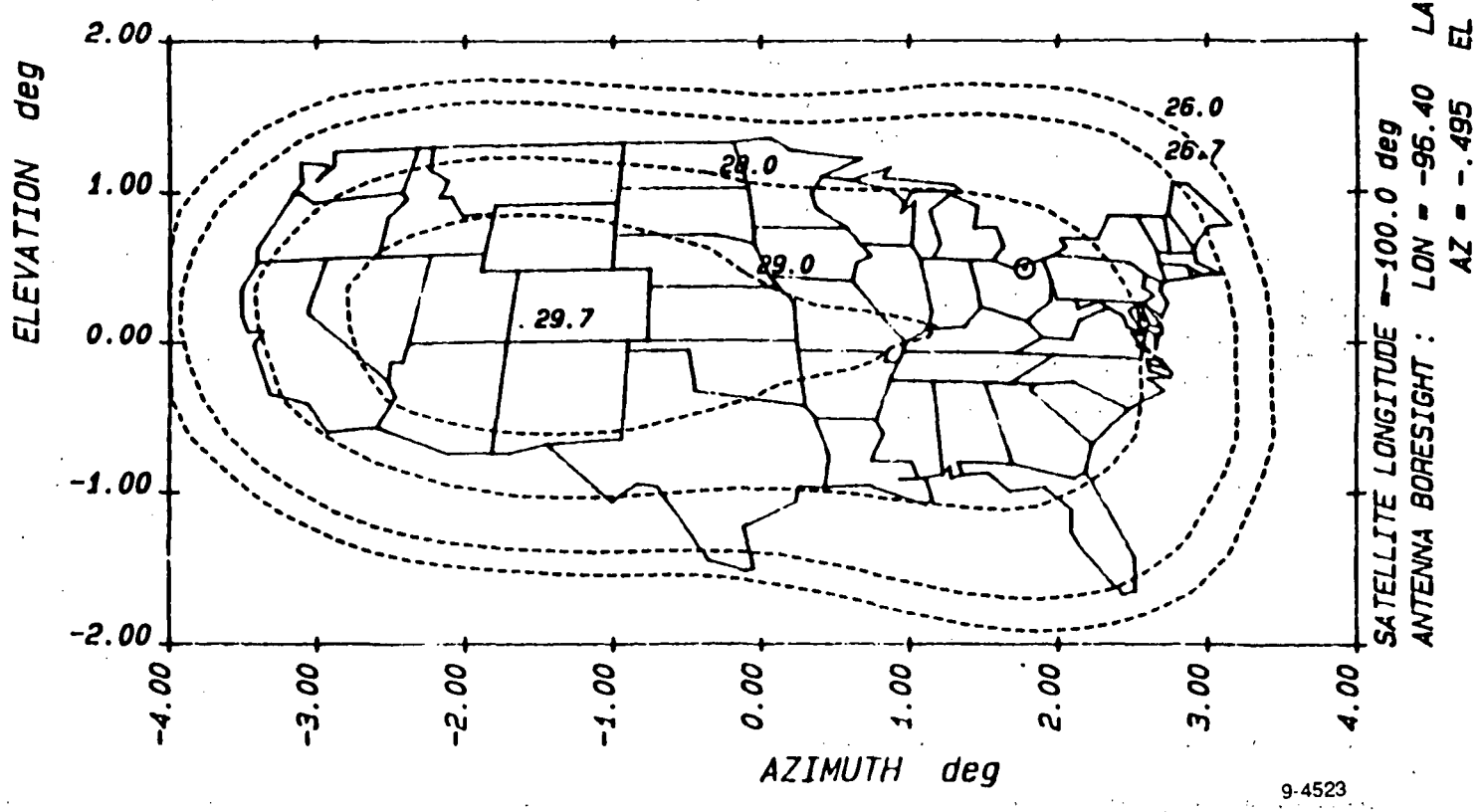

ACTS Spacecraft Beacon Characteristics

20.2 GHz Ka-Band Beacon Transmitter

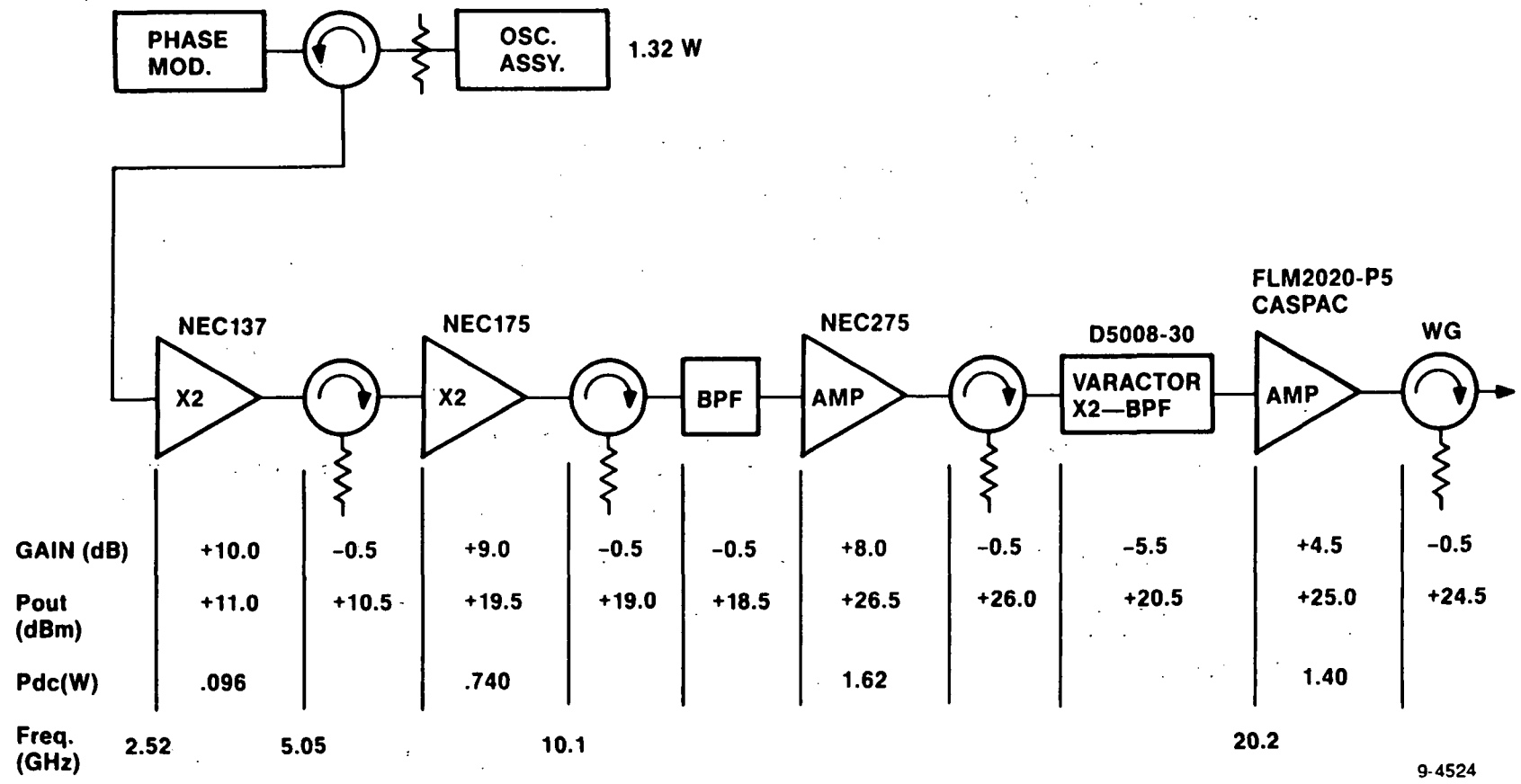

ACTS Spacecraft Beacon Characteristics

Ka-Band Beacon Transmitter Requirements and Measured Values

PARAMETER	REQUIREMENTS	MEASURED VALUES
OPERATING FREQUENCY	20185 AND 20195 MHz ± 0.3 MHz	20.195250 GHz
LONG TERM FREQUENCY STABILITY WITH HEATER	±10 PPM FOR TWO YEARS	7 PPM FOR TWO YEARS (1)
SHORT TERM FREQUENCY STABILITY	4 PPM PEAK TO PEAK FROM -10°C TO +55°C	2.44 PPM PEAK TO PEAK FROM -10°C TO +55°C
WORST CASE FREQUENCY UNCERTAINTY FOR ANY 15 MINUTE PERIOD (1)	—	±555 Hz
PHASE NOISE (SINGLE SIDE BAND)	-51 DBC/Hz MAX. AT 50 Hz OFFSET -61 DBC/Hz MAX. AT 100 Hz OFFSET -68 DBC /Hz MAX. AT 200 Hz OFFSET -72 DBC/Hz MAX.AT 300 Hz OFFSET -76 DBC/Hz MAX. AT 400 Hz OFFSET -92 DBC/Hz AT OR ABOVE 19 KHz OFFSET	-53 -61 -71 -74 -76 SEE NOTE (2)
RF OUTPUT POWER	+22.5 DBM EOL	+23.9 DBM Min. (3)
MODULATION SENSITIVITY	5.0 VOLT PEAK TO PEAK INPUT VOLTAGE RESULTS IN A 1.0 ±10% RADIAN PEAK DEVIATION	1.0 +6%/-4% RADIAN PEAK
ENVELOPE DELAY STABILITY	± 0.05 MICROSECOND	±0.05 MICROSECOND

(1) BY ANALYSIS
(2) UNABLE TO MEASURE DUE TO NOISE FLOOR OF SYSTEM (-92 DBC/Hz)
(3) BY ANALYSIS EOL VALUE + 22.9 DBM

ACTS Spacecraft Beacon Characteristics

Ka-Band Beacon Transmitter
Requirements and Measured Values (Cont'd)

PARAMETER	REQUIREMENTS	MEASURED VALUES
SPURIOUS	2 MHz FROM CARRIER, NO SPUR GREATER THAN -20 DBM (1 MHz BW)	-14.5 DBM @ 25.25 GHz(4)
	2 MHz FROM CARRIER WITHIN 27.5 TO 30.0 GHz NO SPUR GREATER THAN -97 DBM (1 MHz BW)	-75 DBM(5)
	2 MHz FROM CARRIER WITHIN 30.0 TO 34.9 GHz NO SPUR GREATER THAN -47 DBM (1 MHz BW)	-37 DBM @ 30.3 GHz(4)
ACCEPTANCE TEMPERATURE	-10°C TO +55°C	-10°C TO +55°C
QUALIFICATION TEMPERATURE	-15°C TO +60°C	-15°C TO +60°C
INPUT VOLTAGE (DC)	+21.0 TO +35.5 VOLTS	+21.0 AND +35.5 VOLTS
DC POWER CONSUMPTION	10.0 WATTS (PER BEACON)	9.44 WATTS
WEIGHT	4.25 LBS (PER BEACON)	4.05 LBS

(4) TO BE CORRECTED IN FLIGHT UNITS
(5) SYSTEM CAPABILITY

ACTS Spacecraft Beacon Characteristics

KBT Frequency Stability (Utilized as a Fade Beacon)

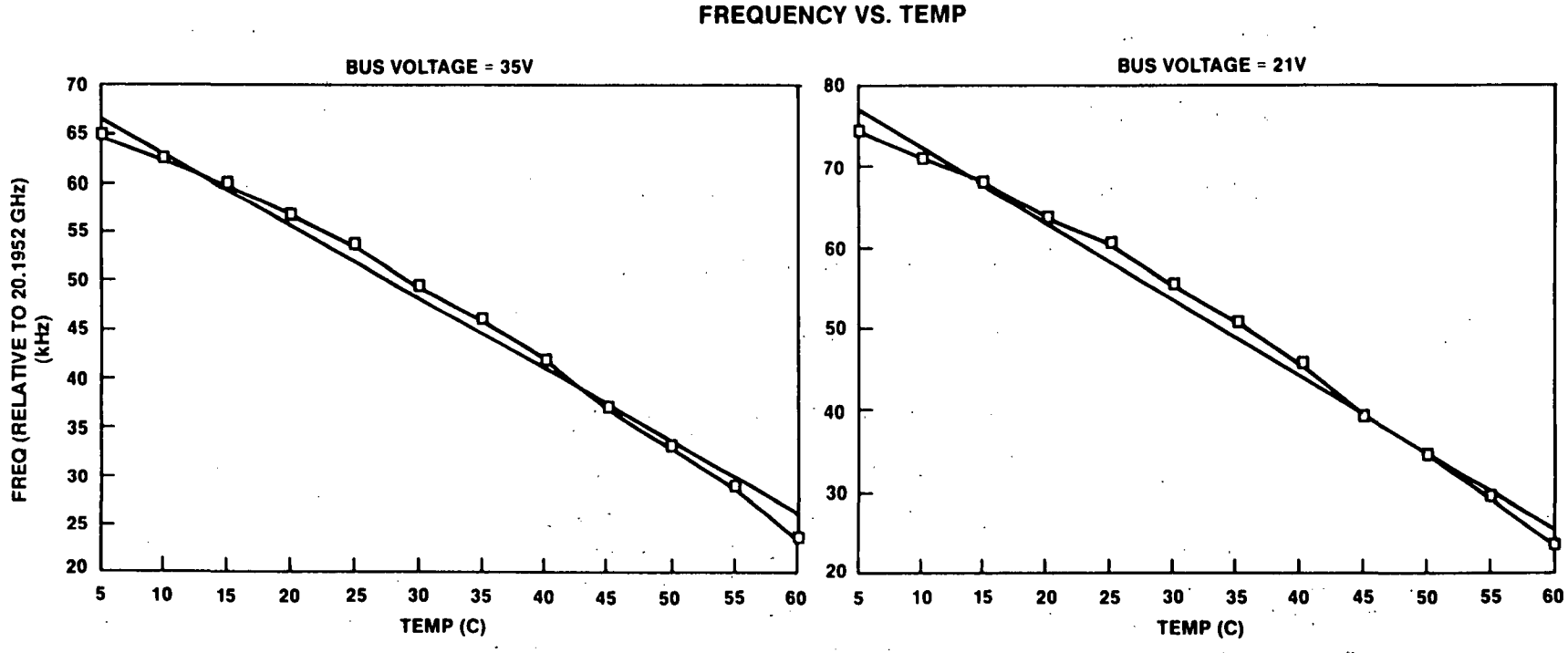

9-4525

ACTS Spacecraft Beacon Characteristics

KBT Output Power Stability

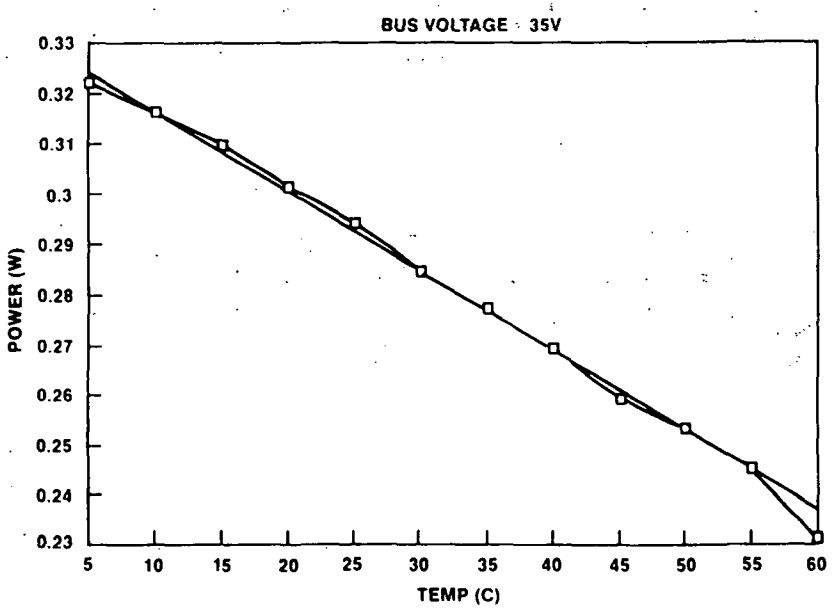

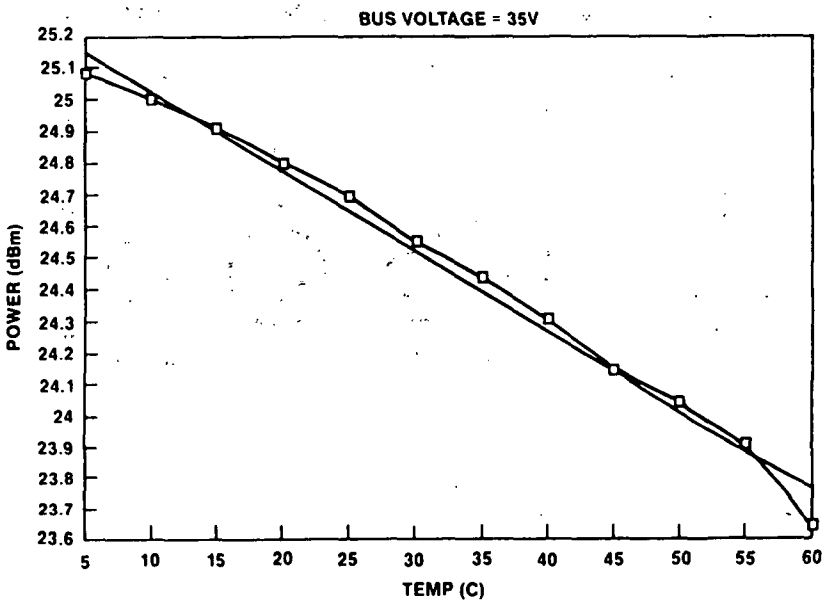

9-4526

ACTS Spacecraft Beacon Characteristics

27.505 GHz Uplink Fade Beacon

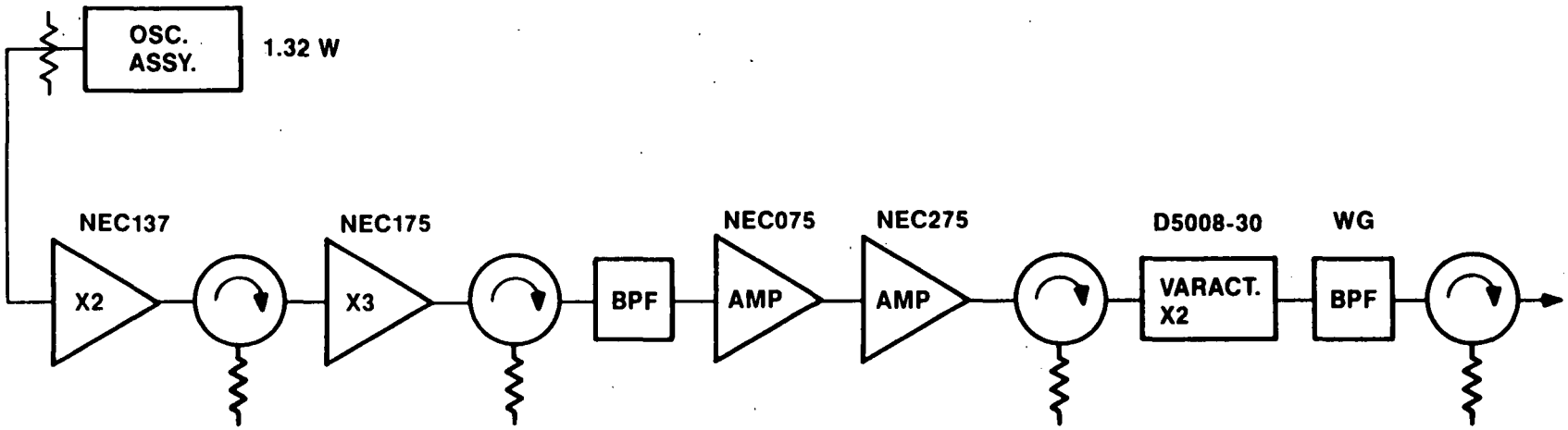

GAIN (dB)	+10.0	-0.5	+4.5	-0.5	-1.5	+7.0	+6.5	-0.5	-4.5	-0.5	-0.5
Pout (dBm)	+11.0	+10.5	+15.0	+14.5	+13.0	+20.0	+26.5	+26.0	+21.5	+21.0	+20.5
Pdc(W)	.072		.580			.540	1.80				
Freq. (GHz)	2.29	4.58		13.753						27.505	

9-4527

ACTS Spacecraft Beacon Characteristics

Uplink Fade Beacon Transmitter Requirements and Measured Values

PARAMETER	REQUIREMENTS	MEASURED VALUES
OPERATING FREQUENCY	27.505 GHz ±0.5 MHz	27.505415 MHz
LONG TERM FREQUENCY STABILITY WITH HEATER	±10 PPM FOR TWO YEARS	6.8 PPM FOR TWO YEARS (1)
SHORT TERM FREQUENCY STABILITY	4 PPM PEAK-TO-PEAK FROM -10°C TO +55°C	2.44 PPM PEAK-TO-PEAK FROM -10°C TO +55°C
WORST CASE FREQUENCY UNCERTAINTY FOR ANY 15 MINUTE PERIOD (1)	—	±757 Hz
PHASE NOISE (SINGLE SIDE BAND)	-49 DBC/Hz AT 50 Hz OFFSET -58 DBC/Hz AT 100 Hz OFFSET -65 DBC/Hz AT 200 Hz OFFSET -69 DBC/Hz AT 300 Hz OFFSET -73 DBC/Hz AT 400 Hz OFFSET -76 DBC/Hz AT 1000 Hz OFFSET -80 DBC/Hz AT 3000 Hz OFFSET	-51 -60 -66 -73 -73 -80 -83
RF OUTPUT POWER	-19 DBM MIN. EOL (2-YEARS, BOTH UFB'S CONSIDERED)	20.12
SPURIOUS	>2 MHz FROM CARRIER NO SPUR GREATER THAN -20 DBM (1 MHz BW)	-20

(1) BY ANALYSIS

ACTS Spacecraft Beacon Characteristics

Uplink Fade Beacon Transmitter Requirements and Measured Values (Cont'd)

PARAMETER	REQUIREMENTS	MEASURED VALUES
SPURIOUS (CONT'D)	>2 MHz FROM CARRIER WITHIN 28.9 TO 30.0 GHz NO SPUR GREATER THAN -74 DBM (1 MHz BW)	−75
	>2 MHz FROM CARRIER WITHIN 30.0 TO 34.9 GHz NO SPUR GREATER THAN -47 DBM (1 MHz BW)	−50
ACCEPTANCE TEMPERATURE	-10°C TO +55°C	-10°C TO +55°C
PROTOFLIGHT TEMPERATURE	-15°C TO +60°C	-15°C TO +60°C
INPUT VOLTAGE (DC)	+21.0 TO +35.5 VOLTS	+21.0 TO +35.5 VOLTS
DC POWER CONSUMPTION	8.50 WATTS (PER BEACON)	8.22 WATTS (2)
WEIGHT	4.25 LBS (PER BEACON)	4.1 LBS (2)

(2) ESTIMATE

ACTS Spacecraft Beacon Characteristics

Beacon Diurnal Temperature Variation - Summer Solstice

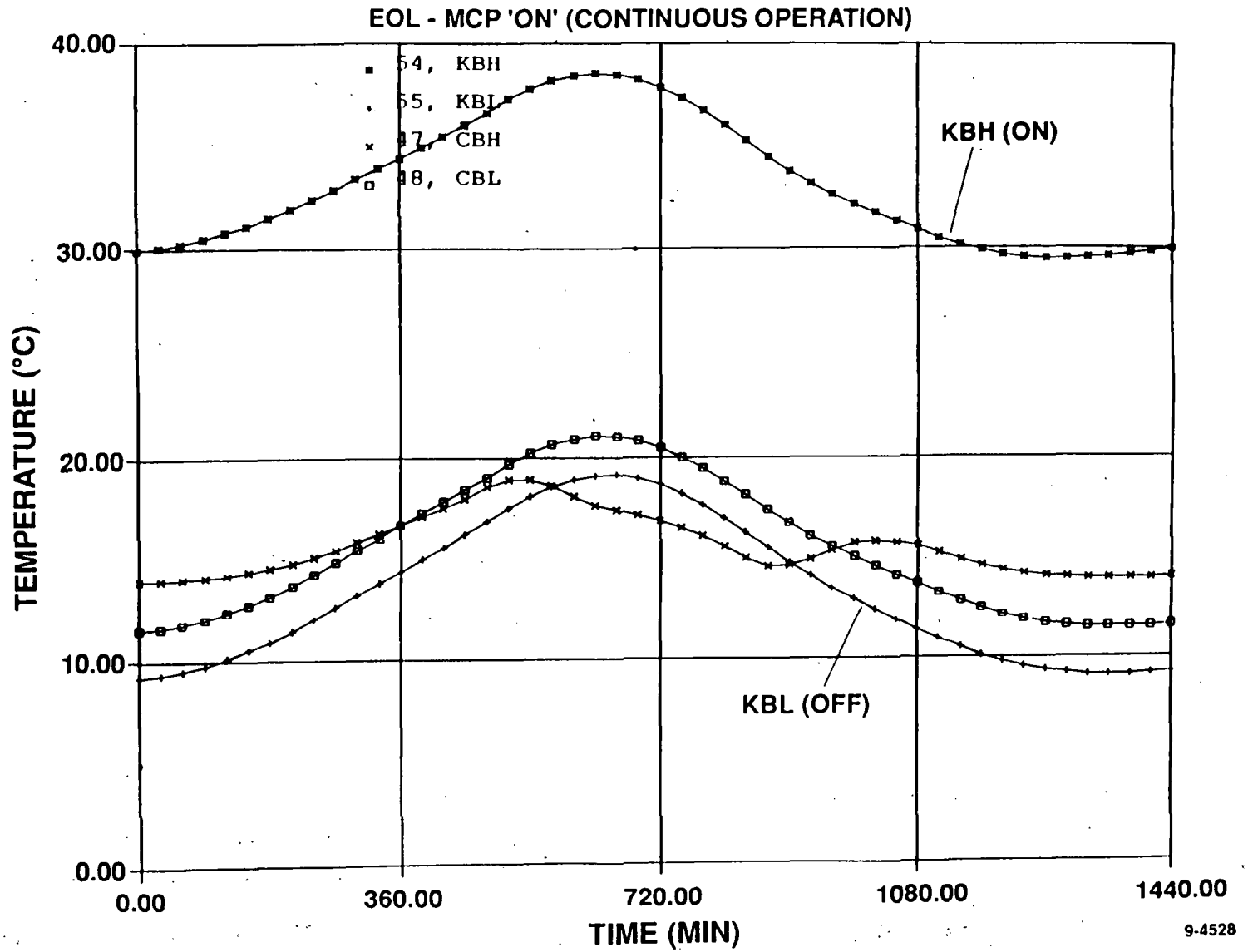

ACTS Spacecraft Beacon Characteristics

Beacon Diurnal Temperature Variation - Equinox

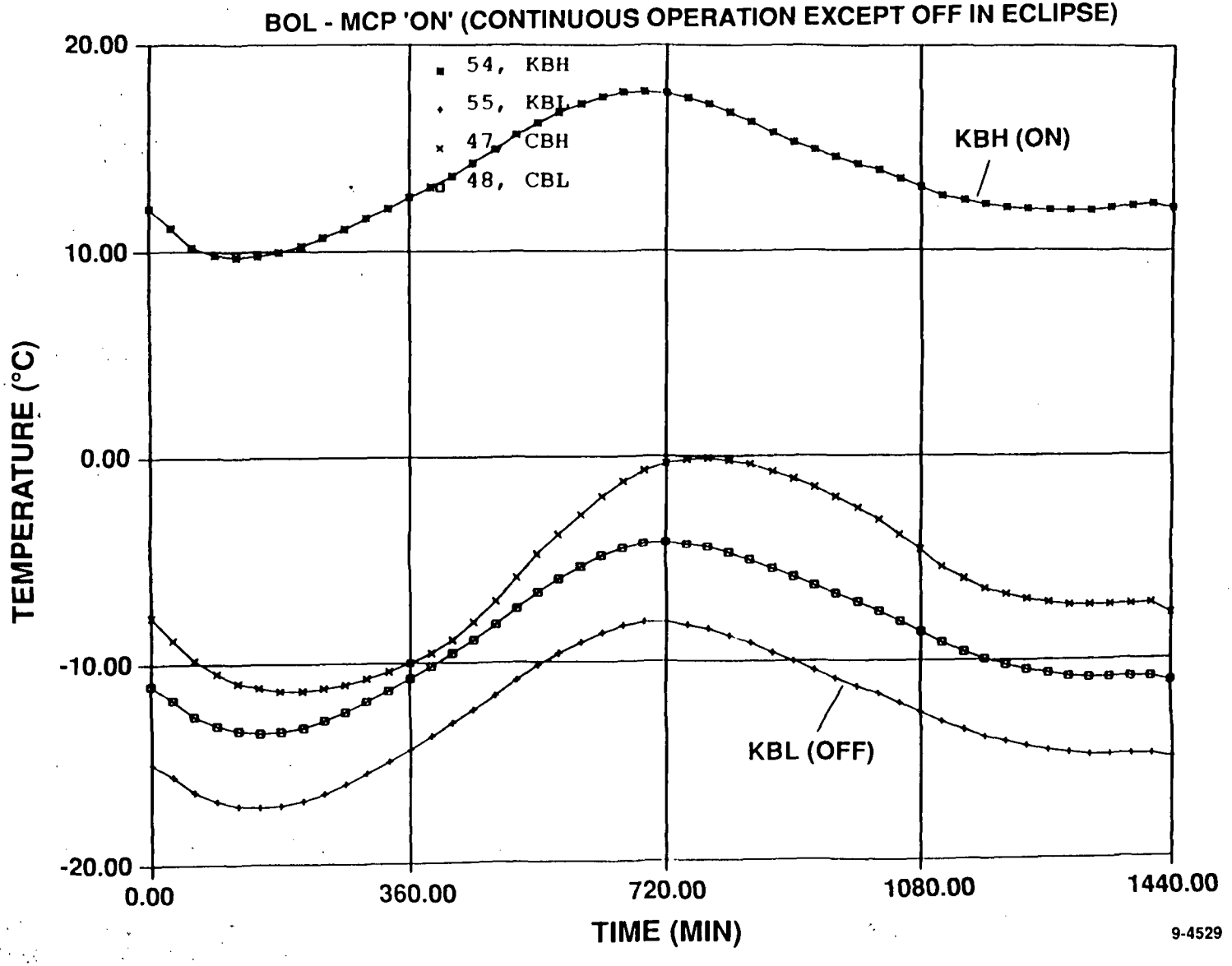

ACTS Spacecraft Beacon Characteristics

Beacon Modulation by Telemetry Modes

RTM Mode	Output Signal	Modulation Level (Radians)
Analog Subcarrier Dwell	14.5 kHz FM Subcarrier	1.0
Attitude Monitor Mode	14.5 kHz Subcarrier	1.0
Ranging Mode	27.777 kHz or 19 kHz FM Subcarrier (Square Wave)	1.0
Direct PCM	1024 Biphase-L PCM	1.0
Direct PCM Dwell	1024 Biphase-L PCM	1.0
Subcarrier PCM	1024 Biphase-L PCM phase-modulating 64 kHz Subcarrier	0.72
	Unmodulated 32 kHz Subcarrier	0.72
Subcarrier PCM Dwell	1024 Biphase-L PCM phase-modulating 64 kHz Subcarrier	0.72
	Unmodulated 32 kHz Subcarrier	0.72
Simultaneous (Ranging/PCM)	1024 Biphase-L PCM modulating 64 kHz Subcarrier	0.72
	27.777 kHz or 19 kHz Subcarrier (Square Wave)	0.50

Constant Carrier Power Level In Last Three Modes Only

ACTS Spacecraft Beacon Characteristics

Beacon Spectrum Showing 64 KHz Telemetry and 32 KHz Placeholder Tone

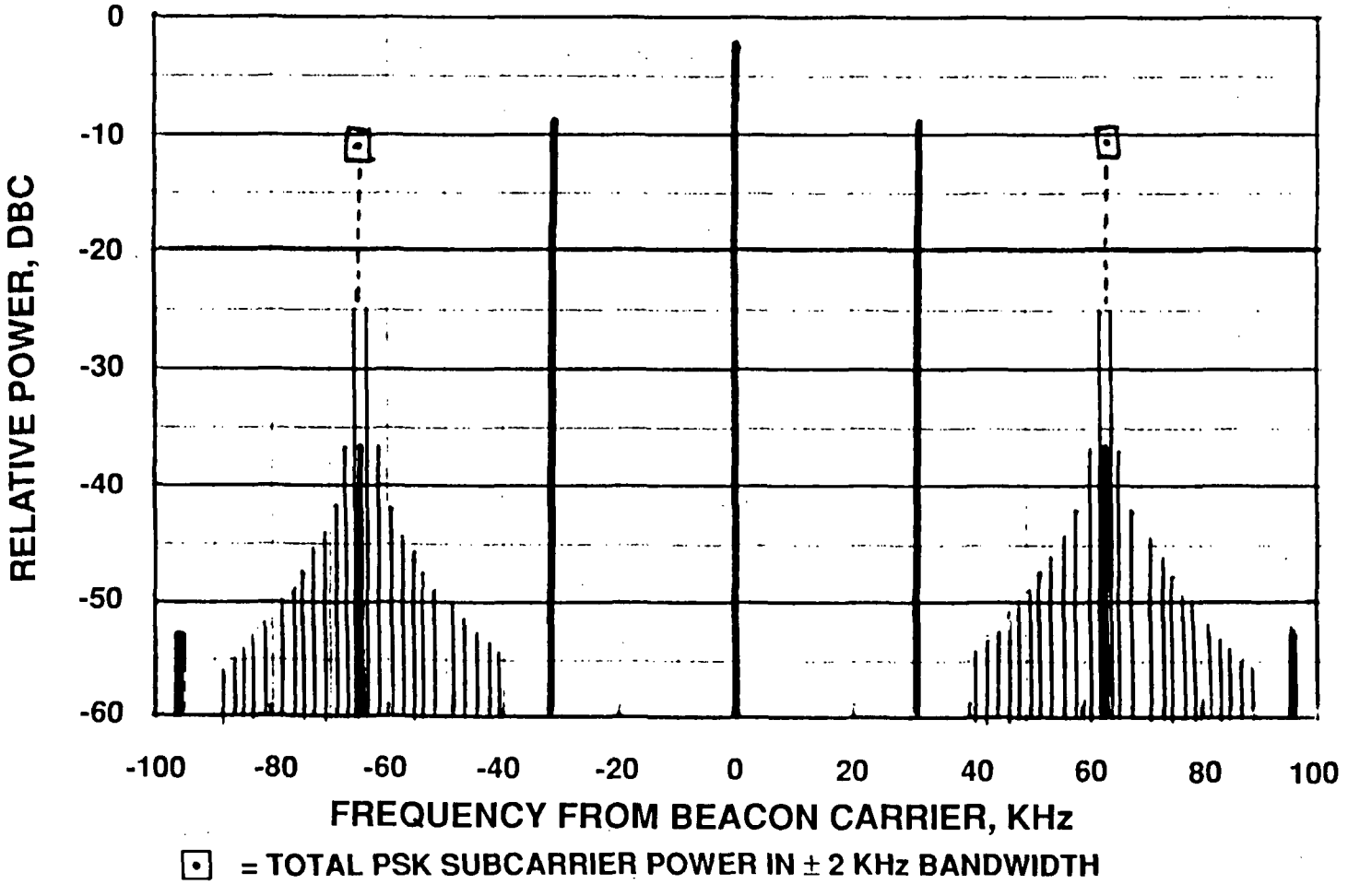

9-4530

ACTS Spacecraft Beacon Characteristics

Beacon Spectrum Showing 64 KHz Telemetry and 27 KHz Fine Ranging Tone

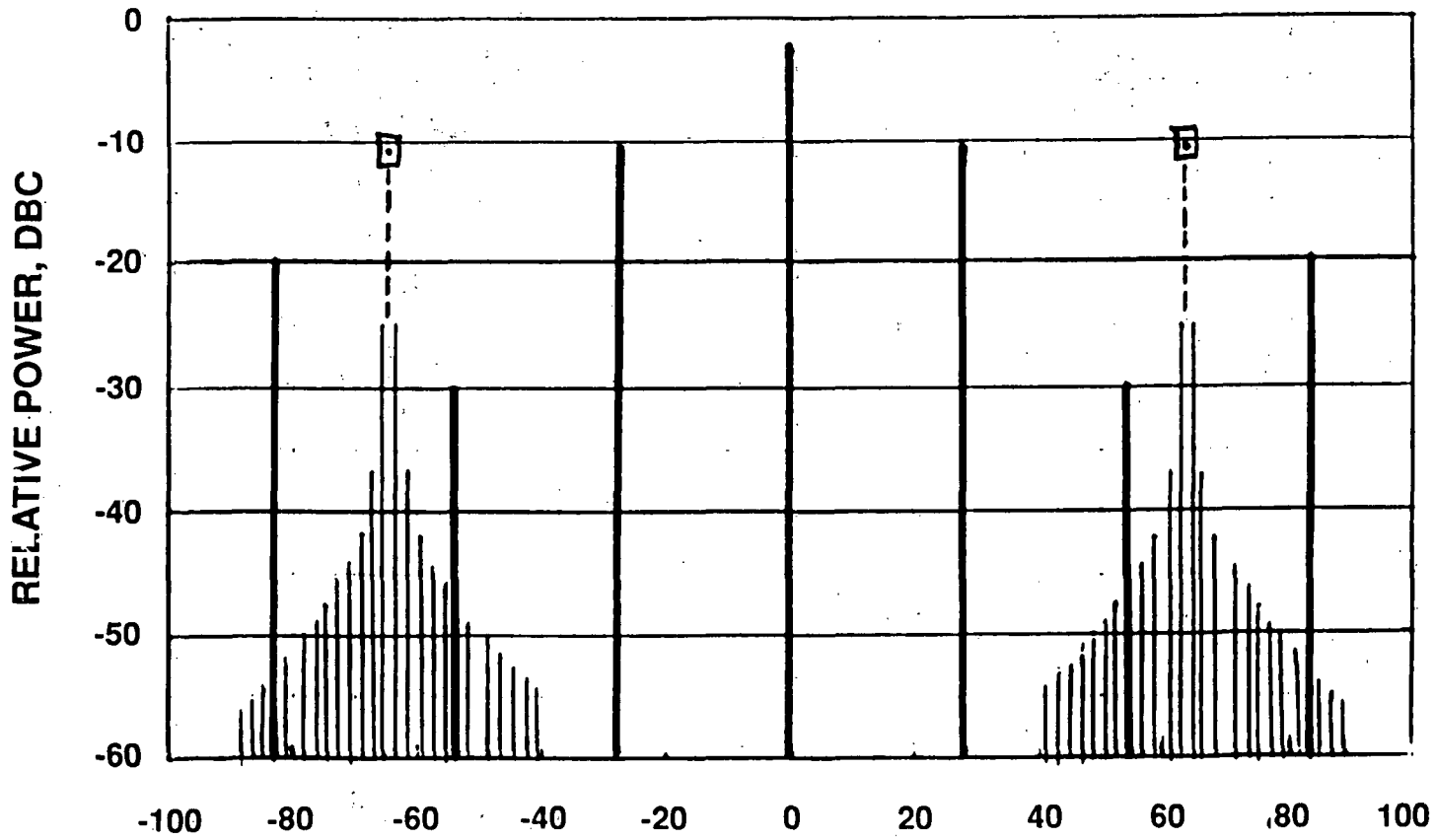

[•] = TOTAL PSK SUBCARRIER POWER IN ± 2 KHz BANDWIDTH

ACTS Spacecraft Beacon Characteristics

Beacon Spectrum Showing 64 KHz Telemetry and 19 KHz Coarse Ranging Tones

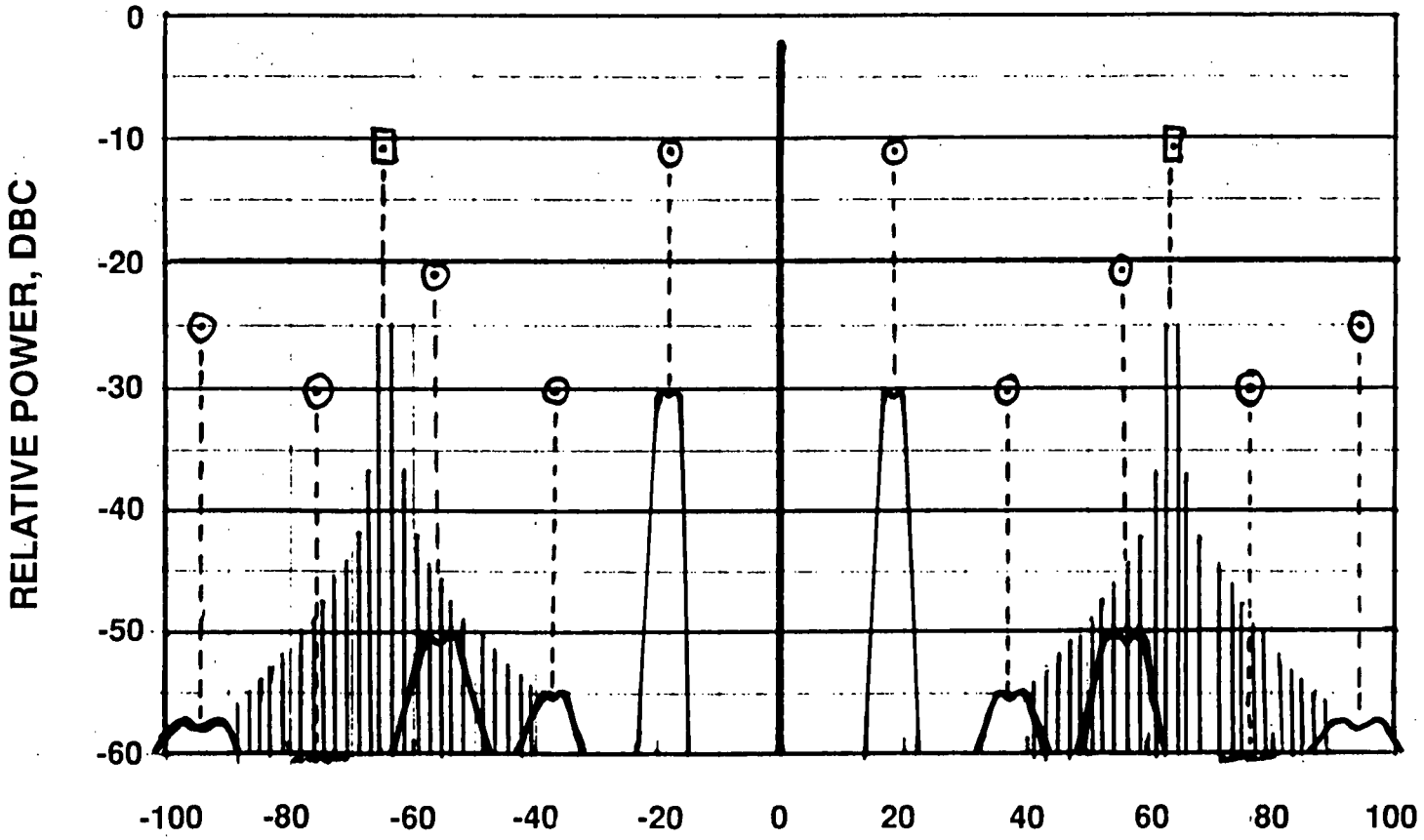

⊙ = TOTAL POWER IN HARMONIC OF 19 KHz RANGING

⊡ = TOTAL PSK SUBCARRIER POWER IN ± 2 KHz BANDWIDTH

9-4532

ACTS Spacecraft Beacon Characteristics

CONCLUSIONS

- FADE MEASUREMENTS AT THE UPLINK FREQUENCY ARE UNDISTURBED BY MODULATION BUT AVAILABLE FOR THE VERTICAL POLARIZATION ONLY
- FADE MEASUREMENTS AT THE DOWNLINK FREQUENCY ARE PRACTICALLY UNAFFECTED BY THE BEACON MODULATION IN THE OPERATIONAL TELEMETRY MODES OR BY THE CONTENTS OF THE TELEMETRY DATA
- THE SHORT TERM STABILITY OF THE BEACONS PERMITS THE USE OF SIMPLER RECEIVERS WITH EASY SIGNAL RECOVERY AFTER EVEN THE DEEPEST FADES
- THE TWO BEACONS ARE NOT PHASE-LOCKED. THIS PROVIDES HIGHER RELIABILITY FOR THE S/C TELEMETRY SYSTEM SINCE EACH BEACON CONTAINS ITS OWN FREQUENCY SOURCE

LBR-2 EARTH STATIONS FOR THE ACTS PROGRAM

Michael O'Reilly
Harris Corporation, Melbourne, FL

N91-11971

Russell Jirberg and Ernie Spisz
NASA Lewis Research Center, Cleveland, OH

ABSTRACT

Described in this paper is the "LBR-2" earth station being developed for NASA's Advanced Communications Technology Satellite (ACTS). The LBR-2 is one of two earth station types that operate through the satellite's baseband processor. The LBR-2 is a small VSAT-like earth station that is easily sited on a user's premises, and provides up to 1.792 megabits per second (MBPS) of voice, video, and data communications. Addressed in the paper is the design of the antenna, the rf subsystems, the digital processing equipment, and the user interface equipment.

BACKGROUND

NASA is currently developing two general classes of earth stations, an "LBR" class and an "HBR" class, for its Advanced Communications Technology Satellite (ACTS). The LBR variety operates through the satellite's Baseband Processor (BBP), whereas the HBR variety operates through its Microwave Switch Matrix (MSM). The basic system architecture for ACTS, as well as the details associated with the BBP and the MSM modes of operation have been described in earlier papers[1,2,3].

For the BBP mode of operation NASA has defined two different types of LBR earth station: an LBR-1 and an LBR-2. In most respects the LBR earth stations are similar. Both are small VSAT-like earth stations that can be easily sited on the users' premises. Both operate in the ACTS' TDMA, demand-assigned multiple access (DAMA) environment. They differ only in terms of their throughput capacities and TDMA burst rates. The LBR-1 earth stations transmit at an uplink burst rate of 110 MBPS, and provide a total throughput capability of 46.528 MBPS. The LBR-1's are intended primarily for those users with a T3 (44.736 MBPS) requirement. The LBR-2's, on the other hand, are considered to be more of a general purpose earth station. They transmit at an uplink burst rate of 27.5 MBPS, and provide 1.792 MBPS of throughput capacity. This allows the LBR-2 earth station to meet the needs of those users whose requirements do not exceed that of a single T1 (1.544 MBPS). Described in this paper is the basic design that is being implemented for the LBR-2 earth station.

DESIGN OVERVIEW

Physically the LBR-2 earth station in many respects resembles the current generation of Ku-band VSAT's. It consists of an outdoor unit and an indoor unit as illustrated in Figure 1. Contained in the outdoor unit are the antenna, the receiver, and the transmitter. Contained in the indoor unit are the digital processing and control portions of the earth station, and the Terrestrial Interface Equipment (TIE) which is the interface to the user's telecommunications equipment.

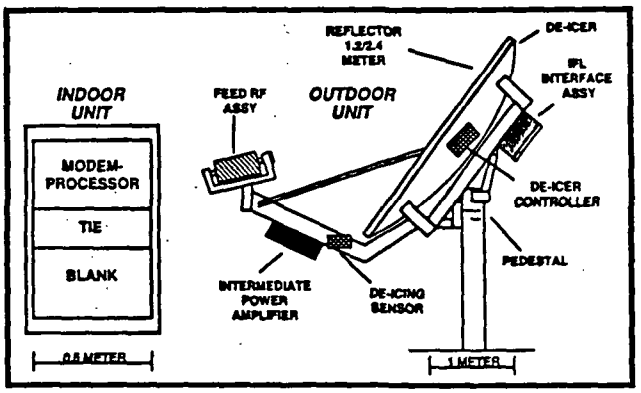

Figure 1. The LBR-2 Physical Configuration

The various subsystems that comprise the earth stations are indicated in Figure 2. The Modem-Processor performs a number of digital processing and control functions including multiplexing and demultiplexing of the uplink and downlink traffic, rate buffering, FEC encoding and decoding, and modulation and demodulation. It is also generates the various frequency and clock signals used throughout the earth station, and manages the various timing and control functions required to operate within the TDMA environment of the ACTS system.

The indoor and outdoor units are interconnected at IF. Uplink signals from the modulator are transferred to the upconverter located on the rear of the antenna using an IF of 700 MHz. Downlink

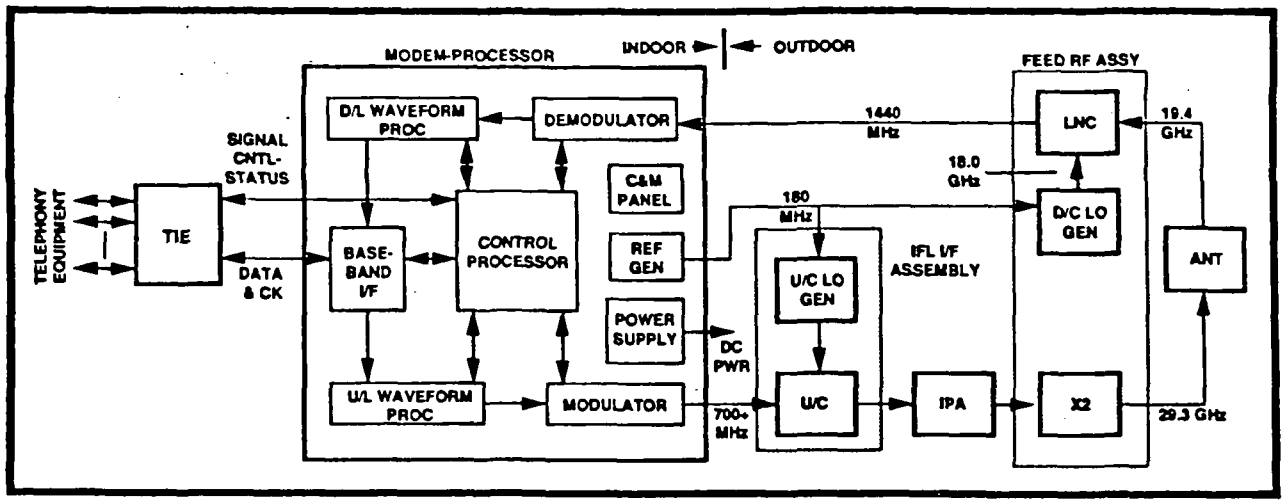

Figure 2. LBR-2 Functional Block Diagram

signals from the receiver, which along with thetransmitter is mounted on the feed support arm of the antenna, are transferred to the demodulator using an IF of 1440 MHz. The indoor-to-outdoor interconnect also includes a 180 MHz reference frequency for the up and down frequency converters. Because of the relatively low IF's used for the interconnect, the indoor and outdoor units may be separated by 100-foot long cable runs. For those installations requiring longer or shorter cable runs, amplifiers or pads may be used to boost or attenuate the signals accordingly.

OUTDOOR UNIT

Antenna

The LBR-2 earth station may be equipped with either one of two antennas: a 1.2-meter diameter antenna or a 2.4-meter diameter antenna. Both are offset prime focus designs with single-piece reflectors. This design was selected on the basis of its rf performance and its reduced tendency for ice and snow buildup.

Both the 1.2-m and 2.4-m antennas are improved versions of an existing Ku-band VSAT design. Typically, reflectors designed for commercial Ku-band service will exhibit 15-20 mils of surface roughness. In a 40 mph wind these antenna may deform by as much as 30 mils. At 30 GHz surface deformities of this magnitude would result in an unacceptably large 3.8 dB loss of gain. Consequently, changes were made to the old design to improve the inherent surface accuracy of the reflector and to stiffen it structurally against wind induced deformities. Measurements made on a 2.4-m prototype antenna indicate that the surface deformities in the new design due to simulated 40 mph wind loads were reduced to 13 mils. Hence, the wind induced losses in performance at 30 GHz will be limited to an acceptable 0.7 dB.

The reflector and its supporting structure, together with the feed support structure, are mounted on an EL-over-AZ positioner. The feed support structure is a tubular member that provides the primary support for the feed rf assembly and for the transmitter. The rf and power cables for the receiver and transmitter are routed through this tube. The feed rf assembly is mounted to the feed support structure by means of a feed saddle which allows three degrees of freedom of movement for focusing adjustments. The feed is located and aligned using three precision rods which are bolted to the reflector and feed saddle through precisely located alignment holes. Once aligned, two of the alignment rods remain an integral part of the assembly to stabilize the feed under windy conditions.

The antennas are designed to be mounted on a single vertical kingpost. For rooftop locations the antennas may be mounted on the non-penetrating platform shown in Figure 3. The mount is designed to maintain an azimuth and elevation pointing accuracy of 0.06° under 40 mph wind conditions. Ballast is provided by a set of concrete blocks which are contained in the four aluminum boxes. The boxes are bolted to the aluminum sandwich panels to eliminate unauthorized removal. Under 80 mph winds this mount will limit the combined live and dead load of the larger 2.4-meter antenna to no more than 48.5 pounds per square foot. Tethers can be attached to contain the antenna in winds that exceed 80 mph.

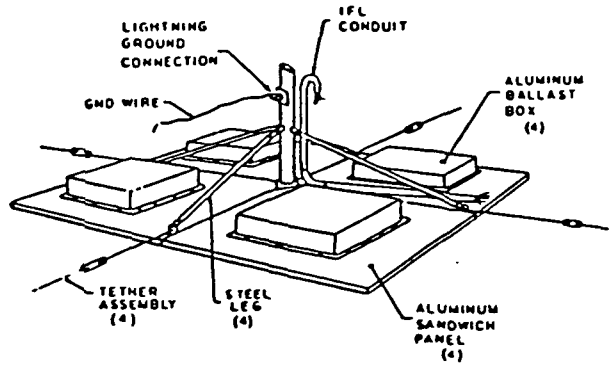

Figure 3. Non-Penetrating Roof Mount

Hydrophobic coatings will be used on the antennas as a rain repellent. Active de-icing in the form of radiant heating can be added to prevent ice and snow buildup. The heaters will be able to uniformly supply approximately 50 watts per square foot of radiant heating.

Transmitter

The transmitter design is unconventional in that it uses a Ku-band power amplifier driving a frequency doubler to generate the Ka-band uplink signal. To compensate for the bandwidth expansion that accompanies the frequency doubling, the signal generated by the modulator is first distorted by passing it through a divide-by-two circuit. After upconversion and amplification at Ku-band, the original modulation bandwidth is then regenerated by the doubler. Analysis, spectral measurements, and BER testing have shown that this ÷2/x2 technique is a viable approach for SMSK modulation. The advantage of this approach is that it avoids the need for costly 30 GHz upconverters and power amplifiers.

The basic design of the transmitter is indicated in Figure 4. It employs a Ku-band upconverter, a Ku-band TWTA as an intermediate power amplifier (IPA), and a high power diode doubler as the final stage. The upconverter is a conventional design implemented with standard commercial components. The 13.860 GHz local oscillator is phase-locked to the 180 MHz reference frequency generated in the indoor unit.

The IPA is implemented using a conventional, commercially available unit. (This unit is currently in production for Ku-band VSAT applications.) It contains a 60-watt TWT, a fault-tolerant power supply, and a controller. The entire unit is packaged in a compact, outdoor, weather-proof enclosure. An air-coldplate heat exchanger with dual redundant fans are used for cooling. Powered tests of this unit were successfully performed with the unit, including the fans, totally submerged in water. The IPA has the capability to deliver 50 watts of output power. With less than 40 watts required to drive the doubler, adequate design margins exists for end-of-life degradations.

The high-power frequency doubler utilizes a pair of epitaxially stacked varactor diodes. Similar frequency multipliers have been developed for EHF transmitter applications for use in a number of major military communications and radar programs. The simplicity of fabrication of these devices and their associated circuits make them ideally suited for commercial applications which require a simple, inexpensive means of generating millimeter-wave power. In addition, these devices have high projected reliabilities due to the fact that they operate with relatively high conversion efficiencies (diode efficiency > 75%), and, hence, low junction temperatures. The median life expectancy of the complete doubler for the earth stations is estimated to be over 66,000 hours.

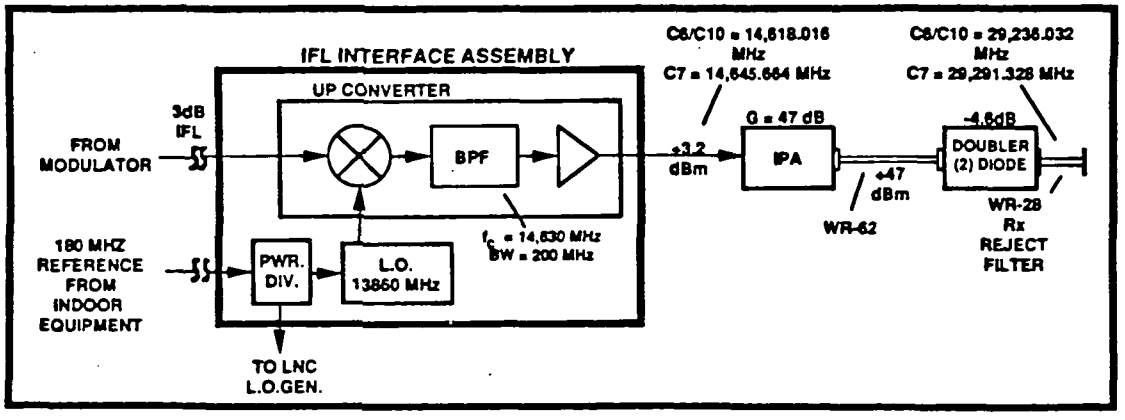

Figure 4. Transmitter Block Diagram

The complete doubler consists of an input isolator followed by a power divider, two diode modules, a power combiner, and an output isolator. Preliminary tests indicated that the conversion efficiency of the doubler, including circuit losses, is 60%. These CW tests also demonstrate that the two diode doubler approach is capable of producing the required 12 watts of output power.

Receiver

The receiver block diagram and downlink frequency plan are illustrated in Figure 5.

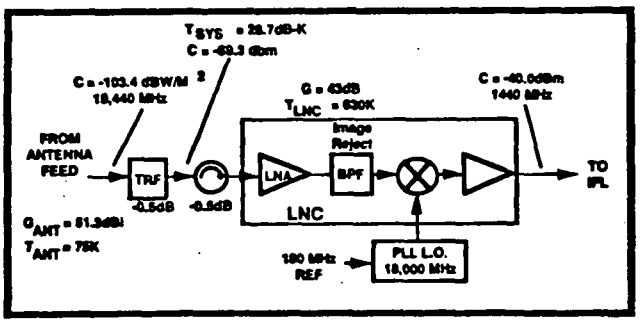

Figure 5. LBR-2 19 GHz Receiver

The transmit reject filter (TRF) together with the ortho-mode transducer (OMT) in the feed provide about 60 dB attenuation of the transmitted signal at the input to the low noise converter (LNC), thus eliminating any potential performance degradation to the LNC from the transmitter. The low noise amplifier (LNA) is a low cost design that uses packaged HEMT devices mounted on a single soft substrate. The IF amplifier is comprised of two low cost packaged Si MMIC devices. The 18 GHz local oscillator is phase locked to the same 180 MHz reference signal used by the upconverter. The TRF, the LNC, and local oscillator are all contained in the weatherproof feed rf assembly which is located at the focal point of the antenna.

The LNA portion of the LNC has a gain of 23 dB, with a demonstrated noise figure of 2.5 dB at room temperature. The G/T performance of the earth stations is therefore estimated to be 16.1 dBi/K with the smaller (1.2-m) antenna and 22.1 dBi/K with the larger (2.4-m) antenna.

INDOOR UNIT

The Modem Processor consisting of the modem, the digital processing equipment, the monitor and control equipment, the frequency sources, and the low voltage power supplies are all integrated within a single chassis. The Modem-Processor, together with the TIE, constitute the indoor unit. The entire unit is contained within a standard EIA 19-inch half-height equipment rack. Additional user equipment may be mounted in the space that remains in the equipment rack. The small size of the indoor unit allows it to be conveniently located within an office environment.

Modulator

The modulated uplink signal is generated using the implementation shown in Figure 6. The digital data from uplink rate buffer is first phase modulated, producing a BPSK spectrum centered at 630 MHz. The signal is then transformed into an SMSK signal centered at 636.575 MHz by passing it through an offset conversion filter. A SAW filter is used to produce the (sin x)/x transfer function required for this conversion filter. The SMSK signal is then upconverted to one of two electrically selected frequencies, either 1,516 MHz or 1,571 MHz, depending on which one of two uplink channels the station is assigned: 29,236.032 GHz or 29,291.328 GHz. The filter bandwidths in the modulator and in the transmitter are sufficiently broad to pass either channel without the need for any switching or retuning of the filters.

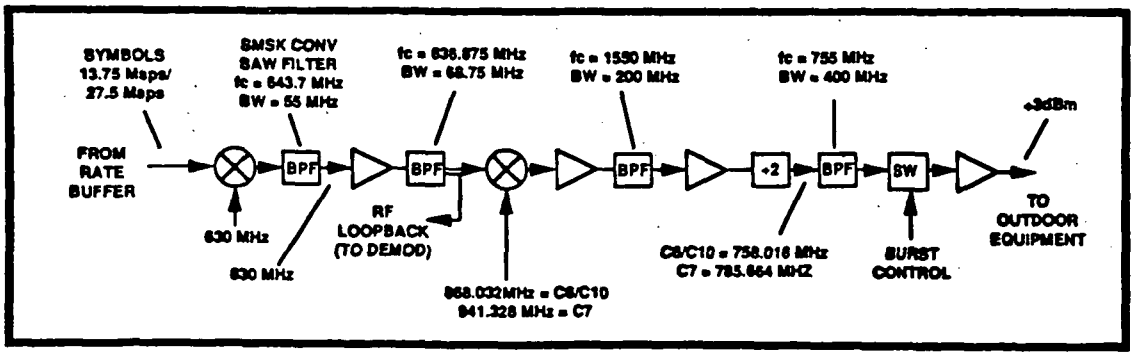

Figure 6. SMSK Modulator Block Diagram

The modulated IF is then divided by 2 so that the signal produced by the frequency doubler in the transmitter will have the proper modulation index. Finally, the signal is passed through a pair of switches whose function is to create the TDMA uplink bursts. The signal emitted by the transmitter between bursts is attenuated by more than 50 dB by the action of the burst switch.

Demodulator

A block diagram of the demodulator is shown in Figure 7. The 1440 MHz SMSK downlink signal from the outdoor unit is first downconverted to 630 MHz. The signal is then leveled by an AGC loop prior to the carrier recovery processing. The AGC is designed to provide a dynamic signal range of 35 dB with level variations in excess of 0.5 dB/second.

The 630 MHz IF signal is then split, one half going to the matched filter and the other half going to a frequency doubler. The matched filter is another SAW device which in this case is matched to the bit rate of the uncoded downlink signal (110.592 MBPS). The 1,260 MHz output from the doubler is downconverted to 180 MHz, where the relatively narrow filter used for carrier recovery is realized. The output of the carrier recovery filter is then upconverted to 1,260 MHz and applied to a divide-by-two circuit. This produces a 630 MHz coherent carrier for demodulating the signal obtained from the output of the matched filter.

The bit synchronizer utilizes two sampling analog-to-digital (A/D) converters for data and clock recovery. These A/D converters are driven by two clocks that are 180° out of phase, both of which are derived from the numerically controlled oscillator (NCO). The A/D converter in the data path samples the eye pattern at its point of maximum opening where little intersymbol interference exists. The A/D converter in the clock recovery path samples the eye pattern at the zero crossings. The clock recovery A/D in combination with the loop filter function as a timing error detector that updates the NCO at every bit transition. Since the downlink burst rate varies by no more than 1 part in 10^5, the burst-to-burst frequency error will be very small. Consequently, the corrections made to the NCO, which is locked to the reference oscillator in the earth station, effectively adjust only the phase of the clock. The performance of this demodulator is within 1.5 dB of ideal.

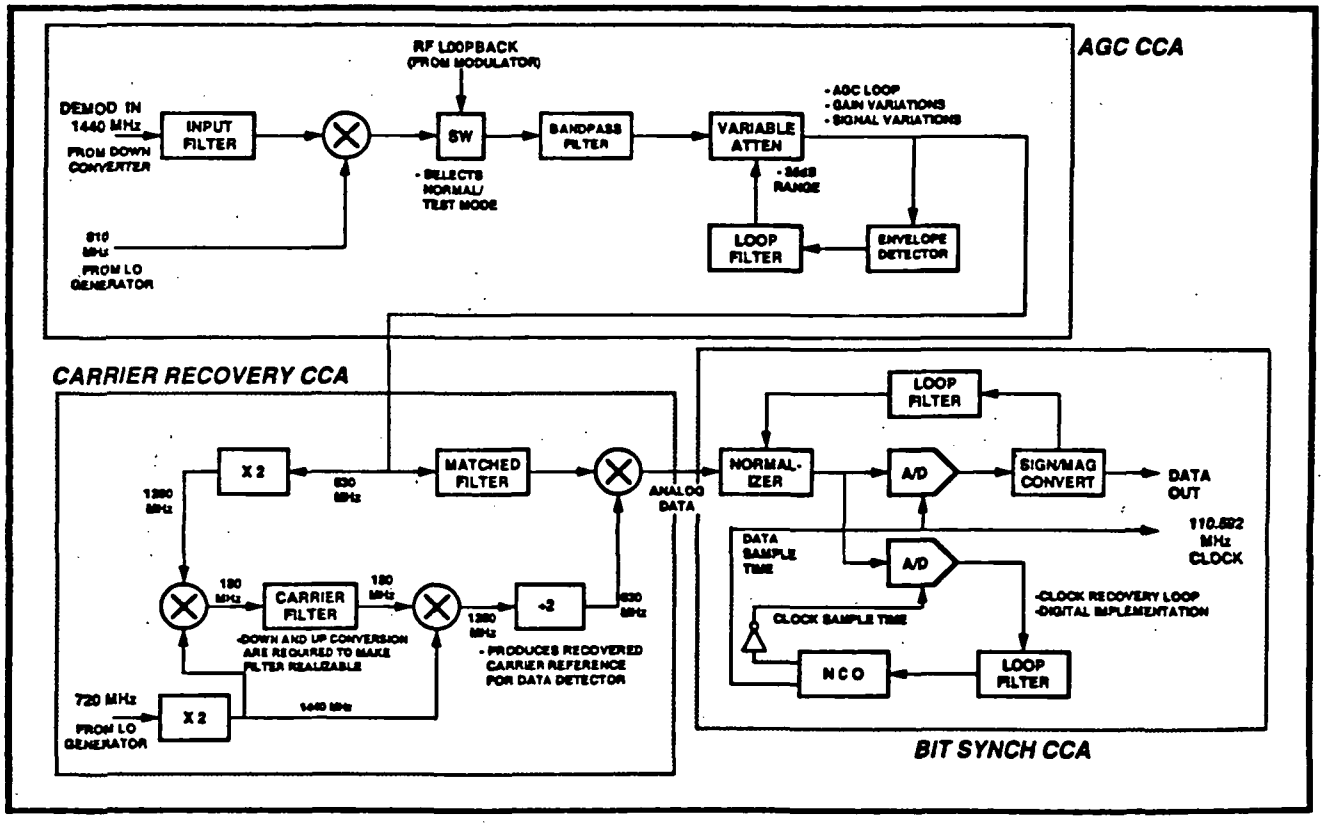

Figure 7. The LBR-2 Demodulator Block Diagram

FEC Codec

Under rain fade conditions the BER can be maintained below $5x10^{-7}$ by the combined effect of a 2:1 reduction in the burst rate and the application of forward error correction (FEC) coding. Using a rate 1/2, constraint length 5, convolutional code, ACTS can provide approximately 10 dB of rain fade protection. The FEC coding is applied adaptively only to those uplinks and downlinks requiring the added protection. In general, the uplinks and downlinks may be independently coded. However, for the LBR-2 earth stations, the FEC coding is always applied simultaneously to both links.

The decoder used in the Modem-Processor is a single chip, 1.5μm CMOS gate array. It implements a Viterbi (maximum likelihood) decoding algorithm for the rate 1/2 convolutional code used by ACTS. The encoder is also a single chip device. It, along with the uplink data scrambler, share a common programmable logic array. (Data scrambling is used to maintain the bit transition density of the uplinks and downlinks at or near 50%.)

TDMA Processor

Indicated in Figure 8 are the TDMA processing and control functions performed by the Modem-Processor. The signal from the demodulator (upper right) is first examined by the unique word detector which senses the unique word embedded in the downlink preamble. (The unique word is used to establish 64-bit word synchronization.) The signal then is rate buffered down to 6.912 MBPS, decoded (if necessary), and descrambled. At this point the outbound orderwire (OBOW) messages from the Master Control Station (MCS) and from other earth stations are demultiplexed and routed to the control processor. The remaining message traffic is then buffered in an elastic buffer and routed to the TIE.

On the uplink, the user traffic from the TIE is buffered in an elastic buffer and then multiplexed together with the inbound orderwire (IBOW) messages from the control processor. The message data is then scrambled and, if necessary, FEC encoded. An uplink preamble is then attached to the message data. The entire message is then rate buffered up to either the 27.648 MBPS rate used for clear-sky (i.e. uncoded) operations, or to the 13.824 MBPS rate used during rain fades.

All TDMA timing and control functions are managed by a single microprocessor. Stored programs automatically perform the following functions without the need for operator intervention:

- station initialization and status
- IBOW and OBOW processing
- U/L and D/L frame processing
- burst time plan management
- TIE signaling and control
- rain fade sensing and control
- fault isolation
- man/machine interface

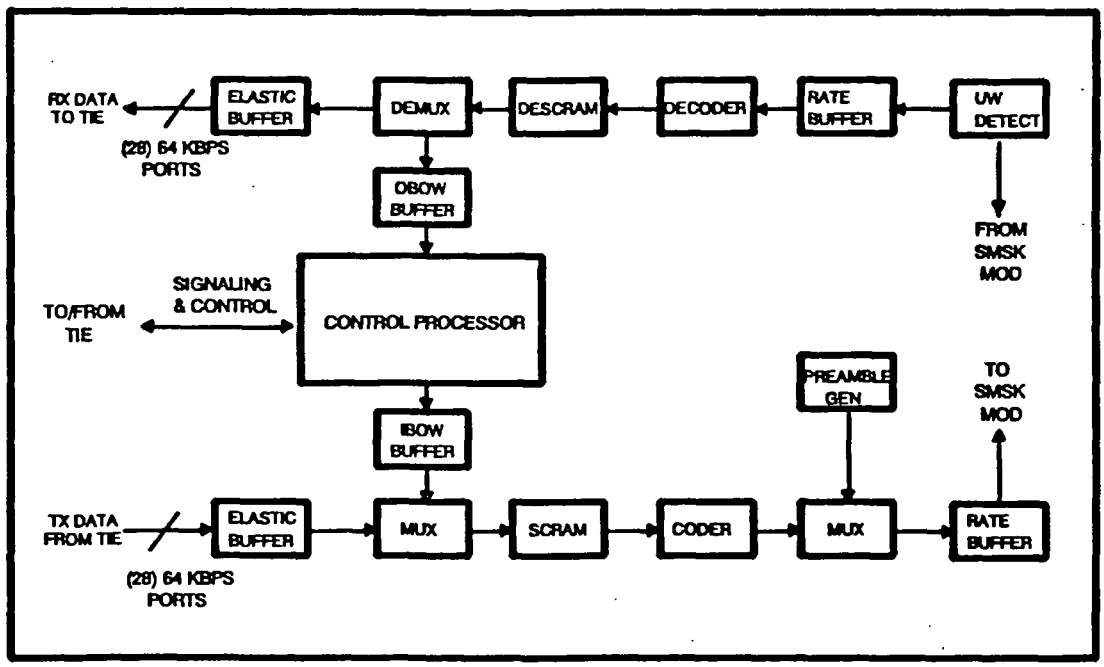

Figure 8. TDMA Processing Flow

Separate foreground and background control maps are used to manage the network burst time plans established by the MCS. In this way the control processor is able to maintain an uninterrupted flow of traffic across the burst time plan change boundaries.

The control processor is also responsible for monitoring the performance of the earth station. Built into the earth station are a number of sensors, stimulators, and test loops which the control processor continuously monitors to check the health of the earth station and to isolate faults. The operating conditions are displayed on a front panel mounted readout as illustrated in Figure 9. A 4x40 character alpha-numeric display is used to indicate the station's operating mode, its health status, the occurrence of any on-line fault indications, and the link quality status. In the off-line fault isolation mode, the appropriate failure indication is displayed.

In order to maintain uplink synchronization, the earth station must have an accurate internal timing source that is stable to ±1 part in 10^9. Contained in the Modem-Processor is a small 10 MHz rubidium cell atomic clock. All timing signals and frequency sources are derived from that clock. The rubidium cell is not only a cost effective means of providing a stable reference, it has the distinct advantage of enabling the earth stations to operate in excess of two years without recalibration.

Rain Fade Control

Link degradations due to rain fades are detected by sensing the E_b/N_o of the downlink traffic-bearing signal. This method of fade detection has three advantages: (1) it avoids the expense of a beacon receiver, (2) it allows the earth station to be operated outside the coverage area of the beacons, and (3) it allows the system to automatically compensate for equipment degradations that affect the station's G/T performance.

The method is based on a statistical measurement of the signal plus noise. The E_b/N_o of the downlink signal is estimated by determining the ratio of the mean (μ^2) to the variance (s^2) of the signal. Analysis indicates that the measurement will be accurate to within ±0.6 dB over the required 10 dB dynamic fade range. The computations required to determine E_b/N_o are done by the control computer in the Modem-Processor. The fade status is automatically communicated to the MCS by means of the inbound orderwire. The decision to invoke and remove FEC coding may be done either at the earth station or by the MCS. The fade thresholds for invoking and removing FEC coding at the onset and cession of a fade event may be adjusted so as to adapt the station to its specific rain fade environment.

For the purposes of experimentation, attenuators may be inserted in the transmitter and receiver to independently restrict the earth station's clear-sky uplink margin and downlink margin. This will allow the speed and effectiveness of the rain fade control algorithms to be evaluated.

TERRESTRIAL INTERFACE

The TIE (Figure 10) is connected to the Modem-Processor by means of 28 duplex synchronous data lines operating at 64 KBPS. Clock rate difference between terrestrial circuits and the space segment are absorbed by elastic (plesiochronous) buffers at the input and output ports to the TDMA Processor. A 2400 baud asynchronous data link is used to convey signaling and control information between the user and the Modem-Processor.

The TIE is a commercial piece of telecommunications equipment. It is equipped with a number of field-changeable modules that will enable the user to configure the interface to meet his particular set of requirements for voice, video, and data services. The user may connect any one or more of the following:

- two-wire analog telephones
- ground/loop start lines and trunks
- two-wire and four-wire E&M trunks
- T1 (DS-1) digital lines
- synchronous serial data (8 - 64 KBPS)
- asynchronous serial data (300 - 9600 baud)

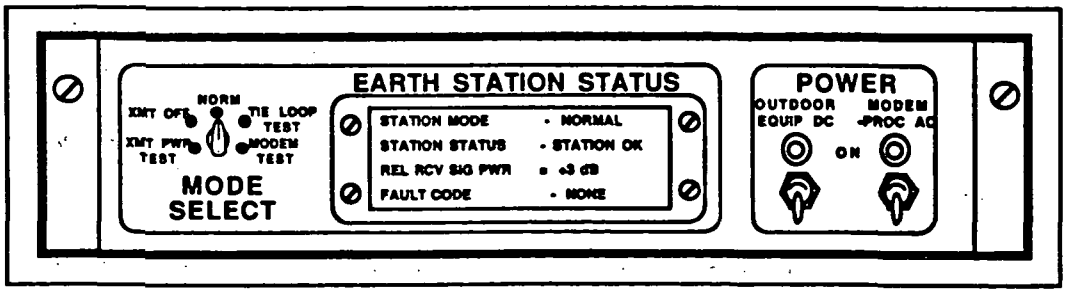

Figure 9. The Control and Monitor Panel

The mix of circuit types is limited only by the throughput capacity of the station (1.792 MBPS). The user may therefore, for example, connect one full T1 (1.544 MBPS) circuit plus four DS-0 (64 KBPS) circuits, or any other equivalent combination of 28 DS-0 circuits. The electrical and signaling protocols for the various interfaces adhere to the conventional Bell standards.

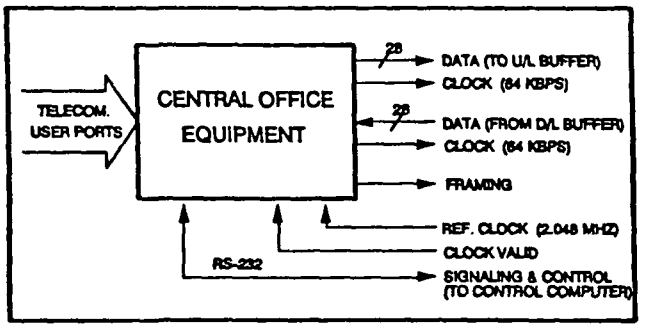

Figure 10. Terrestrial Interface Equipment

Functionally the TIE, in conjunction with the signaling and control software that resides in the control computer of the Modem-Processor, is equivalent to a local telephone central office. Call set-ups and tear-downs are managed using the customary DTMF signaling tones, call progress tones, and cadences. The signaling that takes place between the earth station and the MCS is totally transparent to the user.

All circuits connected to the TIE do not necessarily have to be routed over the satellite. The earth station has the capability to interconnect circuits locally in the same manner as commercial central offices do. This gives the earth station the flexibility to function as a true communications center.

INSTALLATION

The earth station is specifically designed to facilitate its installation on users' premises. It is shipped partially disassembled, the largest single piece being the 2.4-meter reflector. Once on site, the earth station can be reassembled, installed, and checked out by two installers. Two signals that are generated in the indoor unit are cabled out to the antenna: a downlink lock indicator and an analog AGC signal. These signals provide a measure of the received signal strength to assist the installers in aligning the antenna. With the proper site preparation, the installation can be completed in less than 8 hours.

RELIABILITY

The mean-time-between-failures (MTBF) of the earth station is projected to be in excess of 2,200 hours. The self-test capability built into the earth station should allow over 90% of all equipment failures to be detected and isolated. Because of the modular construction of the earth station, the mean-time-to-repair (MTTR) is estimated to be less than one hour.

To eliminate failures due to infant mortality, each earth station will be thermally stress tested by repeatedly cycling the equipment between 0°C and 55°C with power on. Following the thermal stress test, each earth station will be run for a minimum of 200 consecutive failure-free hours. Experience has shown that this type of testing reduces the failure rate of equipment in the first two years of its operation by as much as 50%.

REFERENCES

1. J. C. Graebner and W. F. Cashman, "Advanced Communications Technology Satellite: System Description," IEEE Global Communications Conference, Vol. 1, pp. 559-567, Dec. 1986.

2. F. M. Naderi and S. J. Campanella, "NASA's Advanced Communications Technology Satellite (ACTS): An Overview of the Satellite, the Network, and the Underlying Technologies, "AIAA 12th International Communications Conference, Arlington, Virginia, March 1988.

3. T. Inuaki, D. Juplin, R. Lindstrom, D. Meadows, "ACTS TDMA Network Control Architecture," Proceedings 12th International AIAA Communications Satellite System's Conference, March 1988, Washington, D.C.

N91-11972

A Review of Fade Detection Techniques

F. J. Pergal

Jet Propulsion Laboratory
California Institute of Technology
Pasadena, California

ABSTRACT Several proposed propagation fade detection techniques are reviewed in light of general requirements presented for beacon fade characterization. The discussion includes an analysis of phase lock versus frequency lock beacon tracking loops and of excess noise injection type radiometers. The ACTS beacon fade detection schemes proposed by COMSAT and JPL are examined along with the fade detection technique used by Harris in their ACTS LBR terminal.

1. Introduction

This paper is intended as a review and comparison of several proposed fade detection techniques as applied to the ACTS experiment. The discussion of specific implementations is preceded by a general analysis of beacon tracking receivers in which the ACTS propagation beacon parameters are referenced.

In the event that a fade is detected at a transmitting terminal, compensation procedures would be initiated. The eventual compensation algorithm will depend strongly on fade statistics which will only be compiled during the ACTS experiment itself. Fade compensation algorithms will not be discussed here.

The performance of phase and frequency locked receivers is compared for the ACTS beacon dynamics. Threshold tracking performance is displayed as a function of beacon phase noise and receiver C/N_o. A brief treatment of the associated radiometer design requirements is also included, anticipating the discussion of the proposed JPL beacon receiver.

COMSAT has designed a receiver for the ACTS Beacon Measurement System at the NASA Lewis Research Center which is based on the Hewlett Packard 3586A Selective Level Meter (SLM). The SLM is controlled via PC based hardware with algorithms of COMSAT's design. Reported performance of the system is excellent (Zaks, 1989). The suitability of the COMSAT approach for a VSAT architecture, as is proposed for the ACTS Propagation Experimenter's Terminal, is investigated in detail below.

A novel technique for fade detection has been developed by the Harris Corporation for use in their ACTS LBR terminal (Manning, 1989). The Harris technique uses the LBR signal to estimate the

received SNR. The algorithm operates on relatively coarse (6 bit) samples of the LBR symbol matched filter output. Differences between the averaged outputs of absolute value and square law detectors applied to the matched filter output are exploited to generate very accurate estimates of the channel SNR. Fade compensation is based on this SNR measurement without the need for a separate beacon receiver.

In the proposed JPL receiver the beacon signal is digitized at IF in a relatively wide bandwidth of 2.5 MHz. IF sampling produces complex I/Q sample pairs which are phase rotated and then filtered. Coarse and then fine filtering is accomplished using a cascade of two windowed FFTs. A frequency discriminator is implemented using outputs of the second FFT and a beacon tracking loop is then closed on the phase rotator. Radiometer measurements can be made easily using existing signals within the digital receiver as discussed below.

2.0 General Beacon Receiver Design Requirements

Referring to the Proceedings of the First ACTS Propagation Workshop (Rogers, 1989), the fundamental requirement imposed on a propagation experimenter's terminal is the measurement of fade amplitude with +/-0.1 dB accuracy. Implicit in this requirement is the capability of determining the clear sky baseline path attenuation. Presumably, satellite EIRP variations will be resolvable by means other than measurements at isolated terminals.

For a VSAT type terminal the clear sky beacon C/N_o will be on the order of 40 to 45 dB Hz (Davarian et al., 1990). Signal dynamics include phase noise of -20 dBc/Hz at 5 Hz offset and diurnal frequency drift of up to +/-1.5 ppM (Davarian, loc. cit.). Assuming that the diurnal frequency drift profile is sinusoidal, for the uplink fade beacon at 27.5 GHz, maximum drift rates of 180 Hz/minute could be experienced.

Since only beacon amplitude measurements are required, some frequency tracking error is allowable. The amount of frequency error that can be tolerated will be determined by the beacon pre-detection bandwidth. The minimum predetection bandwidth is determined by the bandwidth of the fade process. The maximum bandwidth, on the other hand, will be determined by the measurement accuracy requirement and the minimum beacon signal level for which that accuracy is to be maintained.

Assume a generic receiver as shown in Figure 1. Referring to the figure, down conversion to baseband is optional; COMSAT, for example, detects the beacon signal at IF. With baseband detection, as shown in the figure, I and Q are low pass filtered and then accurately squared to produce a harmonic free I^2+Q^2 detection statistic. For a clear sky C/N_o of 42 dB Hz and a dynamic range of 15 dB, the minimum predetection C/N_o will be 27

dB Hz. Neglecting squaring loss, the input SNR corresponding to +/-0.1 dB detector accuracy at the bottom of the dynamic range will occur with a predetection lowpass bandwidth, B_{pd}, of 7.7 dB Hz.

Assuming a fade process bandwidth on the order of 5 Hz, this indicates that, in a sense, the ACTS transmitted EIRP is nearly optimal for a propagation experiment using the VSAT architecture. It should also be noted that the post detection noise spectrum will be triangular extending out to $2*B_{pd}$. To avoid noise aliasing either post detection filtering or an output sample rate of at least $4*B_{pd}$ should be used.

If a larger measurement tolerance is possible at the lower end of the dynamic range, or a bank of detectors could be used, then the predetection bandwidth could be opened up proportionately. In any case, the beacon tracking system must maintain the beacon within the predetection bandwidth over the dynamic range of interest. In addition, the tracking system should allow for easy initial acquisition or reacquisition after a long fade. The acquisition process should be fully automatic allowing for unattended operation and, in the case of the 20.2 GHz receiver, should be highly resistant to false locking on modulation sidelobes.

2.0.1 Phase Locked vs. Frequency Locked Tracking

Additive bandpass Gaussian noise and beacon phase noise will introduce angle jitter on the beacon tracking oscillator. In the case of additive noise, the narrower the loop bandwidth, the more accurately the receiver will track the beacon. To track out beacon phase noise, however, the loop should be as wide as possible. For the ACTS beacons, phase noise is significant enough that for a VSAT receiver using either phase or frequency locked tracking, loop bandwidth has to be carefully chosen. The best choice minimizes the total angle tracking error variance.

The contribution to tracking phase jitter variance due to additive noise is $[C/N_oB_L]^{-1}$ radians^2 for the phase locked loop. For the frequency locked loop the situation is more complicated (Natali, 1984) and depends on the predetection SNR and on details of the discriminator design. For a predetection SNR >> 1 and $B_L << B_I$, where B_I is the equivalent predetection IF bandwidth, assuming a cross product discriminator with integrate and dump filtering, the frequency tracking error variance is given by:

$$[0.051(B_L/B_I)B_I^2]/SNR_I$$

As an example, the VPI Olympus 12.5 GHz beacon receiver frequency locked loop has a noise bandwidth of approximately 10 Hz with a predetection bandwidth of 200 Hz. For a C/N_o of 30 dB Hz, the above expression gives an RMS frequency tracking error of roughly 4.5 Hz.

In the case of beacon phase noise the tracking angle error variance is given by the integrated product of the linearized loop error response and the beacon angle noise power spectral density (Gardner, 1979). For the range of B_L in question, the beacon phase noise power spectral density in dBc/Hz has close to a pure flicker of frequency characteristic. The phase noise power spectral density, $S_{phase}(f)$, will equal h_3/f^3, where f is the frequency offset from the beacon carrier frequency and h_3 is a proportionality constant. Expressed as frequency noise the beacon angle modulation PSD will simply be h_3/f, i.e. 1/f or "flicker" noise. For the ACTS beacons h_3 is approximately equal to 1.25.

The total angle error variance will be the sum of the two component variances due to additive and phase noise. For the phase locked loop with a sinusoidal phase detector the commonly accepted threshold corresponds to an RMS phase error of .316 radians. For the frequency locked loop the situation is again slightly more complicated. The frequency error that can be tolerated depends on details of the discriminator design (Natali, 1984).

Generally, the discriminator range will be from $+/-0.2B_I$ to $+/-0.5B_I$, where B_I is the effective prediscriminator IF bandwidth. Allowing for three sigma excursions, the RMS frequency error that can be tolerated will be approximately one third of the discriminator range. The larger the range the greater the frequency error that can be tolerated before thresholding occurs.

There are of course constraints on the discriminator range. Usually, discriminator action is obtained by comparing the phase of a signal with that of a delayed version of itself, i.e. by delay and multiply operations or by differencing the power measured in two frequency offset filters. The multiplication and power measurement operations introduce squaring loss. In order to avoid significant squaring loss in the loop, the effective prediscriminator bandwidth cannot be too large.

For both the phase locked and frequency locked loops there are also practical constraints on the predetection bandwidth. These arise because of component tolerances and voltage offsets. About the best that can be said is that the optimal tracking strategy and parameter settings have to be determined on a case by case basis.

2.0.2 Radiometer Design Considerations

To meet the fade measurement accuracy requirement, for the propagation terminal, a baseline clear sky path attenuation must be established. An excess noise injection radiometer such as used in VPI&SU's Olympus terminal suite (Stutzman, 1990) and shown in block diagram form in Figure 3. is one means to this end. Referring to the figure, a directional coupler at the receiver front end is alternately switched at a low rate (dwell times of

two to five seconds would be typical) between a diode excess noise source and a termination.

Assume that the diode excess noise ratio (ENR) and the physical temperature of the switch, coupler and any other connecting hardware are well regulated. This scheme then will provide constant differential noise power against which to measure changes in the system noise temperature (and receiver gain).

Loss mechanisms in the excess noise path will make a contribution to system noise temperature; but, it is possible to keep these losses in the range of a few dB. Components are mounted on a temperature regulated plate in an effort to stabilize the differential noise temperature. In addition, the system would also be periodically calibrated against hot/cold loads.

Elektronik Centrallen has cited (1988) the results of a two year life test of 35 GHz noise diodes with ENRs on the order of 23 dB which shows ENR variations of roughly +/-.03 dB. From the data records it appears that much of this small variation may even be due to seasonal changes in the test environment.

The radiometer is used to measure differences in system noise temperature, the varying sky noise temperature being the component of system noise that is of interest. At any particular system noise temperature, the accuracy of an absolute system noise temperature measurement is given by $T_{sys}/(BT)^{1/2}$, where B is the equivalent predetection IF noise bandwidth and T is the measurement integration time. Differences in absolute noise measurements will have an accuracy of $(2)^{1/2}$ times this number.

The following heuristic argument is intended as motivation for choosing the excess noise injection radiometer IF bandwidth. The detected excess injected noise provides the "yardstick" against which changes in absolute system noise temperature are measured. The excess noise should therefore be as large, and as accurately determined as practical. Along these lines, if changes in receiver gain are very slow, long term averaging of the detected excess noise differences would remove most of the random measurement inaccuracy. For a system noise temperature, T_{sys}, of 1500 ^{o}K, and an integration time of 3 seconds, a 1 ^{o}K accuracy could be produced with an IF bandwidth of 2.5 MHz.

2.1 The Harris Algorithm and Implementation

The Harris fade detection technique operates on the coded LBR signal and makes use of the output of the receiver's coherent amplitude detector. The input signal is MSK with additive bandpass noise. The receiver signal which is processed is the output of a baseband matched filter. The density of the filter output at the sampling instants is a zero mean Gaussian density convolved with delta functions at +/-A, where A is the signal amplitude at the matched filter output.

The quantized matched filter output is operated on by two parallel detector stages. One stage is a square law detector, the other an absolute value detector. Following each detector operation are two identical accumulation and scaling stages. The processing is illustrated in Figure 3.

For sufficiently high input SNRs, the two Gaussian components (centered at +/-A) of the matched filter output density will have very little overlap. Under these conditions the outputs of the absolute value and square law detector chains are proportional to A and $(A^2 + s^2)$, respectively, where s^2 is the variance of the Gaussian components of the matched filter output density.

The accumulated absolute value detector output is squared to produce an estimate of A^2. The ratio, $A^2/(A^2 + s^2)$, is then formed and used to drive a lookup table. Since this ratio is a monotonic function of SNR (i.e. of A^2/s^2), it easy to compute true SNR via the lookup. At the same time by modifying the lookup table the overlap effect mentioned above can be compensated. The result is an SNR estimate that is accurate over a wide dynamic range.

The number of baseband matched filter samples accumulated for an SNR estimate is 640. Further a minimum of 900 of these ratios (conditioned by the lookup) are averaged to generate the final SNR estimate used by the fade compensator. The noise densities at the outputs of the square law and absolute value detectors will be similar (Blachman, 1966). For input SNRs (in the matched filter bandwidth) of 6 dB or better there will be very little squaring loss so that the variance of the resulting SNR estimate can be easily calculated.

The main advantage of the Harris technique from a receiver design viewpoint is that it is independent of AGC effects. There is also the potential for excellent dynamic range. This will to some extent depend on Bit Synchronizer performance degradations with low SNRs and the resulting inaccuracies in estimated symbol amplitude. Finally the Harris algorithm as implemented does not require an independent beacon receiver which can amount to a large cost savings.

2.2 The COMSAT Fade Detection Receiver

The COMSAT fade detection receiver operates on the ACTS uplink and/or downlink fade beacons. In the fully configured Beacon Measurement System three Hewlett Packard 3586A Selective Level Meters (SLM) are used to track and measure three independent beacons simultaneously. For the BMS, the clear sky C/N_o is 62.1 dB Hz for the 20.2 GHz beacons and 58.5 dB Hz for the 27.5 GHz beacon.

Referring to Figure 4., the down converted beacon signal is input to the SLM. The signal is frequency converted to a 15.625 KHz IF

and band pass filtered to a selectable IF bandwidth. The filtered signal is RMS/log detected with a detector time constant of .011 seconds and the conditioned, detected signal is sampled at a 6&2/3 Hz rate. A self calibration feature is also available in the instrument under bus control.

Receiver tuning information is derived from the bandpass limited 15.625 KHz IF signal. The limited signal drives a second order phase locked loop with B_L of approximately 600Hz (Hewlett Packard, 1990). The phase locked loop VCO runs at 20 times the IF signal frequency. The VCO frequency is counted over a very accurate 0.5 second time interval to obtain the average signal frequency reading. Frequency tracking is essentially open loop with the first LO being set via bus commands from an algorithm of COMSAT's design. The 0.1 Hz frequency resolution and long term stability available with the external clock option allow extremely accurate tuning under bus control.

For a VSAT architecture C/N_o is approximately 15 dB less than what COMSAT is working with in the BMS. To track a VSAT beacon signal the IF bandwidth would probably have to be lowered to 20 Hz. At that IF bandwidth the detector time constant might become a problem. Furthermore, beacon tracking in the open loop mode may require developing a sophisticated frequency estimation algorithm to assure quick reacquisition after fades. In summary, it is probably safe to say that fairly extensive testing would be required to ascertain the suitability of the COMSAT approach in the VSAT application.

2.3 The JPL Digital Beacon Receiver

A block diagram of the JPL Beacon Receiver is shown in Figure 5. Relatively coarse quantization is used to sample the signal at a nominal IF of 20 MHz. Note that the ratio of the nominal IF center frequency to the sampling clock frequency is of the form: $(1 + 1/4)$.

The choice of IF and sampling frequencies allows I and Q relative to a reference sinusoid at the nominal IF frequency to be reconstructed from the IF samples. In the general case, the same will be true if $f_{IF}=f_S*(N +/- 1/4)$, where f_{IF} is the IF frequency, f_S is the sampling clock frequency and N is any integer. The only restriction on f_S is that it be at least twice the band width of the sampled IF signal.

It has been known for some time that a high degree of measurement accuracy is possible with coarse quantization in the presence of a dithering signal (Widrow, 1955). It is also well known that, in general, the quantizing levels have to be extremely accurate. Blachman (1984) has shown that for a memoryless quantizer operating on a noisy signal, the effective quantizer transfer function will be the noise free transfer function convolved with the noise density. The noise essentially smooths over A/D

nonlinearities. By operating at a low enough SNR (<-20 dB), the A/D step accuracy problem is avoided in the JPL receiver. The quantization operation is also effectively memoryless because of the independence of the signal and noise.

The A/D output sequence is sorted into an I/Q sample pair stream, then phase rotated using a complex mixer (a look up table) and formatted into blocks. A (complex) FFT is then performed on blocks of I/Q sample pairs. The order of the FFT is determined by acquisition time requirements as discussed below. The FFT operation is equivalent to passing the signal through a filter bank. The time sequences produced by the FFT bins are then detected and filtered. Following which the output from the FFT bin containing the carrier component is identified by the controlling processor.

As part of the acquisition process a fine grained filter bank operation locates the carrier more precisely. This filtering operation is performed by a second or fine FFT taken on the sample stream corresponding to that bin from the first or coarse FFT operation that contains the carrier component.

Carrier tracking is accomplished using an AFC loop closed on the complex mixer through a phase accumulator. The accumulator increment is controlled by an FLL where the discriminator function is implemented using the outputs of the fine FFT (Natali, 1984). Updates to the loop take place at a relatively low rate corresponding to roughly ten times the loop bandwidth.

During acquisition the AFC loop is disabled. In the tracking mode the carrier is downconverted to a frequency close to DC by the complex mixing operation. The loop will keep the carrier centered in a relatively narrow spectral window. The downconverted signal is amplitude detected and filtered in the controlling processor and passed to the terminal computer. The processor will be designed to support a 10 Hz carrier amplitude sampling rate.

The radiometer and signal processing channels share a common IF. The coarse FFT bins not containing beacon, telemetry or ranging components are detected, summed and filtered to estimate the channel noise variance. Currently simulations are being run to test the effectiveness of FFT windowing using coarse A/D quantization.

With an IF filtered to a noise bandwidth of 2.5 MHz as above, the (complex) I/Q process will have a bandwidth (assuming 4 MHz wide filter skirts) of about 2 MHz. With a 16 MHz sampling clock, the process will be oversampled by a factor of 2. With the above choice of IF and sampling clock frequencies, the sample sequence forms a pattern: I, Q, -I, -Q, I, Q, etc. Therefore, samples 2 and 3 modulo 4 can be discarded.

Using a pair of United Technologies UT69532 IQMAC Processor chips clocked at 16 MHz, a 1024 point complex FFT will run in 0.320

milliseconds; 4 chips will do the FFT in .160 milliseconds. Using 1024 points for the coarse FFT channelizes the I/Q stream into bins with noise bandwidth of roughly 4 KHz.

For a C/N_0 of 43 dB Hz this provides a predetection SNR of about 7 dB even without the fine FFT processing. Since acquisition consists in measuring the relatively slowly changing power of the bin outputs, subsampling the outputs is possible. Needless to say very fast acquisition and reacquisition (in the sub-second range) following deep fades becomes possible.

Experience with Olympus indicates that similar tracking loop parameters and carrier amplitude processing will be appropriate for ACTS signal processing. Loop noise bandwidths on the order of 2 to 3 Hz would enable tracking into the 15 dB C/N_0 region. Note that at peak carrier frequency drift rates (180 Hz/minute) some type of loop aiding would be required for such narrow loop bandwidths.

3.0 Conclusion

Three specific fade detection techniques developed for the ACTS program have been examined. A comparison of the techniques points out the advantages of each in its particular application. The COMSAT design is a very clean implementation for the case where C/N_0 is relatively high. Its applicability for a VSAT propagation terminal architecture, however, would have to be carefully investigated.

The Harris receiver only requires a nominal AGC to keep the signal level reasonably positioned in the A/D converter input range. In this sense the Harris approach has a real advantage. The Harris technique could also be adapted to a beacon receiver but then radiometer information is given up. With this the ability to sense clear sky attenuation independent of satellite EIRP variations is also lost.

The JPL receiver has the advantage of simultaneously measuring channel noise along with beacon amplitude. This minimizes the effects of receiver gain variations on the beacon amplitude measurement. All tuning is done digitally after A/D conversion, so that the need for a selective IF along with a tuned LO is eliminated. The all digital implementation is also attractive from the standpoint of trouble free operation in unattended terminals.

Acknowledgement: The research described in this paper was performed by the Jet Propulsion Laboratory, California Institute of Technology, under contract with the National Aeronautics and Space Administration.

References

Blachman, N. M., Noise and its Effects on Communication, p. 93, New York, McGraw Hill, 1966.

Blachman, N. M., "The Effect of a Nonlinearity upon Signals in the Presence of Noise", IEEE Trans. COM-21, pp. 152-154, February 1973.

Davarian, F., F. Pergal, D. Chakraborty and W. Stutzman, "ACTS Propagation Terminal Prototype Planning and Design", Proceedings of NAPEX XIV, May 1990.

Elektronik Centrallen, "20/30 GHz Multi-Frequency Radiometer Feasibility Study", Horsholm, Denmark, May 1988.

Gardner, F. M., Phaselock Techniques, New York, McGraw Hill, 2nd ed., 1979.

Hewlett Packard, Private communications with personnel at the HP Lake Stevens Instrument Division.

Manning, R. M., "The Harris 'Mean Squared over Variance' Technique", Proceedings of the First ACTS Propagation Studies Workshop, December 1989.

Natali, F. D., "AFC Tracking Algorithms", IEEE Trans. COM-32, pp. 935-947, August 1984.

Rogers, D. V., "Report of the Systems Group", Proceedings of the First ACTS Propagation Studies Workshop, December 1989.

Stutzman, W. L., "Olympus Propagation Terminal Hardware and Experiments", Proceedings of NAPEX XIV, May 1990.

Widrow, B., "A Study of Rough Amplitude Quantization by Means of Nyquist Sampling Theory", IRE Trans. CT-5, pp. 266-276, December 1956.

Zaks, C., "NASA Ground Station Beacon Measurement Subsystem", Proceedings of the First ACTS Propagation Studies Workshop, December 1989.

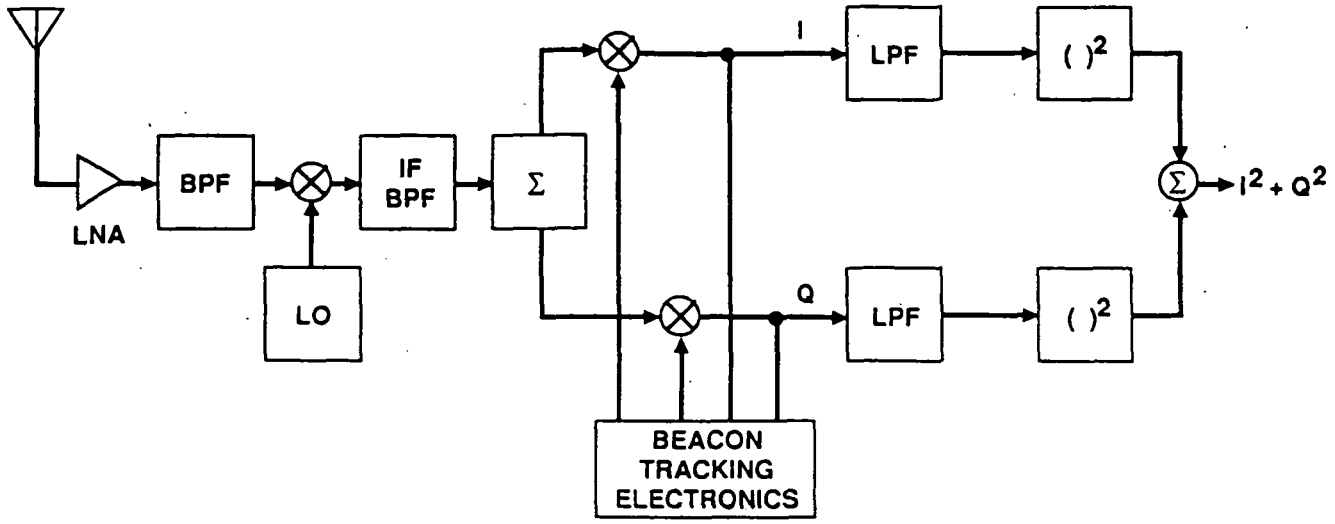

Figure 1. Generic Beacon Receiver Block Diagram

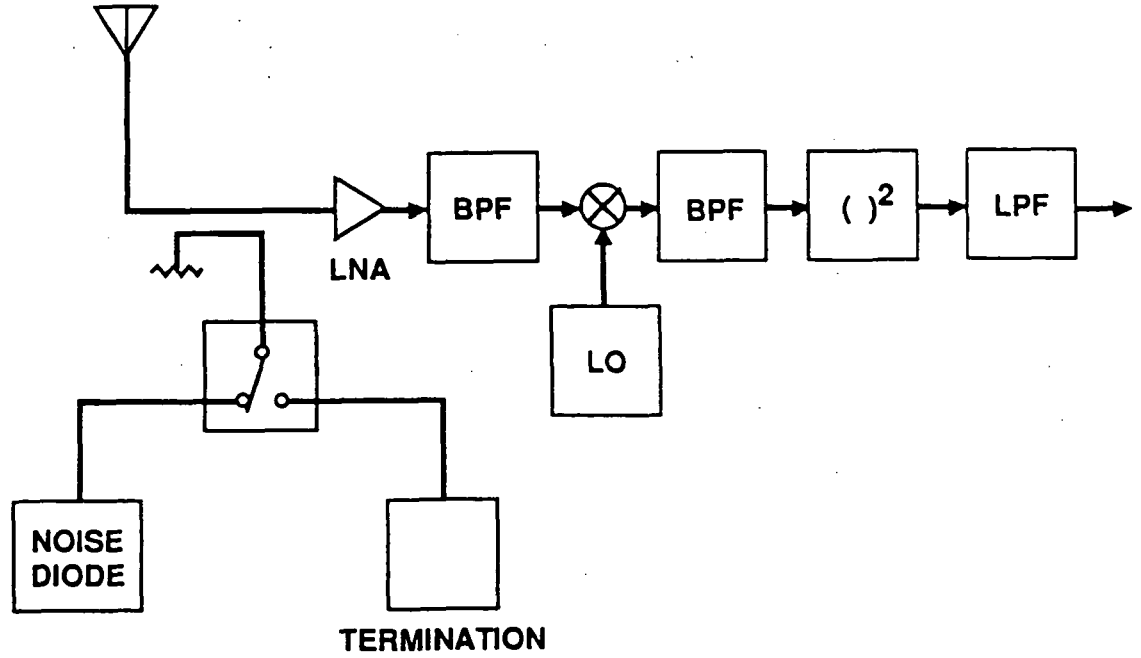

Figure 2. Excess Noise Injection Radiometer Block Diagram.

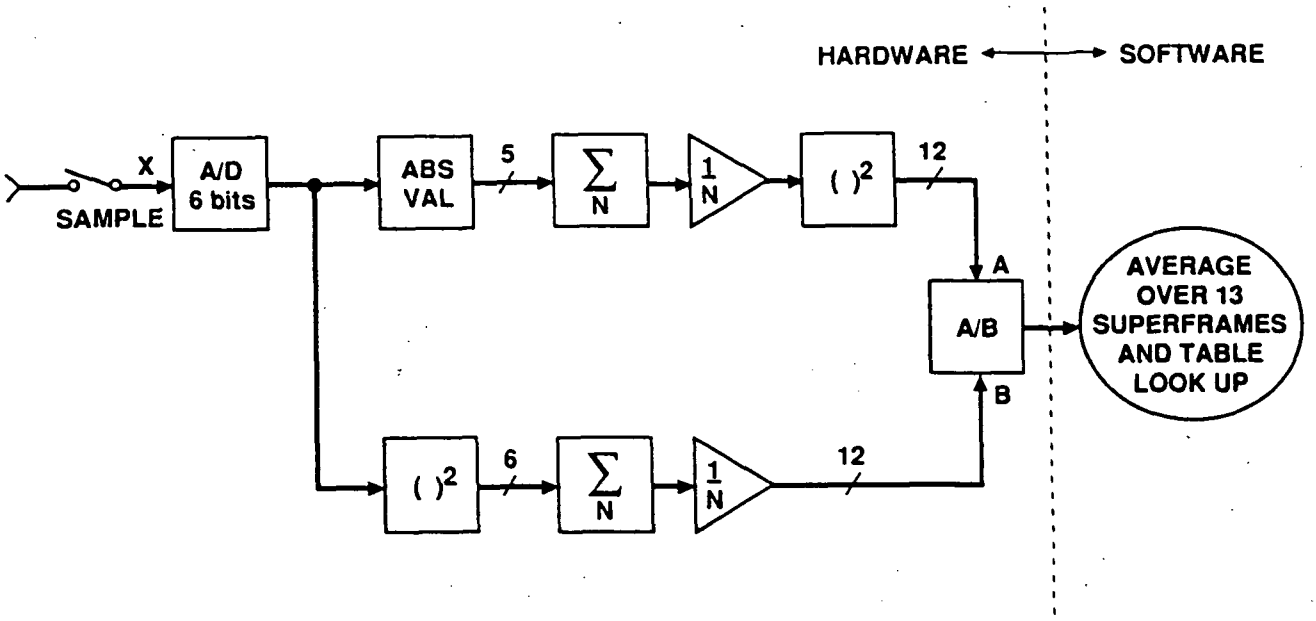

Figure 3. The Harris LBR Fade Detection Technique.

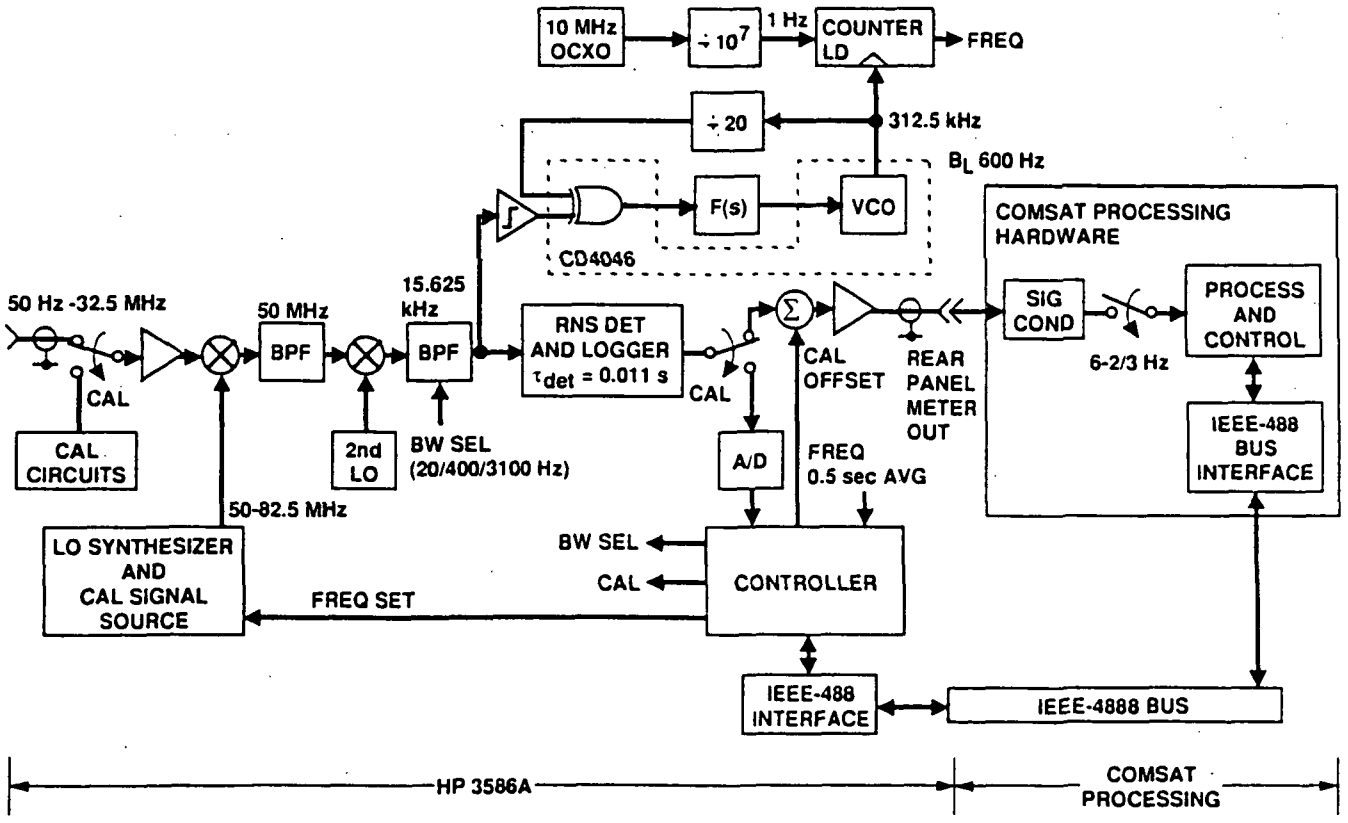

Figure 4. The COMSAT Fade Detection Technique.

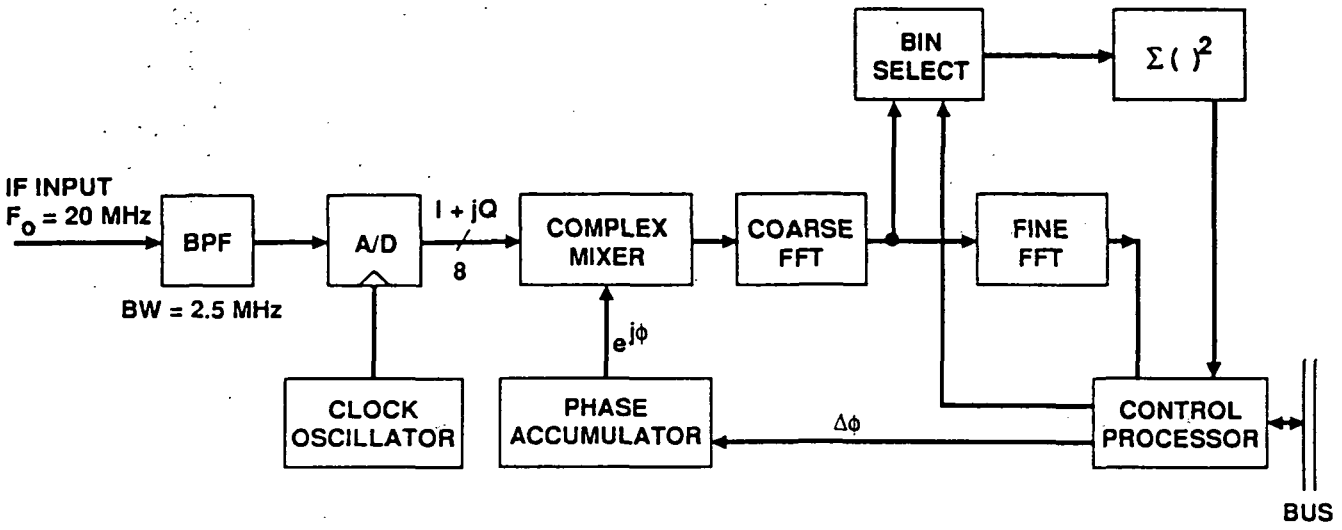

Figure 5. The JPL Digital Beacon Receiver.

TECHNICAL REPORT STANDARD TITLE PAGE

1. Report No. JPL Pub. 90-27	2. Government Accession No.	3. Recipient's Catalog No.
4. Title and Subtitle Proceedings of the Fourteenth NASA Propagation Experimenters Meeting and the Advanced Communications Technology Satellite Propagation Studies Miniworkshop		5. Report Date July 1, 1990 6. Performing Organization Code
7. Author(s) Faramaz Davarian		8. Performing Organization Report No. JPL Publication 90-27
9. Performing Organization Name and Address JET PROPULSION LABORATORY California Institute of Technology 4800 Oak Grove Drive Pasadena, California 91109		10. Work Unit No. 11. Contract or Grant No. NAS7-918 13. Type of Report and Period Covered JPL Publication
12. Sponsoring Agency Name and Address NATIONAL AERONAUTICS AND SPACE ADMINISTRATION Washington, D.C. 20546		14. Sponsoring Agency Code RE4BP-643-10-03-04-00

15. Supplementary Notes

16. Abstract The NASA Propagation Experimenters Meeting (NAPEX), supported by the NASA Propagation Program, is convened annually to discuss studies made on radio wave propagation by investigators from domestic and international organizations. NAPEX XIV was held on May 11, 1990, at the Balcones Research Center, University of Texas, Austin, Texas. Participants included representatives from Canada, Italy, Japan, The Netherlands, United Kingdom, and the United States. The meeting was organized into two technical sessions: The first was devoted to propagation studies for the Advanced Communications Technology Satellite (ACTS) and the Olympus Spacecraft, while the second focused on the fixed and mobile satellite propagation studies and experiments.

Following NAPEX XIV, the ACTS Miniworkshop was held at the Hotel Driskill, Austin, Texas on May 12, 1990, to review ACTS propagation activities since the First ACTS Propagation Studies Workshop was held in Santa Monica, California, on November 28 and 29, 1989. Five papers were presented by contibutors from government agencies, private industries, and research institutions.

17. Key Words (Selected by Author(s))	18. Distribution Statement
Communications Optics Wave Propagation	Unclassified -- Unlimited

19. Security Classif. (of this report)	20. Security Classif. (of this page)	21. No. of Pages	22. Price
Unclassified	Unclassified	258	